Supplementary materials for

Defying the oxidative-addition prerequisite in cross-coupling through artful single-atom catalysts

Jiwei Shi[1,2,3,12], Gang Wang[4,12], Duanshuai Tian[1,12], Xiao Hai[5], Rongwei Meng[1,2,3,12], Yifan Xu[6], Yu Teng[1,2], Lu Ma[7], Shibo Xi[8], Youqing Yang[1], Xin Zhou[1], Xingjie Fu[1,2,3], Hengyu Li[1], Qilong Cai[1], Peng He[1], Huihui Lin[1,8], Jinxing Chen[1], Jiali Li[1], Jinghan Li[1], Qian He[9], Quan-Hong Yang[2,3], Jun Li[4,10], Dongshuang Wu[6*], Yang-Gang Wang[4*], Jie Wu[1*] and Jiong Lu[1,11*]*

[1]Department of Chemistry, National University of Singapore, 3 Science Drive 3, Singapore 117543, Singapore.

[2]Joint School of National University of Singapore and Tianjin University, International Campus of Tianjin University, Binhai New City, Fuzhou 350207, China.

[3]Nanoyang Group, Tianjin Key Laboratory of Advanced Carbon and Electrochemical Energy Storage, School of Chemical Engineering and Technology, National Industry-Education Integration Platform of Energy Storage, and Collaborative Innovation Center of Chemical Science and Engineering (Tianjin), Tianjin University, Tianjin, 300072, China.

[4]Department of Chemistry and Guangdong Provincial Key Laboratory of Catalysis, Southern University of Science and Technology, Shenzhen 518055, Guangdong, China.

[5]School of Materials Science and Engineering, Peking University, Beijing, P.R. China.

[6]School of Materials and Engineering, Nanyang Technological University, Singapore, 639798 Singapore.

[7]National Synchrotron Light Source II Brookhaven National Lab Upton, NY 11973, USA.

[8]Institute of Sustainability for Chemicals, Energy and Environment (ISCE2), Agency for Science, Technology and Research (A*STAR), 1 Pesek Road Jurong Island, Singapore 627833, Republic of Singapore.

[9]Department of Material Science and Engineering, College of Design and Engineering, National University of Singapore, 9 Engineering Drive 1, EA #03-09, 117575, Singapore.

[10]Department of Chemistry and Engineering Research Center of Advanced Rare-Earth Materials of Ministry of Education, Tsinghua University, Beijing, China.

[11]National University of Singapore (Suzhou) Research Institute, No. 377 Linquan Street, 215123 Suzhou, Jiangsu, China.

[12]These authors contributed equally: Jiwei Shi, Gang Wang, Duanshuai Tian, Rongwei Meng

*Corresponding author. Email: xiaohai@pku.edu.cn; dongshuang.wu@ntu.edu.sg; wangyg@sustech.edu.cn; chmjie@nus.edu.sg; chmluj@nus.edu.sg

Table of Contents

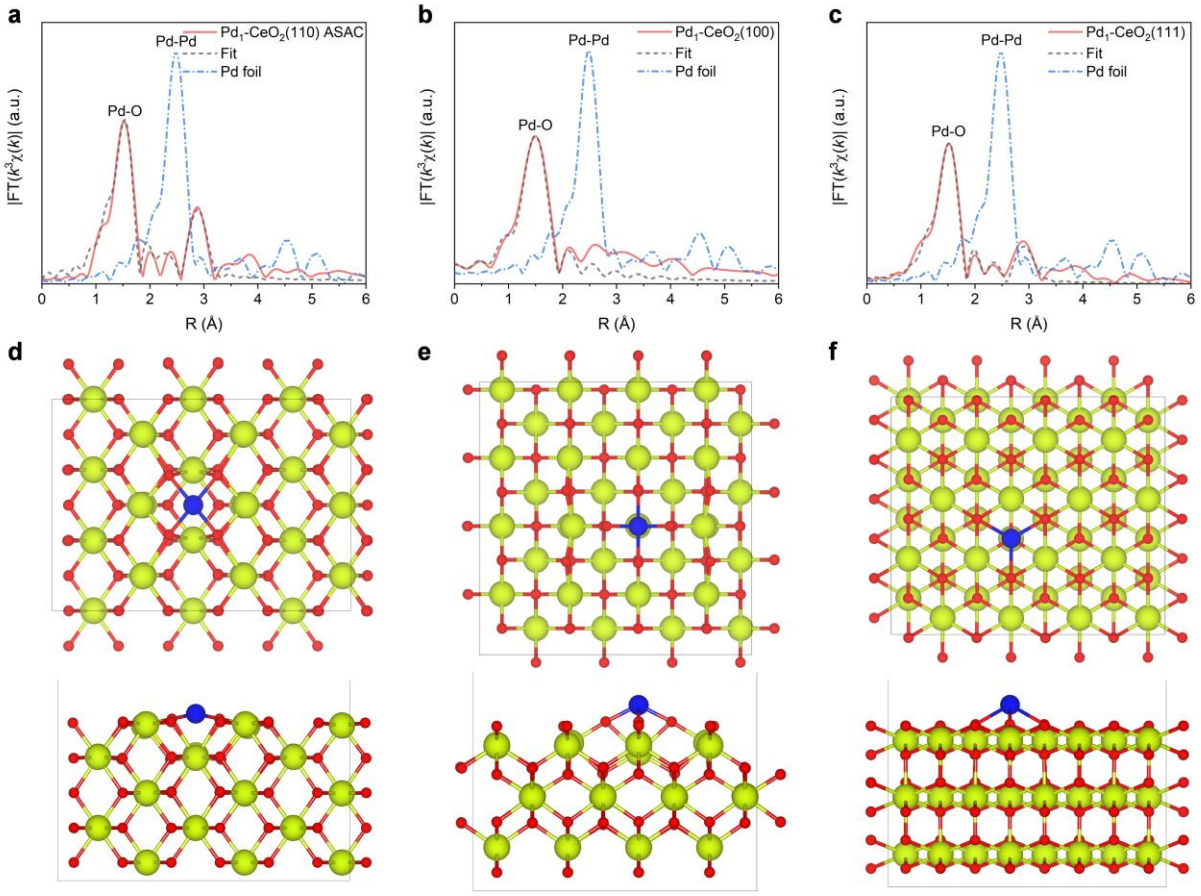

Supplementary Fig. 1 | The experimental and modelled structures of Pd single atoms on facet-dependent CeO_2. Fourier-transformed EXAFS spectra of Pd_1-CeO_2(110) ASAC (**a**), Pd_1-CeO_2(100) (**b**), and Pd_1- CeO_2(111) (**c**). Top views and side views of Pd SACs on CeO_2 with different crystal planes: Pd_1-CeO_2(110) ASAC (**d**), Pd_1-CeO_2(100) (**e**), Pd_1-CeO_2(111) (**f**). The red, yellow, and blue spheres represent oxygen, cerium, and palladium, respectively.

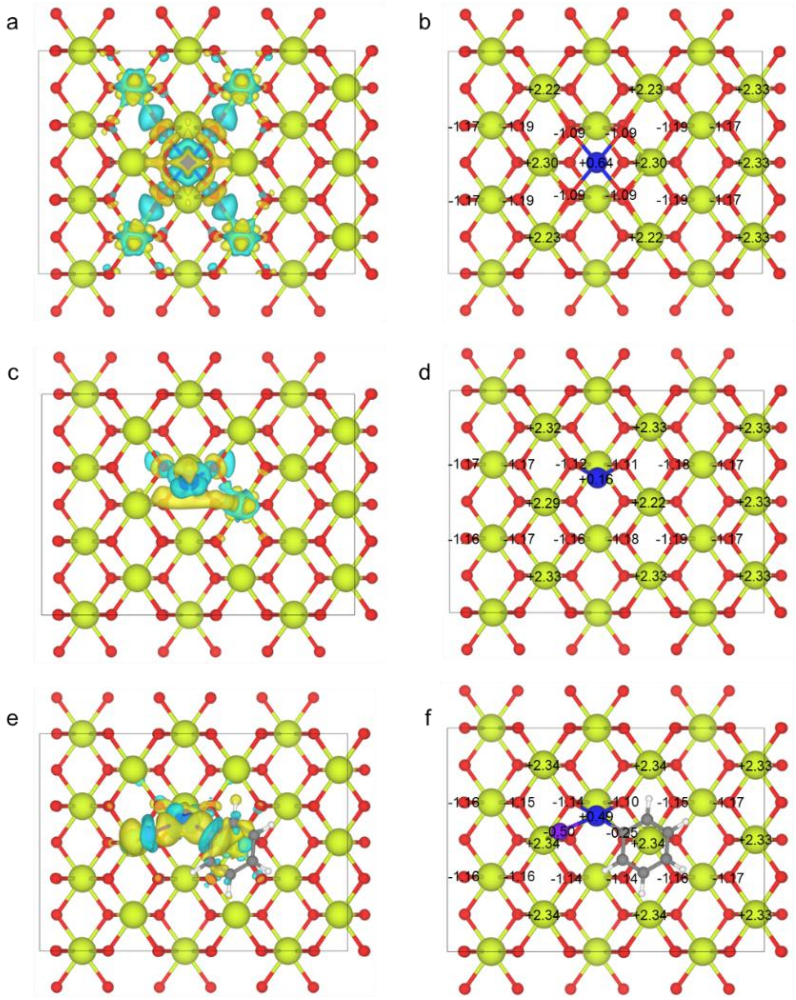

Supplementary Fig. 2 | Charge density differences of Pd_1 ASACs catalyst. The white, grey, purple, red, yellow, and blue spheres represent hydrogen, carbon, bromine, oxygen, cerium, and palladium atoms, respectively.

The Pd in the initially four-coordinated Pd_1 ASACs catalyst is in a high-valence oxidized state, with electrons predominantly transferred to the Ce and O atoms in the Pd-O-Ce linkage (**Supplementary Fig. 2a, b**). During the reaction, the Pd-O bond is cleaved, forming a bicoordinated structure, and the Pd valence state is reduced from +0.64 to +0.16 as electrons transfer back from the Ce and O atoms to the Pd atom (**Supplementary Fig. 2c, d**). Following oxidative addition, the dissociation of bromobenzene results in the bromide ion and phenyl ring gaining 0.5 and 0.25 electrons, respectively, leading to Pd oxidation from +0.16 to +0.49. Concurrently, additional electrons are transferred from the Ce-O-Pd linkage to the Pd atom (**Supplementary Fig. 2e, f**). Thus, the continuous electron transfer between the Pd atom and the O and Ce atoms in the Pd-O-Ce bond ensures the stabilization of the Pd valence state throughout the reaction.

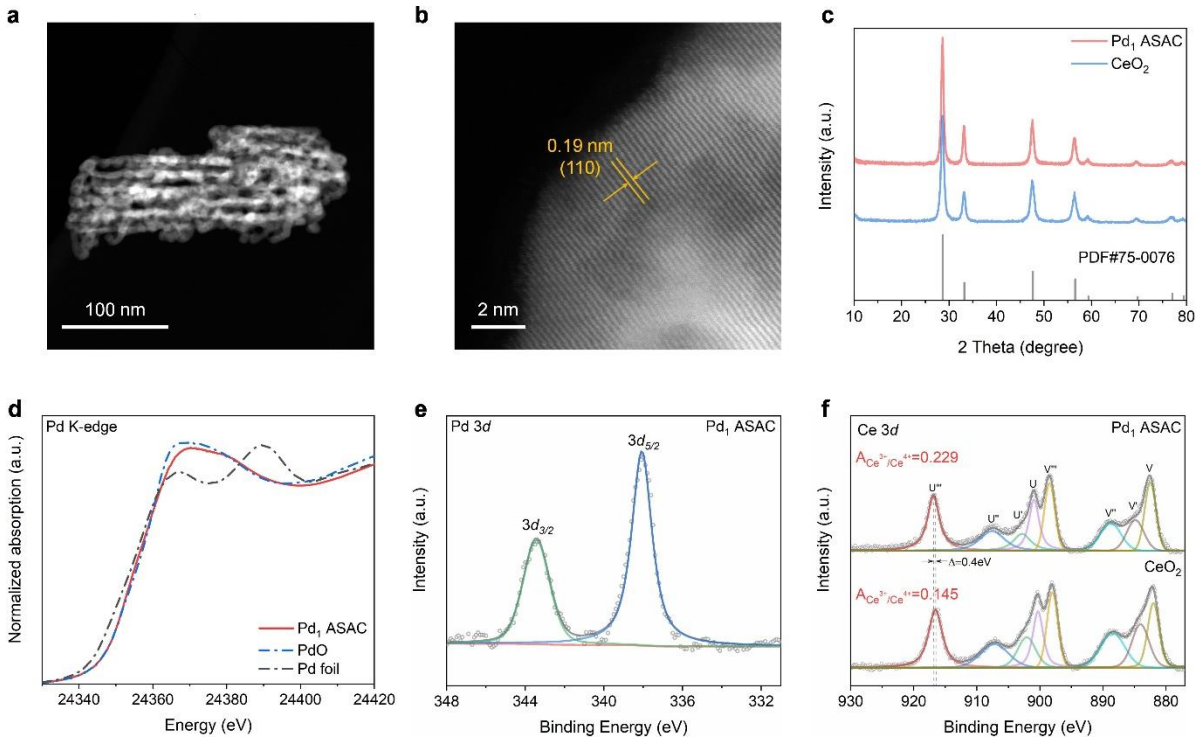

Supplementary Fig. 3 | Characterization of Pd_1 ASAC. a, TEM image of Pd_1 ASAC. **b,** Atomic-resolution ADF-STEM image of Pd_1 ASAC. **c,** XRD patterns of Pd_1 ASAC. **d,** Pd K-edge XANES spectra of Pd_1 ASAC and references (Pd foil and PdO). **e,** Pd 3*d* XPS spectra of Pd_1 ASAC. **f,** Ce 3*d* XPS spectra of Pd_1 ASAC and CeO_2. The peaks V' and U' correspond to the signals of Ce^{3+}species, and the others are assigned to the Ce^{4+} species.

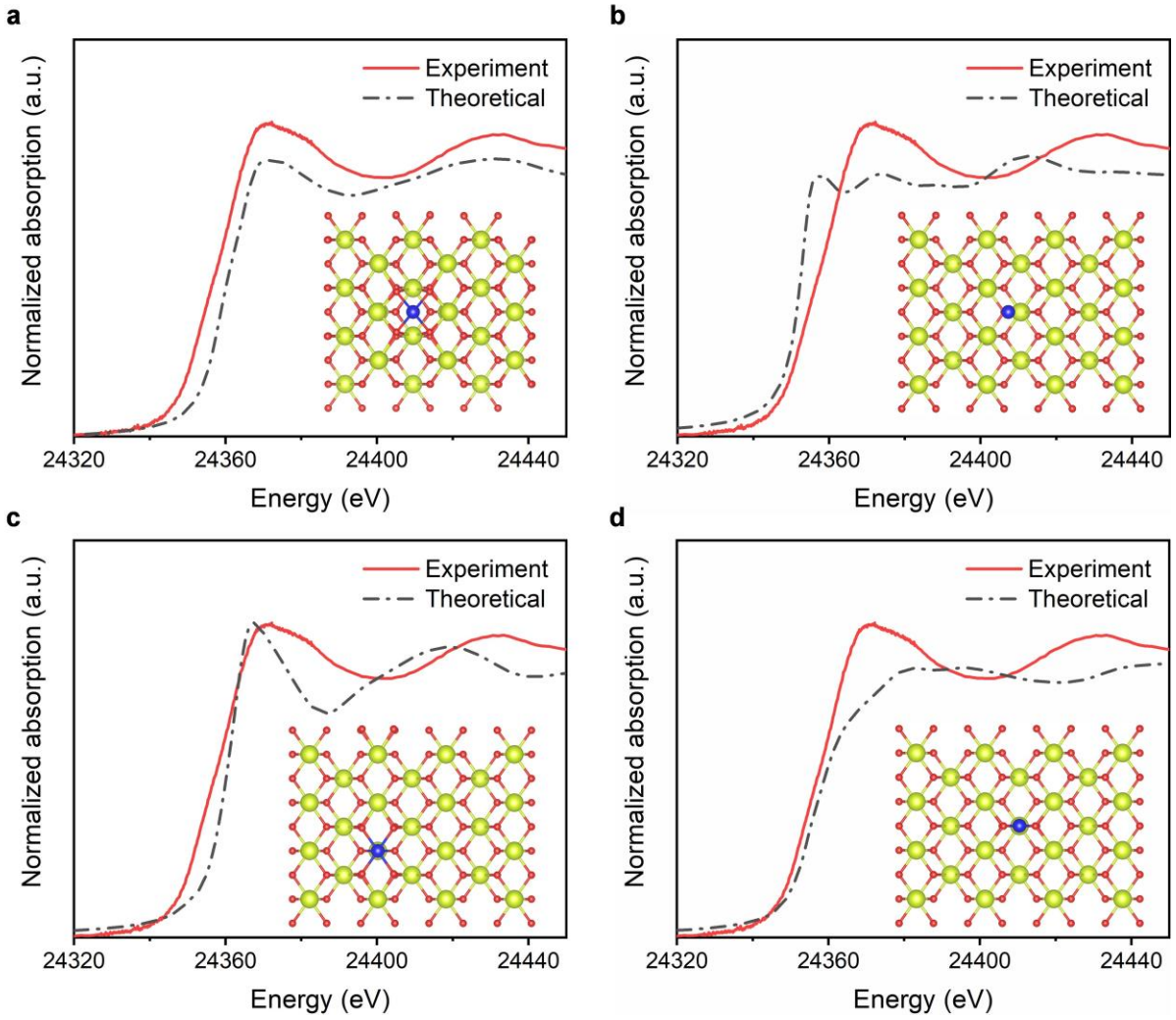

Supplementary Fig. 4 | Comparison of the experimental and modelled Pd K-edge XANES spectra. **a,** Pd single-atom is anchored on the CeO_2(110) facet in a 4-coordinated manner with the surface oxygen atoms. **b,** Pd single-atom is anchored on the oxygen vacancy on the CeO_2(110) facet. **c,** Pd single-atom is anchored on the Ce vacancy on the CeO_2(110) facet. **d,** Pd single-atom is anchored on the CeO_2(110) facet in a 2-coordinated manner with the surface oxygen atoms. The corresponding DFT-modelled atomic structures are shown in the insets. The red, yellow, and blue spheres represent oxygen, cerium, and palladium, respectively.

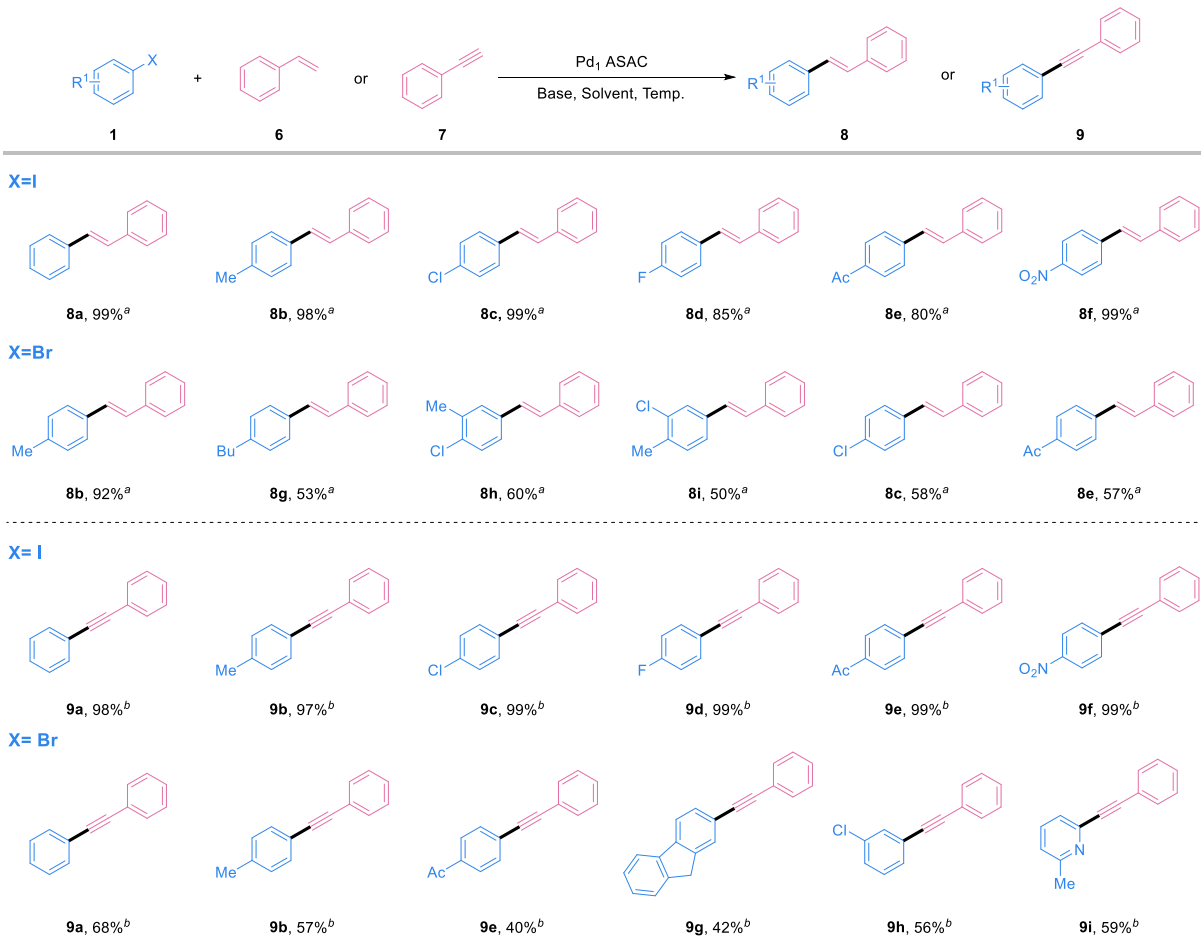

Supplementary Fig. 5 | Substrate scope of Pd_1 ASAC catalyzed Heck and Sonogashira cross-coupling reactions.

Conditions: a: **1** (0.5 mmol), **6** (1 mmol), Pd_1 ASAC (5 mg, 0.35 mol%), K_2CO_3 (1.5 mmol), EtOH/H_2O (2 mL: 2 mL), 100 °C, 10 h, isolated yield. b: **1** (0.5 mmol), **7** (0.75 mmol), Pd_1 ASAC (5 mg, 0.35 mol%), K_2CO_3 (3 mmol), EtOH/H_2O (3.5 mL: 0.5 mL), 100 °C, 10 h, isolated yield.

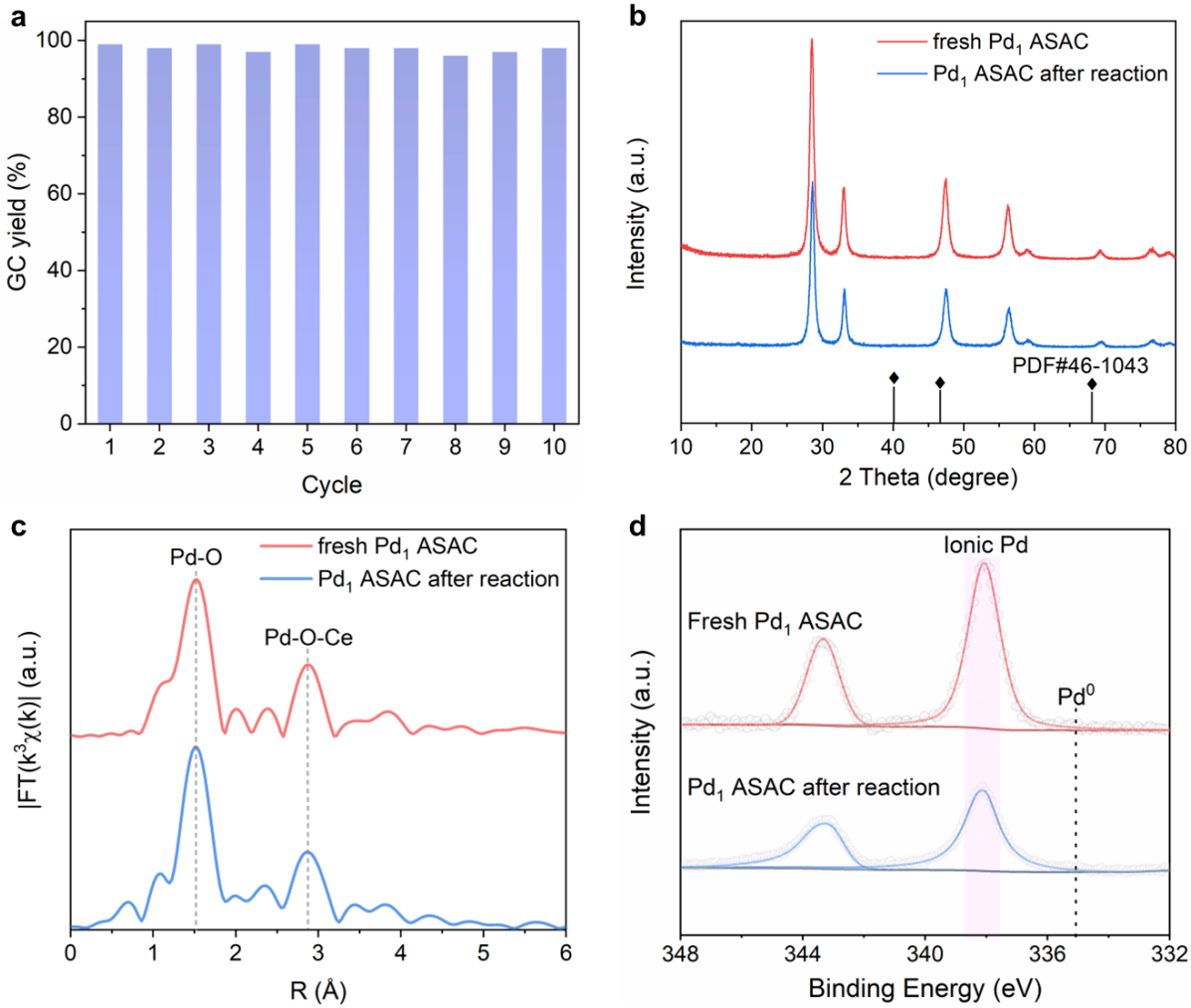

Supplementary Fig. 6 | Stability of Pd_1 ASAC in Suzuki cross-coupling. a, Cycling test for the Suzuki cross-coupling reaction using 4-bromotoluene and phenylboronic acid over Pd_1 ASAC. **b,** XRD patterns, **c,** Fourier transformed EXAFS spectra and **d,** XPS spectra of the fresh Pd_1 ASAC and the Pd_1 ASAC recovered after 10 reaction cycles.

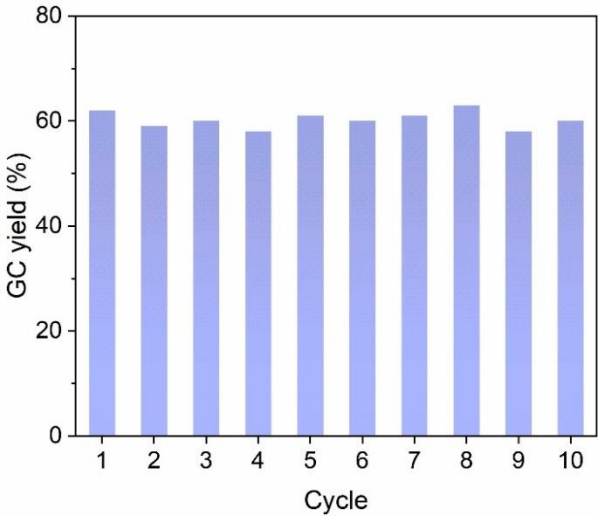

Supplementary Fig. 7 | Cycling test for the Suzuki cross-coupling reaction using 4-bromotoluene and phenylboronic acid over Pd1 ASAC under low-conversion conditions.

Reaction conditions: 4-Bromotoluene (5 mmol), phenylboronic acid (6 mmol), K_2CO_3 (15 mmol), catalyst, EtOH/H_2O (20 mL/20 mL) were sequentially added to the round-bottomed flask. The flask was heated and stirred in a 100 °C oil bath for 10 min. The products were extracted with DCM, and the yield was calculated by GC analysis. The catalyst was isolated by centrifugation, washed with EtOH/H_2O, and dried at 80 °C overnight for the next cycle. To avoid the decrease in efficiency caused by the loss of catalyst during operation, it is necessary to keep the dosage ratio of catalyst, substrate, solvent, and base constant in each cycle.

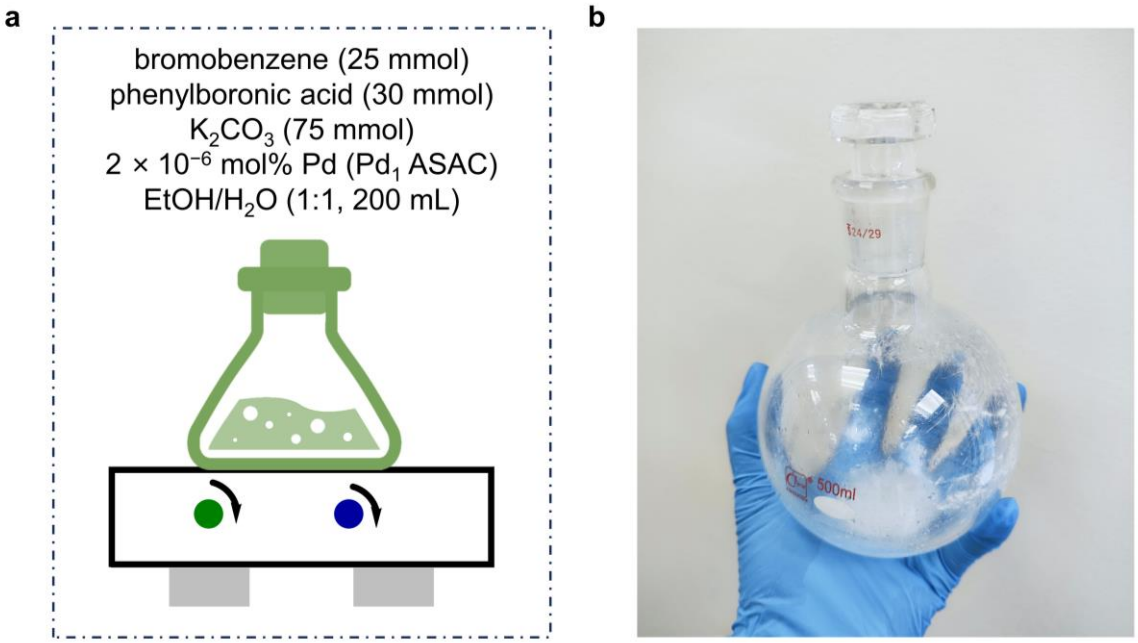

Supplementary Fig. 8 | Turnover number (TON) of Pd_1 ASAC in cross-coupling. **a,** Specific conditions of the TON test experiment. **b,** Photograph of the experimental product biphenyl. *TON = mole of converted aryl halides/mole of Pd catalyst*

Experimental procedure is shown in Supplementary Fig. 8a : Bromobenzene (25 mmol), phenylboronic acid (30 mmol), K_2CO_3 (75 mmol), Pd_1 ASAC (2×10^{-6} mol%, according to Pd), ethanol (100 mL), and H_2O (100 mL) were sequentially added to the flask. The flask was placed in an oil bath preheated to 80 °C, and stirring in an ambient atmosphere, yielding biphenyl (Supplementary Fig. 8b) in approximately 90% yield.

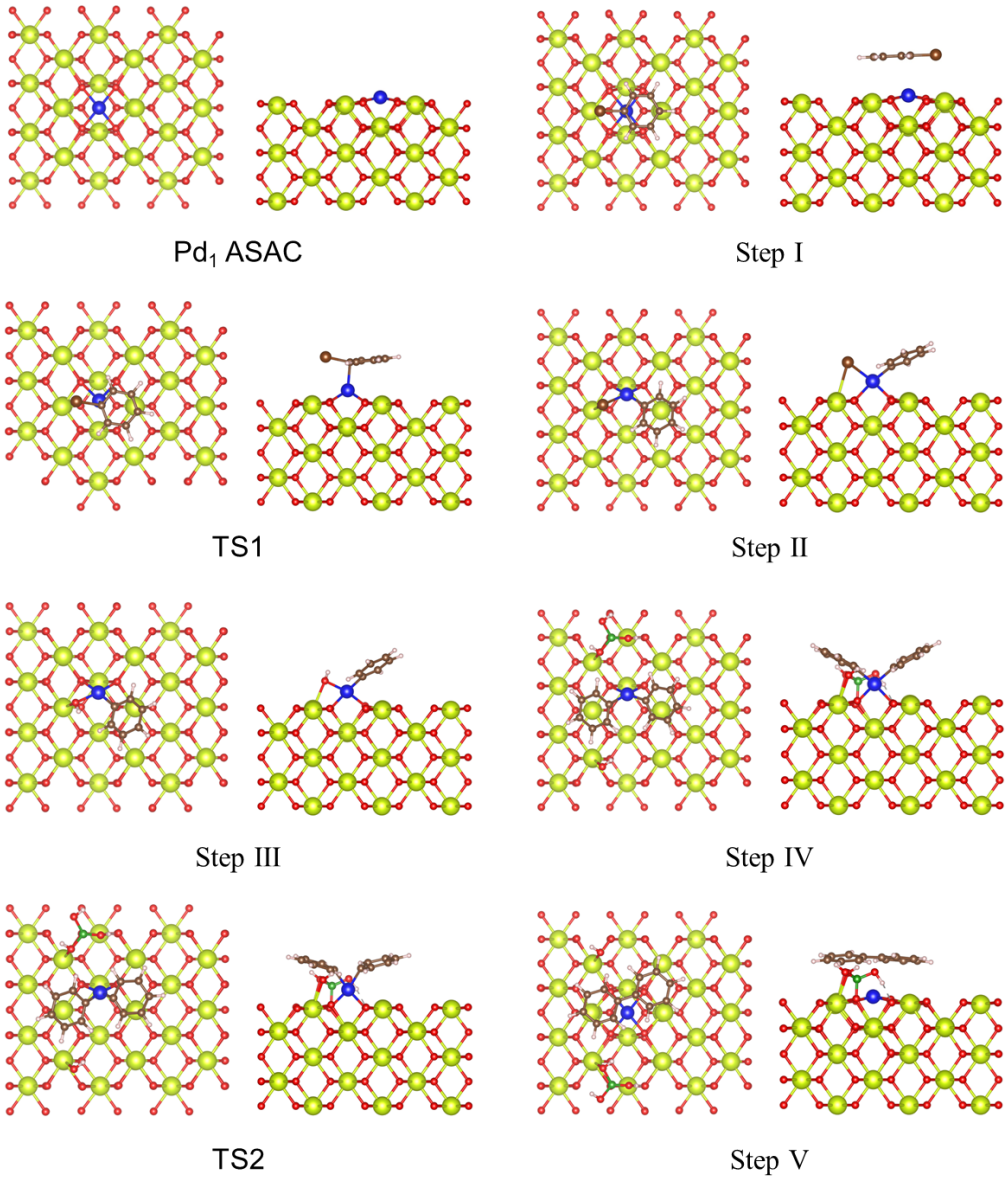

Supplementary Fig. 9 | Atomic structure of Pd_1 ASAC calculated by DFT. Top and side views of the optimized structure of Pd_1 ASAC model in all reaction steps.

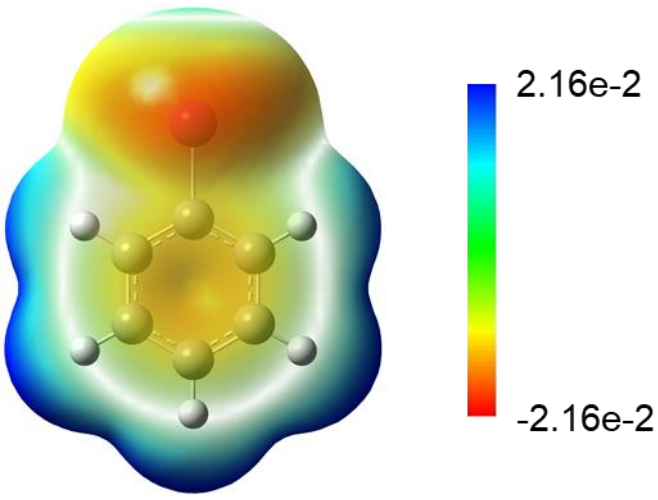

Supplementary Fig. 10 | Electrostatic potential diagram of bromobenzene.

According to the electrostatic potential diagram of bromobenzene, it can be seen that the charges of the molecule tend to gather around the Br atom. As a result, the Br ion after bromobenzene dissociation is adsorbed on the electrophilic Ce site, and the phenyl group is adsorbed on the nucleophilic Pd site.

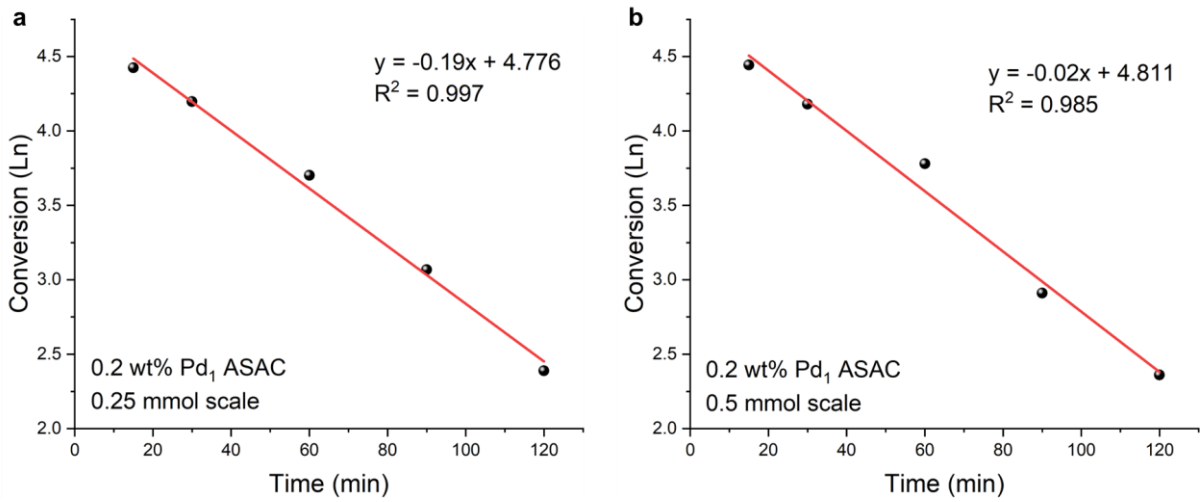

Supplementary Fig. 11 | Kinetic studies of Pd_1 ASAC catalysed Suzuki cross-coupling. The plots of the natural logarithm of the concentration of aryl halide versus time: initial concentration of bromobenzene C_0 = 0.25 M (**a**), C_0 = 0.5 M (**b**). All reactions were conducted with 0.1 mol% Pd.

Experimental procedure: In a capped reaction tube, sequentially add 0.25 mmol (C_0 = 0.25 M) or 0.5 mmol (C_0 = 0.5 M) of bromobenzene, 0.6 mmol of phenylboronic acid, 1.5 mmol of K_2CO_3, Pd_1 ASAC (0.1 mol% Pd, according to Pd), 2 mL of ethanol, 2 mL of H_2O, and 0.5 mmol of decane (as an internal standard for GC analysis). Place the reaction tube in an oil bath at 25 °C and stir under ambient atmosphere for the desired time (10-120 min). After the reaction, remove the cap and transfer a portion of the solution into a vial. Extract with DCM and analyze the conversion of reactants via gas chromatography. Under optimized reaction conditions, the natural logarithm of the bromobenzene concentration versus time plot is linear, indicating a first-order reaction with respect to the aryl halide. This suggests that the aryl halide is involved in the rate-determining step, consistent with DFT studies.

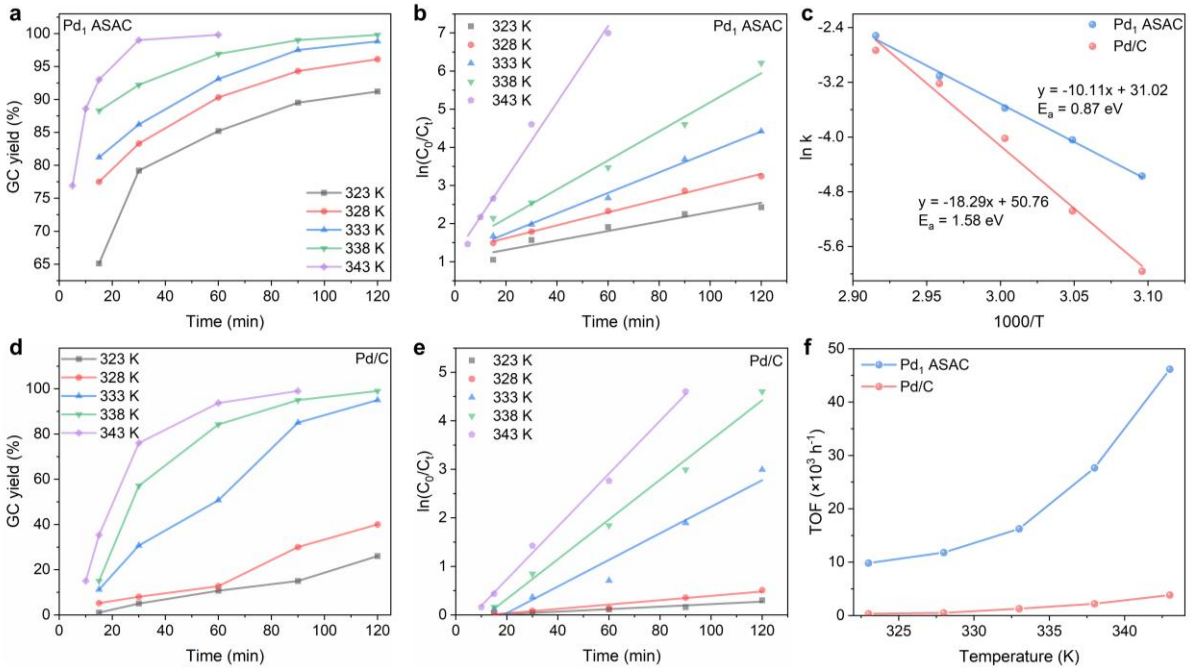

136 **Supplementary Fig. 12 |** Catalytic performance for the Suzuki reaction of bromobenzene and
137 phenylboronic acid. Time-dependent yield of biphenyl over Pd_1 ASAC (**a**) and Pd/C (**d**). The
138 corresponding ln(C_0/C_t)-time curves for Suzuki coupling reactions over Pd_1 ASAC (**b**) and Pd/C (**e**). **c,**
139 Arrhenius plots of the reaction over Pd_1 ASAC and commercial Pd/C. **f,** A TOF comparison of Pd_1
140 ASAC and commercial Pd/C.

141 To further study the reaction kinetics of Pd_1 ASAC, we investigated the coupling reaction of
142 bromobenzene and phenylboronic acid at different temperatures (323, 328, 333, 338, and 343 K)
143 (Supplementary Fig. 12a) and compared them with commercial Pd/C (Supplementary Fig. 12d). The
144 relationship between ln (C_0/C_t) and time is consistent with first-order reaction kinetics (Supplementary
145 Fig. 12b and e). The rate constant (k) of the reaction can be calculated from the slope of the ln (C_0/C_t)-
146 time curve, and then the apparent activation energy can be calculated by plotting ln k as a function of
147 1000/T in an Arrhenius plot (Supplementary Fig. 12c). The results demonstrate that the activation
148 energy of Pd_1 ASAC-catalyzed reaction is much lower than that of commercial Pd/C. Notably, Pd_1
149 ASAC is able to exhibit a significant turnover frequency (TOF) of 46,149 h^{-1} at 343 K (Supplementary
150 Fig. 12f), outperforming all listed catalysts by about an order of magnitude or more in the Suzuki cross-
151 coupling reactions (Supplementary Table 3).

152

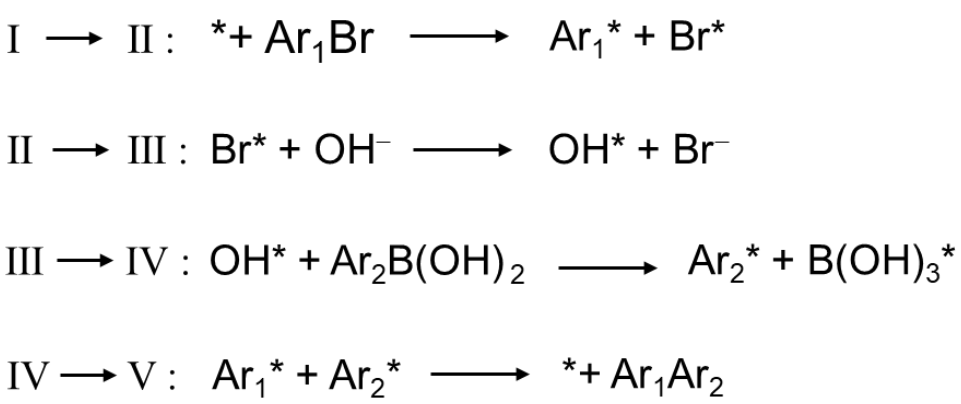

153

154 **Supplementary Fig. 13 |** The chemical reaction equation of the entire reaction process.

155

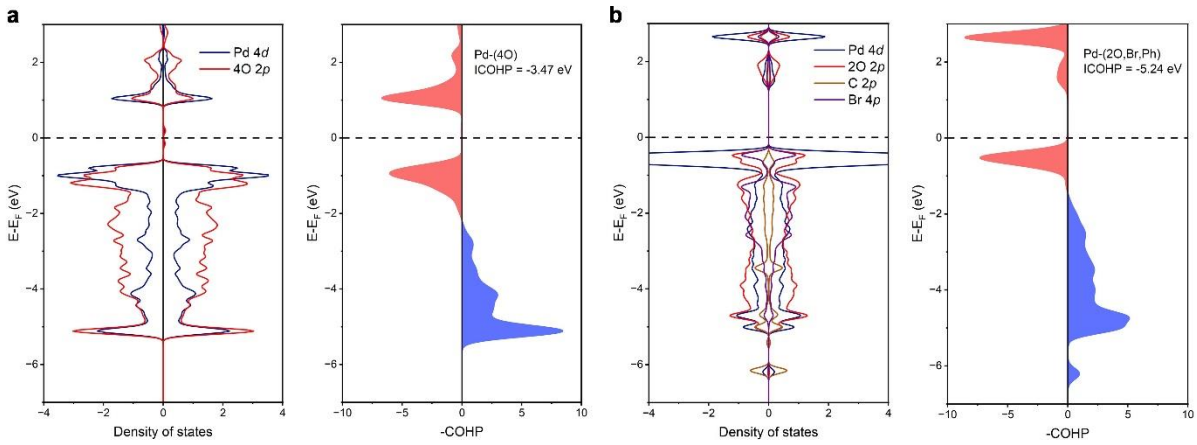

Supplementary Fig. 14 | Electronic structure of Pd_1 ASAC with different coordination configurations. a, DOS and ICOHP of the initial Pd-(4O) coordination structure. **b,** DOS and ICOHP of the Pd-(2O, Br, Ph) coordination structure after oxidative addition. The square-planar coordinated Pd-O bonds have obvious occupation of the antibonding orbital near E_F, while the occupation of the antibonding orbital near E_F is significantly weakened in the new tetra-coordinated structure formed by the dissociation of bromobenzene. The calculated ICOHP also confirms that Pd center has stronger bond interaction after bromobenzene dissociation (−5.24 eV *vs.* −3.47 eV), which is believed to be the driving force for the opening of Pd-O bonds.

The Pd *d*-orbital center of the four-coordinated PdO_4 motif lies further below E_F and once two Pd-O bonds are opened to form new four-coordinated structures, the Pd *d*-orbital centers shift significantly closer to E_F. Therefore, the Pd-adsorbate interactions are enhanced and show better catalytic activity. As a result, the Pd_1 ASAC can adaptively regulate the Pd electronic structure to facilitate catalysis through dynamic coordination configuration tuning during the reaction. The 5*d*-orbitals of adjacent Ce revealed a slight decrease in the integrated occupied state below E_F and a gradual increase in empty states, with these empty states shifting toward E_F. All these observations indicate the accumulation of positive charge over Ce as the reaction proceeds.

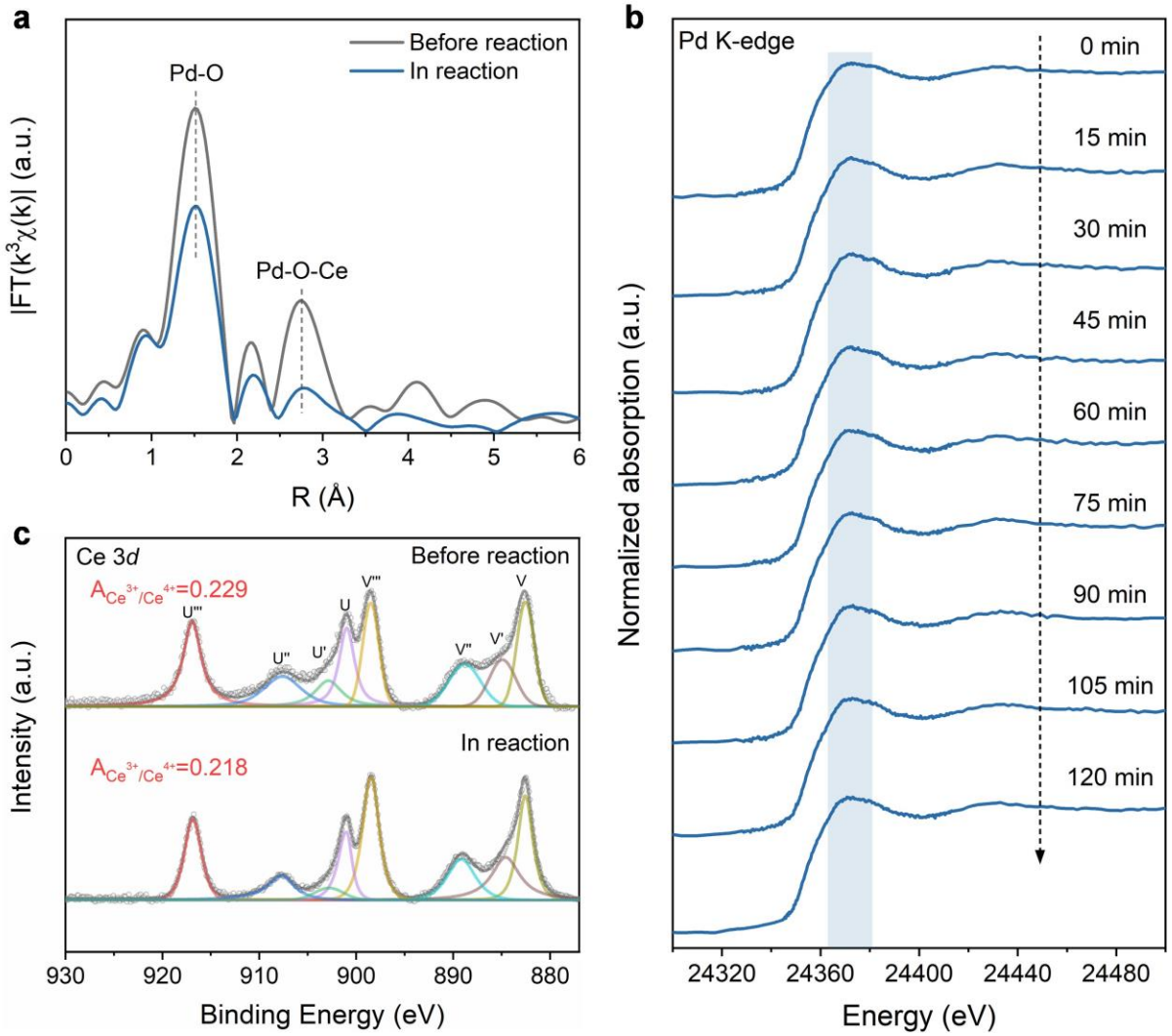

175

176 **Supplementary Fig. 15 | Operando XANES and ex situ XPS spectra during Suzuki cross-**
177 **coupling reaction. a**, Fourier-transformed EXAFS spectra of Pd_1 ASAC collected before and during
178 the Suzuki cross-coupling reaction. **b**, Operando Pd K-edge XANES of Pd_1 ASAC recorded at
179 different times in the Suzuki cross-coupling reaction. **c**, Ex situ XPS spectra of Pd_1 ASAC measured
180 before and in the Suzuki cross-coupling reaction. The peaks V' and U' correspond to the signals of
181 Ce^{3+}species, and the others are assigned to the Ce^{4+} species.

182 The changes in the chemical state of Pd_1 ASAC during the Suzuki cross-coupling reaction can be
183 observed from the in situ Pd K-edge XANES. Throughout the reaction, there are no significant peak
184 shifts or intensity changes, indicating that the valence state of Pd does not undergo substantial changes.
185 In the Fourier-transformed EXAFS spectra, the intensity of the main peaks associated with the first
186 coordination shell path Pd-O and the second coordination shell path Pd-O-Ce decreases, indicating a

reduction in the coordination number of Pd-O. This demonstrates that during the reaction, Pd_1 ASAC transfers from the initial Pd-O_4 planar four-coordination structure through the opening of two Pd-O bonds, with the Pd atom being pulled up and bonded by dissociated phenyl and bromide ions, forming a new four-coordinated configuration, consistent with DFT calculations. Ex situ XPS results showed a slight increase in Ce^{3+}/Ce^{4+} ratio during the reaction, which may be due to the transfer of electrons from Ce atoms to Pd atoms in ASAC during the oxidative addition process, thus ensuring that the valence state of Pd remains constant.

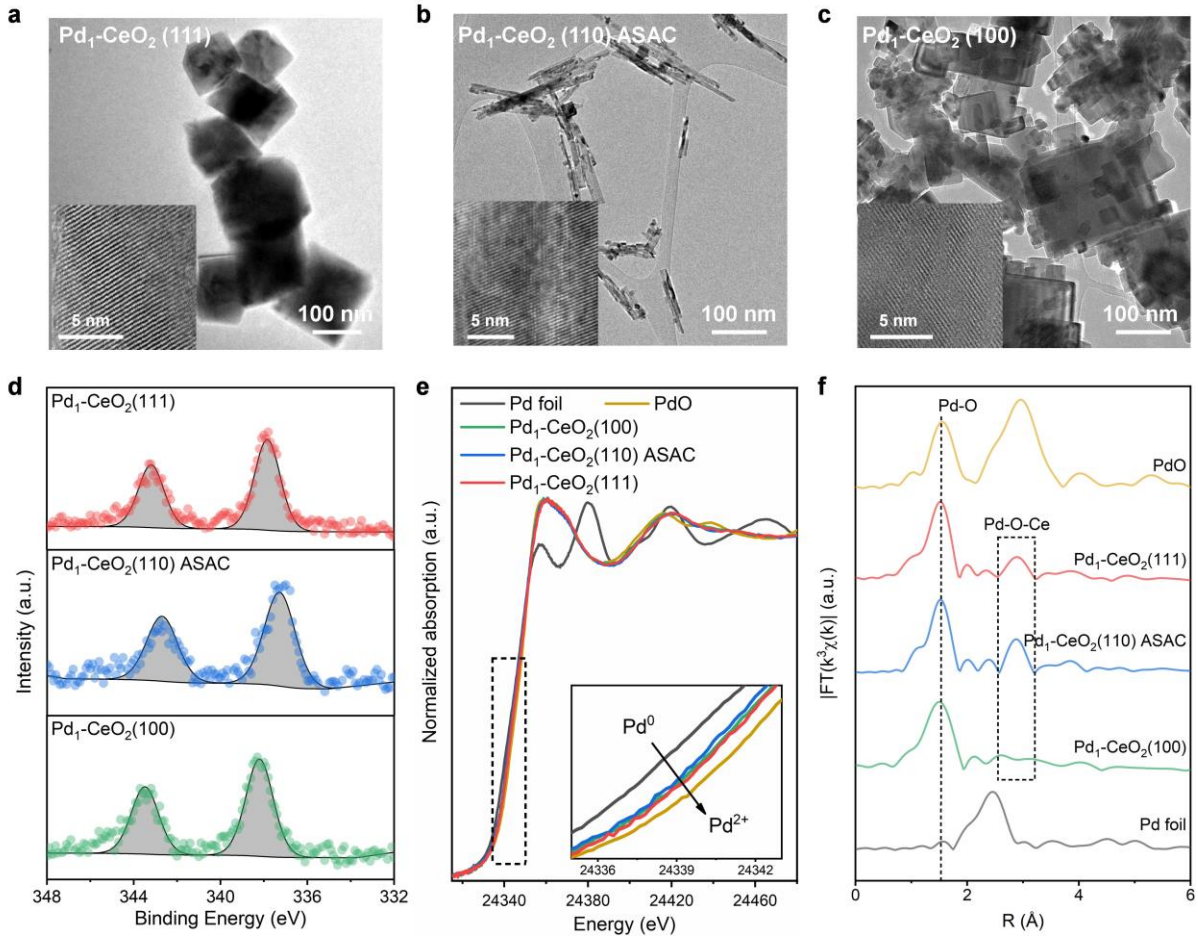

Supplementary Fig. 16 | characterizations of Pd_1 anchored on facet-dependent CeO_2. TEM images of Pd_1-CeO_2(111) (**a**), Pd_1-CeO_2(110) ASAC (**b**), Pd_1-CeO_2(100) (**c**), inserts are their HRTEM images respectively. **d,** Pd 3*d* XPS spectra, **e,** Pd K-edge XANES spectra, **f,** Pd K-edge Fourier transformed EXAFS spectra of Pd single atoms on facet-dependent CeO_2.

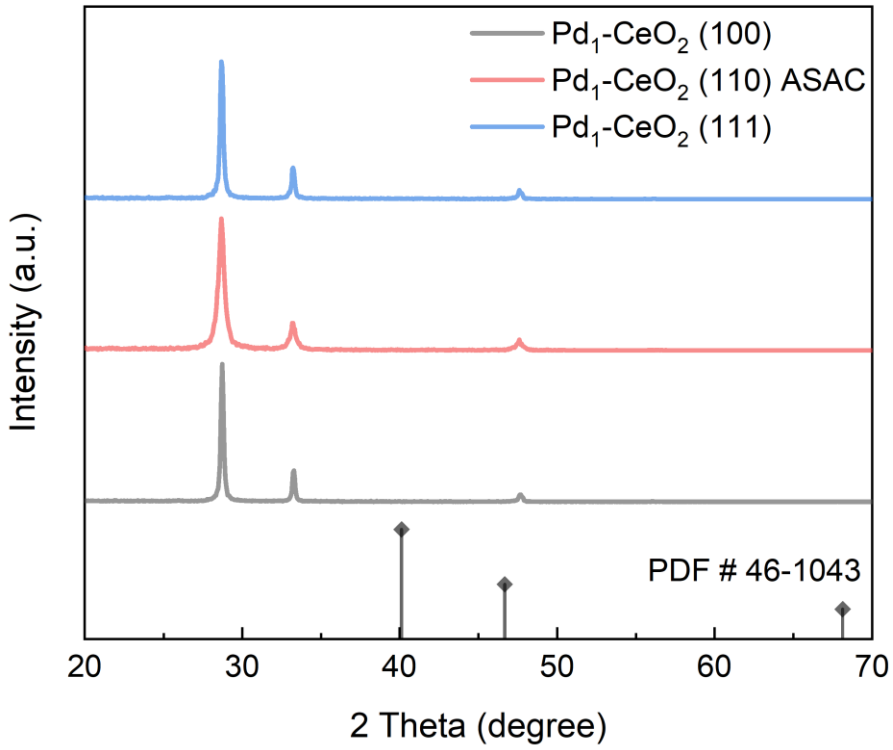

Supplementary Fig. 17 | XRD patterns of Pd_1-CeO_2(100), Pd_1-CeO_2(110) ASAC, and Pd_1-CeO_2(111).

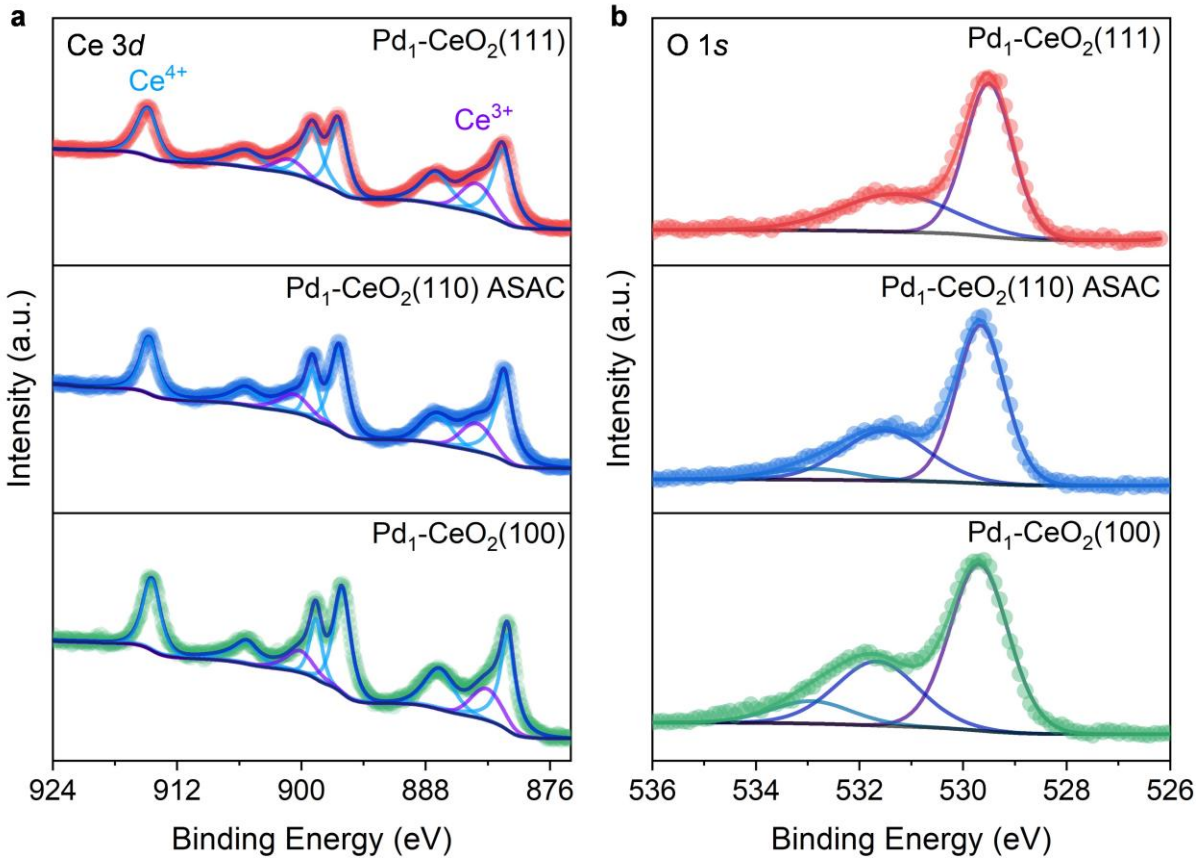

206

207 **Supplementary Fig. 18 |** Characterization of catalysts. **a,** Ce 3*d* XPS spectra, **b,** O 1*s* XPS spectra of

208 Pd single atoms on facet-dependent CeO_2.

209

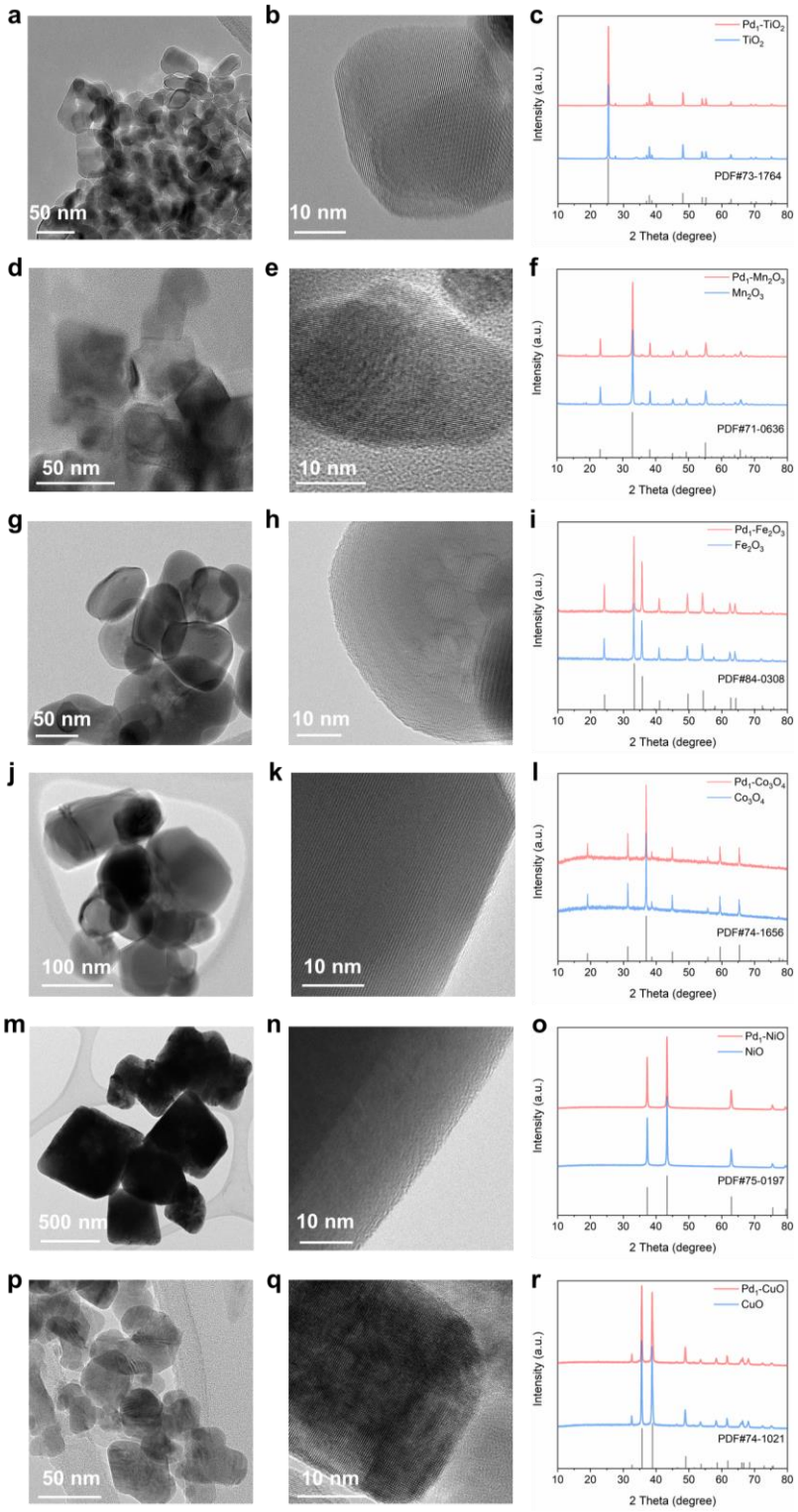

Supplementary Fig. 19 | Characterization of catalysts. Low-magnification TEM images of Pd_1-TiO_2 (**a**), Pd_1-Mn_2O_3 (**d**), Pd_1-Fe_2O_3 (**g**), Pd_1-Co_3O_4 (**j**), Pd_1-NiO (**m**), and Pd_1- CuO (**p**). High-resolution TEM images of Pd_1-TiO_2 (**b**), Pd_1-Mn_2O_3 (**e**), Pd_1-Fe_2O_3 (**h**), Pd_1-Co_3O_4 (**k**), Pd_1-NiO (**n**), and Pd_1- CuO (**q**). XRD patterns of Pd_1-TiO_2 (**c**), Pd_1-Mn_2O_3 (**f**), Pd_1-Fe_2O_3 (**i**), Pd_1-Co_3O_4 (**l**), Pd_1-NiO (**o**), and Pd_1-CuO (**r**).

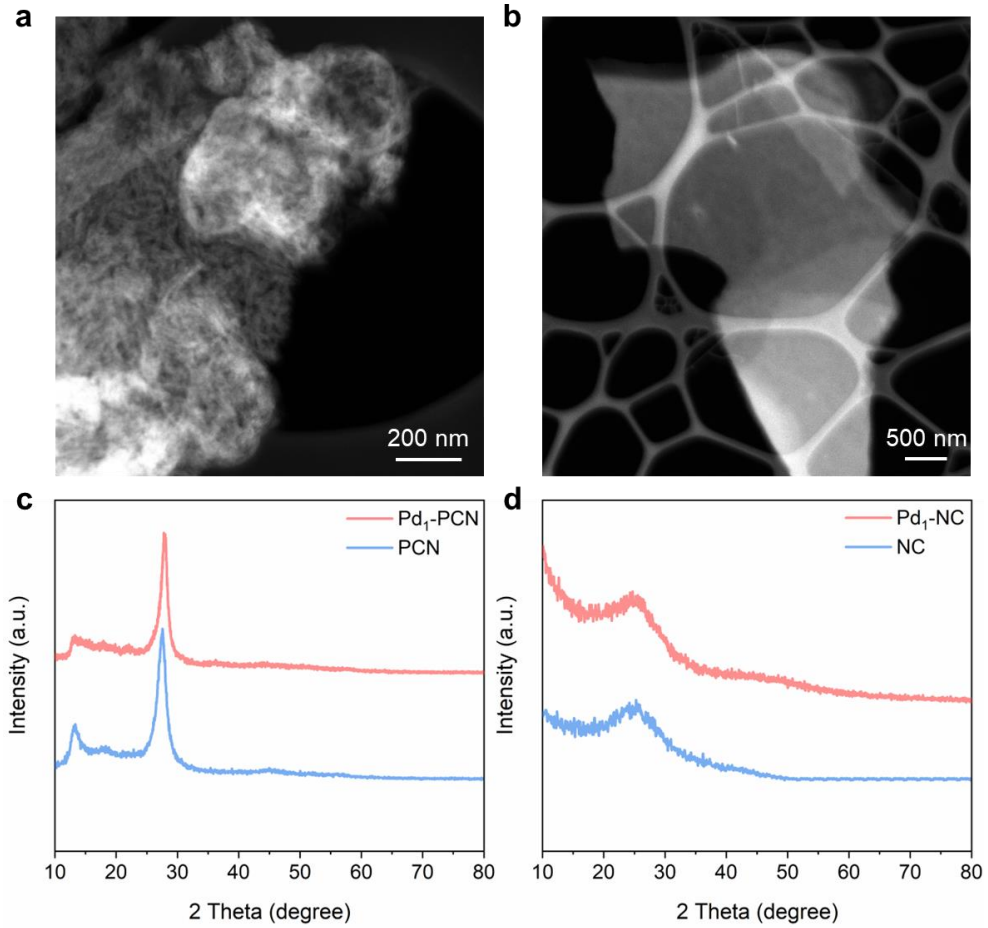

Supplementary Fig. 20 | Characterization of catalysts. TEM images of Pd_1-PCN (**a**), Pd_1-NC (**b**). XRD patterns of Pd_1-PCN (**c**), Pd_1-NC (**d**).

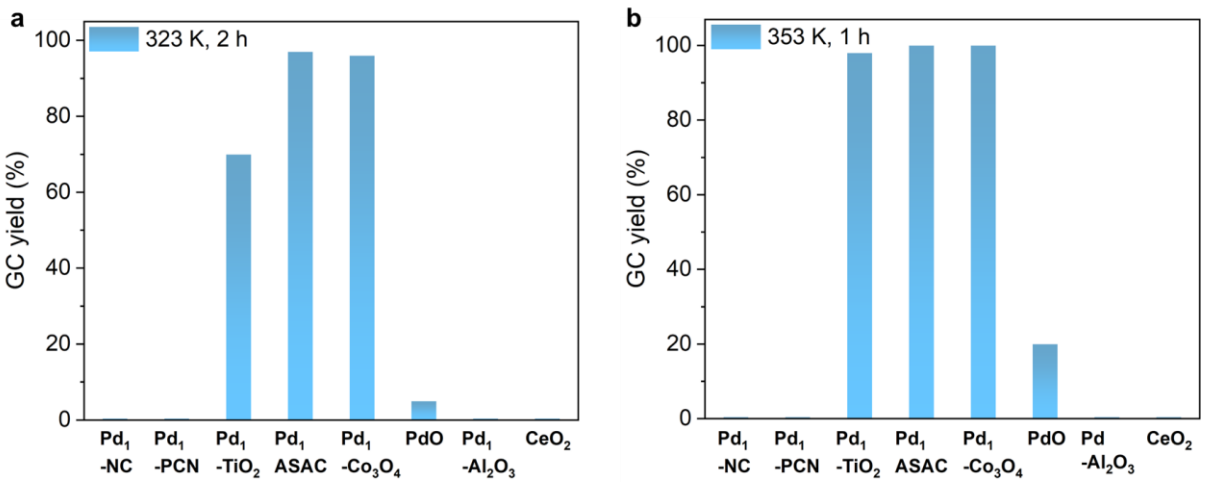

219 **Supplementary Fig. 21 |** Yield of biphenyl for reactions at 323 K (**a**) and 353 K (**b**).

220

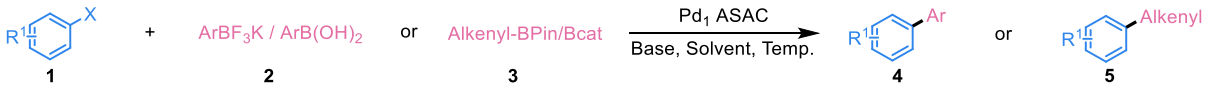

Supplementary Fig. 22 | The schematic illustration of Suzuki cross-coupling reactions.

General procedures: Compounds **1**, **2**, or **3**, Pd_1 ASAC, and the base were dissolved in the specified solvent. The reaction mixture was stirred at the designated temperature for the required duration. After completion, the solvent was evaporated under reduced pressure, and the residue was re-dissolved in a mixture of ethyl acetate and water. The organic phase was separated and dried over anhydrous sodium sulfate. The solvent was again evaporated under reduced pressure, yielding the crude product mixture. Further purification by silica gel column chromatography afforded compound **4** or **5**.

Diffierent conditions for diverse substrates, refer to Fig. 3: Conditions: a: **1** (0.5 mmol), **2** ($ArB(OH)_2$, 0.6 mmol), Pd_1 ASAC (5 mg, 0.35 mol%), K_2CO_3 (1.5 mmol), $EtOH/H_2O$ (2 mL: 2 mL), 80 °C, 10 h. b: **1** (0.5 mmol), **2** ($ArB(OH)_2$, 0.6 mmol), Pd_1 ASAC (5 mg, 0.35 mol%), K_2CO_3 (1.5 mmol), $EtOH/H_2O$ (2 mL: 2 mL), 100 °C, 20 h. c: **1** (0.5 mmol), **2** ($ArB(OH)_2$,0.6 mmol), Pd_1 ASAC (5 mg, 0.35 mol%), K_2CO_3 (1.5 mmol), THF/H_2O (2 mL: 2 mL), 100 °C, 24 h. d: **1** (0.2 mmol), **2** ($ArBF_3K$, 0.3 mmol), $KHCO_3$ (0.6 mmol), Pd_1 ASAC (10.5 mg, 0.35 mol%), $EtOH/H_2O$ (1.5 mL: 0.5 mL), 100 °C, 24 h. e: **1** (0.5 mmol), **2** ($ArB(OH)_2$, 1.2 mmol), Pd_1 ASAC (5 mg, 0.35 mol%), K_2CO_3 (3 mmol), $EtOH/H_2O$ (2 mL: 2 mL), 80 °C, 10 h, isolated yield. f: **1** (0.2 mmol), **3** (0.24 mmol), K_3PO_4 (0.6 mmol), Pd_1 ASAC (10.5 mg, 0.35 mol%), $EtOH/H_2O$ (1.6 mL: 0.4 mL), 80 °C, 24 h. g: **1** (0.2 mmol), **3** (0.24 mmol), K_3PO_4 (0.6 mmol), Pd_1 ASAC (10.5 mg, 0.35 mol%), $EtOH/H_2O$ (1.6 mL: 0.4 mL), 80 °C, 63 h, isolated yield.

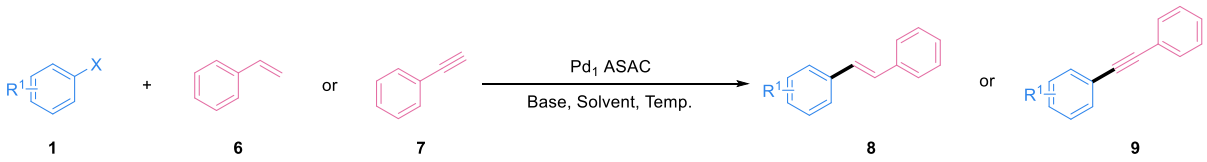

240 **1** **6** **7** **8** **9**

241 **Supplementary Fig. 23 |** The schematic illustration of the Heck and Sonogashira cross-coupling
242 reactions.

243 General procedures: Compounds **1**, **6**, or **7**, Pd_1 ASAC, and the base were dissolved in the specified
244 solvent. The reaction mixture was stirred at the designated temperature for the required duration. After
245 completion, the solvent was evaporated under reduced pressure, and the residue was re-dissolved in a
246 mixture of ethyl acetate and water. The organic phase was separated and dried over anhydrous sodium
247 sulfate. The solvent was again evaporated under reduced pressure, yielding the crude product mixture.
248 Further purification by silica gel column chromatography afforded compound **8** or **9**.

249 Diffierent conditions for diverse substrates: a: **1** (0.5 mmol), **6** (1 mmol), Pd_1 ASAC (5.3 mg, 0.07
250 mol%), K_2CO_3 (1.5 mmol), EtOH/H_2O (2 mL: 2 mL), 100 °C, 10 h, isolated yield. b: **1** (0.5 mmol), **7**
251 (0.75 mmol), Pd_1 ASAC (5.3 mg, 0.07 mol%), K_2CO_3 (3 mmol), EtOH/H_2O (3.5 mL: 0.5 mL), 100 °C,
252 10 h, isolated yield.

253

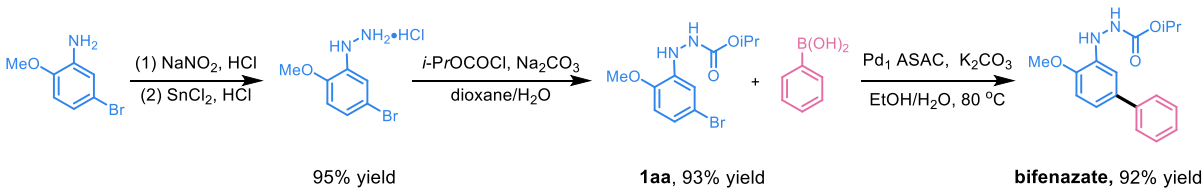

95% yield **1aa**, 93% yield **bifenazate,** 92% yield

Supplementary Fig. 24 | Synthesis of bifenazate.

Procedure for the preparation of 5-Bromo-2-methoxyphenylhydrazine hydro-chloride: The reaction mixture was maintained at 0 °C during this procedure. 5-Bromo-2-methoxyaniline (2.00 g, 10.0 mmol) was added to vigorously stirred concentrated HCl (17 mL) and aged for 10 min. A solution of $NaNO_2$ (691 mg, 10.0 mmol) in distilled water (4 mL) was added dropwise over 10 min and the mixture was stirred for an additional 15 min. A solution of $SnCl_2 \cdot H_2O$ (498 mg, 22.0 mol) in concentrated HCl (5 mL) was added dropwise. The reaction mixture was stirred for 30 min and filtered. The product was dried in vacuo overnight to afford 5-bromo-2-methoxyphenylhydrazine hydrochloride as a brown solid (2.38 g, 95% yield).

Procedure for the preparation of compound **1aa**: A solution of 5-bromo-2-methoxyphenylhydrazine hydrochloride (2.00 g, 7.90 mmol) and triethylamine (2.28 mL, 16.6 mmol) in CH_2Cl_2 (16 mL) was cooled to 0 °C and a solution of isopropyl chloroformate (0.93 mL, 8.08 mmol) in CH_2Cl_2 (8 mL) was added dropwise at a rate that maintained a temperature below 0 °C. When the addition was complete, the reaction mixture was allowed to warm to room temperature. The reaction mixture was stirred for 3h and concentrated in vacuo. The residue was purified by flash column chromatography on silica gel (n-hexane/EtOAc, 2:1) to afford isopropyl 3-(5-bromo-2-methoxyphenyl)carbazate as a colorless solid (2.21 g, 93% yield).

Procedure for the preparation of bifenazate: In a 20-mL round-bottom flask with a stir bar, added isopropyl 3-(5-bromo-2-methoxyphenyl)carbazate (151 mg, 0.5 mmol), phenylboronic acid (92 mg, 0.75 mmol), K_2CO_3 (207 mg, 1.5 mmol), Pd_1 ASAC (5 mg, 0.35 mol%), H_2O (2 mL), and EtOH (2 mL) and the system was sealed with a septum. The mixture was stirred at 80 °C for 12 h. The mixture was diluted with H_2O (50 mL) and EtOAc (50 mL), and filtered through a Celite pad. The filtrate was separated into two layers and the aqueous layer was extracted with EtOAc (2 × 50 mL). The combined organic layers were washed with brine (50 mL), dried over Na_2SO_4, and concentrated in vacuo. The

residue was purified by flash column chromatography on silica gel (n-hexane/EtOAc, 50:1 to 5:1) to afford bifenazate as a yellow solid (138 mg, 92% yield).

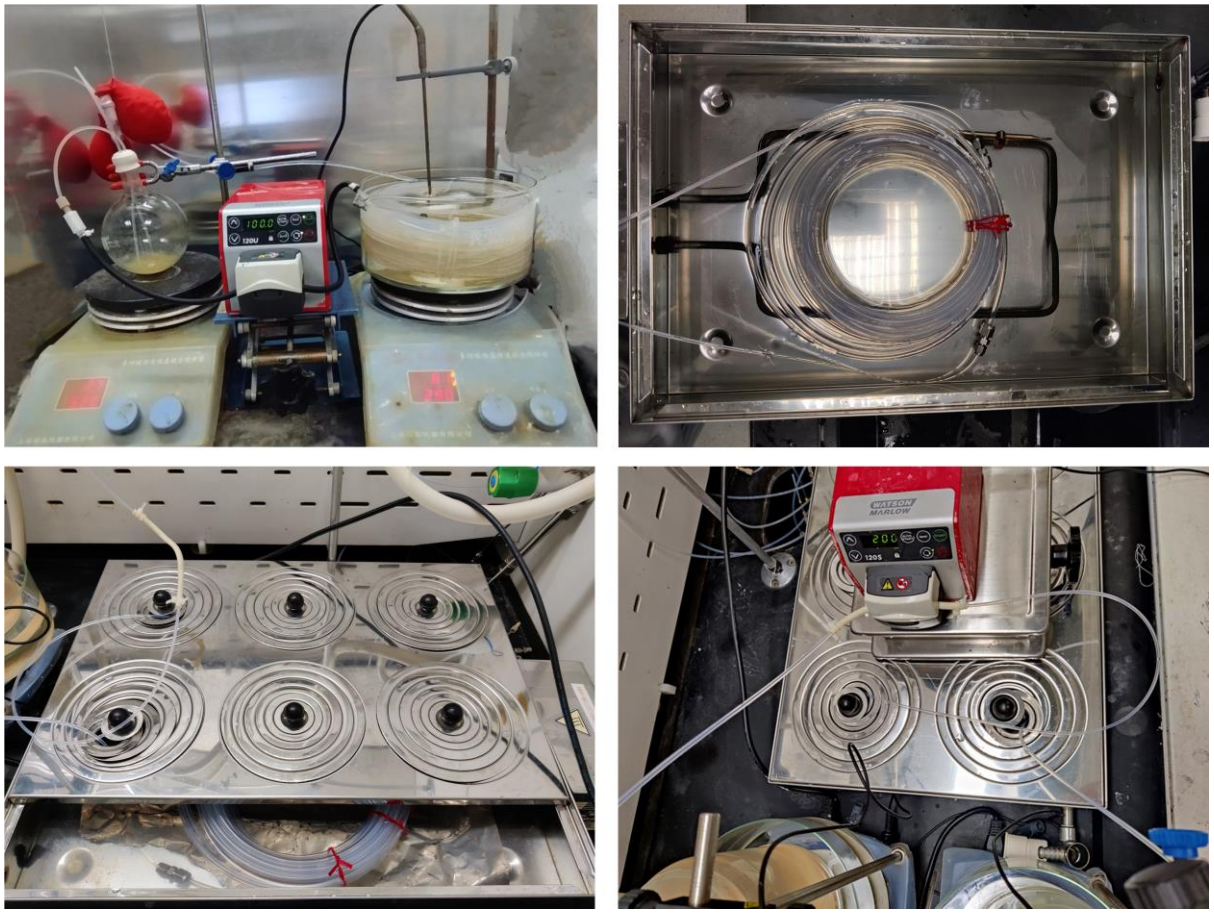

Supplementary Fig. 25 | High-rate circulation flow devices for evaluating catalytic performance. Reaction tubing, PFA tubing reactor (outer diameter (O.D.) = 4.8 mm, inner diameter (I.D.) = 3.2 mm, volume (V) = 240 mL) Contherm stainless steel water bath; load 2300W; set temperature: 80 ° C. **d,** Watson-Marlow 100 series cased pump; 120S control, drive with 114DV Pumphead; 4 rollers, Max. operating pressure 2bar, Max.; Tygon® Norprene® Peristaltic Pump.

Conditions optimization:

Entries	Pd-CeO_2 (X mg)	Equivalents of boronic acid and base	Flow rate	Solvent	Temp.	Conversion
1[a]	20	1.5	10 mL/min	EtOH/H_2O (1:1)	80°C.	0
2[a]	50	1.5	10 mL/min	EtOH/H_2O (1:1)	80°C.	30%
3[b]	50	3	10 mL/min	EtOH/H_2O (1:1)	80°C.	70% (block)
4[a]	50	3	10 mL/min	THF/H_2O (1:1)	80°C.	0
5[c]	50	3	10 mL/min	EtOH/H_2O (2:1)	80°C.	100% (91% yield)

Conditions: [a] Reaction time = 12 h, [b] Reaction time = 3 h, [c] Reaction time = 5 h.

Supplementary Fig. 26 | Conditions optimization for flow synthesis.

Blockage of the reaction tube is a limiting factor for heterogeneous catalysts in flow synthesis experiments. As illustrated in **Supplementary Fig. 26**, at 1 g scale, insufficient feeding of the catalyst and phenylboronic acid results in low reaction conversion. However, increasing the amounts of catalysts and phenylboronic acid leads to micro-tubing reactor blocking. To address this issue, we optimized the flow rate (10 mL/min), catalyst feeding (50 mg), K_2CO_3 and boronic acid (3 equiv.), and solvent ratio (EtOH/H_2O, 2:1), achieving both sufficient reagent solubility and high reaction yields. Consequently, this modified condition was adopted for circulation flow synthesis.

Note: When we performed a larger scale (10 g) synthesis, we further increased the amount of catalyst (400 mg) to achieve efficient reaction and flow rate (40 mL/min) to avoid clogging.

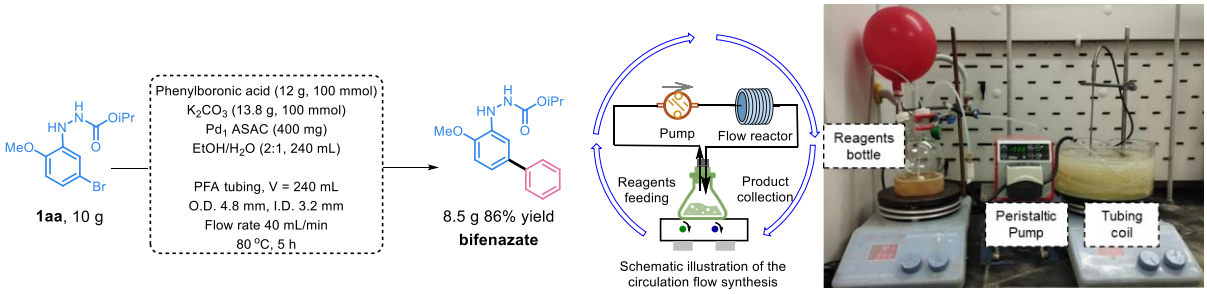

300

301 **Supplementary Fig. 27** | Large-scale circulated flow synthesis of bifenazate. High-purity
302 perfluoroalkoxy polymer (HPFA) tubing and fittings were purchased from IDEX Health & Science
303 Technologies. The peristaltic pump was purchased from Watson-Marlow.

304 Substrate **1aa** was mixed with 400 mg Pd_1 ASAC, 12 g phenylboronic acid and 13.8 g potassium
305 carbonate in 240 mL of EtOH/H_2O (2:1) to create a slurry. The slurry was continuously pumped at 40
306 mL/min using a peristaltic pump and directed to the PFA tubing reactor (outer diameter (O.D.) = 4.8
307 mm, inner diameter (I.D.) = 3.2 mm, volume (V) = 240 mL) which was heated to 80 °C with the heating
308 module. The reaction mixture was recirculated to the original reservoir until the reaction was completed
309 to afford bifenazate in 86% isolated yield.

310

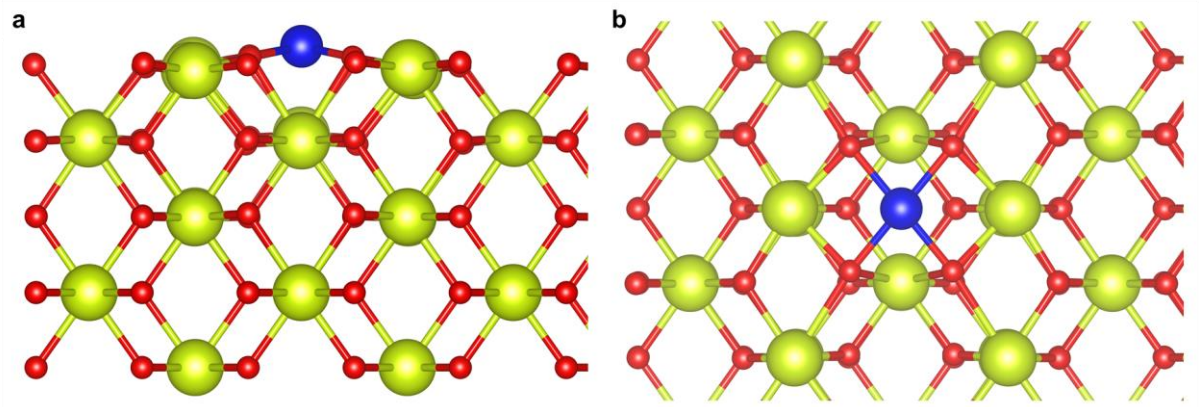

Supplementary Fig. 28 | Structure of Pd_1 ASAC calculated by DFT. Side **(a)** and top **(b)** views of the optimized structure of Pd_1 ASAC model. The red, yellow, and blue spheres represent oxygen, cerium, and palladium, respectively.

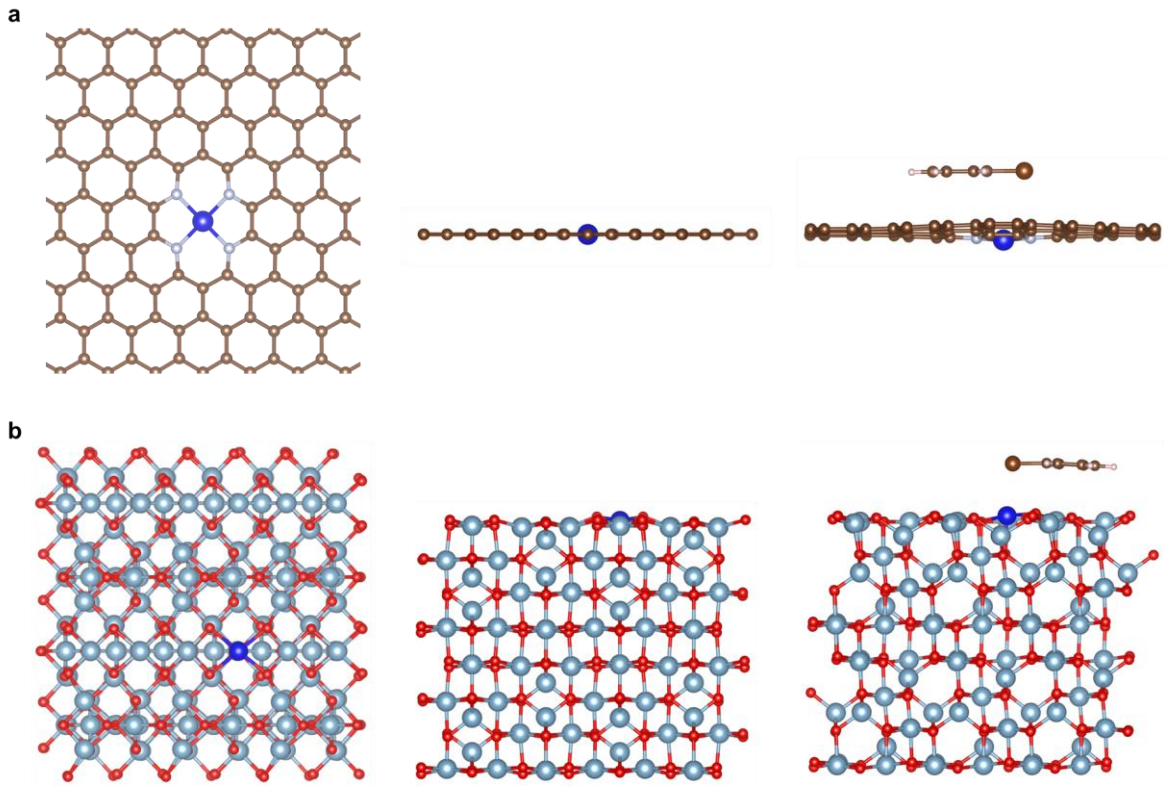

Supplementary Fig. 29 | Structural models of Pd_1-NC (**a**) and Pd_1-Al_2O_3 (**b**) and optimized structures in the oxidative addition step calculated by DFT.

Reducible support is essential for the design of highly active catalysts for cross-coupling reactions, as it functions as electron reservoirs to address the high reaction energy barriers associated with the bivalent elevation at a single metal site. Moreover, achieving a dynamic and reversible coordination transition between Pd single atoms and the support is essential to regulate the electronic structure of the metal center during the reaction. However, in the case of NC, the Pd-N bonds lack the ability to undergo dynamic transitions during the reaction, resulting in catalytic inactivity. In addition, carbon is known to be a conduct but not to be a reducible support that has the excellent capability to accept/donor the electrons. As illustrated in **Supplementary Fig. 29a**, the dissociation of the C-Br bond in bromobenzene was adsorbed on Pd_1-NC, followed by structural optimization. However, the system reverted to the initial bromobenzene configuration, which was also shown in the case of Al_2O_3 (**Supplementary Fig. 29b**),demonstrating that single atom Pd on a non-reducible support is incapable of activating bromobenzene (**Supplementary Video 2 and 3**).

Supplementary Table 1 | The formation energies of Pd single-atom on different crystal planes of CeO_2.

Crystal planes	E_{form} (eV)
Pd_1-CeO_2(110) ASAC	−1.37
Pd_1-CeO_2(100)	−1.66
Pd_1-CeO_2(111)	0.84
Pd_1-NC	−2.76
Pd_1-Al_2O_3	−5.52

Supplementary Table 2 | Results of EXAFS fittings of catalysts.

Sample	Shell	*N*	*R* (Å)	σ^2 (10^{-3}Å^2)	R factor
Pd_1 ASAC	Pd-O	4.0 ± 0.5	2.01 ± 0.01	0.0024 ± 0.0013	0.026
	Pd-Ce	3.9 ± 1.3	3.14 ± 0.02	0.0068 ± 0.0018	
Pd_1-CeO_2 (110) ASAC	Pd-O	4.0±0.5	1.99±0.01	0.0014±0.0008	0.024
	Pd-Ce	3.7±1.5	3.15±0.02	0.0055±0.0019	
Pd_1-CeO_2 (100)	Pd-O	4.1±0.6	1.99±0.01	0.0012±0.0009	0.007
Pd_1-CeO_2 (111)	Pd-O	3.9±0.3	1.99±0.01	0.0010±0.0009	0.019
	Pd-Ce	3.4±1.0	3.18±0.02	0.0081±0.0026	
Pd_1-NC	Pd-N	4.3±0.2	1.95±0.02	0.0032±0.0009	0.009
Pd_1-Al_2O_3	Pd-O	3.9±0.5	2.19±0.01	0.0061±0.0009	0.029

N, coordination number; *R*, distance between absorbing and backscattering atoms; σ^2, Debye-Waller factor to account for thermal and structural disorders; R factor as a measure of the goodness of fit.

Supplementary Table 3 | Comparison of turnover frequencies of reported Pd catalysts in Suzuki cross-coupling reaction.

Entry	Catalyst	Substrate	Conditions	Reaction mode	TOF (h^{-1})	Ref.
1	$C_{18}H_{25}C_{l2}N_3O_4Pd$		333 K/24 h	homogeneous	2.0	[1]
2	$C_{24}H_{45}NP_2Pd$		338 K/16 h	homogeneous	3.2	[2]
3	$(PPh_3)_2PdCl_2$		383 K/24 h	homogeneous	8.2	[3]
4	$Pd(OAc)_2$	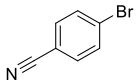	333 K/6 h	homogeneous	15	[4]
5	Pd/C		393 K/2 h	heterogeneous	10000	[5]
6	Pd/CeO_2	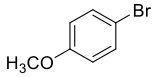	393 K/4 h	heterogeneous	4100	[5]
7	Pd/Graphene	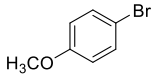	353 K/20 h	heterogeneous	57	[6]
8	Pd/NMC		323 K/2 h	heterogeneous	137	[7]
9	$Pd_{0.10}/g\text{-}C_3N_4$		298 K/30 min	heterogeneous	120.93	[8]
10	Pd@mZ-x-H		333 K/30 min	heterogeneous	4050	[9]
11	Pd@CMK-3		333 K/5 min	heterogeneous	2800	[10]
12	Pd(0)-MCM-41		353 K/12 h	heterogeneous	6990	[11]
13	Pd/Pyr-GDY		353 K/5 h	heterogeneous	18000	[12]
14	$Pd_1/UiO\text{-}66\text{-}NH_2$		333 K/2 h	heterogeneous (SAC)	13043	[13]
15	Pd-ECN		393 K/10 min	heterogeneous (SAC)	549	[14]

16	Pd-SAs/3DOM-CeO_2		298 K/15 min	heterogeneous (SAC)	520.01	[15]
17	Pd-N_3C_1		373 K/24 h	heterogeneous (SAC)	4.2	[16]
18	Pd_1/C_3N_4/rGO	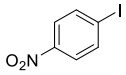	333 K/60 min	heterogeneous (SAC)	362.37	[17]
19	Pd/C		323 K/2 h	heterogeneous	325	This work
20	Pd_1 ASAC		298 K/15 min	heterogeneous (SAC)	2820	This work
21	Pd_1 ASAC		323 K/15 min	heterogeneous (SAC)	9820	This work
22	Pd_1 ASAC		343 K/5 min	heterogeneous (SAC)	46149	This work

TOF = [(mole of converted aryl halides / mole of Pd catalyst) / reaction time].

Supplementary Table 4 | Comparison of Pd content in catalysts before and after reaction.

Catalyst	Pd content (wt.%)		
	Before reaction	After reaction (80 ℃)	After reaction (50 ℃)
Pd_1-TiO_2	0.23	0.22	0.22
Pd_1-Mn_2O_3	0.36	0.16	0.33
		0.14	0.35
Pd_1-Fe_2O_3	0.29	0.29	0.28
Pd_1-Co_3O_4	0.29	0.29	0.28
		0.30	0.29
Pd_1-NiO	0.32	0.19	0.12
		0.21	0.21
Pd_1-CuO	0.32	0.08	0.10
		0.09	0.11
Pd_1 ASAC	0.27	0.27	0.28
	0.93	0.94	0.93

Experimental procedure: Bromobenzene (0.5 mmol), phenylboronic acid (0.6 mmol), K_2CO_3 (1.5 mmol), Pd_1 ASAC (0.07 mol%, according to Pd), ethanol (2 mL), and H_2O (2 mL) were sequentially added to the screw-top reaction tube. The reaction tube was placed in an oil bath preheated to 80 ° C, and stirring in an ambient atmosphere. After the reaction, the catalyst was filtered out, and fresh phenylboronic acid and base were added to the filtrate for a subsequent reaction. GC-MS analysis detected 0% conversion of the new substrate, indicating no leaching of Pd ions into the filtrate. This finding was supported by ICP-AES analysis, which showed that the Pd content in the catalyst remained virtually unchanged before and after the reaction, with no detectable Pd ions in the solution

CP2K input file for structural optimization:

```
&GLOBAL
  PROJECT         Pd1-CeO2
  RUN_TYPE        GEO_OPT
  PRINT_LEVEL MEDIUM
&END GLOBAL

&MOTION
   &GEO_OPT
     OPTIMIZER    BFGS
     MAX_ITER                  1300
     MAX_FORCE         4.50E-04
   &END GEO_OPT
   &CONSTRAINT
     &FIXED_ATOMS
       LIST       12..47    130..147
     &END FIXED_ATOMS
   &END CONSTRAINT
   &PRINT
     &TRAJECTORY SILENT
       ADD_LAST NUMERIC
       FILENAME ./MD_TRAJECTORY.xyz
       &EACH
         MD                    5
       &END EACH
     &END TRAJECTORY
     &VELOCITIES    SILENT
       &EACH
         MD                    5
       &END EACH
     &END VELOCITIES
     &RESTART SILENT
       &EACH
         MD                    10
       &END EACH
     &END RESTART
   &END PRINT
&END MOTION

&FORCE_EVAL
  METHOD Quickstep
  &DFT
      CHARGE 0
```

```
  POTENTIAL_FILE_NAME    GTH_POTENTIALS
  BASIS_SET_FILE_NAME    BASIS_MOLOPT
  WFN_RESTART_FILE_NAME ./XXX-RESTART.wfn
        UKS    T
 &MGRID
    CUTOFF 400
    NGRIDS 20
    REL_CUTOFF 60
 &END MGRID
 &QS
    EPS_DEFAULT 1.0E-12
    EPS_PGF_ORB 1.0E-6
    EXTRAPOLATION ASPC
    EXTRAPOLATION_ORDER 3
 &END QS
 &SCF
    EPS_SCF 1.0E-6
    MAX_SCF 60
    SCF_GUESS RESTART
     &OT
       PRECONDITIONER FULL_ALL
       MINIMIZER    BROYDEN
       BROYDEN_BETA         0.9
       BROYDEN_SIGMA         0.1
       LINESEARCH    2PNT
     &END OT
     &OUTER_SCF
       EPS_SCF 1.0E-6
       MAX_SCF 5
     &END OUTER_SCF
     &MIXING ON
       ALPHA 0.1
       BETA    0.5
     &END MIXING
     &PRINT
        &RESTART_HISTORY
          FILENAME = MD_RESTART_HISTORY.wfn
          ADD_LAST NUMERIC
          BACKUP_COPIES 5
          &EACH
          &END EACH
        &END RESTART_HISTORY
    &END PRINT
 &END SCF
```

```
    &XC
      &XC_FUNCTIONAL PBE
      &END XC_FUNCTIONAL
      &XC_GRID
        XC_SMOOTH_RHO NN10
        XC_DERIV SPLINE2_SMOOTH
      &END XC_GRID
      &vdW_POTENTIAL
         POTENTIAL_TYPE PAIR_POTENTIAL
         &PAIR_POTENTIAL
            TYPE DFTD3
            PARAMETER_FILE_NAME dftd3.dat
            REFERENCE_FUNCTIONAL PBE
            R_CUTOFF 10.
         &END PAIR_POTENTIAL
      &END vdW_POTENTIAL
    &END XC
    &PRINT
      &MULLIKEN    SILENT
        FILENAME =CHARGE.mulliken
        &EACH
           MD       5
        &END EACH
      &END MULLIKEN
    &END PRINT
  &END DFT
  &SUBSYS
    &CELL
      A       16.233000 0.000000 0.000000
      B       0.000000 11.478460 0.000000
      C       0.000000 0.000000 27.652310
      PERIODIC XYZ
    &END CELL

    &TOPOLOGY
      COORD_FILE_NAME init.xyz
      COORD_FILE_FORMAT xyz
    &END TOPOLOGY

    &KIND H
      BASIS_SET DZVP-MOLOPT-SR-GTH
      POTENTIAL GTH-PBE-q1
    &END KIND
```

```
      &KIND Br
        BASIS_SET DZVP-MOLOPT-SR-GTH
        POTENTIAL GTH-PBE-q7
      &END KIND
      &KIND C
        BASIS_SET DZVP-MOLOPT-SR-GTH
        POTENTIAL GTH-PBE-q4
      &END KIND
      &KIND O
        BASIS_SET DZVP-MOLOPT-SR-GTH
        POTENTIAL GTH-PBE-q6
      &END KIND
      &KIND Pd
        BASIS_SET DZVP-MOLOPT-SR-GTH
        POTENTIAL GTH-PBE-q18
      &END KIND
      &KIND Ce
        BASIS_SET DZVP-MOLOPT-SR-GTH
        POTENTIAL GTH-PBE-q12
        &DFT_PLUS_U    T
          L    3
          U_MINUS_J [eV] 5
        &END DFT_PLUS_U
      &END KIND

    &END SUBSYS
  &END FORCE_EVAL

```

Supplementary References

1. Steeples, E., Kelling, A., Schilde, U. & Esposito, D. Amino acid-derived N-heterocyclic carbene palladium complexes for aqueous phase Suzuki-Miyaura couplings. *New J. Chem*. **40**, 4922-4930 (2016).
2. van der Vlugt, J. I., Siegler, M. A., Janssen, M., Vogt, D. & Spek, A. L. A cationic AgI(PNPtBu) species acting as PNP transfer agent: facile synthesis of Pd(PNPtBu)(alkyl) complexes and their reactivity compared to PCPtBu analogues. *Organometallics*. **28**, 7025-7032 (2009).
3. Asachenko, A. F., Sorochkina, K. R., Dzhevakov, P. B., Topchiy, M. A. & Nechaev, M. S. Suzuki-Miyaura cross-coupling under solvent-free conditions. *Adv. Synth. Catal*. **355**, 3553-3557 (2013).
4. Myslinska, M., Heise, G. L. & Walsh, D. J. Practical and efficient applications of novel dioxaborolanes and dioxaborinanes in the synthesis of corresponding boronates and their use in the palladium-catalyzed cross coupling reactions. *Tetrahedron Lett*. **53**, 2937-2941 (2012).
5. Köhler, K., Heidenreich, R.G., Soomro, S.S. & Pröckl, S.S. Supported palladium catalysts for Suzuki reactions: structure-property relationships, optimized reaction protocol and control of palladium leaching. *Adv. Synth. Catal.* **350**, 2930-2936 (2008).
6. Gómez-Martínez, M., Buxaderas, E., Pastor, I. M. & Alonso, D. A. Palladium nanoparticles supported on graphene and reduced graphene oxide as efficient recyclable catalyst for the Suzuki-Miyaura reaction of potassium aryltrifluoroborates. *J. Mol. Catal. A: Chem*. **404-405**, 1-7 (2015).
7. Sun, J. et al. Green Suzuki-Miyaura coupling reaction catalyzed by palladium nanoparticles supported on graphitic carbon nitride. *Applied Catalysis B: Environmental*. **165**, 661-667 (2015).
8. Sun, J. et al. Green Suzuki–Miyaura coupling reaction catalyzed by palladium nanoparticles supported on graphitic carbon nitride. *Applied Catalysis B: Environmental*. **165**, 661-667 (2015).
9. Ke, W, et al. Mesoporous H-ZSM-5 nanocrystals with programmable number of acid sites as “solid ligands” to activate Pd nanoparticles for C–C coupling reactions. *Nano Research*. **11**, 874-881 (2018).
10. Wang, Z, et al. Pd embedded in porous carbon (Pd@CMK-3) as an active catalyst for Suzuki reactions: Accelerating mass transfer to enhance the reaction rate. *Nano research*. **7**, 1254-1262 (2014).
11. Jana, S., Haldar, S. & Koner, S. Heterogeneous Suzuki and Stille coupling reactions using highly efficient palladium (0) immobilized MCM-41 catalyst. *Tetrahedron Lett.* **50**, 4820-4823 (2009).
12. Yang, L.L. et al. A graphdiyne-based carbon material for electroless deposition and stabilization of sub-nanometric Pd catalysts with extremely high catalytic activity. *J. Mater. Chem. A* **7**, 13142-13148 (2019).
13. Ji, S. et al. Construction of a single-atom palladium catalyst by electronic metal-support interaction and interface confinement effect with remarkable performance in Suzuki coupling reaction. *Chem. Eng. J.* **452**, 139205 (2023).
14. Chen, Z. et al. A heterogeneous single-atom palladium catalyst surpassing homogeneous systems for Suzuki coupling. *Nat. Nanotechnol*. **13**, 702-707 (2018).
15. Tao, X. et al. Anchoring positively charged Pd single atoms in ordered porous ceria to boost

catalytic activity and stability in Suzuki coupling reactions. *Small*. **16**, 2001782 (2020).
16. Liu, J. et al. Molecular engineered palladium single atom catalysts with an M-C_1N_3 subunit for Suzuki coupling. *Journal of Materials Chemistry A*. **9**, 11427-11432 (2021).
17. Fu, N. et al. Fabricating Pd isolated single atom sites on C_3N_4/rGO for heterogenization of homogeneous catalysis. *Nano Research*. **13**, 947-951 (2020).

Analysis of the NMR data

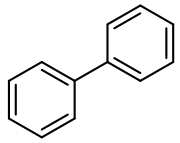

1,1'-biphenyl (4a). The compound was prepared in 99% yield when X=I, Br and Cl. **^{1}H NMR** (500 MHz, Chloroform-*d*) δ [ppm] 7.65-7.56 (m, 4H), 7.45 (dd, J = 8.4, 7.0 Hz, 4H), 7.39-7.31 (m, 2H); **^{13}C NMR** (125 MHz, Chloroform-d) δ [ppm] 141.21, 128.72, 127.14.

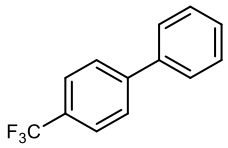

4-(trifluoromethyl)-1,1'-biphenyl (4b). The compound was prepared in 99% yield. **^{1}H NMR** (500 MHz, Chloroform-*d*) δ [ppm] 7.70 (s, 4H), 7.62-7.60 (m, 2H), 7.49-7.45 (m, 2H), 7.41-7.33 (m, 1H); **^{13}C NMR** (125 MHz, Chloroform-d) δ [ppm] 144.71, 139.75, 128.96, 128.73, 128.16, 127.40, 127.26, 127.15, 125.67. **^{19}F NMR** (471 MHz, Chloroform-d) δ [ppm] -62.39.

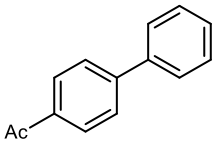

1-([1,1'-biphenyl]-4-yl) ethan-1-one (4c). The compound was prepared in 98% yield when X=I and Br. **^{1}H NMR** (400 MHz, Chloroform-*d*) δ [ppm] 8.07-8.01 (m, 2H), 7.72-7.67 (m, 2H), 7.66-7.60 (m, 2H), 7.52-7.44 (m, 2H), 7.44-7.38 (m, 1H), 2.64 (s, 3H); **^{13}C NMR** (125 MHz, Chloroform-d) δ [ppm] 197.74, 145.75, 139.84, 135.82, 128.93, 128.89, 128.20, 127.24, 127.19, 26.64.

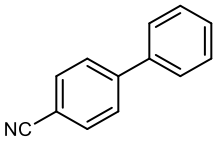

[1,1'-biphenyl]-4-carbonitrile (4d). The compound was prepared in 99% yield when X=I, Br and Cl. **^{1}H NMR** (500 MHz, Chloroform-*d*) δ [ppm] 7.78-7.71 (m, 2H), 7.71-7.66 (m, 2H), 7.61-7.57 (m, 2H), 7.49 (dd, J = 10.4, 4.8 Hz, 2H), 7.45-7.41 (m, 1H); **^{13}C NMR** (125 MHz, Chloroform-d) δ [ppm] 145.68, 139.18, 132.59, 129.10, 128.64, 127.73, 127.22, 118.93, 110.91.

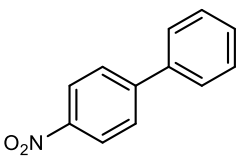

4-nitro-1,1'-biphenyl (4e). The compound was prepared in 99%, 99% and 93% yield when X=I, Br and Cl, respectively. **^{1}H NMR** (500 MHz, Chloroform-*d*) δ [ppm] 8.30 (d, J = 8.9 Hz, 2H), 7.79-7.70 (m, 2H), 7.67-7.59 (m, 2H), 7.55-7.47 (m, 2H), 7.47-7.42 (m, 1H); **^{13}C NMR** (125 MHz, Chloroform-

d) δ [ppm] 147.60, 147.05, 138.74, 129.12, 128.88, 127.77, 127.35, 124.07.

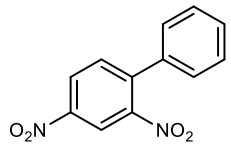

2,4-dinitro-1,1'-biphenyl (4f). The compound was prepared in 99% yield when X=I and Cl. **^{1}H NMR** (500 MHz, Chloroform-*d*) *δ* [ppm] 8.74-8.68 (m, 1H), 8.47 (ddd, J = 8.5, 2.3, 1.1 Hz, 1H), 7.73-7.64 (m, 1H), 7.53-7.44 (m, 3H), 7.40-7.30 (m, 2H); **^{13}C NMR** (125 MHz, Chloroform-d) δ [ppm] 149.03, 146.80, 142.21, 135.16, 133.19, 129.52, 129.05, 127.63, 126.44, 119.67.

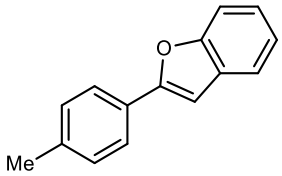

2-(p-tolyl) benzofuran (4g). The compound was prepared in 99% yield when X=I and Br. **^{1}H NMR** (500 MHz, Chloroform-*d*) *δ* [ppm] 7.87 (d, J = 8.2 Hz, 2H), 7.69-7.60 (m, 2H), 7.41-7.30 (m, 4H), 7.06 (s, 1H), 2.50 (s, 3H); **^{13}C NMR** (125 MHz, Chloroform-d) δ [ppm] 156.16, 154.74, 138.54, 129.45, 129.32, 127.72, 124.85, 123.96, 122.82, 120.71, 111.05, 100.53, 21.34.

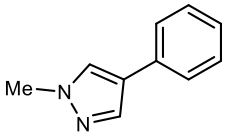

1-methyl-4-phenyl-1H-pyrazole (4h). The compound was prepared in 89% yield. **^{1}H NMR** (500 MHz, Chloroform-*d*) *δ* [ppm] 7.76 (d, J = 0.8 Hz, 1H), 7.60 (d, J = 0.7 Hz, 1H), 7.50 – 7.44 (m, 2H), 7.40 – 7.32 (m, 2H), 7.25 – 7.19 (m, 1H), 3.94 (s, 3H); **^{13}C NMR** (125 MHz, Chloroform-d) δ [ppm] 136.73, 132.61, 128.82, 126.86, 126.32, 125.48, 123.23, 39.07.

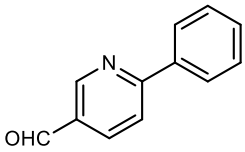

6-phenylnicotinaldehyde (4i). The compound was prepared in 93% yield. **^{1}H NMR** (500 MHz, Chloroform-*d*) *δ* [ppm] 10.13 (s, 1H), 9.13 (d, J = 2.1 Hz, 1H), 8.22 (dd, J = 8.2, 2.2 Hz, 1H), 8.11-8.05 (m, 2H), 7.90 (d, J = 8.2 Hz, 1H), 7.55-7.47 (m, 3H); **^{13}C NMR** (125 MHz, Chloroform-d) δ [ppm] 190.44, 162.18, 152.37, 137.94, 136.50, 130.36, 129.82, 128.97, 127.52, 120.58.

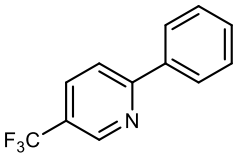

2-phenyl-5-(trifluoromethyl) pyridine (4j). The compound was prepared in 89% yield. **^{1}H NMR** (500 MHz, Chloroform-*d*) *δ* [ppm] 8.98-8.93 (m, 1H), 8.07-8.01 (m, 2H), 7.98 (dd, J = 8.3, 2.4 Hz, 1H), 7.85 (d, J = 8.3 Hz, 1H), 7.55-7.45 (m, 3H); **^{13}C NMR** (125 MHz, Chloroform-d) δ [ppm] 160.66, 146.60, 137.93, 133.92, 130.04, 128.95, 127.25, 124.94, 124.82, 124.67, 122.66, 119.94. **^{19}F NMR** (471 MHz, Chloroform-d) δ [ppm] -62.24.

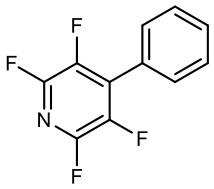

2,3,5,6-tetrafluoro-4-phenylpyridine (4k). The compound was prepared in 92% yield. **^{1}H NMR** (500 MHz, Chloroform-*d*) *δ* [ppm] 7.54-7.47 (m, 5H); **^{13}C NMR** (125 MHz, Chloroform-d) δ [ppm] 145.41, 143.42, 141.30, 139.31, 136.49, 136.26, 134.26, 129.84, 129.82, 127.07. **^{19}F NMR** (471 MHz, Chloroform-d) δ [ppm] -94.28, -94.34 (d, J = 6.9 Hz), -94.39, -145.48 – -145.51 (m), -145.54 – -145.57 (m).

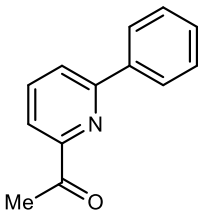

1-(6-phenylpyridin-2-yl) ethan-1-one (4l). The compound was prepared in 98% yield. **^{1}H NMR** (500 MHz, Chloroform-*d*) *δ* [ppm] 8.10 (dd, J = 7.2, 1.7 Hz, 2H), 7.96 (dd, J = 7.5, 1.2 Hz, 1H), 7.92-7.82 (m, 2H), 7.51 (dd, J = 8.3, 6.5 Hz, 2H), 7.47-7.42 (m, 1H), 2.82 (s, 3H); **^{13}C NMR** 200.41, 156.28, 153.23, 138.25, 137.50, 129.35, 128.74, 126.76, 123.30, 119.65, 25.66.

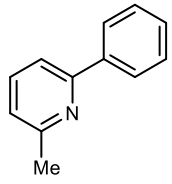

2-methyl-6-phenylpyridine (4m). The compound was prepared in 91% yield. **^{1}H NMR** (500 MHz, Chloroform-*d*) *δ* [ppm] 8.09-7.95 (m, 2H), 7.62 (t, J = 7.7 Hz, 1H), 7.54-7.45 (m, 3H), 7.42 (d, J = 7.4 Hz, 1H), 7.09 (d, J = 7.6 Hz, 1H), 2.65 (s, 3H); **^{13}C NMR** (125 MHz, Chloroform-d) δ [ppm] 158.20, 156.82, 139.63, 136.77, 128.59, 128.56, 126.89, 121.48, 117.50, 24.63.

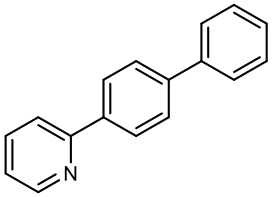

2-([1,1'-biphenyl]-4-yl) pyridine (4n). The compound was prepared in 99% yield. **^{1}H NMR** (500 MHz,

Chloroform-*d*) δ [ppm] 8.81-8.67 (m, 1H), 8.19-8.05 (m, 2H), 7.80-7.74 (m, 3H), 7.74-7.65 (m, 3H), 7.48 (dd, J = 8.4, 7.0 Hz, 2H), 7.44-7.35 (m, 1H), 7.27-7.20 (m, 1H); **^{13}C NMR** (125 MHz, Chloroform-d) δ [ppm] 156.82, 149.54, 141.60, 140.42, 138.06, 136.71, 128.73, 127.43, 127.35, 127.21, 126.98, 122.02, 120.35.

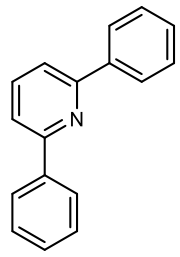

2,6-diphenylpyridine (4o). The compound was prepared in 99% yield. **^{1}H NMR** (500 MHz, Chloroform-*d*) δ [ppm] 8.23-8.11 (m, 4H), 7.83 (td, J = 7.6, 3.0 Hz, 1H), 7.71 (td, J = 7.6, 3.5 Hz, 2H), 7.52 (qd, J = 7.5, 2.3 Hz, 4H), 7.47-7.41 (m, 2H); **^{13}C NMR** 156.81, 139.47, 137.46, 128.95, 128.66, 126.97, 118.62.

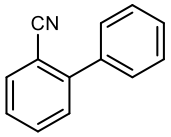

[1,1'-biphenyl]-2-carbonitrile (4p). The compound was prepared in 99% yield. **^{1}H NMR** (500 MHz, Chloroform-*d*) δ [ppm] 7.77 (dd, J = 7.8, 1.3 Hz, 1H), 7.65 (td, J = 7.7, 1.3 Hz, 1H), 7.59 – 7.55 (m, 2H), 7.54 – 7.42 (m, 5H); **^{13}C NMR** (125 MHz, Chloroform-d) δ [ppm] 145.42, 138.06, 133.69, 132.76, 130.02, 128.69, 128.66, 127.48, 118.67, 111.20.

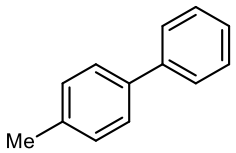

4-methyl-1,1'-biphenyl (4q). The compound was prepared in 99% yield when X=I and Br. **^{1}H NMR** (500 MHz, Chloroform-*d*) δ [ppm] 7.59 (dd, J = 8.2, 1.3 Hz, 2H), 7.50 (d, J = 8.1 Hz, 2H), 7.43 (t, J = 7.7 Hz, 2H), 7.37-.31 (m, 1H), 7.28-7.24 (m, 2H), 2.41 (s, 3H); **^{13}C NMR** (125 MHz, Chloroform-d) δ [ppm] 141.13, 138.33, 136.99, 129.45, 128.68, 126.97, 126.94, 21.08.

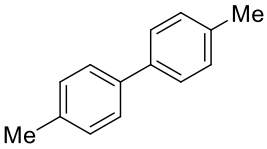

4,4'-dimethyl-1,1'-biphenyl (4r). The compound was prepared in 99% yield. **^{1}H NMR** (500 MHz, Chloroform-*d*) δ [ppm] 7.63-7.55 (m, 4H), 7.38-7.30 (m, 4H), 2.49 (s, 6H); **^{13}C NMR** (125 MHz, Chloroform-d) δ [ppm] 138.24, 136.62, 129.39, 126.76, 21.04.

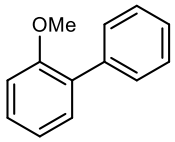

2-methoxy-1,1'-biphenyl (4s). The compound was prepared in 80% yield. **^{1}H NMR** (400 MHz, Chloroform-*d*) δ [ppm] 7.60-7.54 (m, 2H), 7.48-7.41 (m, 2H), 7.39-7.32 (m, 3H), 7.11-6.99 (m, 2H), 3.84 (s, 3H); **^{13}C NMR** (125 MHz, Chloroform-d) δ [ppm] 156.42, 138.51, 130.86, 130.69, 129.51, 128.57, 127.94, 126.87, 120.79, 111.19, 55.50.

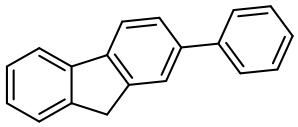

2-phenyl-9H-fluorene (4t). The compound was prepared in 99% yield. **^{1}H NMR** (500 MHz, Chloroform-*d*) δ [ppm] 7.93-7.75 (m, 3H), 7.67 (d, J = 8.1 Hz, 2H), 7.63 (d, J = 7.7 Hz, 1H), 7.57 (d, J = 7.4 Hz, 1H), 7.47 (dd, J = 8.3, 7.1 Hz, 2H), 7.43-7.29 (m, 3H), 3.98 (s, 2H); **^{13}C NMR** (125 MHz, Chloroform-d) δ [ppm] 143.85, 143.43, 141.46, 141.36, 140.89, 139.83, 128.74, 127.15, 127.08, 126.79, 126.70, 125.97, 125.02, 123.77, 120.08, 119.93, 36.98.

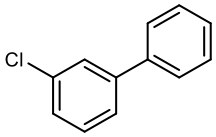

3-chloro-1,1'-biphenyl (4u). The compound was prepared in 99% yield. **^{1}H NMR** (500 MHz, Chloroform-*d*) δ [ppm] 7.68-7.59 (m, 3H), 7.50 (ddd, J = 9.9, 6.8, 1.8 Hz, 3H), 7.47-7.34 (m, 3H); **^{13}C NMR** (125 MHz, Chloroform-d) δ [ppm] 142.99, 139.72, 134.59, 129.92, 128.84, 127.80, 127.22, 127.20, 127.04, 125.23.

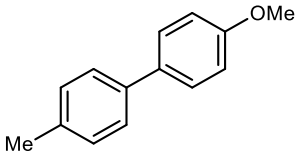

4-methoxy-4'-methyl-1,1'-biphenyl (4v). The compound was prepared in 99% yield. **^{1}H NMR** (500 MHz, Chloroform-*d*) δ [ppm] 7.59 (d, J = 8.8 Hz, 2H), 7.53 (d, J = 8.2 Hz, 2H), 7.30 (d, J = 7.5 Hz, 2H), 7.04 (d, J = 8.8 Hz, 2H), 3.90 (s, 3H), 2.46 (s, 3H); **^{13}C NMR** (125 MHz, Chloroform-d) δ [ppm] 158.86, 137.88, 136.25, 133.64, 129.38, 127.87, 126.50, 114.08, 55.21, 20.99.

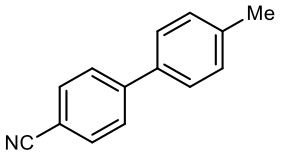

2-methyl-6-(phenylethynyl) pyridine (4w). The compound was prepared in 99% yield. **^{1}H NMR** (500 MHz, Chloroform-*d*) δ [ppm] 7.76-7.61 (m, 4H), 7.50 (d, J = 8.1 Hz, 2H), 7.30 (d, J = 8.0 Hz, 2H), 2.42 (s, 3H); **^{13}C NMR** (125 MHz, Chloroform-d) δ [ppm] 145.48, 138.65, 136.13, 132.45, 129.74, 127.34,

126.95, 118.96, 110.42, 21.10.

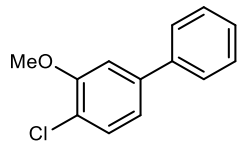

4-chloro-3-methoxy-1,1'-biphenyl (4x). The compound was prepared in 90% yield. **^{1}H NMR** (400 MHz, Chloroform-*d*) δ [ppm] 7.52-7.47 (m, 2H), 7.45-7.38 (m, 2H), 7.37-7.32 (m, 1H), 7.27-7.23 (m, 1H), 7.03 (dd, J = 8.1, 2.0 Hz, 1H), 6.98 (d, J = 2.0 Hz, 1H), 3.81 (s, 3H); **^{13}C NMR** (125 MHz, Chloroform-d) δ [ppm] 156.97, 137.46, 133.88, 131.50, 129.38, 129.22, 128.06, 127.19, 120.81, 111.85, 55.75.

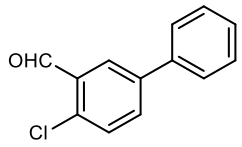

4-chloro-[1,1'-biphenyl]-3-carbaldehyde (4y). The compound was prepared in 75% yield. **^{1}H NMR** (400 MHz, Chloroform-*d*) δ [ppm] 10.53 (s, 1H), 8.15 (d, J = 2.4 Hz, 1H), 7.76 (dd, J = 8.3, 2.4 Hz, 1H), 7.63-7.57 (m 2H), 7.53 (d, J = 8.3 Hz, 1H), 7.50-7.43 (m, 2H), 7.43-7.36 (m, 1H); **^{13}C NMR** (125 MHz, Chloroform-d) δ [ppm] 189.78, 140.52, 138.61, 136.82, 133.47, 132.53, 130.98, 129.04, 128.23, 127.62, 126.93.

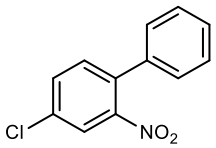

4-chloro-2-nitro-1,1'-biphenyl (4z). The compound was prepared in 81% yield. **^{1}H NMR** (500 MHz, Chloroform-*d*) δ [ppm] 7.86 (dd, J = 3.4, 2.3 Hz, 1H), 7.68 (d, J = 8.6 Hz, 1H), 7.60 (dd, J = 8.3, 2.2 Hz, 1H), 7.44-7.41 (m, 2H), 7.41-7.38 (m, 1H), 7.30-7.25 (m, 2H); **^{13}C NMR** (125 MHz, Chloroform-d) δ [ppm] 135.94, 133.31, 132.99, 132.36, 128.79, 128.54, 127.80, 125.77, 124.20.

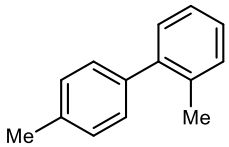

2,4'-dimethyl-1,1'-biphenyl (4aa). The compound was prepared in 99% yield. **^{1}H NMR** (500 MHz, Chloroform-*d*) δ [ppm] 7.42-7.22 (m, 8H), 2.56-2.43 (m, 3H), 2.42-2.26 (m, 3H); **^{13}C NMR** (125 MHz, Chloroform-d) δ [ppm] 141.84, 138.99, 136.31, 135.34, 130.23, 129.81, 129.03, 128.73, 127.02, 125.70, 21.14, 20.48.

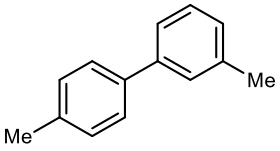

3,4'-dimethyl-1,1'-biphenyl (4ab). The compound was prepared in 99% yield. **^{1}H NMR** (500 MHz, Chloroform-*d*) *δ* [ppm] 7.60 (d, J = 8.2 Hz, 2H), 7.50 (d, J = 12.4 Hz, 2H), 7.43 (t, J = 7.6 Hz, 1H), 7.35 (d, J = 7.8 Hz, 2H), 7.26 (t, J = 8.1 Hz, 1H), 2.53 (s, 3H), 2.50 (s, 3H); **^{13}C NMR** (125 MHz, Chloroform-d) δ [ppm] 141.11, 138.42, 138.19, 136.83, 129.37, 128.58, 127.73, 127.67, 126.95, 124.04, 21.51, 21.05.

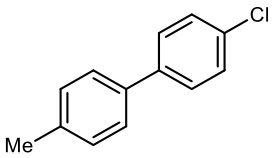

4-chloro-4'-methyl-1,1'-biphenyl (4ac). The compound was prepared in 99% yield when X=I and Br. **^{1}H NMR** (500 MHz, Chloroform-*d*) *δ* [ppm] 7.49 (ddd, J = 18.6, 8.0, 1.8 Hz, 3H), 7.38 – 7.28 (m, 3H), 7.27 – 7.15 (m, 2H), 2.46 (s, 3H); **^{13}C NMR** (125 MHz, Chloroform-d) δ [ppm] 139.53, 137.37, 137.04, 132.98, 129.55, 128.80, 128.12, 126.75, 21.06.

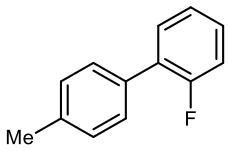

2-fluoro-4'-methyl-1,1'-biphenyl (4ad). The compound was prepared in 99% yield when X=I and Br. **^{1}H NMR** (400 MHz, Chloroform-*d*) *δ* [ppm] 7.50-7.40 (m, 3H), 7.34-7.24 (m, 3H), 7.23-7.11 (m, 2H), 2.42 (s, 3H); **^{13}C NMR** (125 MHz, Chloroform-d) δ [ppm] 159.77 (d, J = 245.8 Hz), 137.46, 132.86, 130.65 (d, J = 3.5 Hz), 129.14, 128.86 (d, J = 2.7 Hz), 128.67, 128.60, 124.26 (d, J = 3.6 Hz), 116.02 (d, J = 22.7 Hz), 21.18. **^{19}F NMR** (377 MHz, Chloroform-d) δ [ppm] -118.05.

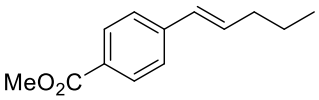

methyl (E)-4-(pent-1-en-1-yl) benzoate (5a). The compound was prepared in 93% yield. **^{1}H NMR** (400 MHz, Chloroform-*d*) *δ* [ppm] 8.00-7.91 (m, 2H), 7.41-7.36 (m, 2H), 6.46-6.30 (m, 2H), 3.90 (s, 3H), 2.22 (td, J = 7.4, 5.9 Hz, 2H), 1.57-1.46 (m, 2H), 0.96 (t, J = 7.4 Hz, 3H); **^{13}C NMR** (125 MHz, Chloroform-d) δ [ppm] 167.01, 142.45, 133.98, 129.86, 129.16, 128.21, 125.73, 51.97, 35.18, 22.33, 13.72.

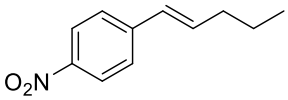

(E)-1-nitro-4-(pent-1-en-1-yl) benzene (5b). The compound was prepared in 93% yield. **^{1}H NMR** (400 MHz, Chloroform-*d*) *δ* [ppm] 8.20-8.10 (m, 2H), 7.47-7.42 (m, 2H), 6.50-6.36 (m, 2H), 2.32-2.15 (m, 2H), 1.58-1.47 (m, 2H), 0.97 (t, J = 7.4 Hz, 3H); **^{13}C NMR** (125 MHz, Chloroform-d) δ [ppm] 146.38, 144.42, 136.40, 128.24, 126.30, 123.94, 35.22, 22.16, 13.70.

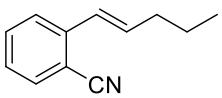

(E)-2-(pent-1-en-1-yl) benzonitrile (5c). The compound was prepared in 88% yield. **^{1}H NMR** (500 MHz, Chloroform-*d*) δ [ppm] 7.64-7.56 (m, 2H), 7.53-7.48 (m, 1H), 7.28-7.24 (m, 1H), 6.79-6.71 (m, 1H), 6.50-6.40 (m, 1H), 2.27 (ddd, J = 14.6, 7.2, 1.5 Hz, 2H), 1.56-1.50 (m, 2H), 0.98 (t, J = 7.4 Hz, 3H); **^{13}C NMR** (125 MHz, Chloroform-d) δ [ppm] 141.24, 136.60, 132.87, 132.56, 126.87, 126.08, 125.36, 118.11, 110.47, 35.19, 22.23, 13.68.

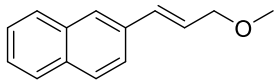

(E)-2-(3-methoxyprop-1-en-1-yl) naphthalene (5d). The compound was prepared in 50% yield. **^{1}H NMR** (400 MHz, Chloroform-*d*) δ [ppm] 7.84-7.77 (m, 3H), 7.75 (s, 1H), 7.62 (dd, J = 8.6, 1.7 Hz, 1H), 7.53-7.40 (m, 2H), 6.79 (d, J = 16.0 Hz, 1H), 6.42 (dt, J = 15.9, 6.0 Hz, 1H), 4.16 (dd, J = 6.0, 1.4 Hz, 2H), 3.43 (s, 3H); **^{13}C NMR** (125 MHz, Chloroform-d) δ [ppm] 134.16, 133.54, 133.01, 132.49, 128.17, 127.96, 127.63, 126.44, 126.32, 126.23, 125.87, 123.55, 73.14, 58.04.

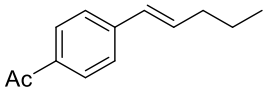

(E)-1-(4-(pent-1-en-1-yl) phenyl) ethan-1-one (5e). The compound was prepared in 99% yield. **^{1}H NMR** (400 MHz, Chloroform-*d*) δ [ppm] 7.94 – 7.84 (m, 2H), 7.45 - 7.37 (m, 2H), 6.47 – 6.25 (m, 2H), 2.58 (s, 3H), 2.22 (td, J = 7.4, 5.8 Hz, 2H), 1.52 (dq, J = 14.6, 7.4 Hz, 2H), 0.96 (t, J = 7.4 Hz, 3H); **^{13}C NMR** (125 MHz, Chloroform-d) δ [ppm] 197.61, 142.66, 135.40, 134.31, 129.09, 128.73, 125.91, 35.21, 26.53, 22.31, 13.73.

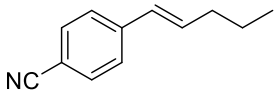

(E)-4-(pent-1-en-1-yl) benzonitrile (5f). The compound was prepared in 70% yield. **^{1}H NMR** (500 MHz, Chloroform-*d*) δ [ppm] 7.61-7.51 (m, 2H), 7.46-7.34 (m, 2H), 6.45-6.29 (m, 2H), 2.26-2.19 (m, 2H), 1.57-1.45 (m, 2H), 0.96 (t, J = 7.4 Hz, 3H); **^{13}C NMR** (125 MHz, Chloroform-d) δ [ppm] 142.38, 135.30, 132.28, 128.55, 126.33, 119.12, 109.87, 35.11, 22.19, 13.67.

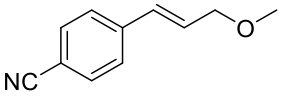

(E)-4-(3-methoxyprop-1-en-1-yl) benzonitrile (5g). The compound was prepared in 81% yield. **^{1}H NMR** (400 MHz, Chloroform-*d*) δ [ppm] 7.62-7.54 (m, 2H), 7.47-7.42 (m, 2H), 6.68-6.54 (m, 1H), 6.39 (dt, J = 16.0, 5.5 Hz, 1H), 4.11 (dd, J = 5.5, 1.6 Hz, 2H), 3.40 (s, 3H); **^{13}C NMR** (125 MHz, Chloroform-d) δ [ppm] 141.20, 132.34, 130.13, 129.93, 126.83, 118.86, 110.74, 72.44, 58.31.

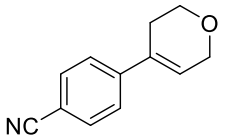

4-(3,6-dihydro-2H-pyran-4-yl) benzonitrile (5h). The compound was prepared in 87% yield. **^{1}H NMR** (500 MHz, Chloroform-*d*) δ [ppm] 7.65-7.56 (m, 2H), 7.50-7.43 (m, 2H), 6.27 (dq, J = 4.5, 1.5 Hz, 1H), 4.34 (q, J = 2.8 Hz, 2H), 3.93 (t, J = 5.4 Hz, 2H), 2.50 (ddq, J = 5.4, 4.5, 2.7 Hz, 2H); **^{13}C NMR** (125 MHz, Chloroform-d) δ [ppm] 144.44, 132.89, 132.24, 125.89, 125.16, 118.87, 110.61, 65.71, 64.12, 26.75.

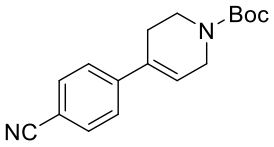

tert-butyl 4-(4-cyanophenyl)-3,6-dihydropyridine-1(2H)-carboxylate (5i). The compound was prepared in 99% yield. **^{1}H NMR** (500 MHz, Chloroform-*d*) δ [ppm] 7.63-7.54 (m, 2H), 7.44 (d, J = 8.4 Hz, 2H), 6.15 (s, 1H), 4.30-3.95 (m, 2H), 3.63 (t, J = 5.7 Hz, 2H), 2.64-2.36 (m, 2H), 1.47 (s, 9H); **^{13}C NMR** (125 MHz, Chloroform-d) δ [ppm] 154.61, 144.87, 134.11, 132.18, 125.37, 124.19, , 118.80, 110.53, 79.83, 43.60, 28.36, 26.97.

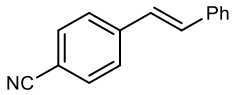

(E)-4-styrylbenzonitrile (5j). The compound was prepared in 99% yield. **^{1}H NMR** (400 MHz, Chloroform-*d*) δ [ppm] 7.67-7.60 (m, 2H), 7.60-7.51 (m, 4H), 7.43-7.36 (m, 2H), 7.36-7.29 (m, 1H), 7.21 (d, J = 16.3 Hz, 1H), 7.09 (d, J = 16.3 Hz, 1H); **^{13}C NMR** (125 MHz, Chloroform-d) δ [ppm] 141.75, 136.21, 132.41, 132.33, 128.79, 128.58, 126.85, 126.79, 126.64, 118.97, 110.48.

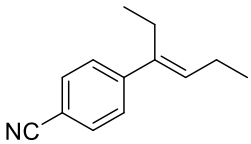

(E)-4-(hex-3-en-3-yl) benzonitrile (5k). The compound was prepared in 99% yield. **^{1}H NMR** (500 MHz, Chloroform-*d*) δ [ppm] 7.62 – 7.51 (m, 2H), 7.47 – 7.39 (m, 2H), 5.74 (t, J = 7.3 Hz, 1H), 2.51 (q, J = 7.5 Hz, 2H), 2.23 (p, J = 7.5 Hz, 2H), 1.07 (t, J = 7.5 Hz, 3H), 0.97 (t, J = 7.6 Hz, 3H); **^{13}C NMR** (125 MHz, Chloroform-d) δ [ppm] 147.64, 139.71, 133.11, 132.00, 126.74, 119.16, 109.79, 22.42, 21.81, 14.16, 13.51..

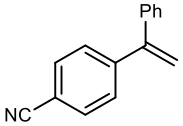

4-(1-phenylvinyl) benzonitrile (5l). The compound was prepared in 99% yield. **^{1}H NMR** (400 MHz, Chloroform-*d*) δ [ppm] 7.66-7.59 (m, 2H), 7.48-7.41 (m, 2H), 7.40-7.32 (m, 3H), 7.32-7.24 (m, 2H), 5.57 (dd, J = 17.3, 0.7 Hz, 2H); **^{13}C NMR** (125 MHz, Chloroform-d) δ [ppm] 148.64, 146.02, 140.14, 132.02, 128.79, 128.41, 128.21, 128.10, 118.81, 116.68, 111.28.

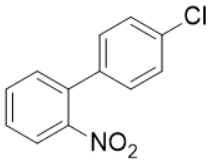

4'-chloro-2-nitro-1,1'-biphenyl (4ae). **^{1}H NMR** (500 MHz, $CDCl_3$) δ 7.91 (dd, J = 8.1, 1.3 Hz, 1H), 7.65 (td, J = 7.5, 1.3 Hz, 1H), 7.53 (ddd, J = 8.0, 7.4, 1.5 Hz, 1H), 7.47 – 7.35 (m, 3H), 7.28 (d, J = 8.3 Hz, 2H). **^{13}C NMR** (126 MHz, $CDCl_3$) δ149.09, 135.94, 135.23, 134.48, 132.53, 131.87, 129.3 0, 128.93, 128.60, 124.29.

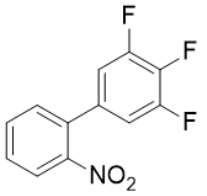

3',4',5'-trifluoro-2-nitro-1,1'-biphenyl (4af). **^{1}H NMR** (500 MHz, $CDCl_3$) δ 7.96 (dd, J = 8.1, 1.3 Hz, 1H), 7.69 (td, J = 7.6, 1.3 Hz, 1H), 7.62 – 7.56 (m, 1H), 7.41 (dd, J = 7.6, 1.5 Hz, 1H), 7.04 – 6.92 (m, 2H). **^{13}C NMR** (126 MHz, $CDCl_3$) δ 151.14 (ddd, J = 251.3, 10.1, 4.2 Hz), 148.72, 139.78 (td, J = 251.3, 15.0 Hz), 133.54, 132.82, 131.67, 129.41, 124.54, 112.61 (d, J = 22.5 Hz), 112.61 (d, J = 11.2 Hz). **^{19}F NMR** (471 MHz, $CDCl_3$) δ -133.43 (d, J = 20.1 Hz), -160.54 (t, J = 20.8 Hz).

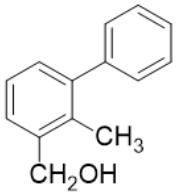

(2-methyl-[1,1'-biphenyl]-3-yl) methanol (4ag). **^{1}H NMR** (500 MHz, $CDCl_3$) δ 7.48 – 7.42 (m, 3H), 7.40 – 7.36 (m, 1H), 7.35 – 7.27 (m, 3H), 7.24 (dd, J = 7.6, 1.6 Hz, 1H), 4.80 (s, 2H), 2.28 (s, 3H). **^{13}C NMR** (126 MHz, $CDCl_3$) δ 142.89, 142.07, 139.25, 133.62, 129.61, 129.40, 128.09, 126.83, 126.78, 125.62, 64.09, 15.91.

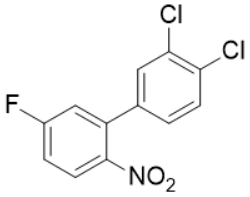

3',4'-dichloro-5-fluoro-2-nitro-1,1'-biphenyl (4ah). **^{1}H NMR** (500 MHz, $CDCl_3$) δ 8.04 (dd, J = 9.0, 5.0 Hz, 1H), 7.53 (d, J = 8.2 Hz, 1H), 7.44 (d, J = 2.1 Hz, 1H), 7.24 (ddd, J = 9.0, 7.3, 2.7 Hz, 1H), 7.15 (dd, J = 8.2, 2.1 Hz, 1H), 7.12 (dd, J = 8.5, 2.8 Hz, 1H). **^{13}C NMR** (126 MHz, $CDCl_3$) δ 164.10 (d, J = 258 Hz), 144.74, 137.32 (d, J = 10 Hz), 136.55, 133.14 (d, J = 22.5 Hz), 130.73, 129.69, 127.43 (d, J = 8.8 Hz), 127.13, 118.89 (d, J = 23.8 Hz), 116.02 (d, J = 23.2 Hz). **^{19}F NMR** (471 MHz, $CDCl_3$) δ -103.57.

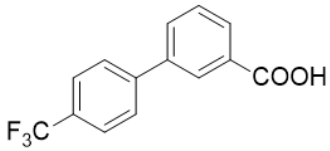

4'-(trifluoromethyl)-[1,1'-biphenyl]-3-carboxylic acid (4ai). **^{1}H NMR** (500 MHz, Methanol-d_4) δ 8.34 (t, J = 1.8 Hz, 1H), 8.09 (dt, J = 7.8, 1.4 Hz, 1H), 7.94 (ddd, J = 7.8, 2.0, 1.1 Hz, 1H), 7.92 – 7.86 (m, 2H), 7.80 (m, 2H), 7.63 (t, J = 7.7 Hz, 1H). **^{13}C NMR** (126 MHz, Methanol-d_4) δ 168.03, 143.82, 139.76, 135.44, 131.45, 131.28, 129.39 (q, J = 32.5 Hz),129.09, 128.95, 127.93, 127.28, 125.53 (q, J = 3.8 Hz) 124.37 (q, J = 270 Hz). **^{19}F NMR** (471 MHz, $CDCl_3$) δ -64.02.

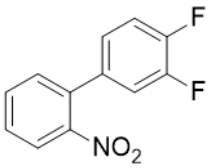

3',4'-difluoro-2-nitro-1,1'-biphenyl (4aj). **^{1}H NMR** (500 MHz, $CDCl_3$) δ 7.92 (dd, J = 8.1, 1.3 Hz, 1H), 7.66 (td, J = 7.5, 1.3 Hz, 1H), 7.55 (td, J = 7.8, 1.4 Hz, 1H), 7.43 (dd, J = 7.8, 1.4 Hz, 1H), 7.30 – 7.15 (m, 2H), 7.07 – 7.04 (m, 1H). **^{13}C NMR** (126 MHz, $CDCl_3$) δ 150.44 (dd, J = 248.8, 12.5 Hz), 150.16 (dd, J = 247.5, 12.5 Hz), 149.00, 134.35 (d, J = 3.8 Hz), 134.29, 132.62, 131.85, 128.93, 124.34, 124.29 (d, J = 3.8 Hz), 117.63 (d, 17.5 Hz). 117.34 (d, 17.5 Hz). **^{19}F NMR** (471 MHz, $CDCl_3$) δ -136.93 (d, J = 21.0 Hz), -138.15 (d, J = 21.6 Hz).

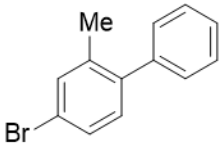

4-bromo-2-methyl-1,1'-biphenyl (4ak). **^{1}H NMR** (500 MHz, $CDCl_3$) δ 7.48 – 7.43 (m, 3H), 7.42 – 7.37 (m, 2H), 7.34 – 7.30 (m, 2H), 7.13 (d, J = 8.1 Hz, 1H), 2.28 (s, 3H). **^{13}C NMR** (126 MHz, $CDCl_3$) δ 140.89, 140.79, 137.67, 133.02, 131.33, 129.04, 128.82, 128.24, 127.15, 121.09, 20.34.

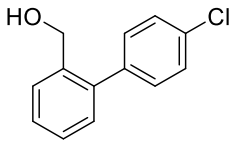

(4'-chloro-[1,1'-biphenyl]-2-yl) methanol (4al). **^{1}H NMR** (400 MHz, Chloroform-d) δ [ppm] 7.57-7.53 (m, 1H), 7.43-7.34 (m, 4H), 7.34-7.29 (m, 2H), 7.28-7.23 (m, 1H), 4.57 (s, 2H), 1.94 (s, 1H); **^{13}C NMR** (125 MHz, Chloroform-d) δ [ppm] 140.08, 138.98, 137.82, 133.31, 130.45, 129.91, 128.58, 128.35, 127.98, 127.76, 62.90.

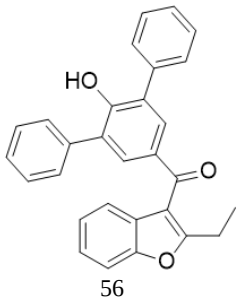

(2-ethylbenzofuran-3-yl) (2'-hydroxy-[1,1':3',1''-terphenyl]-5'-yl) methanone (4am). **^{1}H NMR** (500 MHz, $CDCl_3$) δ 7.88 (s, 2H), 7.61 – 7.57 (m, 5H), 7.54 – 7.48 (m, 5H), 7.45 – 7.41 (m, 2H), 7.35 – 7.26 (m, 2H), 6.00 (s, 1H), 3.02 (q, J = 7.5 Hz, 2H), 1.38 (t, J = 7.5 Hz, 3H). **^{13}C NMR** (126 MHz, $CDCl_3$) δ 190.49, 165.66, 153.65, 136.46, 131.95, 131.71, 129.32, 129.06, 128.92, 128.75, 128.20, 127.21, 124.37, 123.44, 121.32, 116.15, 111.06, 21.88, 12.44.

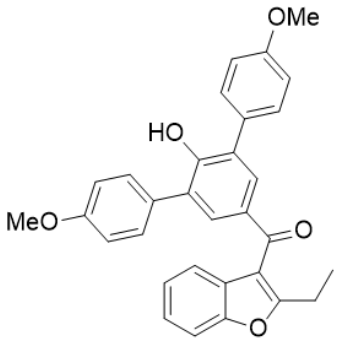

(2-ethylbenzofuran-3-yl) (2'-hydroxy-4,4''-dimethoxy-[1,1':3',1''-terphenyl]-5'-yl) methanone (4an). **^{1}H NMR** (500 MHz, $CDCl_3$) δ 7.83 (s, 2H), 7.62 – 7.58 (m, 1H), 7.54 – 7.49 (m, 4H), 7.39 – 7.25 (m, 2H), 7.08 – 7.00 (m, 4H), 6.03 (s, 1H), 3.86 (s, 6H), 3.01 (q, J = 7.6 Hz, 2H), 1.38 (t, J = 7.5 Hz, 3H). **^{13}C NMR** (126 MHz, $CDCl_3$) δ 190.66, 165.59, 159.50, 153.88, 153.70, 131.80, 131.29, 130.51, 128.68, 128.52, 127.26, 124.35, 123.42, 121.35, 116.20, 116.09, 114.48, 111.05, 55.36, 21.87, 12.44.

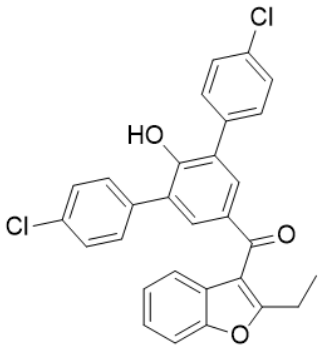

(4,4''-dichloro-2'-hydroxy-[1,1':3',1''-terphenyl]-5'-yl) (2-ethylbenzofuran-3-yl) methanone (4ao). **^{1}H NMR** (500 MHz, $CDCl_3$) δ 7.83 (s, 2H), 7.53 – 7.43 (m, 10H), 7.32 (ddd, J = 8.5, 7.3, 1.4 Hz, 1H), 7.28 – 7.23 (m, 1H), 3.00 (q, J = 7.5 Hz, 2H), 1.36 (t, J = 7.5 Hz, 3H). **^{13}C NMR** (126 MHz, $CDCl_3$) δ 190.16, 165.98, 153.71, 153.38, 134.67, 134.42, 132.16, 131.80, 130.66, 129.30, 127.92, 127.05, 124.47, 123.46, 121.17, 115.96, 111.18, 21.86, 12.40.

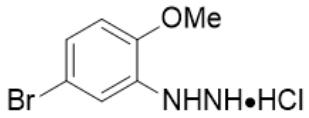

(5-bromo-2-methoxyphenyl) hydrazine. **^{1}H NMR** (500 MHz, Methanol-d4) δ 7.31 – 7.16 (m, 2H), 6.98 (d, J = 8.6 Hz, 1H), 3.92 (s, 3H). **^{13}C NMR** (126 MHz, Methanol-d_4) δ 148.22, 134.99, 126.04, 117.85, 112.46, 55.23.

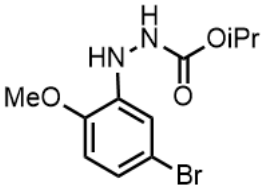

isopropyl 2-(5-bromo-2-methoxyphenyl) hydrazine-1-carboxylate (1aa). **^{1}H NMR** (500 MHz, $CDCl_3$) δ 6.98 (d, J = 2.4 Hz, 1H), 6.94 (dd, J = 8.5, 2.4 Hz, 1H), 6.67 (d, J = 8.5 Hz, 1H), 6.44 (s, 1H), 6.25 (s, 1H), 4.99 (p, J = 6.2 Hz, 1H), 3.85 (s, 3H), 1.42 – 1.04 (m, 6H). **^{13}C NMR** (126 MHz, $CDCl_3$) δ 156.50, 145.96, 138.91, 122.69, 114.95, 113.60, 111.52, 69.86, 55.77, 22.03.

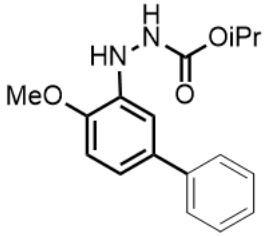

isopropyl 2-(4-methoxy-[1,1'-biphenyl]-3-yl) hydrazine-1-carboxylate (bifenazate). **^{1}H NMR** (500 MHz, $CDCl_3$) δ 7.58 – 7.54 (m, 2H), 7.42 (dd, J = 8.5, 7.0 Hz, 2H), 7.35 – 7.30 (m, 1H), 7.12 (d, J = 2.2 Hz, 1H), 7.10 (dd, J = 8.2, 2.3 Hz, 1H), 6.91 (d, J = 8.3 Hz, 1H), 6.46 (s, 1H), 6.32 (s, 1H), 4.99 (p, J = 6.2 Hz, 1H), 3.92 (s, 3H), 1.41 – 1.10 (m, 6H). **^{13}C NMR** (126 MHz, $CDCl_3$) δ 156.72, 146.64, 141.40, 137.75, 134.36, 128.63, 126.92, 126.67, 119.17, 111.11, 110.49, 69.62, 55.75, 22.06.

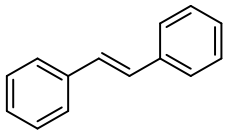

(E)-1,2-diphenylethene (8a). The compound was prepared in 99% yield. **^{1}H NMR** (500 MHz, Chloroform-*d*) δ [ppm] 7.54 (dd, J = 8.2, 1.3 Hz, 4H), 7.38 (dd, J = 8.5, 6.9 Hz, 4H), 7.30-7.26 (m, 2H), 7.13 (s, 2H); **^{13}C NMR** (125 MHz, Chloroform-d) δ [ppm] 137.29, 128.65, 127.59, 126.48.

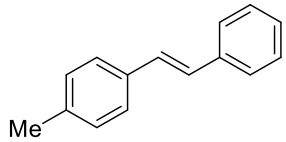

(E)-1-methyl-4-styrylbenzene (8b). The compound was prepared in 97% and 92% yield when X=I and Br, respectively. **^{1}H NMR** (400 MHz, Chloroform-*d*) δ [ppm] 7.55-7.50 (m, 2H), 7.47-7.41 (m, 2H), 7.41-7.35 (m, 2H), 7.30-7.24 (m, 1H), 7.20 (d, J = 7.9 Hz, 2H), 7.16-7.05 (m, 2H), 2.39 (s, 3H); **^{13}C NMR** (125 MHz, Chloroform-d) δ [ppm] 137.49, 134.52, 129.37, 128.62, 128.60, 127.67, 127.38, 126.41, 126.37, 21.23.

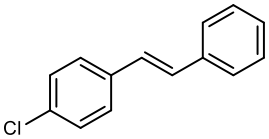

(E)-1-chloro-4-styrylbenzene (8c). The compound was prepared in 99% yield. **^{1}H NMR** (500 MHz, Chloroform-*d*) δ [ppm] 7.56-7.50 (m, 2H), 7.45 (d, J = 8.5 Hz, 2H), 7.39 (dd, J = 8.4, 6.9 Hz, 2H), 7.36-7.32 (m, 2H), 7.32-7.28 (m, 1H), 7.12-7.04 (m, 2H); **^{13}C NMR** (125 MHz, Chloroform-d) δ [ppm] 136.92, 135.78, 133.10, 129.25, 128.78, 128.68, 127.81, 127.61, 127.29, 126.50.

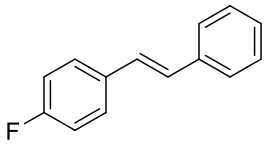

(E)-1-fluoro-4-styrylbenzene (8d). The compound was prepared in 85% yield. **^{1}H NMR** (400 MHz, Chloroform-*d*) δ [ppm] 7.55-7.46 (m, 4H), 7.42-7.34 (m, 2H), 7.32-7.26 (m, 1H), 7.13-6.98 (m, 4H); **^{13}C NMR** (125 MHz, Chloroform-d) δ [ppm] 162.31 (d, J = 245.7 Hz), 137.14, 133.48 (d, J = 3.2 Hz), 128.68, 128.46 (d, J = 2.1 Hz), 127.96 (d, J = 7.9 Hz), 127.64, 127.44, 126.42, 115.59 (d, J = 21.5 Hz). **^{19}F NMR** (377 MHz, Chloroform-d) δ [ppm] -114.20.

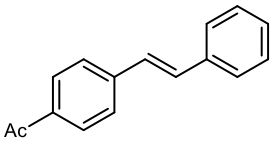

(E)-1-(4-styrylphenyl) ethan-1-one (8e). The compound was prepared in 80% yield. **^{1}H NMR** (400 MHz, Chloroform-*d*) δ 7.98-7.93 (m, 2H), 7.61-7.50 (m, 4H), 7.42-7.34 (m, 2H), 7.33-7.28 (m, 1H), 7.23 (d, J = 16.4 Hz, 1H), 7.13 (d, J = 16.4 Hz, 1H), 2.61 (s, 3H); **^{13}C NMR** (125 MHz, Chloroform-d) δ [ppm] 197.48, 141.99, 136.67, 135.92, 131.45, 128.86, 128.78, 128.30, 127.42, 126.80, 126.48, 26.57.

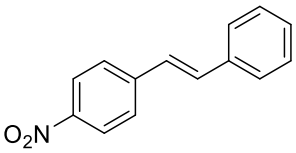

(E)-1-nitro-4-styrylbenzene (8f). The compound was prepared in 99% yield. **^{1}H NMR** (500 MHz, Chloroform-*d*) δ [ppm] 8.28-8.12 (m, 2H), 7.68-7.59 (m, 2H), 7.59-7.51 (m, 2H), 7.45-7.37 (m, 2H), 7.37-7.31 (m, 1H), 7.27 (d, J = 16.4 Hz, 1H), 7.14 (d, J = 16.3 Hz, 1H); **^{13}C NMR** (125 MHz, Chloroform-d) δ [ppm] 146.71, 143.80, 136.13, 133.26, 128.86, 128.81, 126.98, 126.81, 126.23, 124.10.

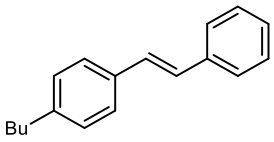

(E)-1-butyl-4-styrylbenzene (8g). The compound was prepared in 53% yield. **^{1}H NMR** (500 MHz, Chloroform-*d*) δ [ppm] 7.55-7.47 (m, 2H), 7.43 (d, J = 8.1 Hz, 2H), 7.39-7.30 (m, 2H), 7.28-7.22 (m, 1H), 7.18 (d, J = 8.1 Hz, 2H), 7.13-7.04 (m, 2H), 2.67-2.58 (m, 2H), 1.63 (ddd, J = 15.3, 11.0, 7.5 Hz, 2H), 1.39 (dq, J = 14.7, 7.4 Hz, 2H), 0.95 (t, J = 7.4 Hz, 3H); **^{13}C NMR** (125 MHz, Chloroform-d) δ [ppm] 142.62, 137.66, 134.87, 128.76, 128.64, 127.84, 127.38, 126.45, 126.42, 35.42, 33.53, 22.34, 13.90.

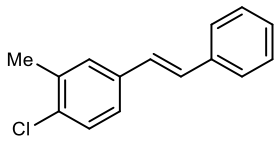

(E)-1-chloro-2-methyl-4-styrylbenzene (8h). The compound was prepared in 60% yield. **^{1}H NMR** (500 MHz, Chloroform-*d*) δ [ppm] 7.56-7.47 (m, 3H), 7.37 (t, J = 7.6 Hz, 2H), 7.32-7.24 (m, 2H), 7.21 (d, J = 7.8 Hz, 1H), 7.04 (q, J = 16.3 Hz, 2H), 2.38 (s, 3H); **^{13}C NMR** (125 MHz, Chloroform-d) δ [ppm] 137.00, 136.71, 135.20, 134.69, 131.08, 129.07, 128.70, 127.79, 127.18, 126.77, 126.52, 124.72, 19.83.

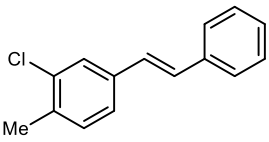

(E)-2-chloro-1-methyl-4-styrylbenzene (8i). The compound was prepared in 50% yield. **^{1}H NMR** (400 MHz, Chloroform-*d*) δ [ppm] 7.54-7.48 (m, 3H), 7.42-7.33 (m, 2H), 7.32-7.26 (m, 2H), 7.23-7.19 (m, 1H), 7.11-6.98 (m, 2H), 2.39 (s, 3H); **^{13}C NMR** (125 MHz, Chloroform-d) δ [ppm] 136.99, 136.70, 135.19, 134.68, 131.07, 129.06, 128.69, 127.78, 127.16, 126.76, 126.51, 124.71, 19.82.

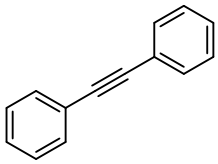

1,2-diphenylethyne (9a). The compound was prepared in 98% and 68% yield when X=I and Br, respectively. **^{1}H NMR** (400 MHz, Chloroform-*d*) δ [ppm] 7.60-7.50 (m, 2H), 7.43-7.30 (m, 3H); **^{13}C NMR** (125 MHz, Chloroform-d) δ [ppm] 131.59, 128.32, 128.23, 123.25, 89.35.

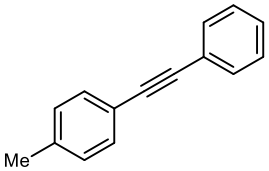

1-methyl-4-(phenylethynyl) benzene (9b). The compound was prepared in 97% and 57% yield when X=I and Br, respectively. **^{1}H NMR** (500 MHz, Chloroform-*d*) δ [ppm] 7.55-7.51 (m, 2H), 7.43 (d, J = 8.1 Hz, 2H), 7.37-7.30 (m, 3H), 7.16 (d, J = 7.9 Hz, 2H), 2.37 (s, 3H); **^{13}C NMR** (125 MHz, Chloroform-d) δ [ppm] 138.38, 131.53, 131.48, 129.10, 128.30, 128.06, 123.46, 120.17, 89.53, 88.69, 21.50.

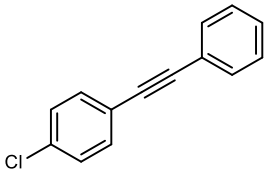

1-chloro-4-(phenylethynyl) benzene (9c). The compound was prepared in 99% yield. **^{1}H NMR** (500 MHz, Chloroform-*d*) δ [ppm] 7.59-7.50 (m, 2H), 7.50-.44 (m, 2H), 7.40-7.29 (m, 5H); **^{13}C NMR** (125

MHz, Chloroform-d) δ [ppm] 134.23, 132.78, 131.57, 128.66, 128.46, 128.37, 122.90, 121.76, 90.30, 88.22.

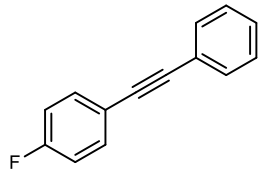

1-fluoro-4-(phenylethynyl) benzene (9d). The compound was prepared in 99% yield. **^{1}H NMR** (500 MHz, Chloroform-*d*) *δ* [ppm] 7.57-7.50 (m, 4H), 7.39-7.32 (m, 3H), 7.09-7.02 (m, 2H); **^{13}C NMR** (125 MHz, Chloroform-d) δ [ppm] 162.48 (d, J = 248.1 Hz), 133.46 (d, J = 8.3 Hz), 131.54, 128.36, 128.32, 123.07, 119.36 (d, J = 3.3 Hz), 115.63 (d, J = 22.0 Hz), 89.02, 88.26. **^{19}F NMR** (377 MHz, Chloroform-d) δ [ppm] -110.94.

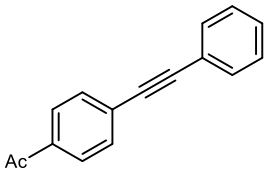

1-(4-(phenylethynyl)phenyl)ethan-1-one (9e). The compound was prepared in 99% and 56% yield when X=I and Br, respectively. **^{1}H NMR** (500 MHz, Chloroform-*d*) *δ* [ppm] 8.01-7.88 (m, 2H), 7.65-7.58 (m, 2H), 7.58-7.53 (m, 2H), 7.41-7.33 (m, 3H), 2.61 (s, 3H); **^{13}C NMR** (125 MHz, Chloroform-d) δ [ppm] 197.28, 136.14, 131.70, 131.65, 128.78, 128.41, 128.23, 128.16, 122.61, 92.68, 88.57, 26.59.

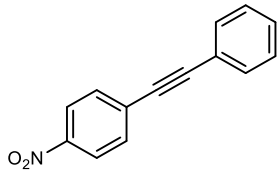

1-nitro-4-(phenylethynyl) benzene (9f). The compound was prepared in 99% yield. **^{1}H NMR** (500 MHz, Chloroform-*d*) *δ* [ppm] 8.27-8.17 (m, 2H), 7.71-7.63 (m, 2H), 7.61-7.51 (m, 2H), 7.44-7.34 (m, 3H); **^{13}C NMR** (125 MHz, Chloroform-d) δ [ppm] 146.95, 132.24, 131.82, 130.24, 129.26, 128.52, 123.61, 122.07, 94.68, 87.52.

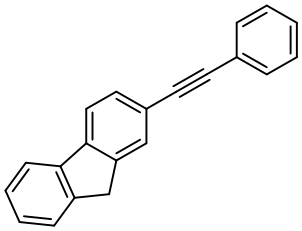

2-(phenylethynyl)-9H-fluorene (9g). The compound was prepared in 42% yield. **^{1}H NMR** (400 MHz, Chloroform-*d*) *δ* [ppm] 7.81-7.74 (m, 2H), 7.74-7.70 (m, 1H), 7.62-7.51 (m, 4H), 7.43-7.30 (m, 5H), 3.92 (s, 2H); **^{13}C NMR** (125 MHz, Chloroform-d) δ [ppm] 143.56, 143.19, 141.88, 141.09, 131.56, 130.50, 128.35, 128.16, 128.13, 127.15, 126.91, 125.09, 123.45, 121.27, 120.18, 119.78, 90.15, 89.37,

36.74.

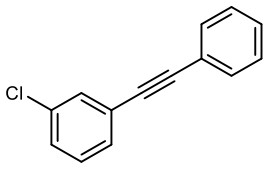

1-chloro-3-(phenylethynyl) benzene (9h). The compound was prepared in 56% yield. **^{1}H NMR** (500 MHz, Chloroform-*d*) *δ* [ppm] 7.55-7.50 (m, 3H), 7.41 (dt, J = 7.3, 1.4 Hz, 1H), 7.39-7.33 (m, 3H), 7.33-7.27 (m, 2H); **^{13}C NMR** (125 MHz, Chloroform-d) δ [ppm] 134.22, 131.69, 131.47, 129.71, 129.54, 128.60, 128.49, 128.40, 125.08, 122.82, 90.57, 87.93.

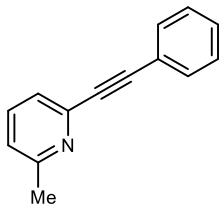

2-methyl-6-(phenylethynyl) pyridine (9i). The compound was prepared in 59% yield. **^{1}H NMR** (500 MHz, Chloroform-*d*) *δ* [ppm] 8.01-7.88 (m, 2H), 7.65-7.58 (m, 2H), 7.58-7.53 (m, 2H), 7.41-7.33 (m, 3H), 2.61 (s, 3H); **^{13}C NMR** (125 MHz, Chloroform-d) δ [ppm] 158.85, 142.50, 136.61, 132.09, 128.90, 128.32, 124.45, 122.69, 122.33, 89.32, 88.51, 24.42.

^{1}H and ^{13}C-NMR spectra of product 4a.

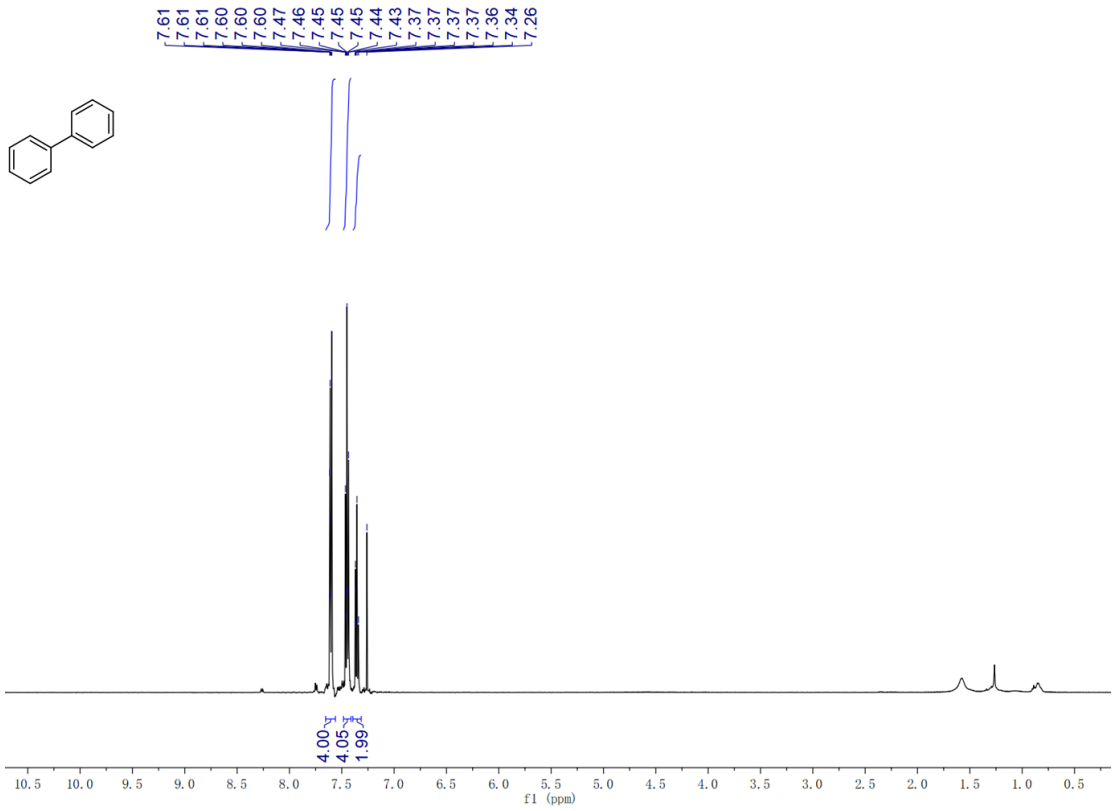

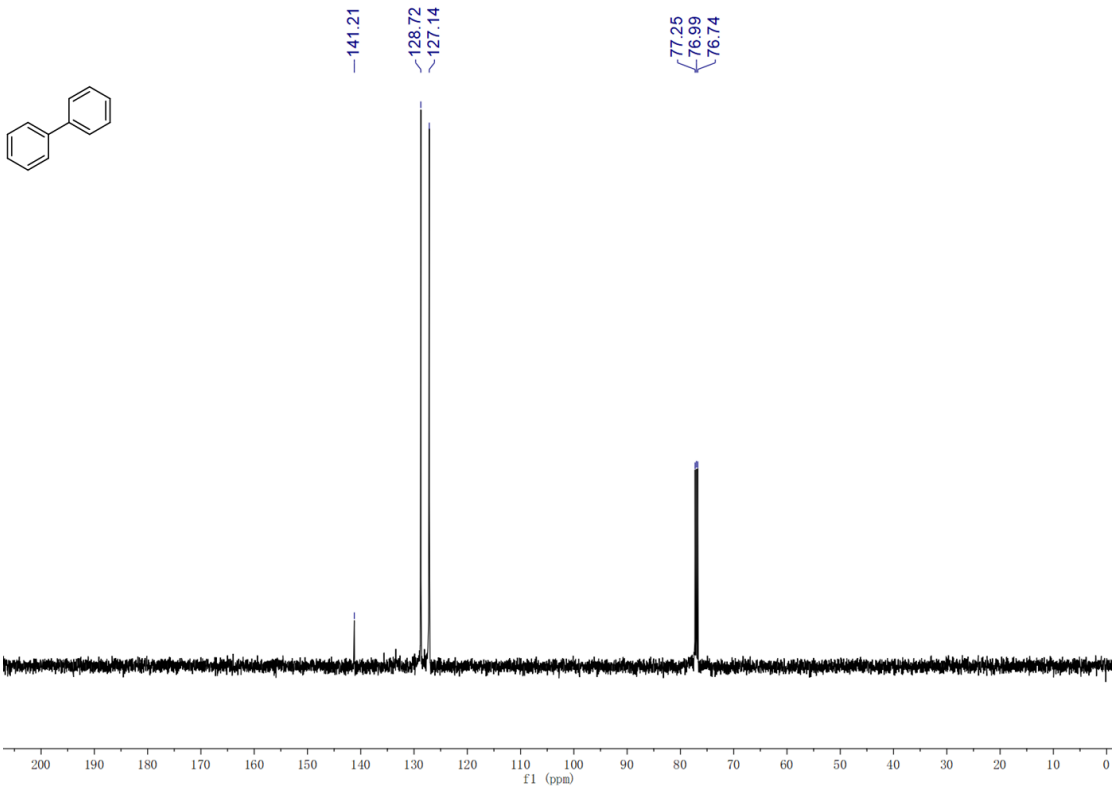

^{1}H and ^{13}C, ^{19}F-NMR spectra of product 4b.

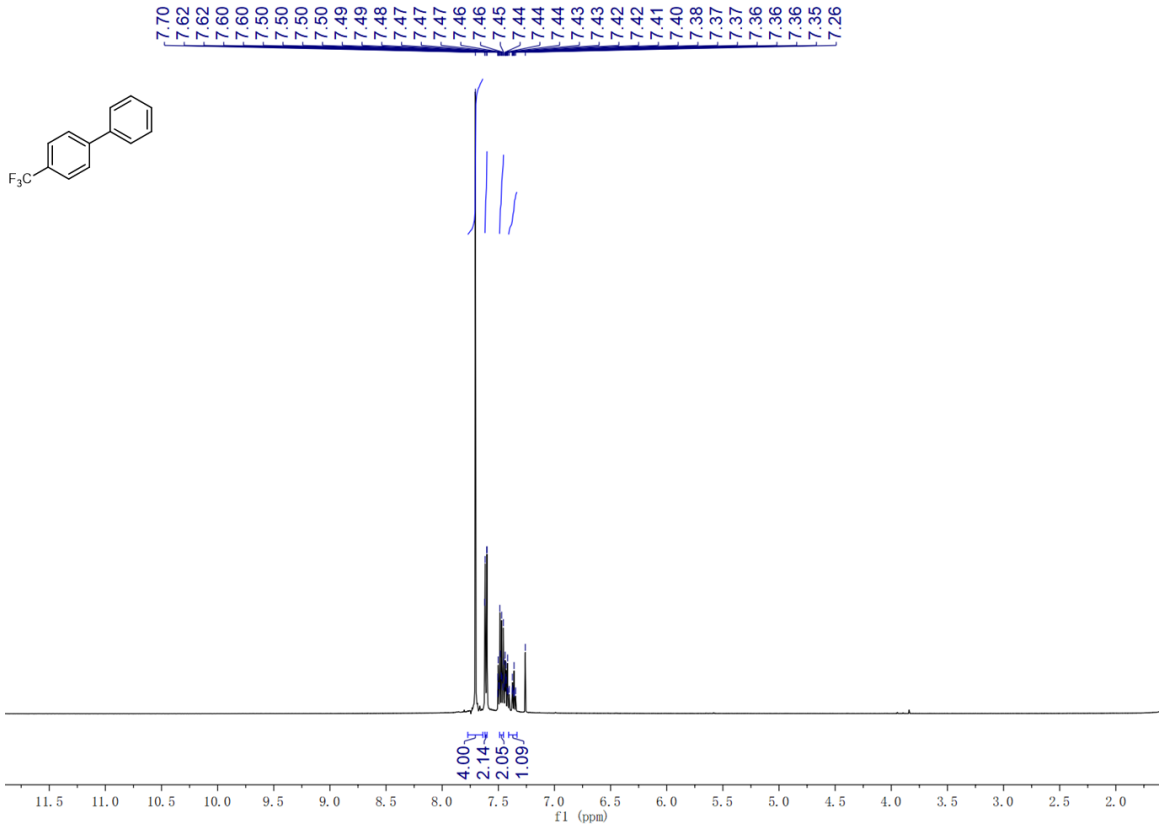

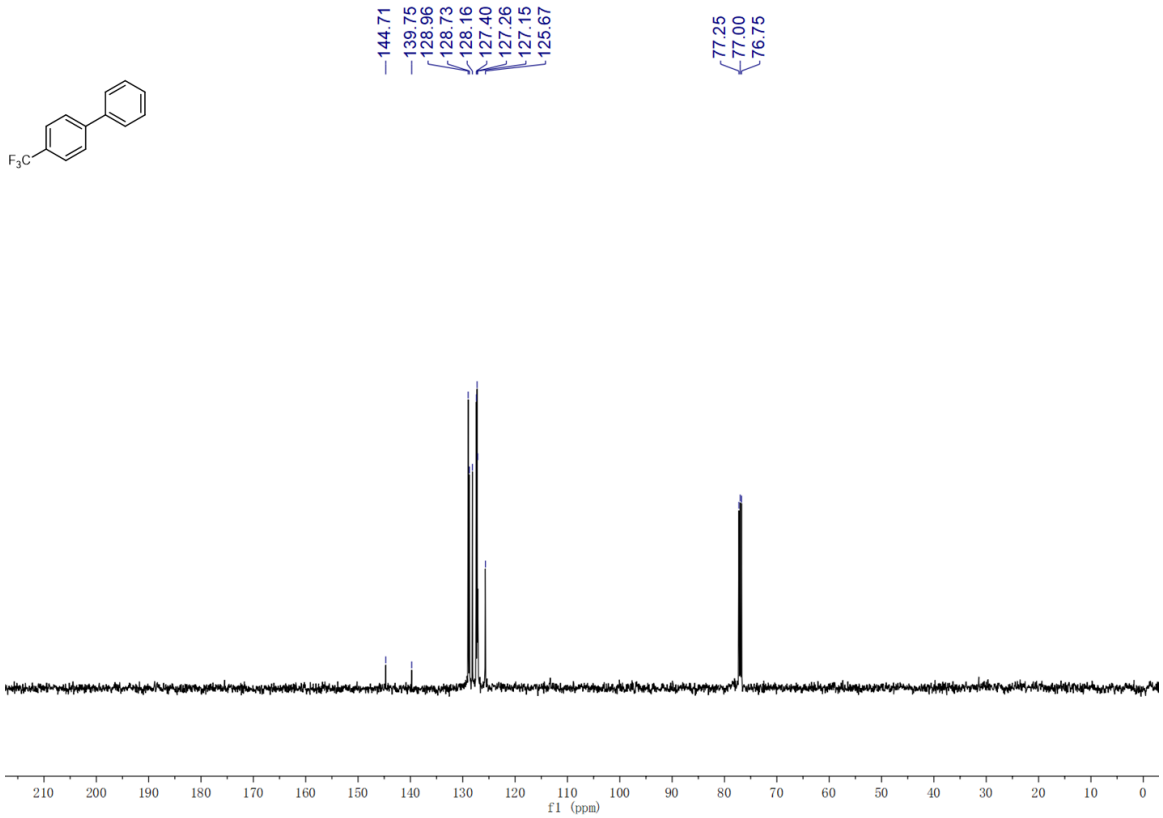

1046

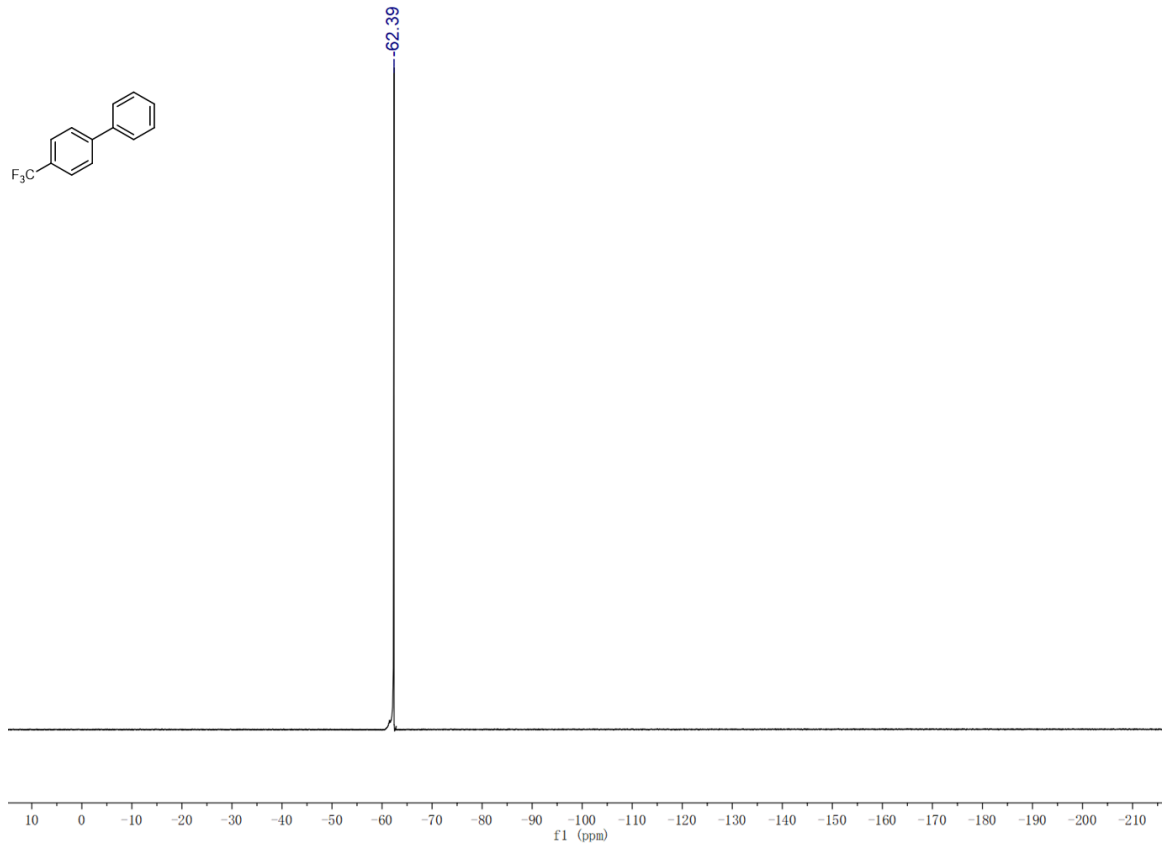

1047

1048

^{1}H and ^{13}C-NMR spectra of product 4c.

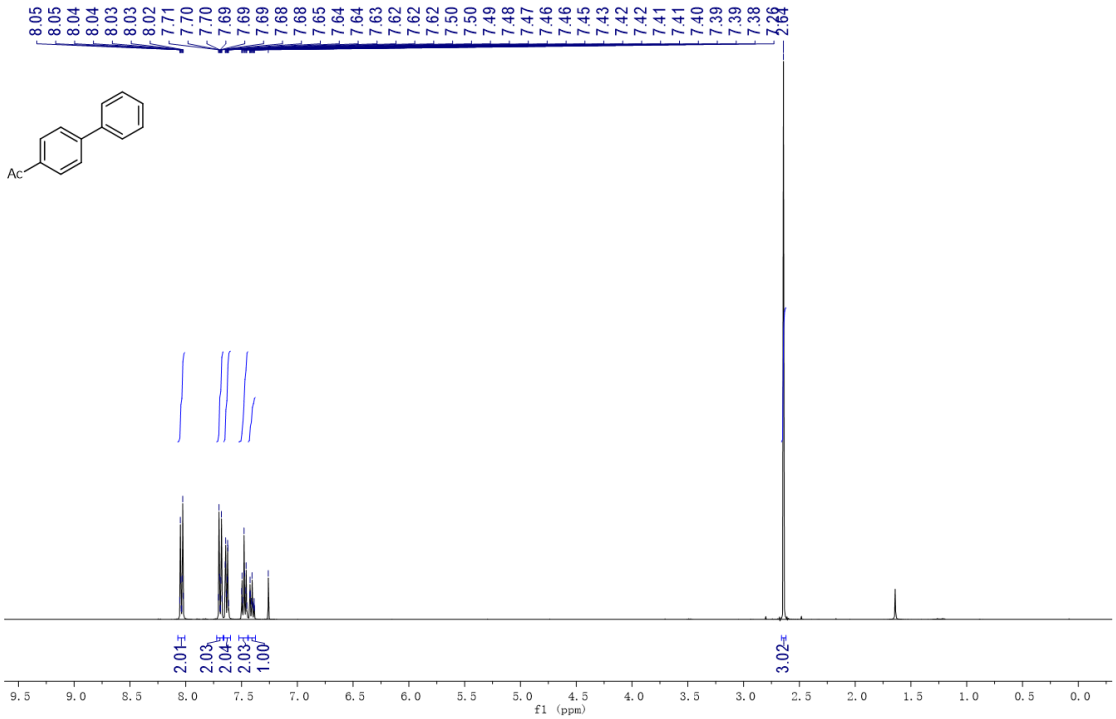

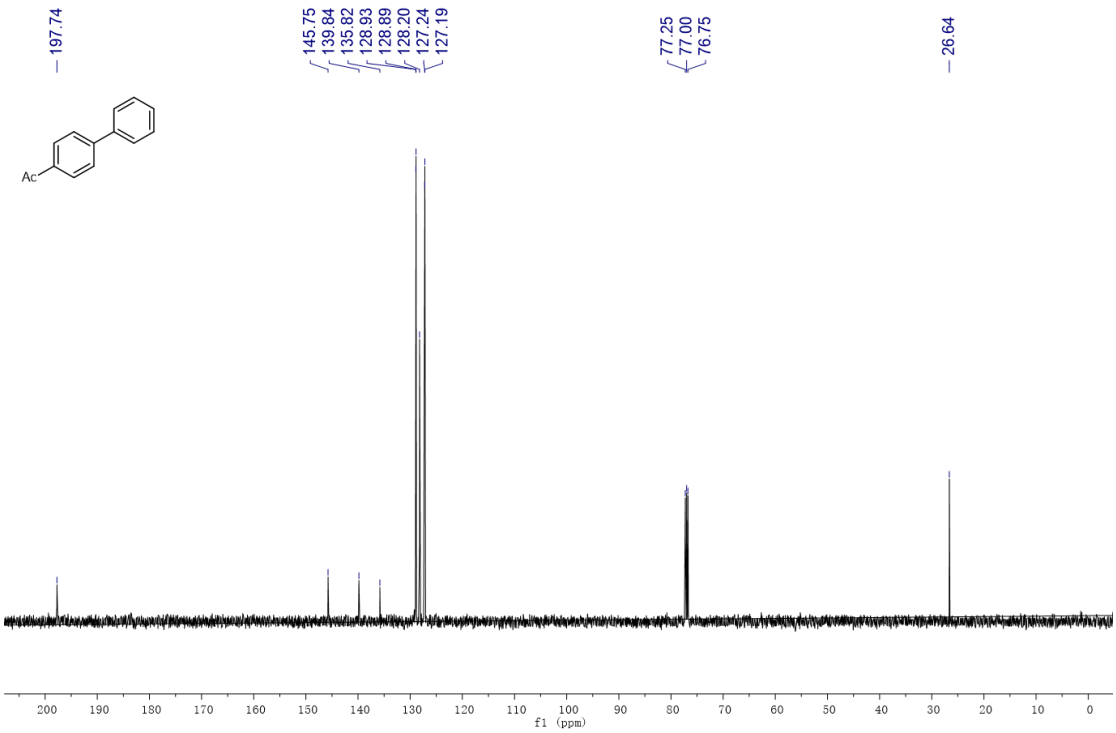

^{1}H and ^{13}C-NMR spectra of product 4d.

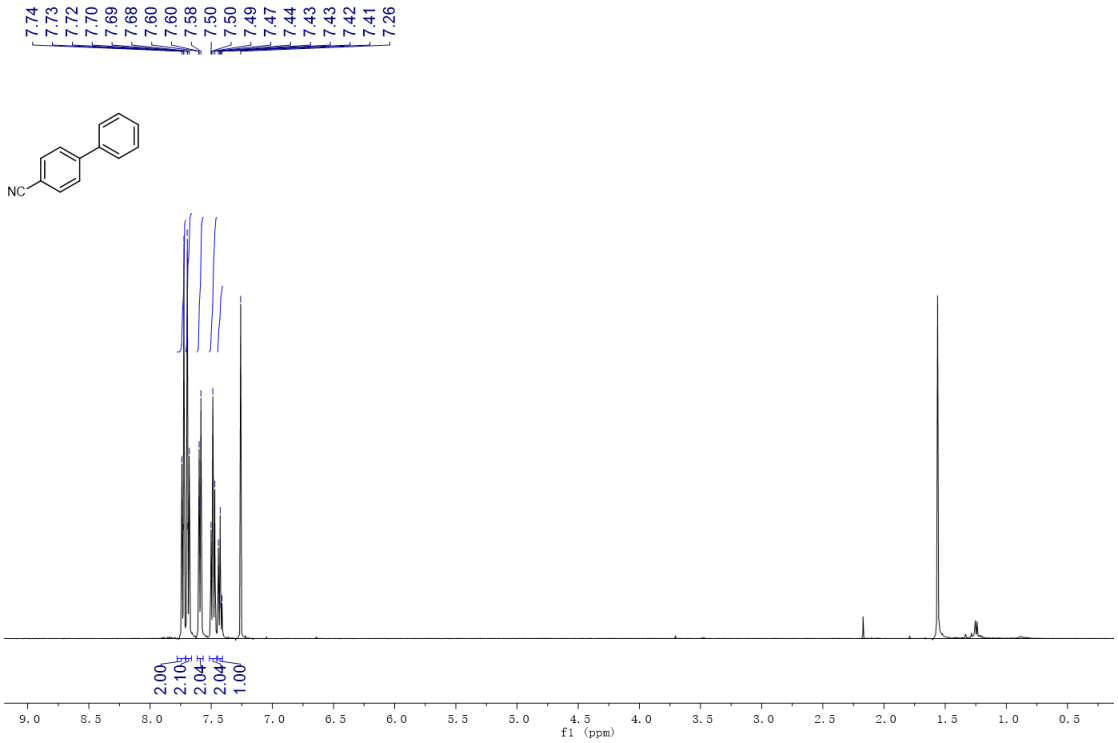

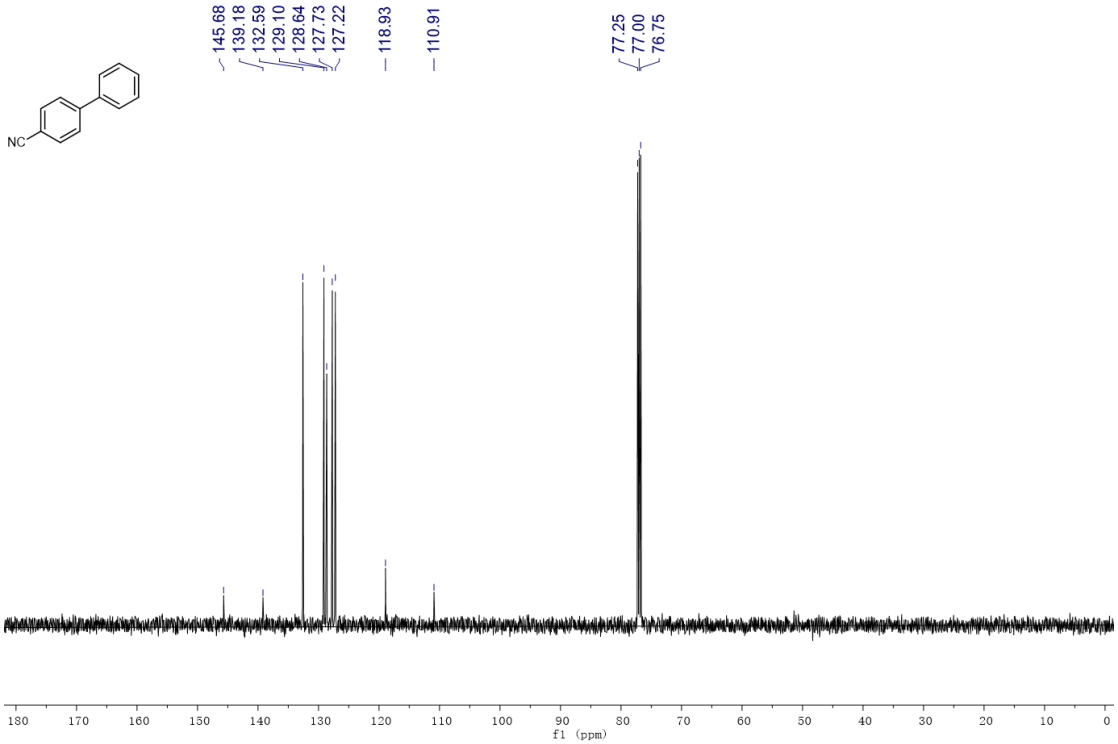

^{1}H and ^{13}C-NMR spectra of product 4e.

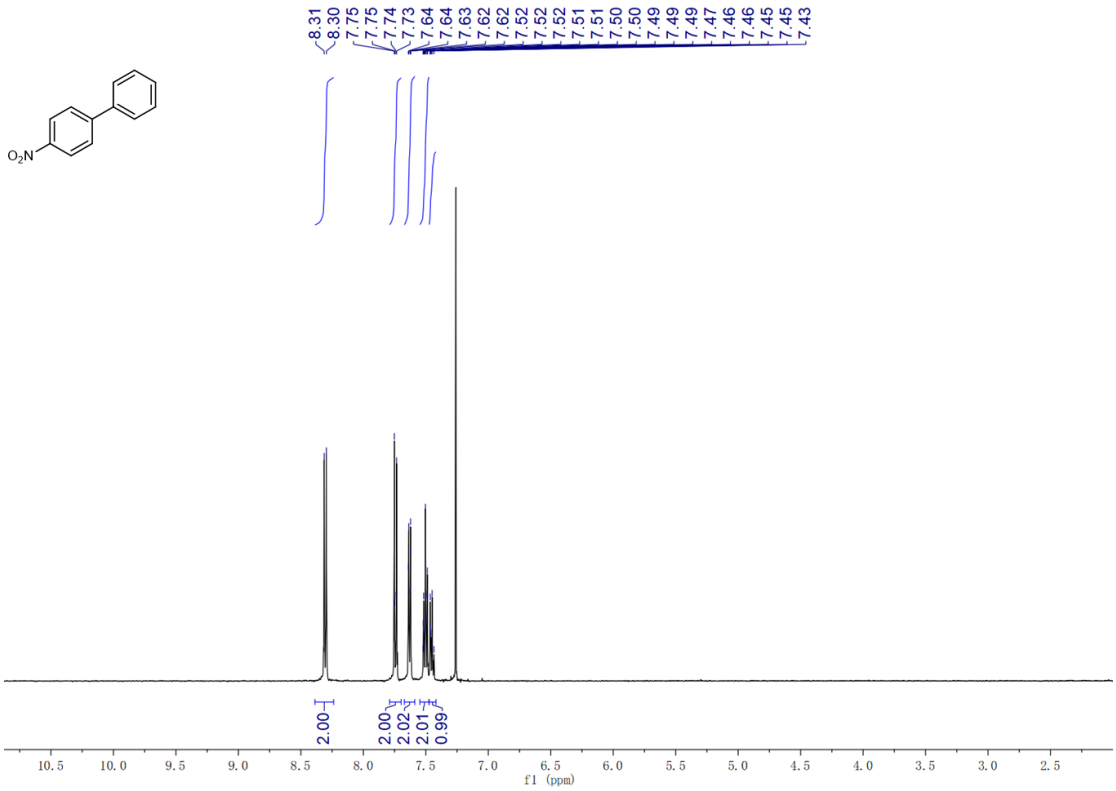

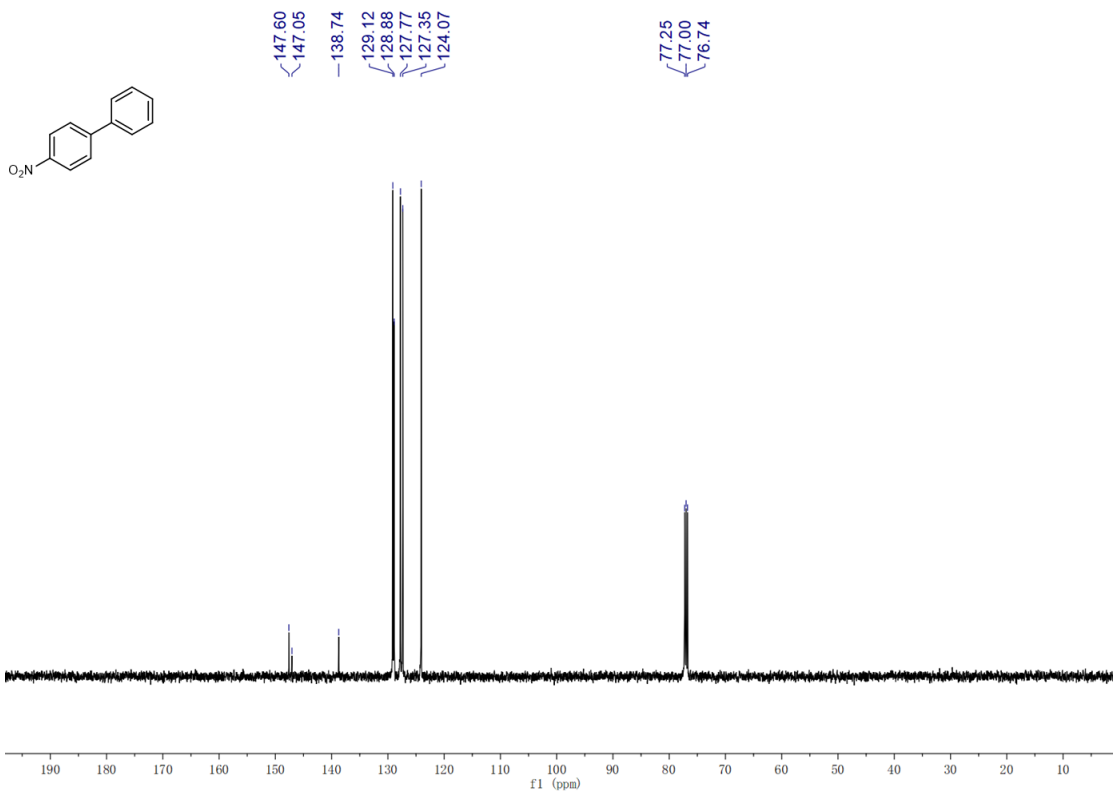

^{1}H and ^{13}C-NMR spectra of product 4f.

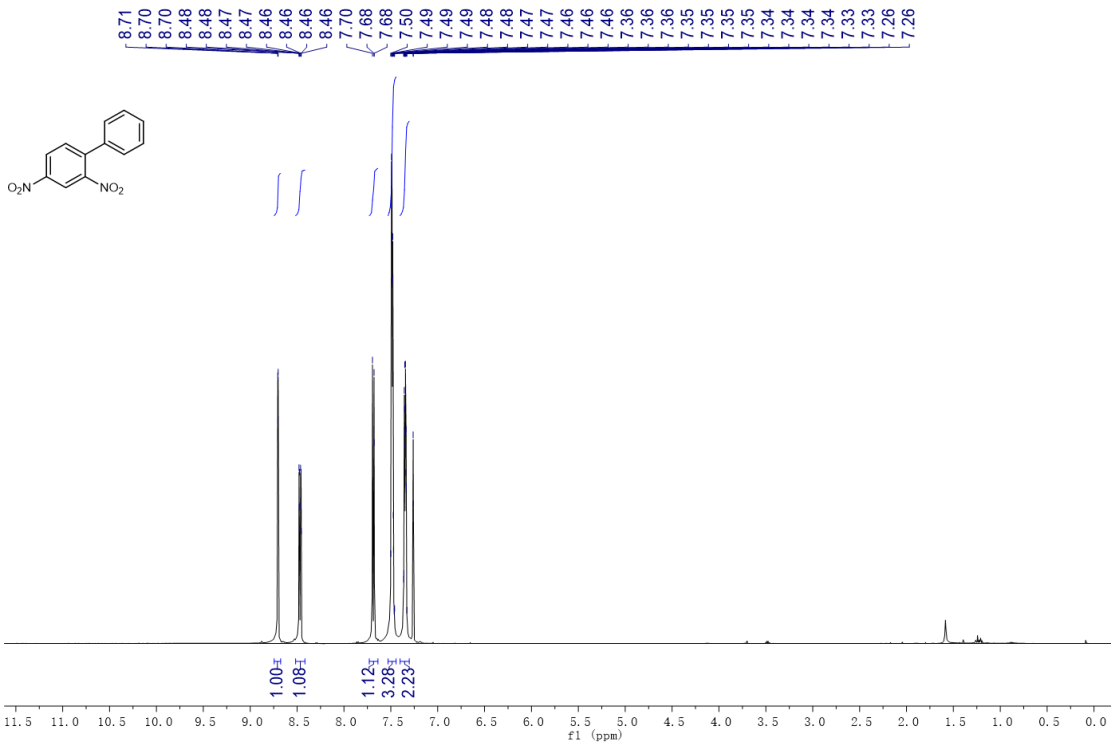

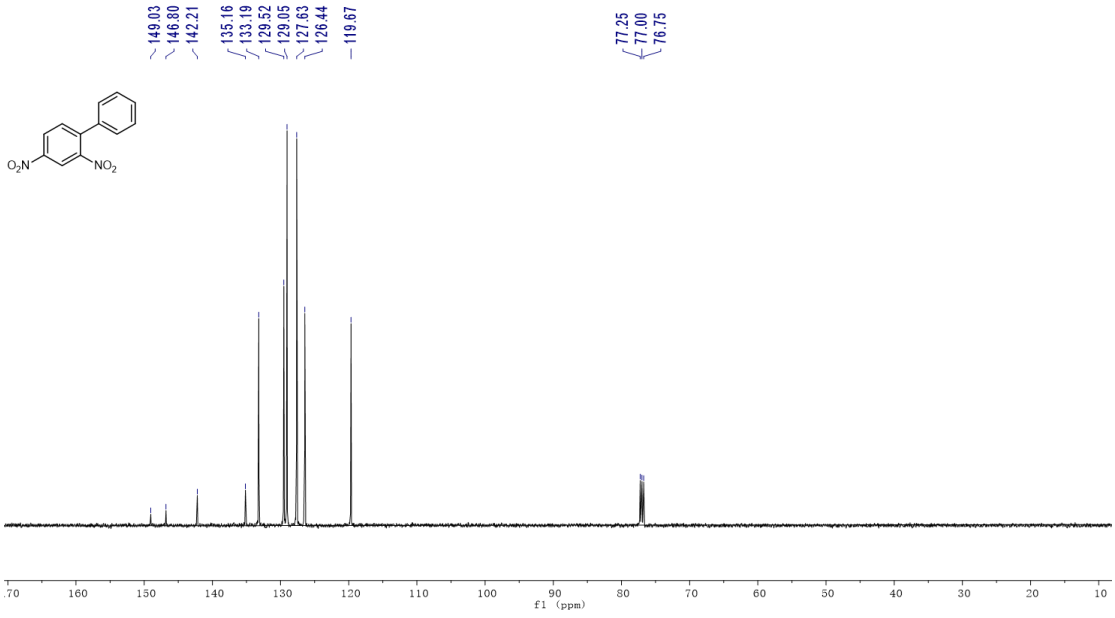

^{1}H and ^{13}C-NMR spectra of product 4g.

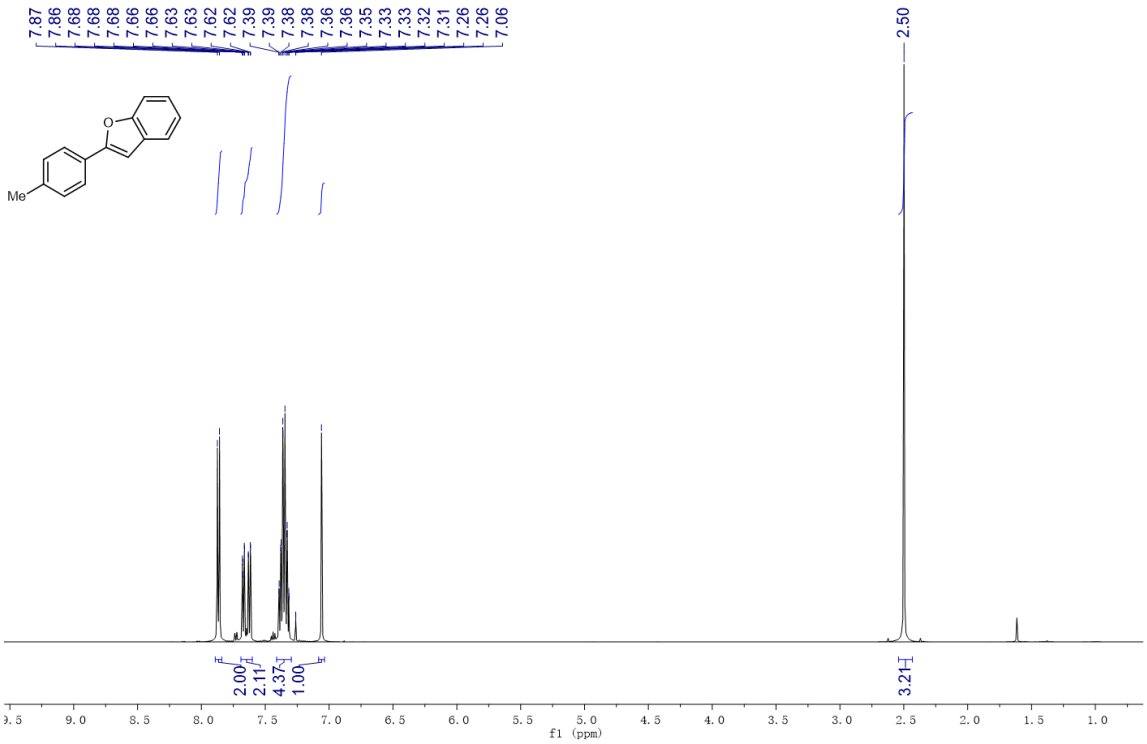

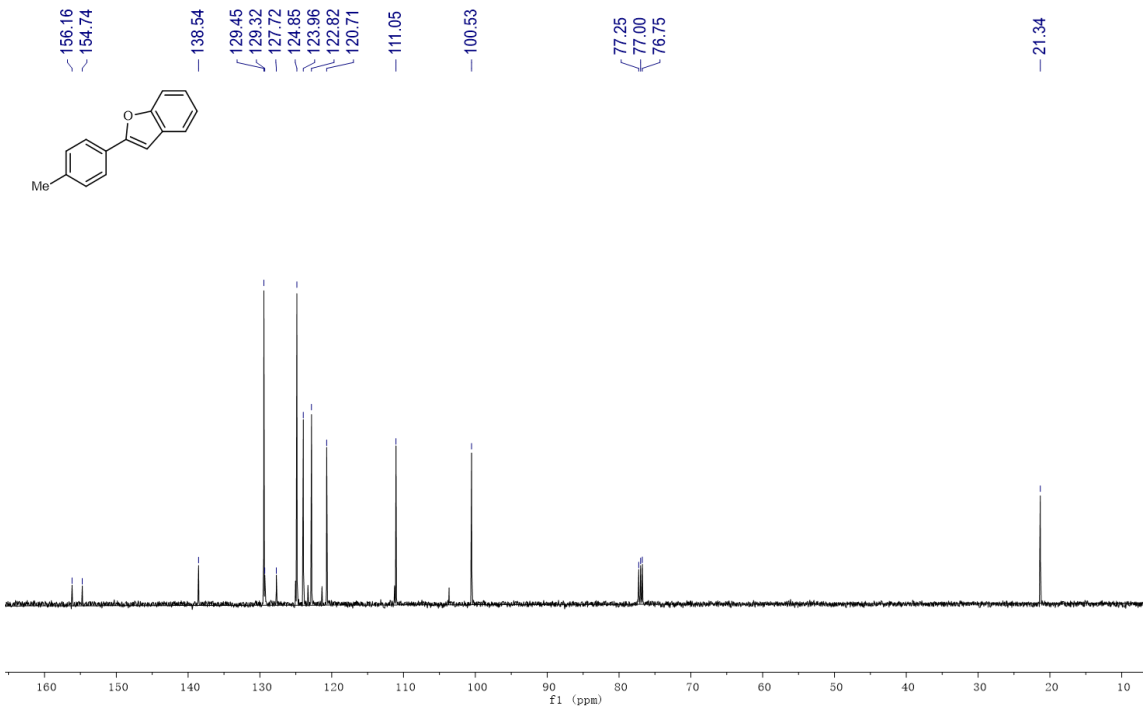

^{1}H and ^{13}C-spectra of product 4h.

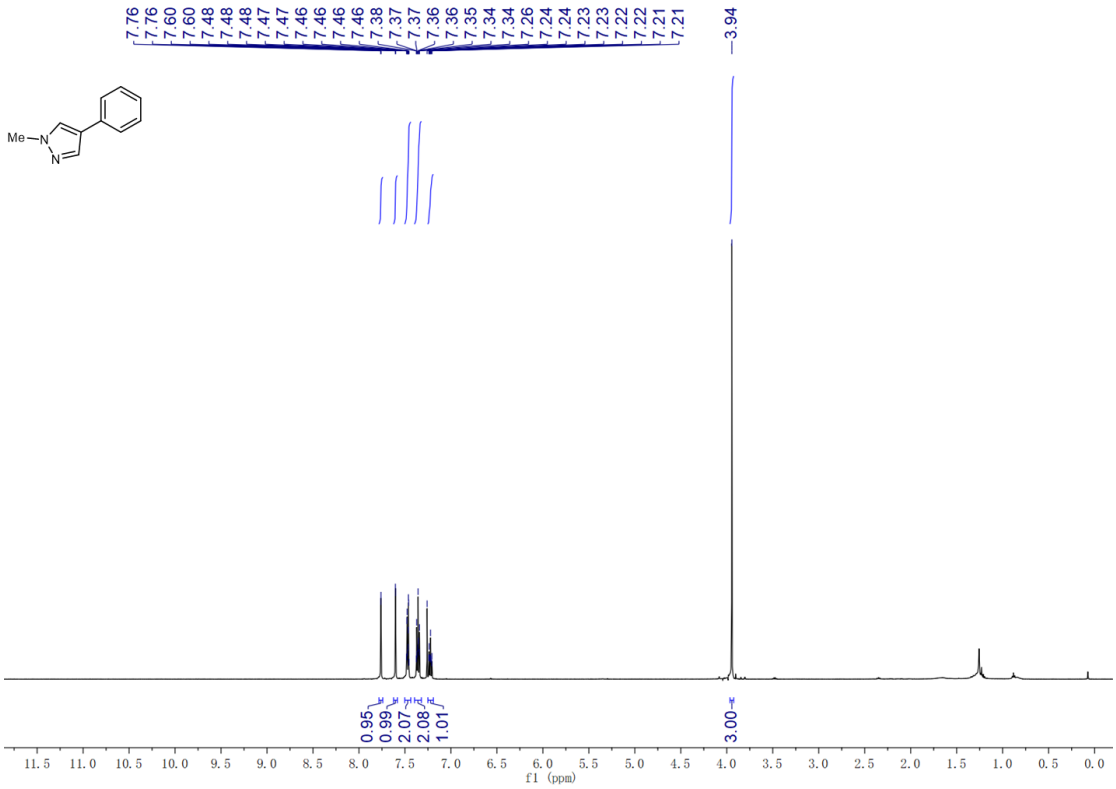

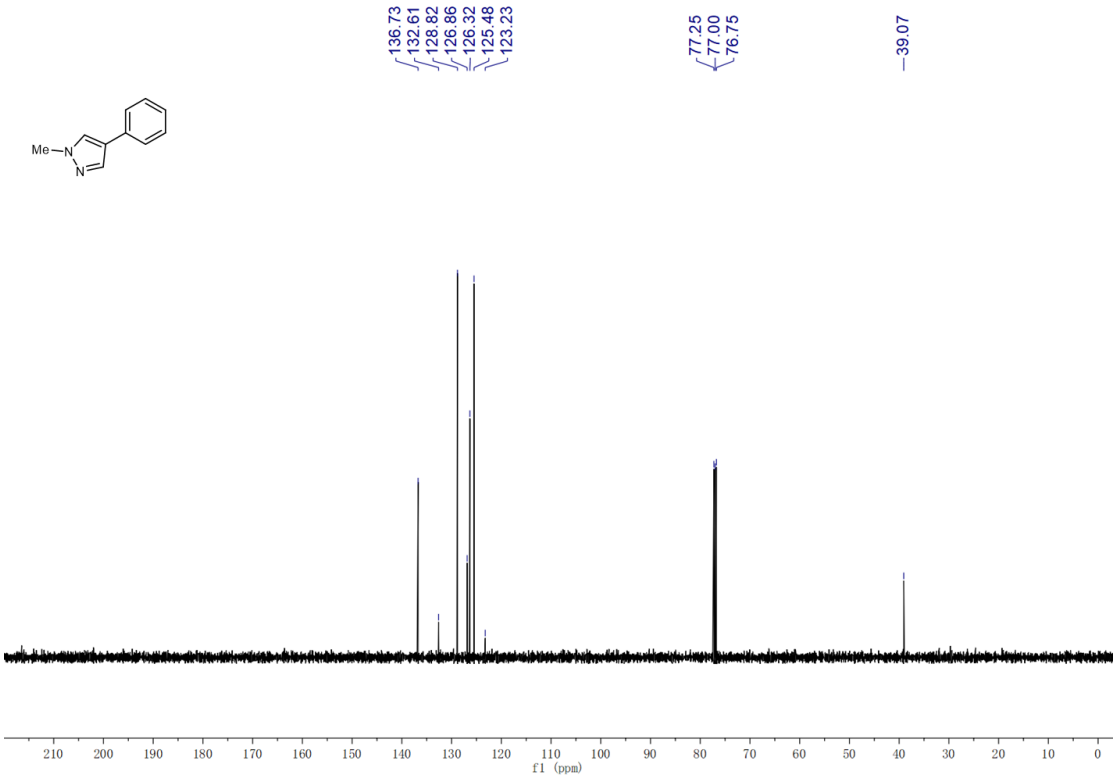

^{1}H, ^{13}C-NMR spectra of product 4i.

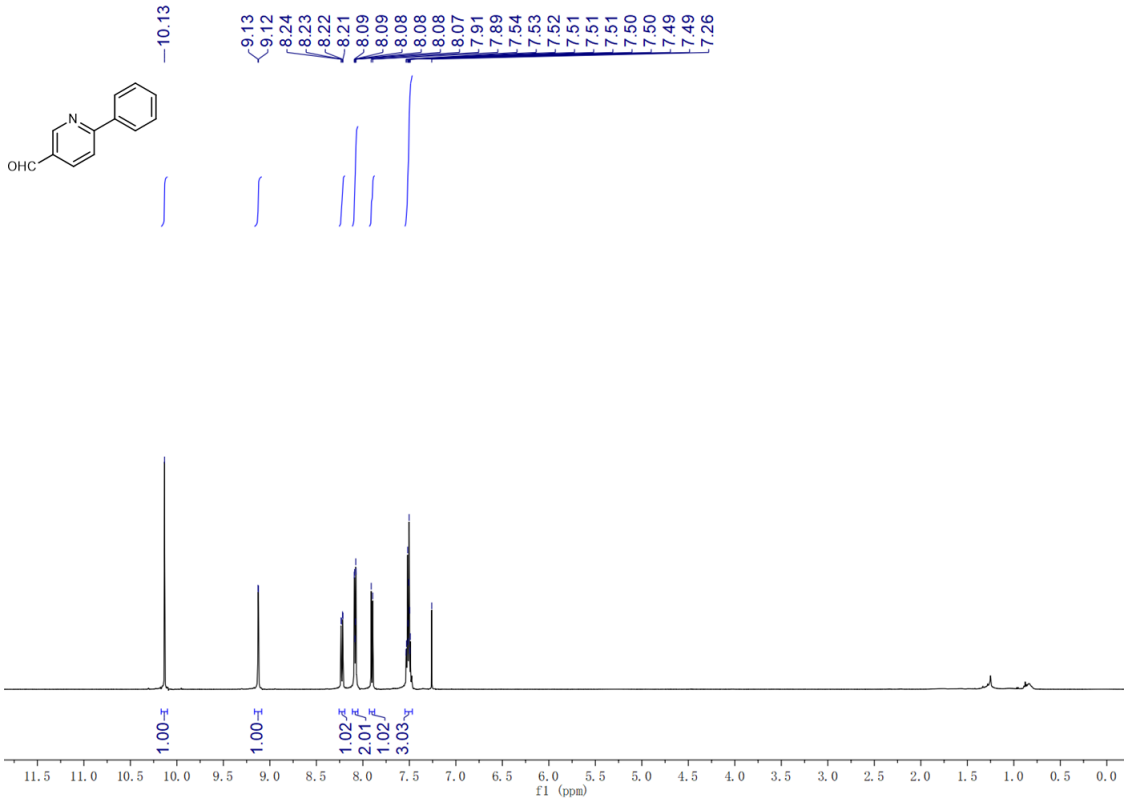

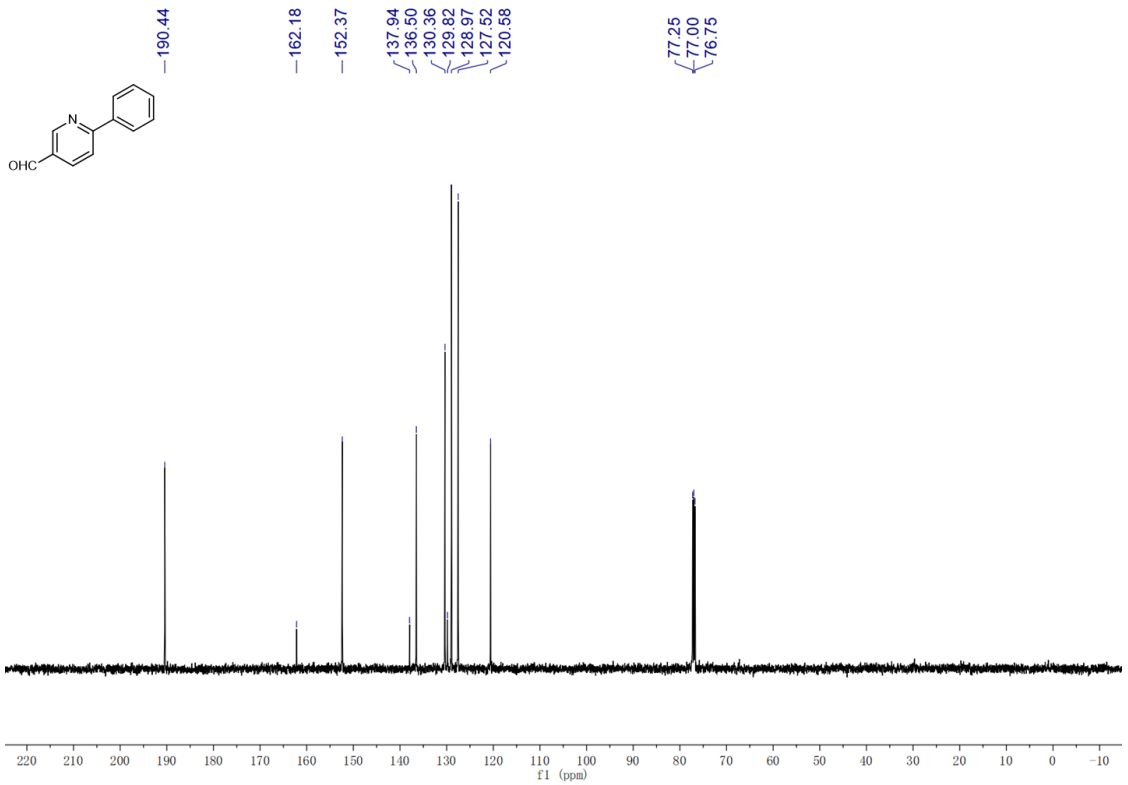

^{1}H and ^{13}C, ^{19}F-NMR spectra of product 4j.

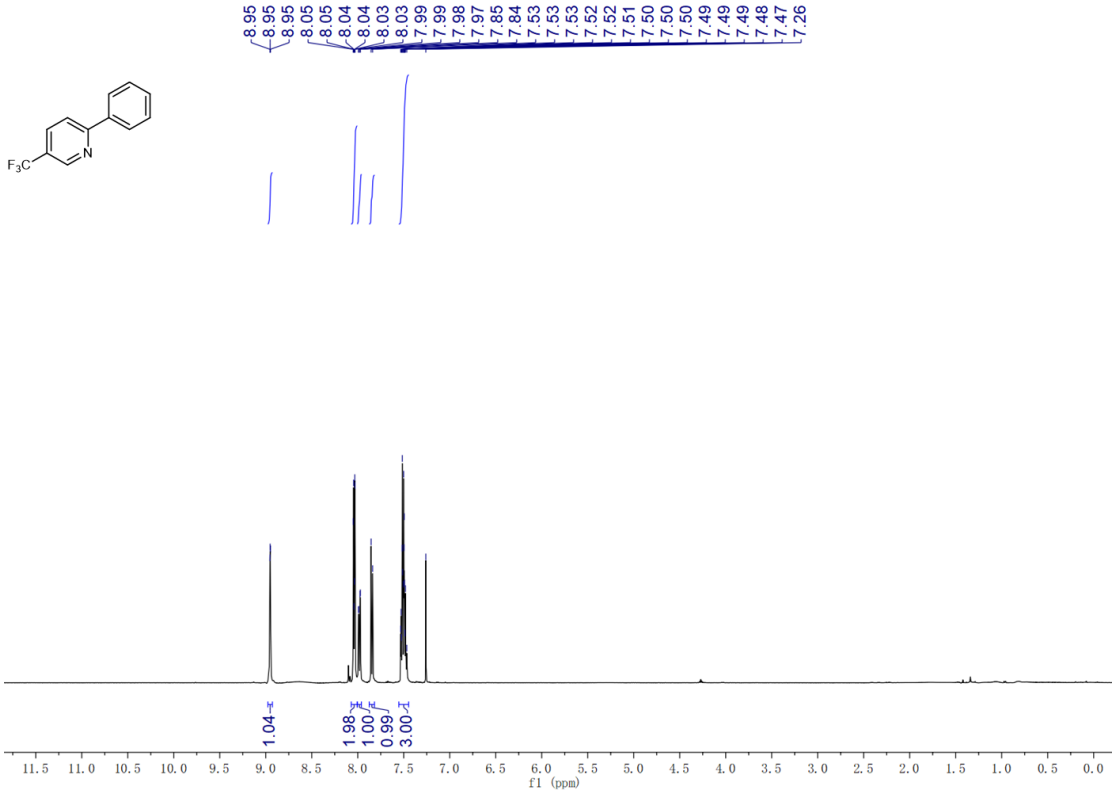

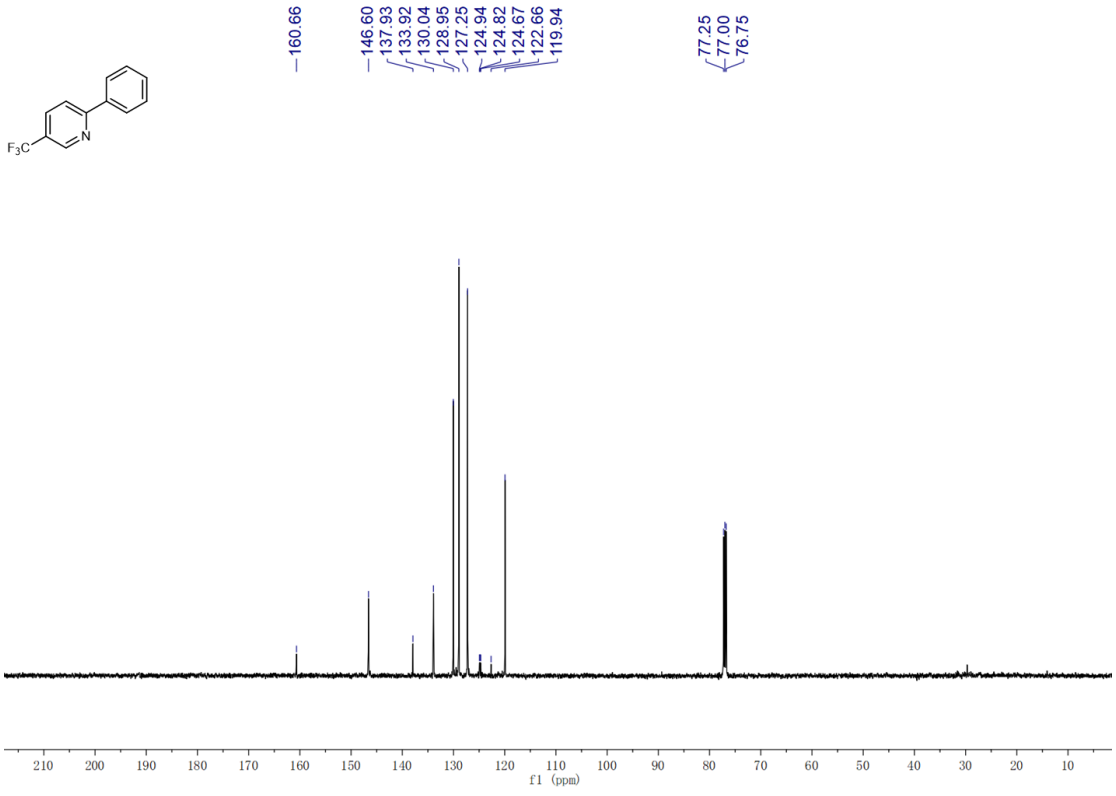

1096

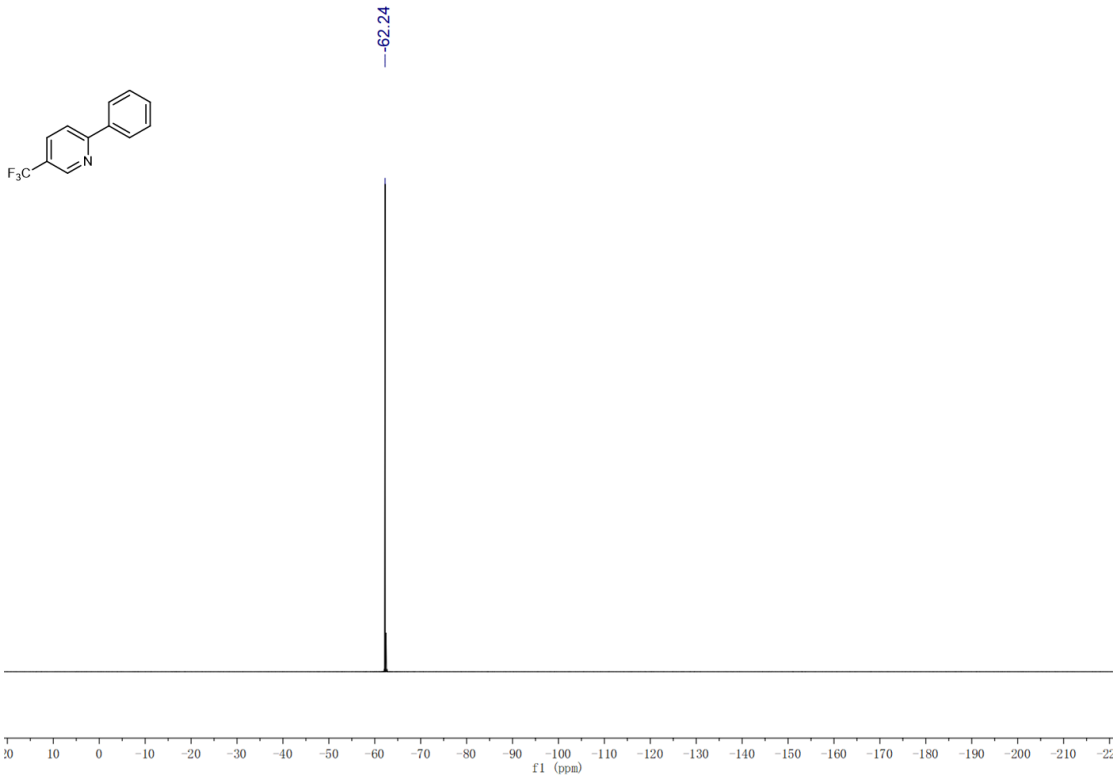
-62.24
F3C
N
10
0
-10
-20
-30
-40
-50
-60
-70
-80
-90
-100
-110
-120
-130
-140
-150
-160
-170
-180
-190
-200
-210
f1 (ppm)

1097

^{1}H and ^{13}C, ^{19}F-NMR spectra of product 4k.

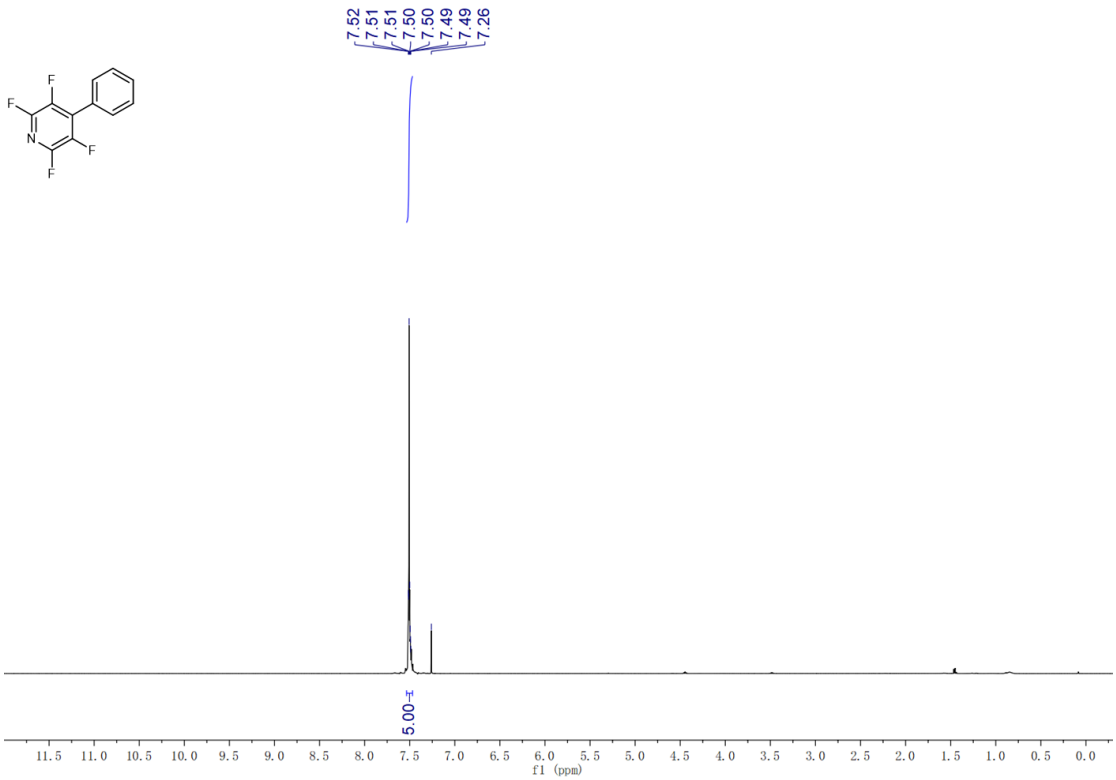

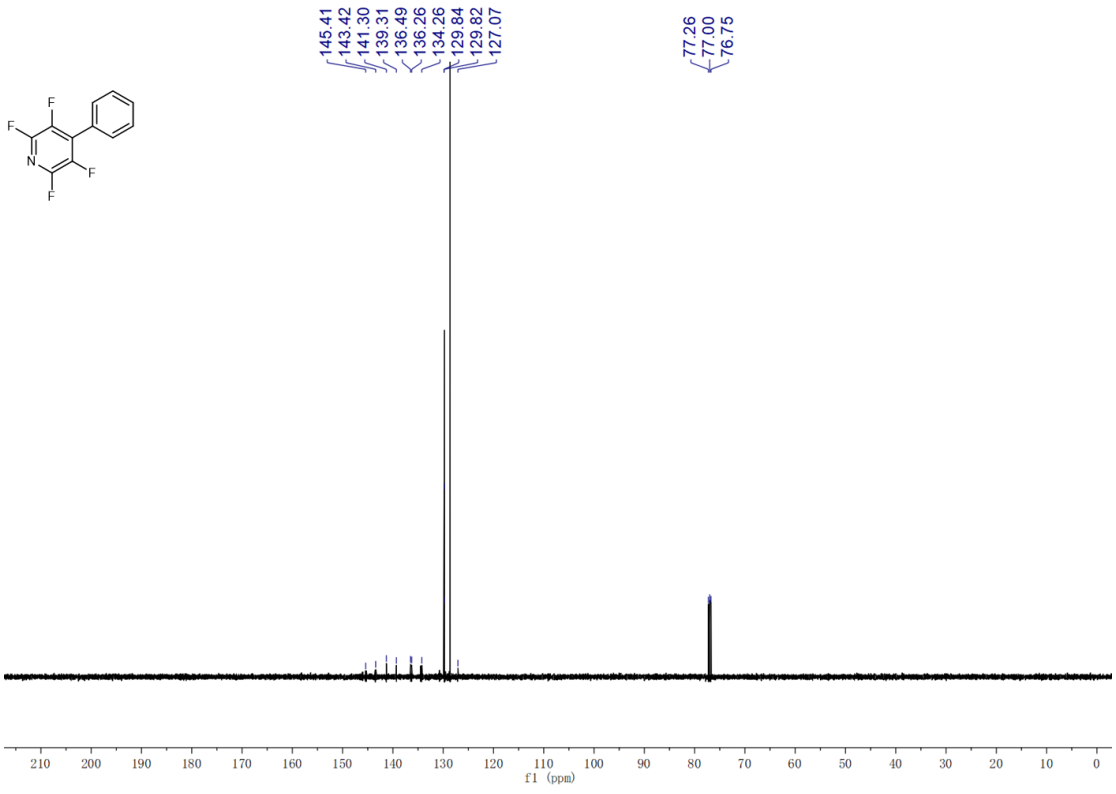

1104

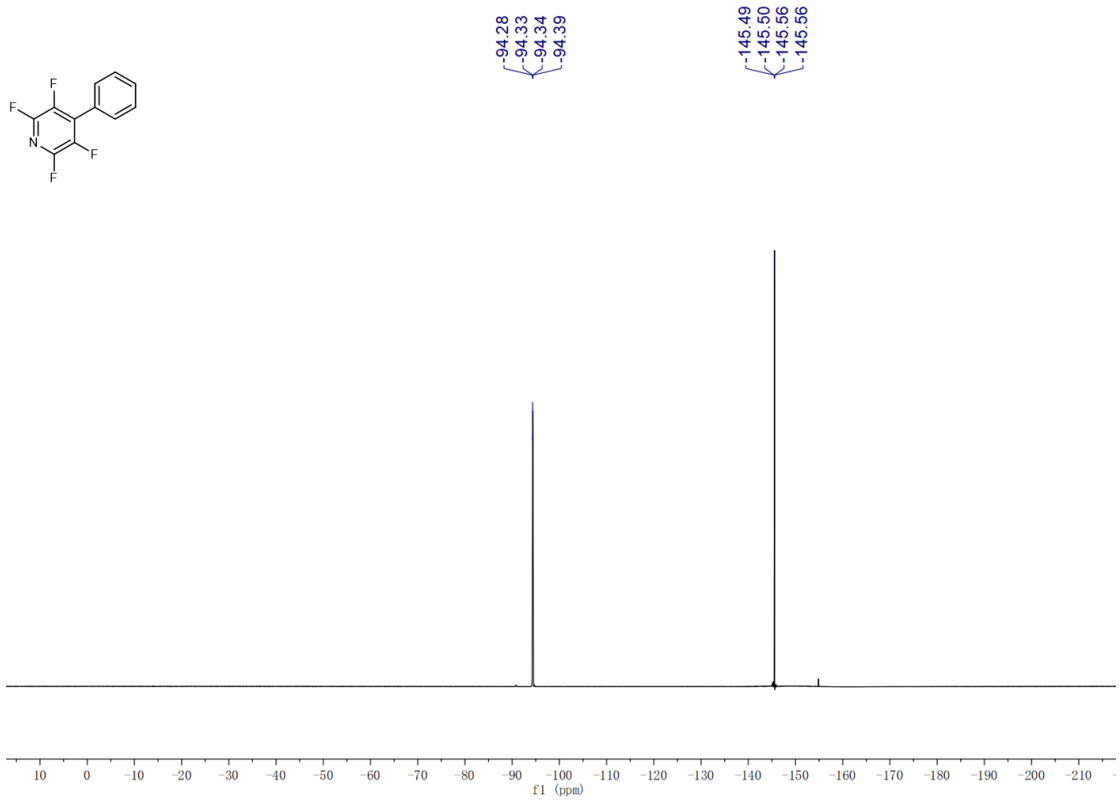

1105

1106

^{1}H and ^{13}C spectra of product 4l.

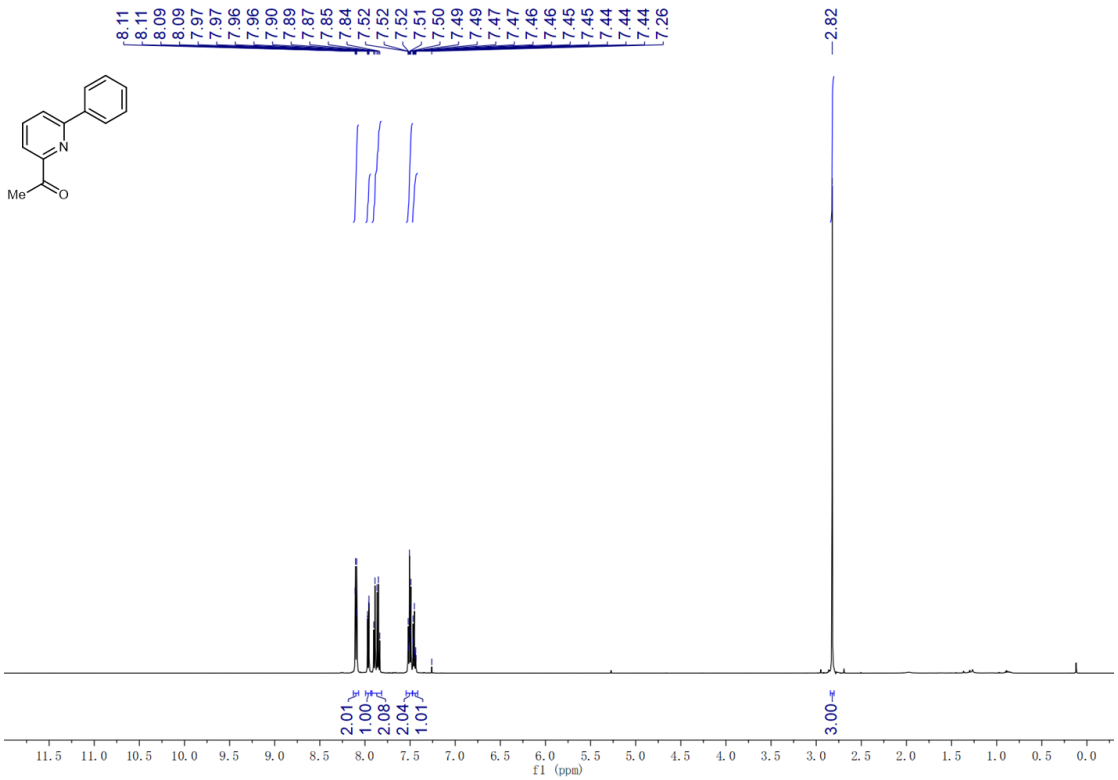

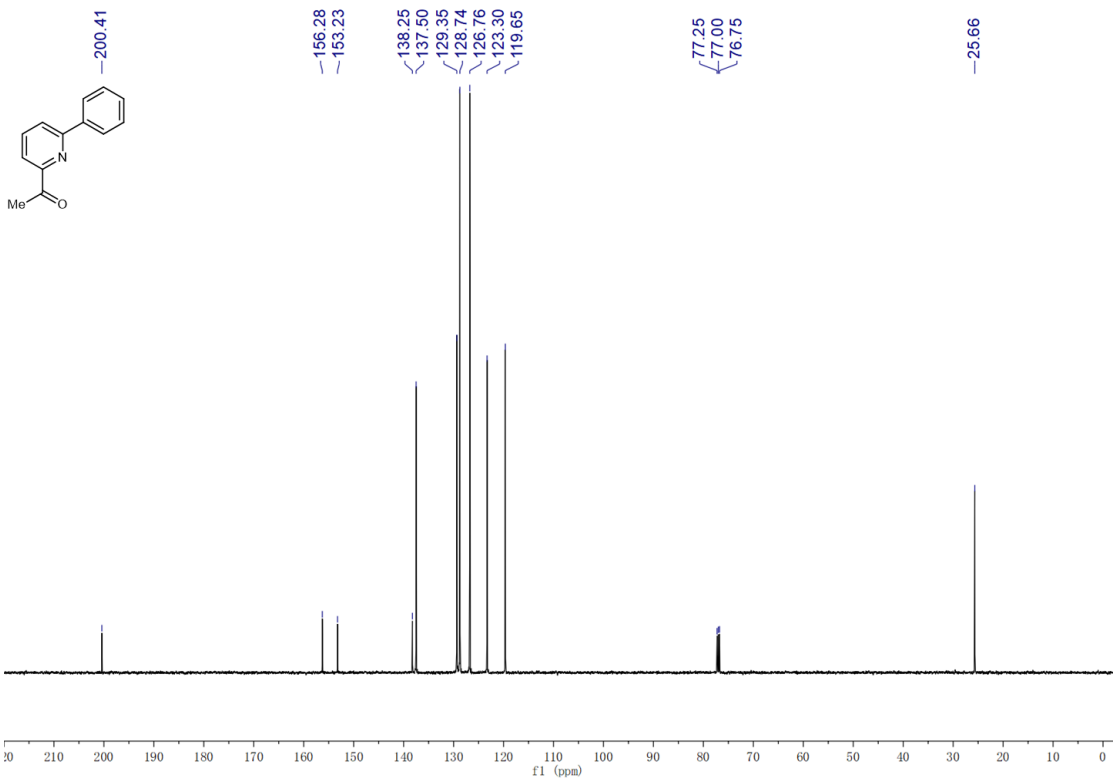

^{1}H and ^{13}C-spectra of product 4m.

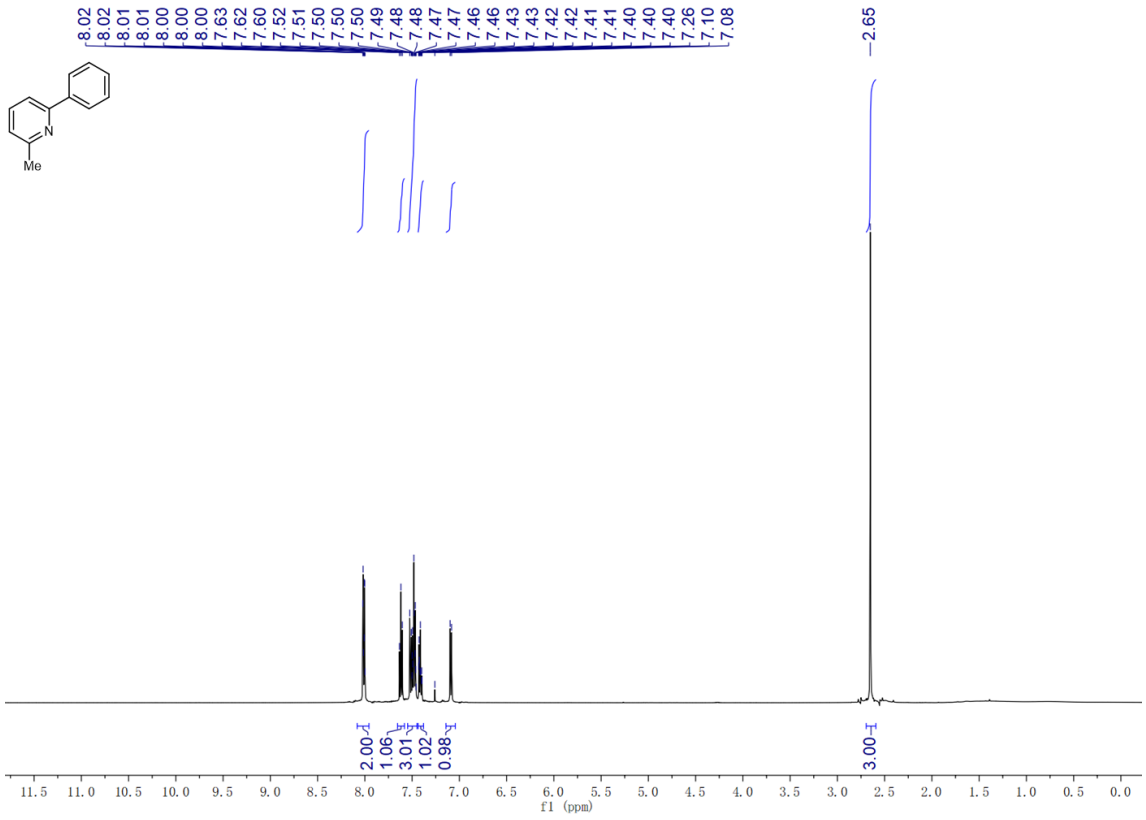

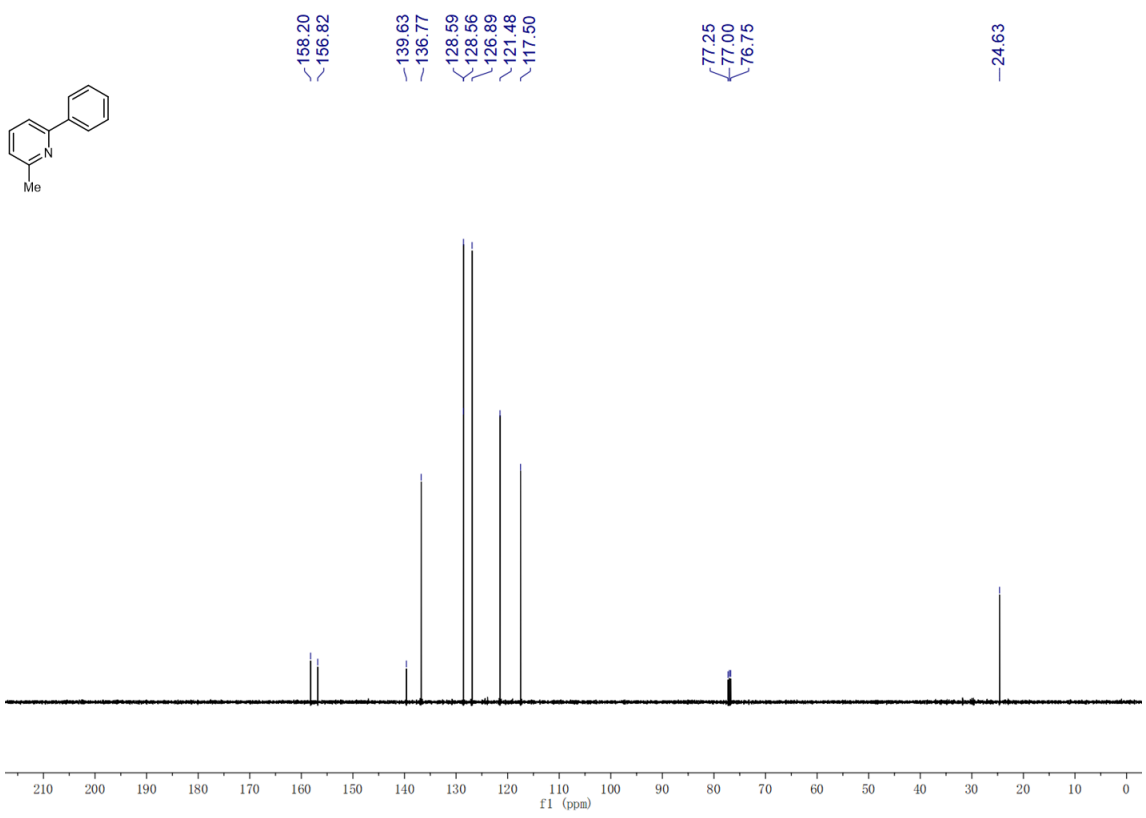

^{1}H and ^{13}C-NMR spectra of product 4n.

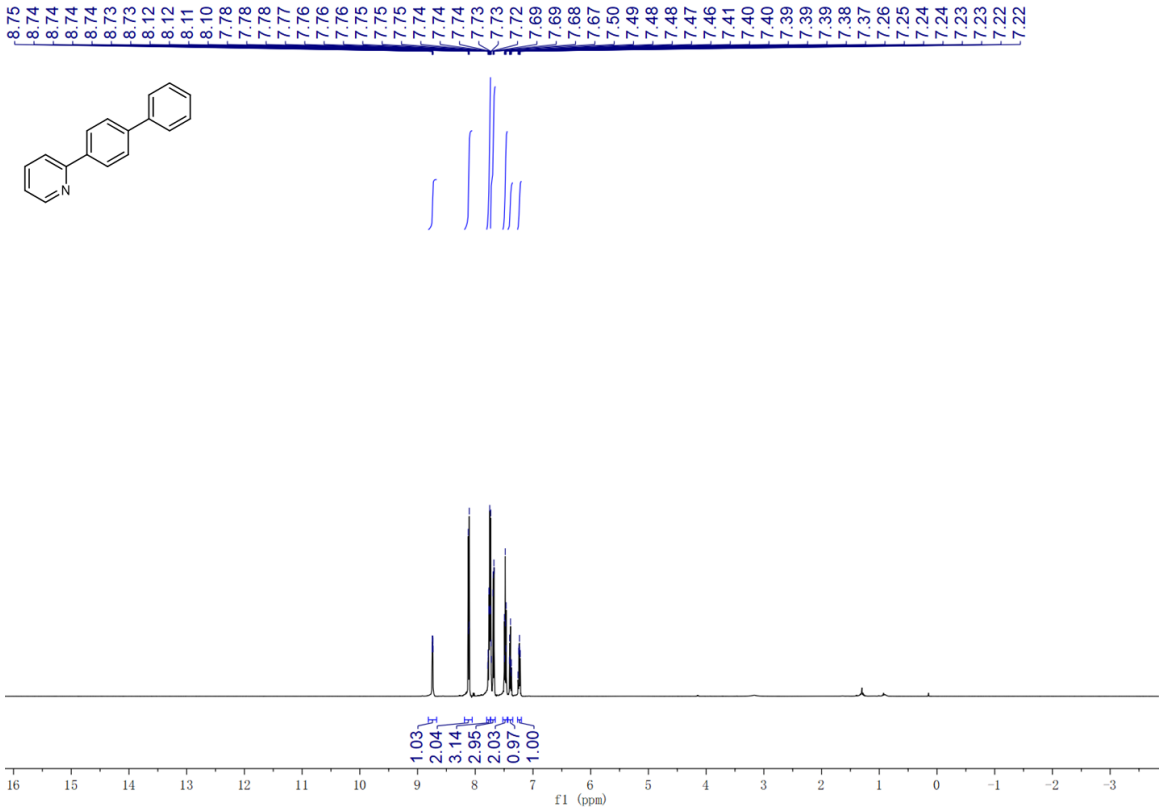

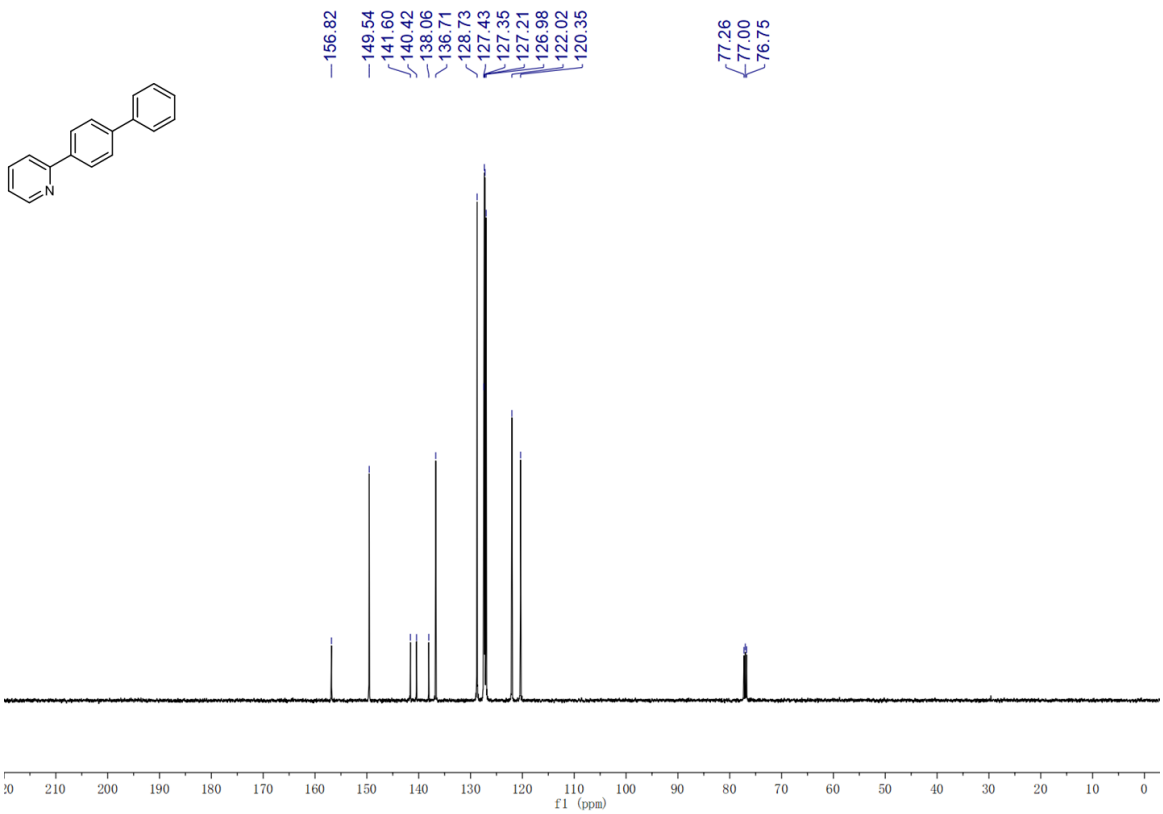

^{1}H and ^{13}C spectra of product 4o.

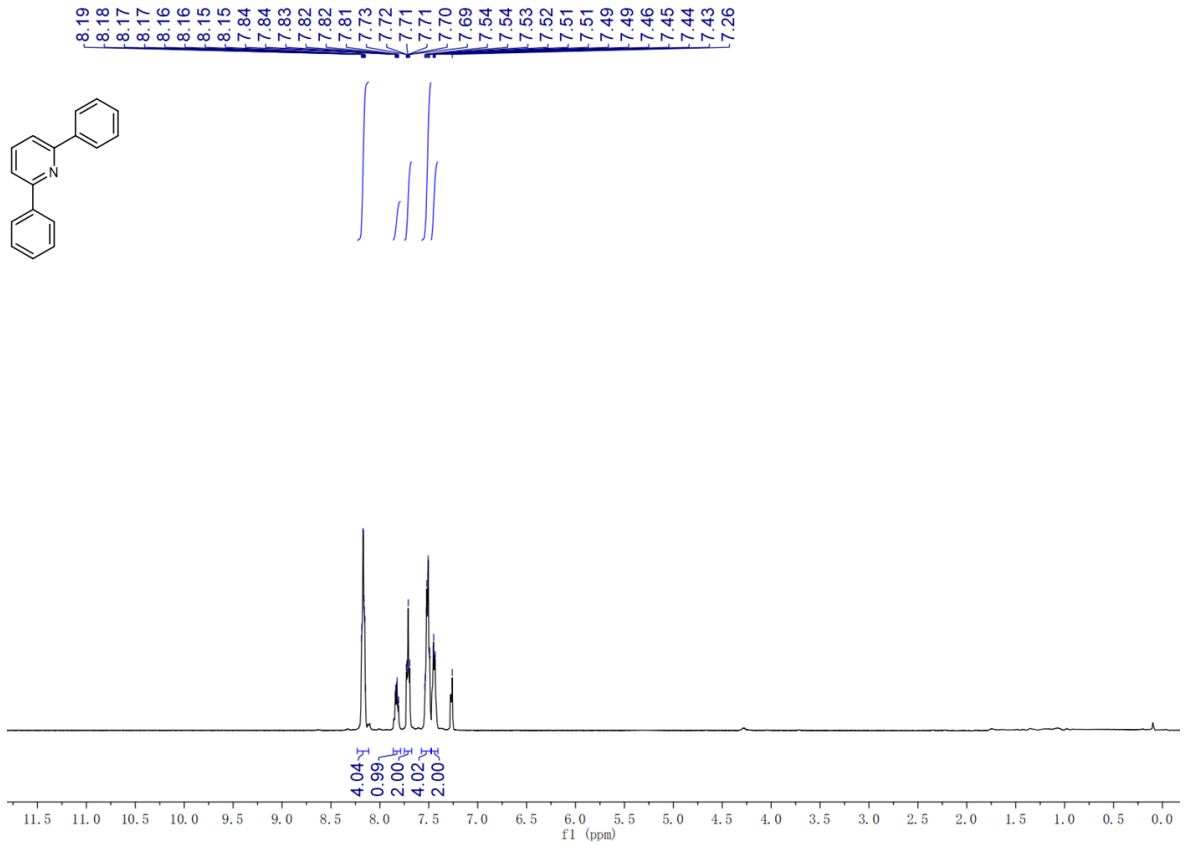

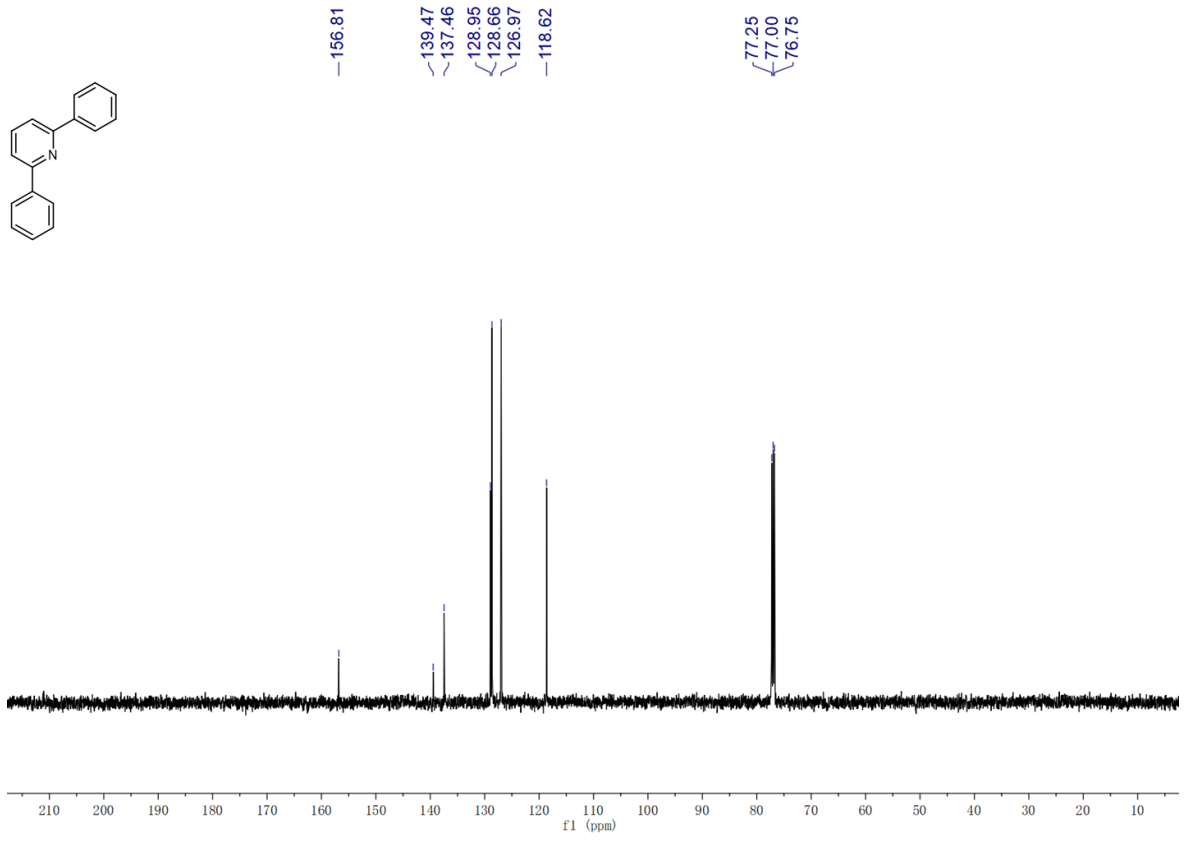

^{1}H and ^{13}C- NMR spectra of product 4p.

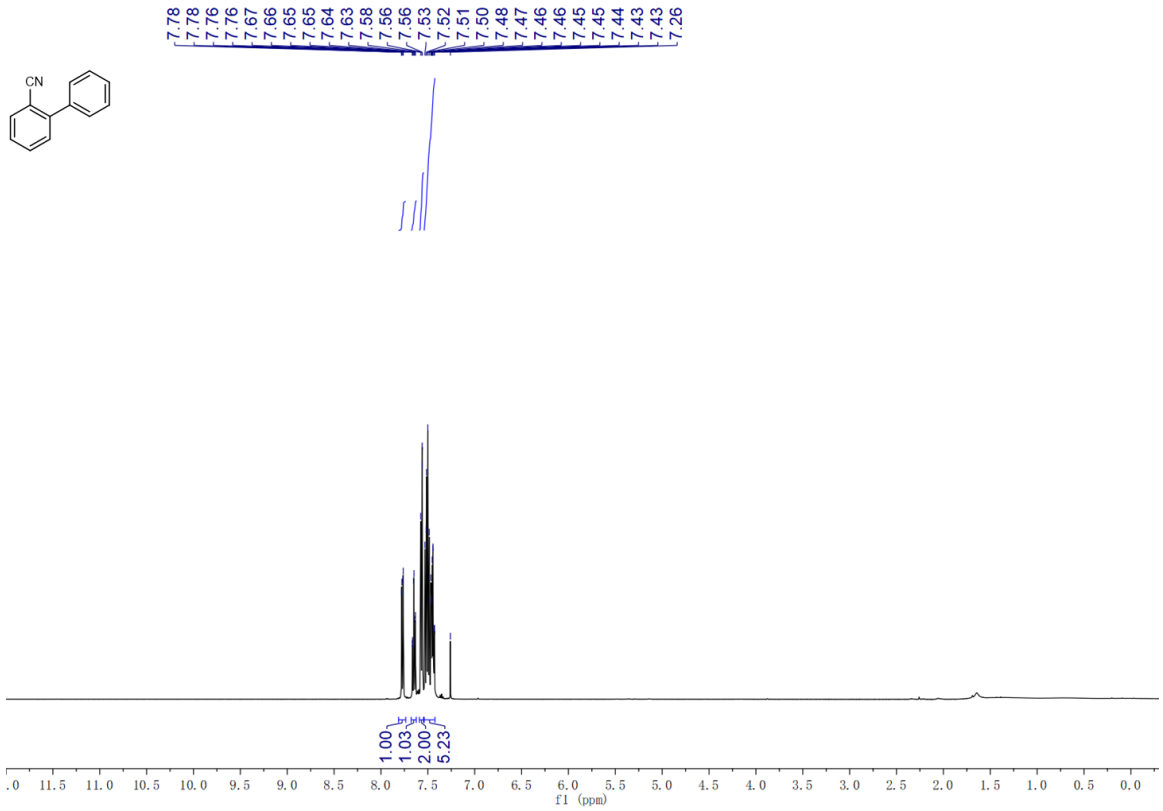

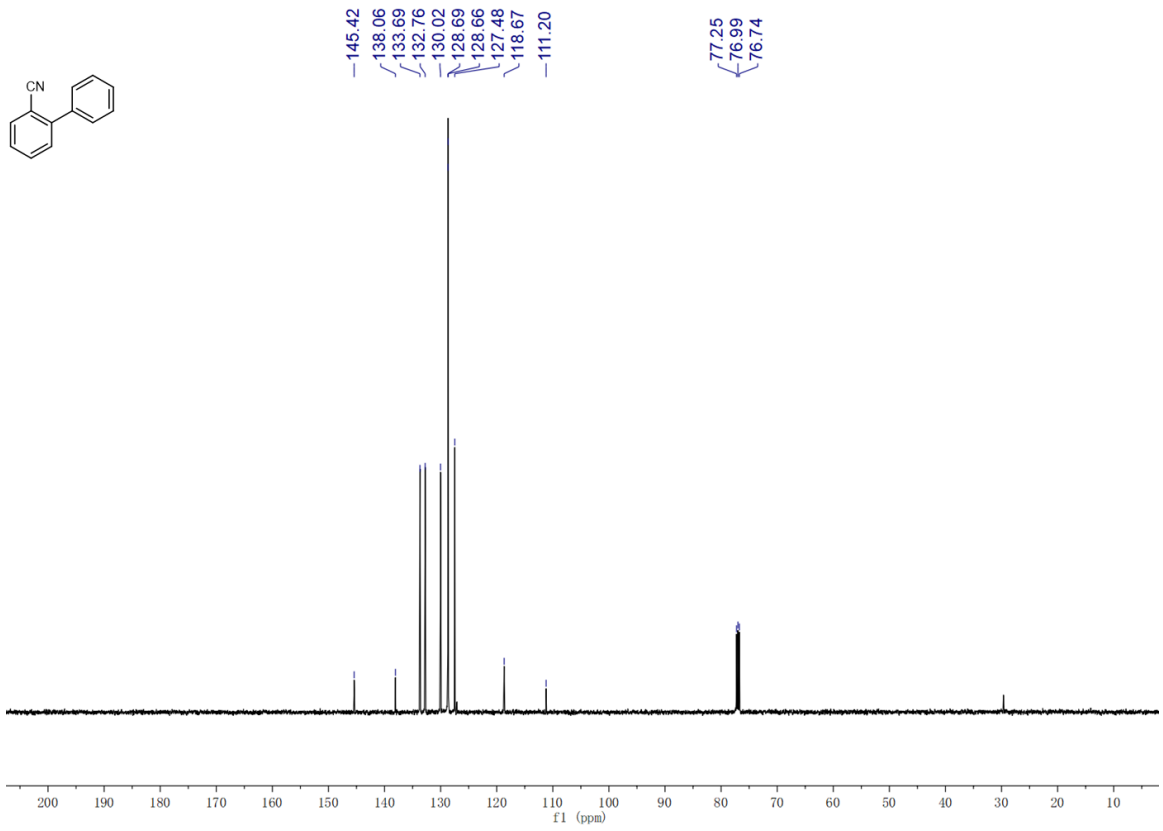

^{1}H and ^{13}C-NMR spectra of product 4q.

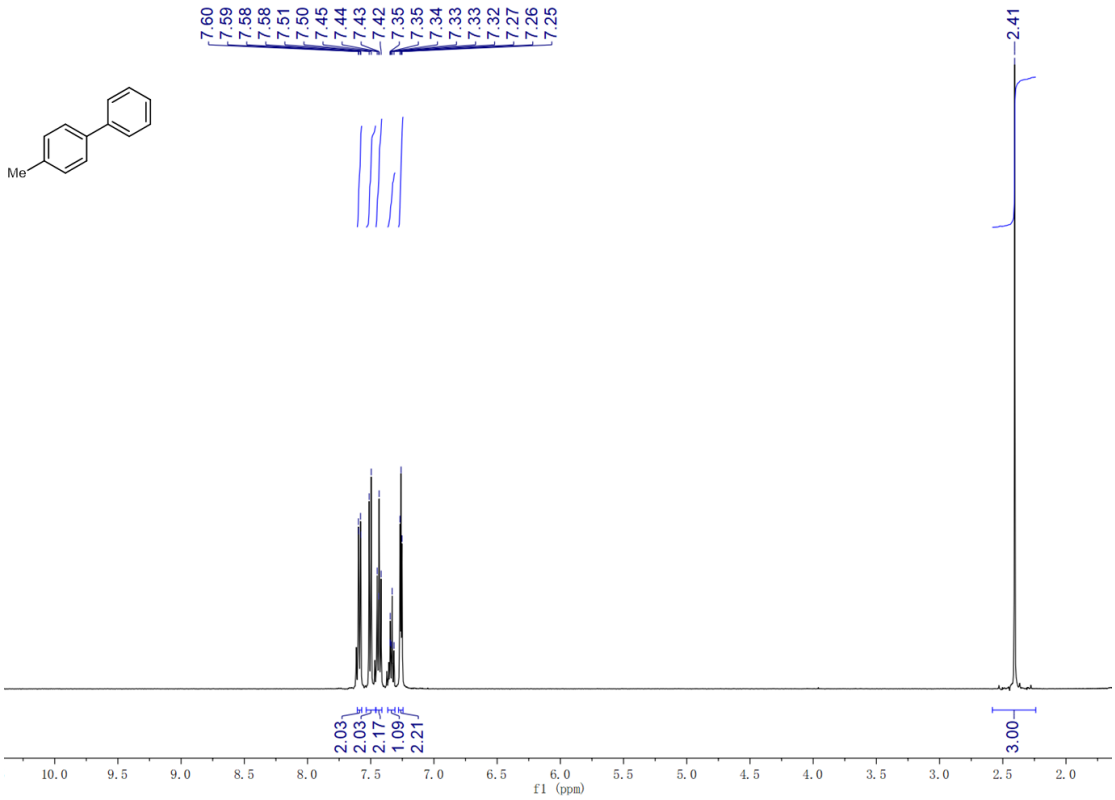

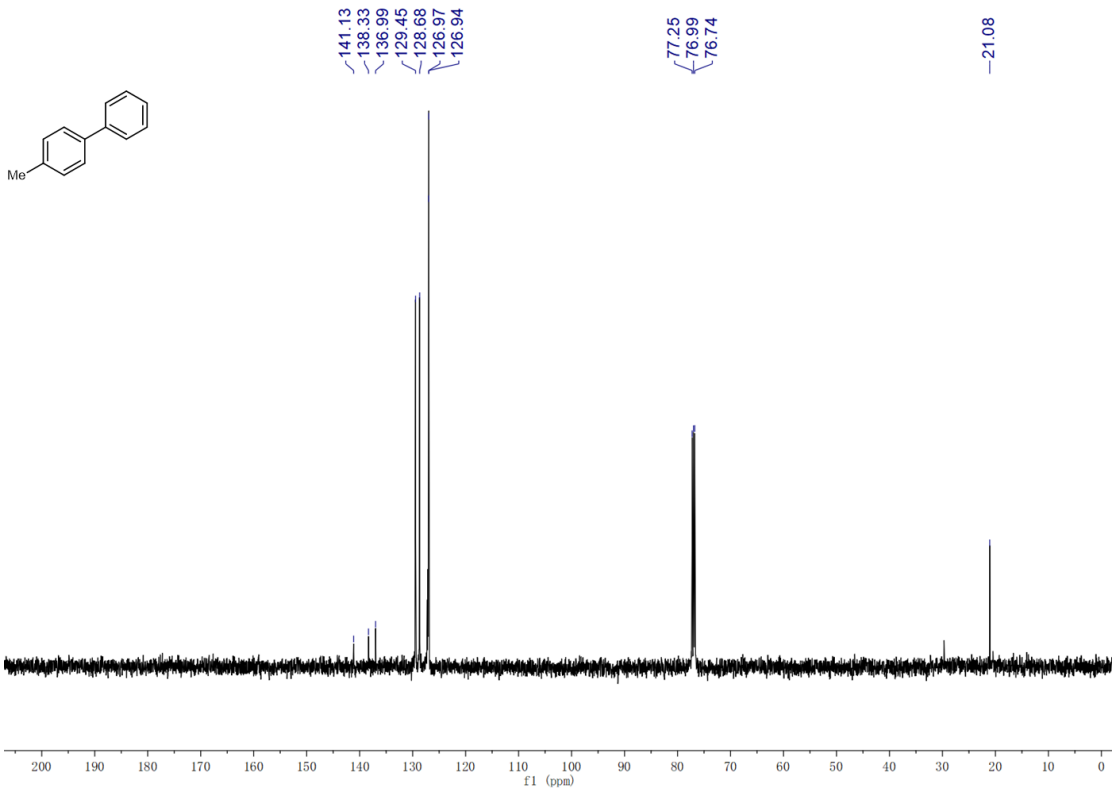

^{1}H and ^{13}C- NMR spectra of product 4r.

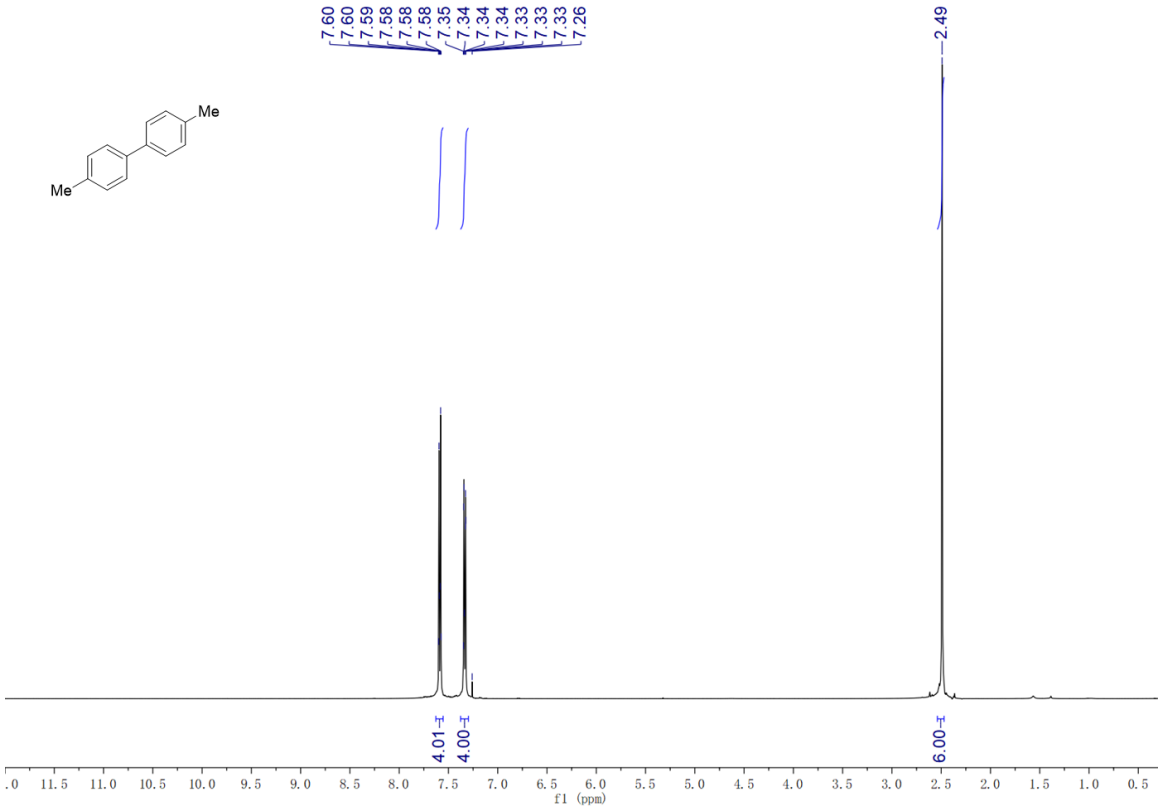

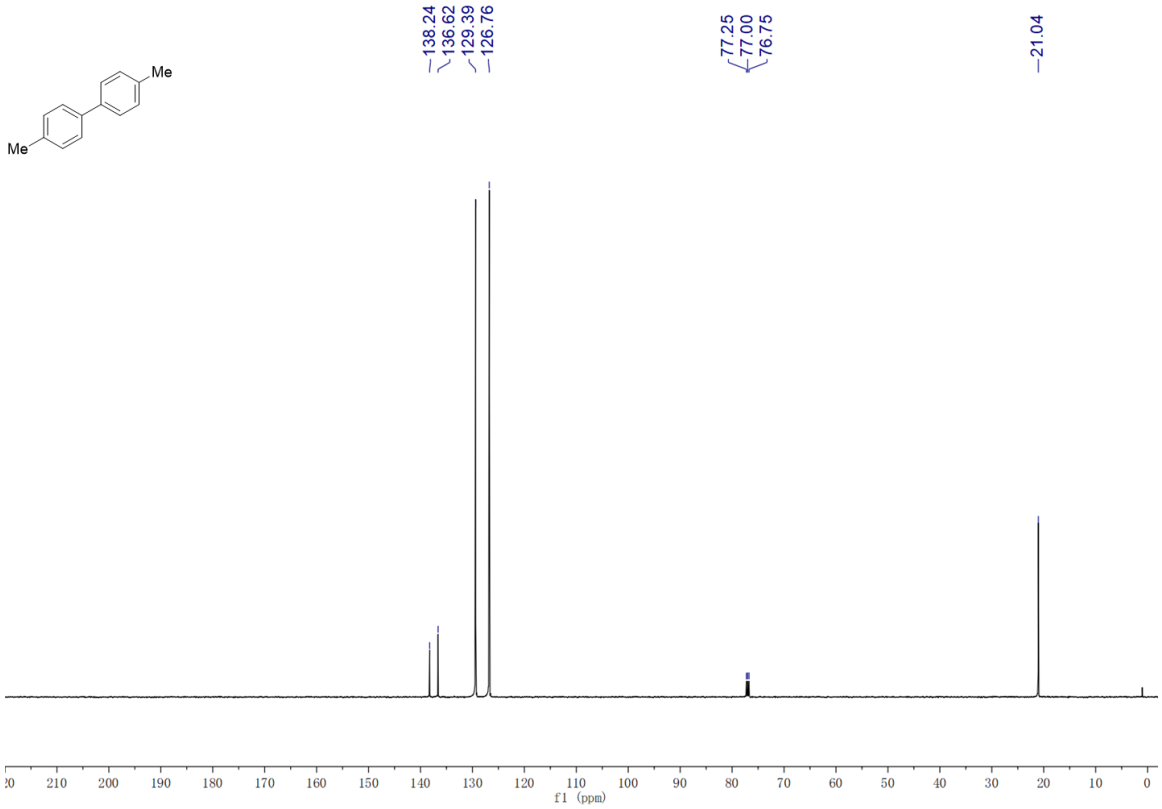

^{1}H and ^{13}C-NMR spectra of product 4s.

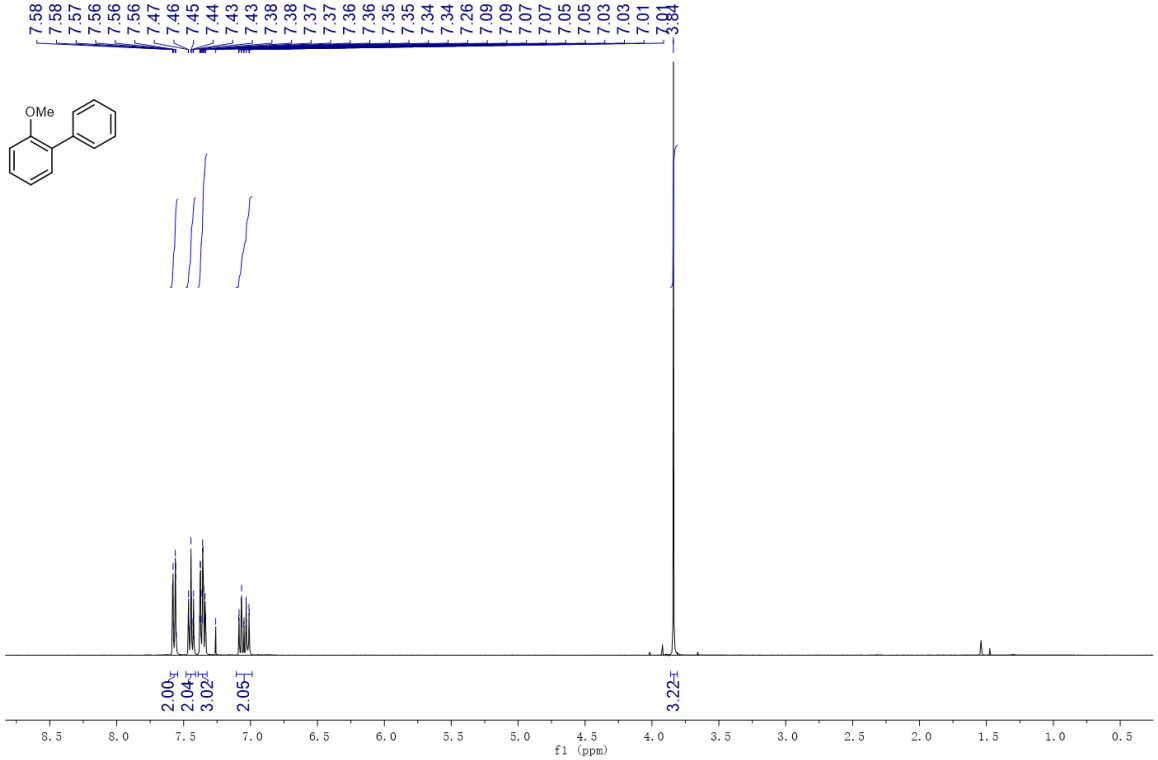

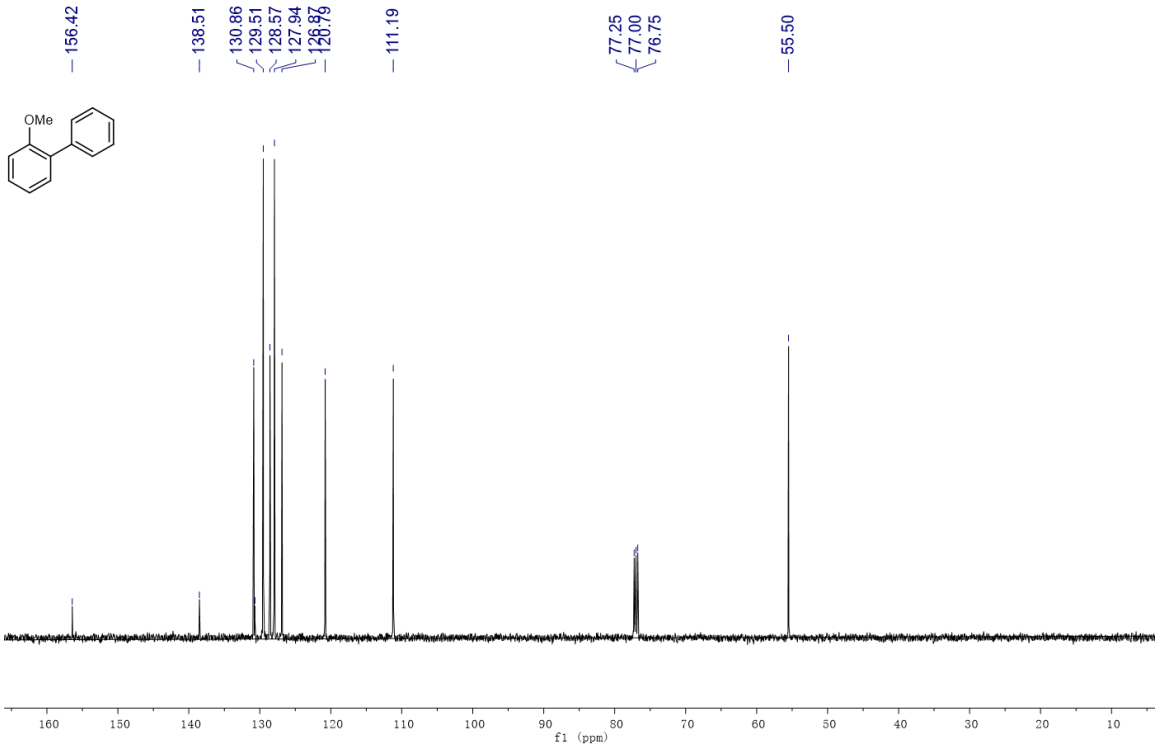

^{1}H and ^{13}C-NMR spectra of product 4t.

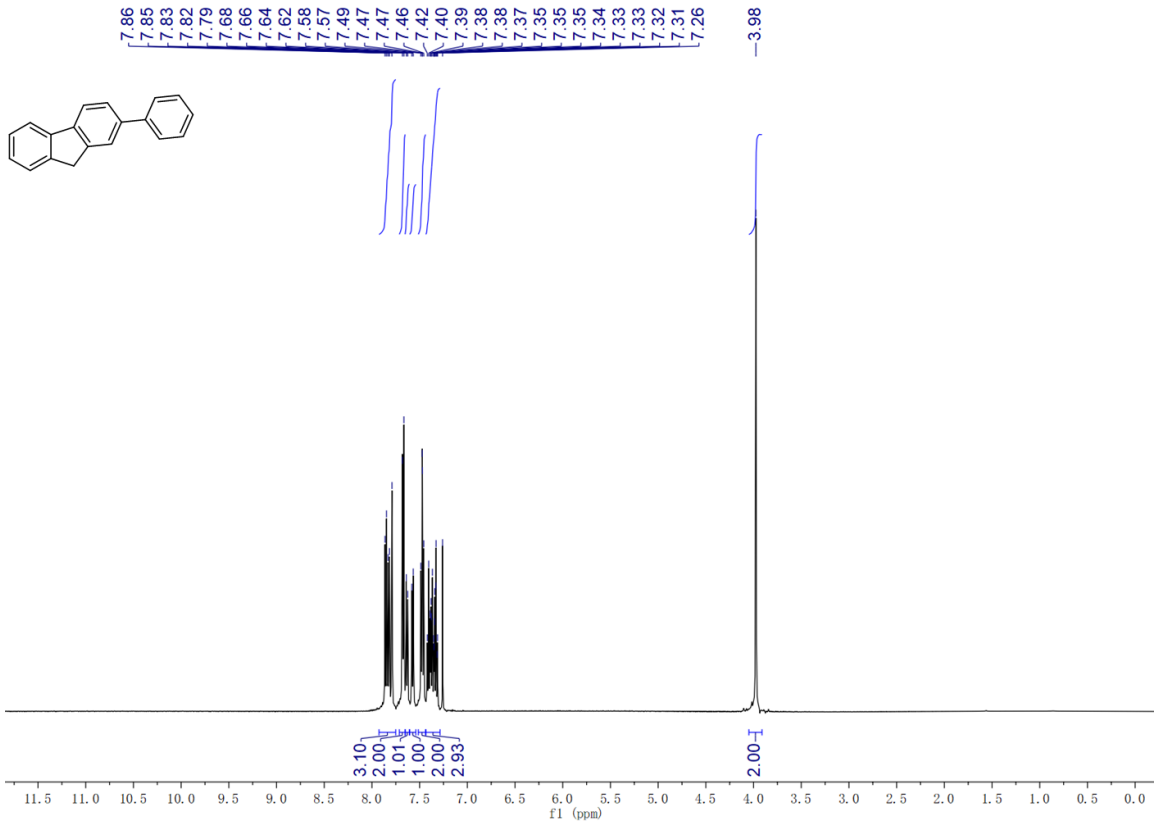

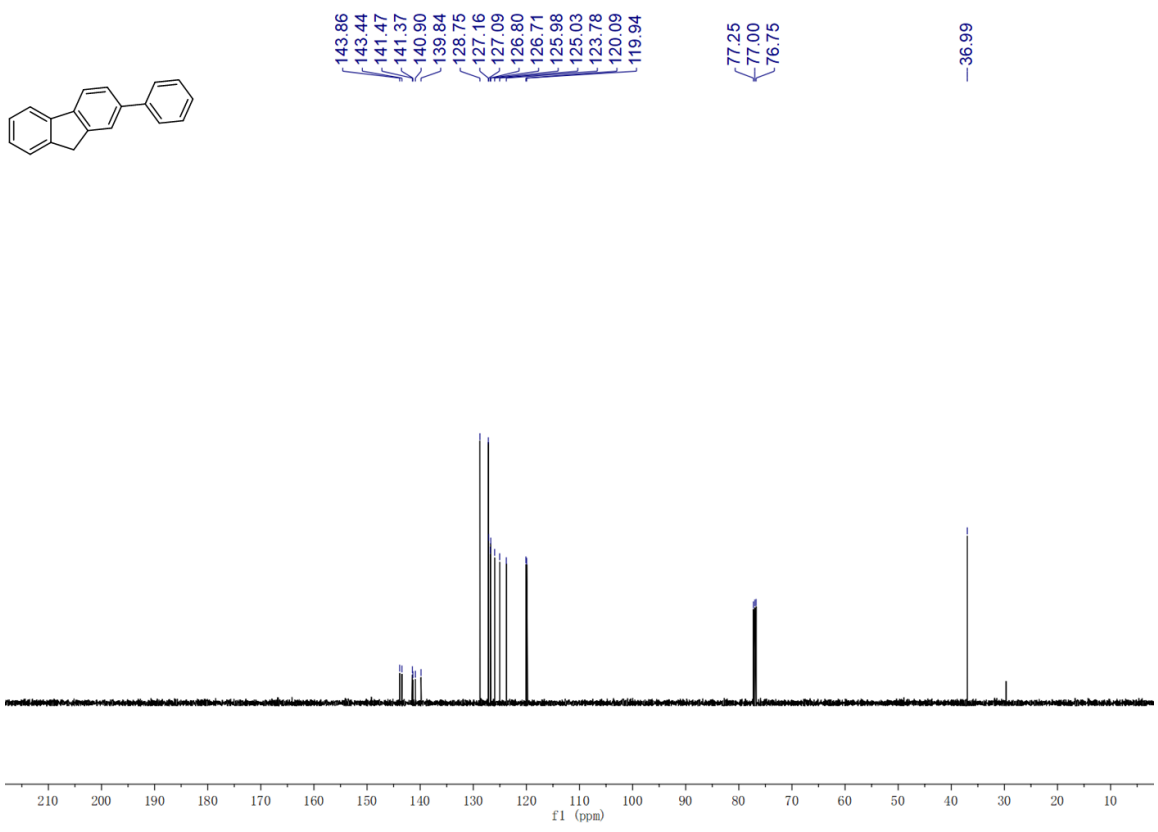

^{1}H and ^{13}C-NMR spectra of product 4u.

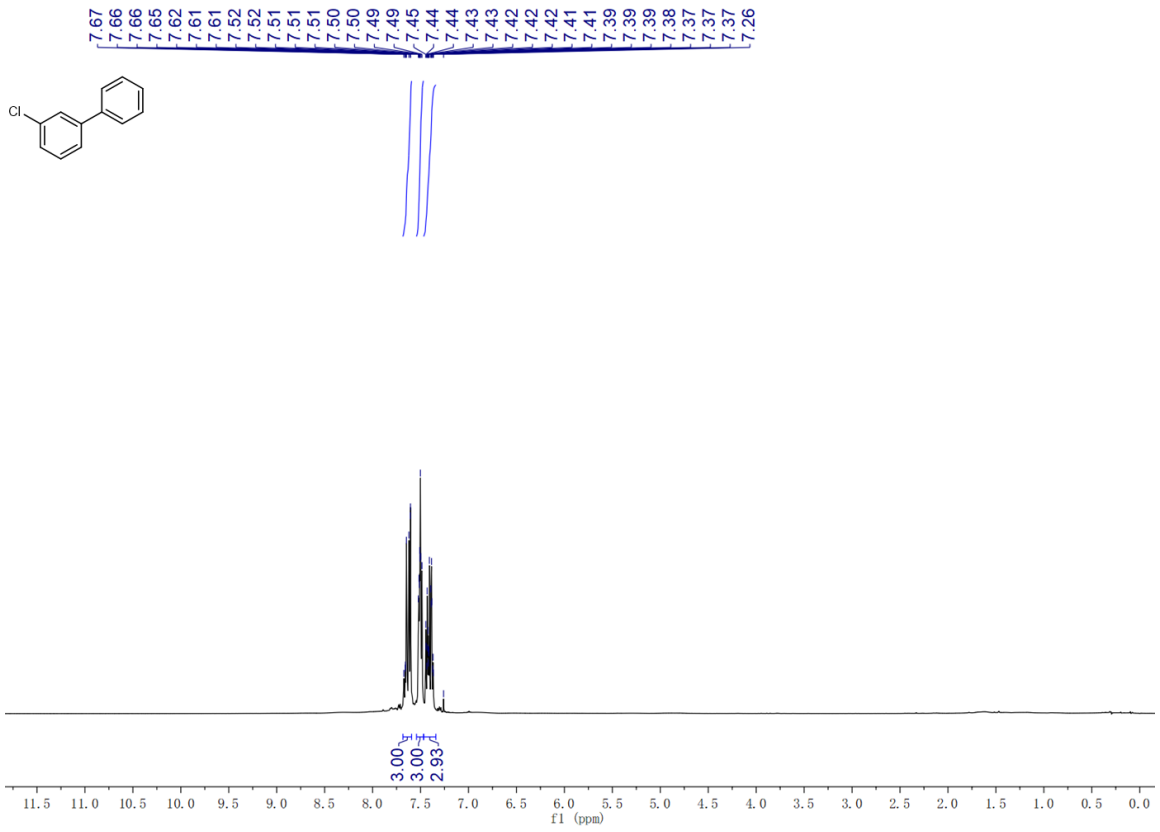

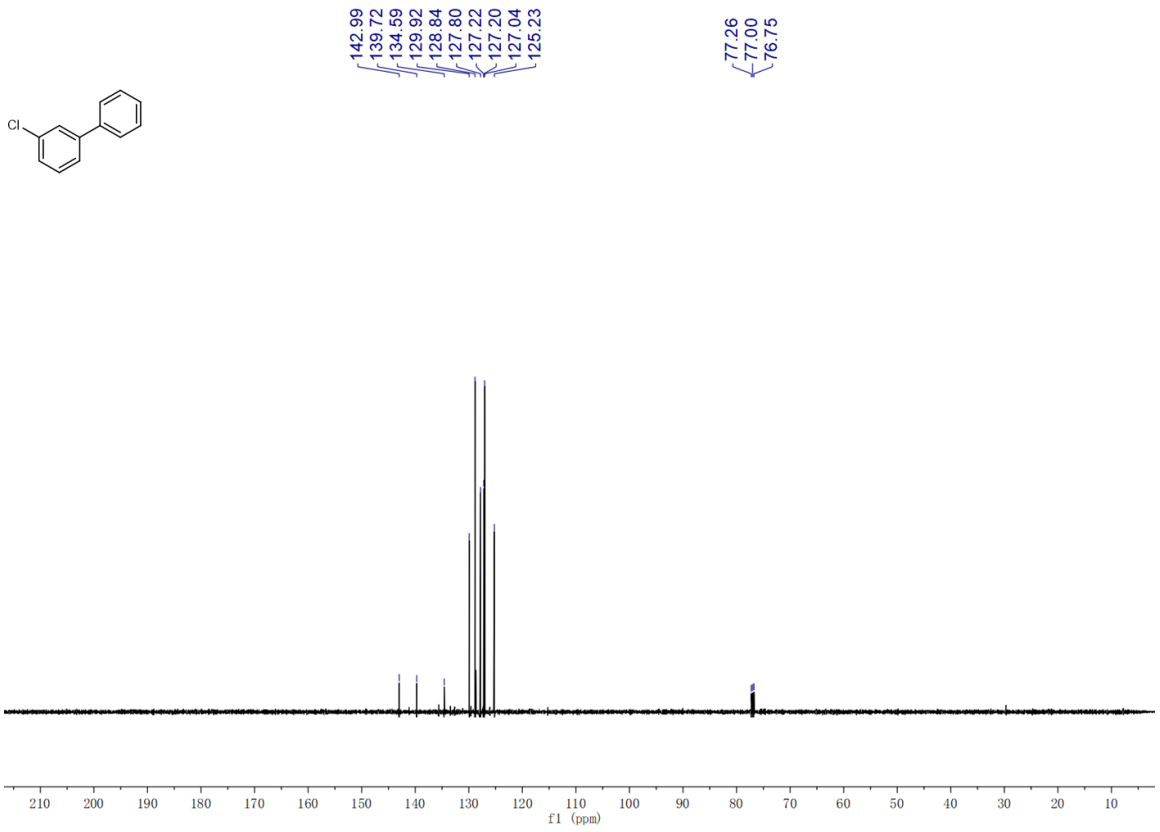

^{1}H and ^{13}C- NMR spectra of product 4v.

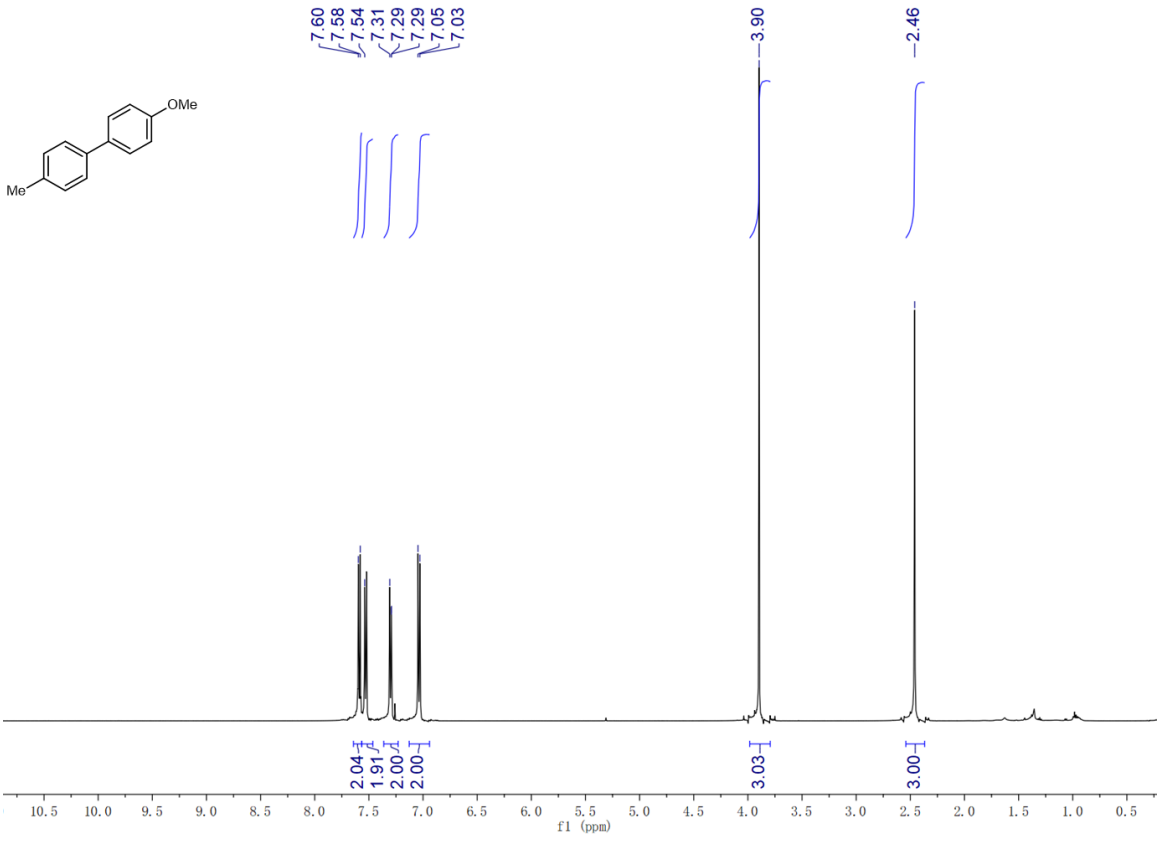

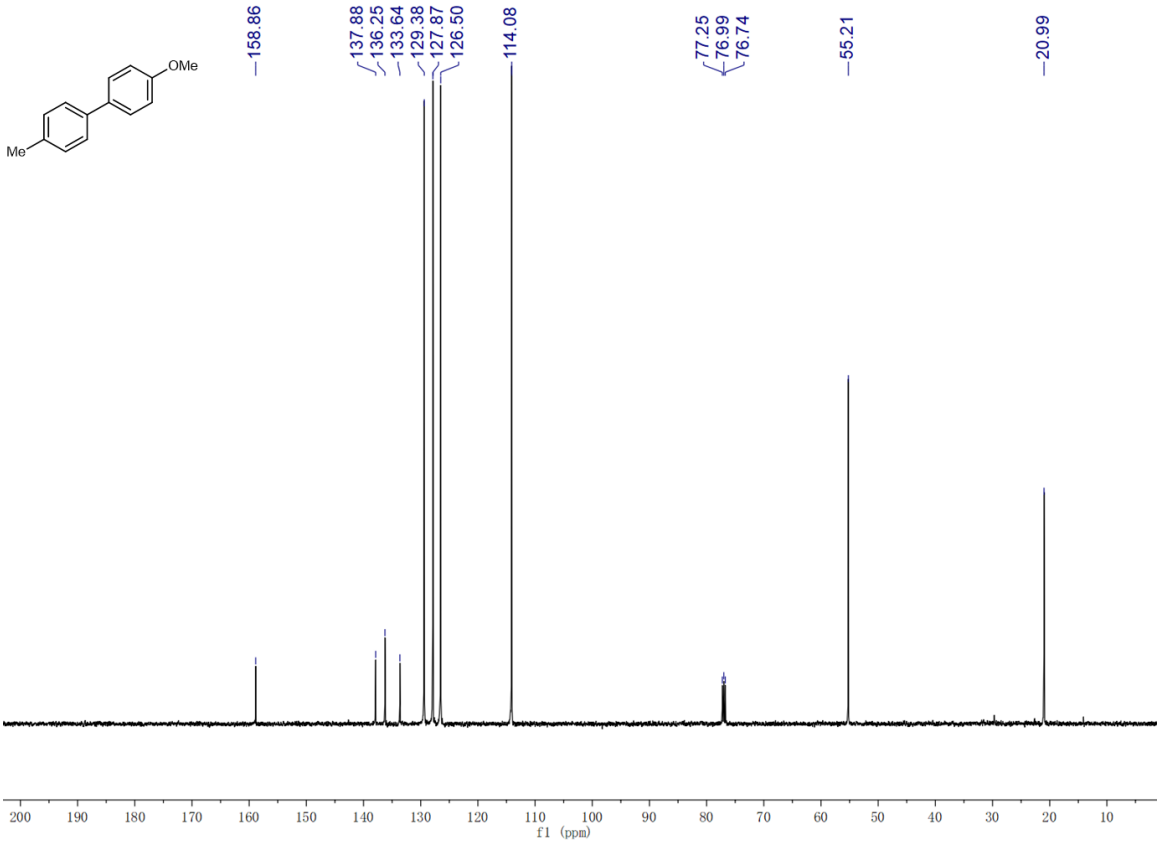

^{1}H and ^{13}C-NMR spectra of product 4w.

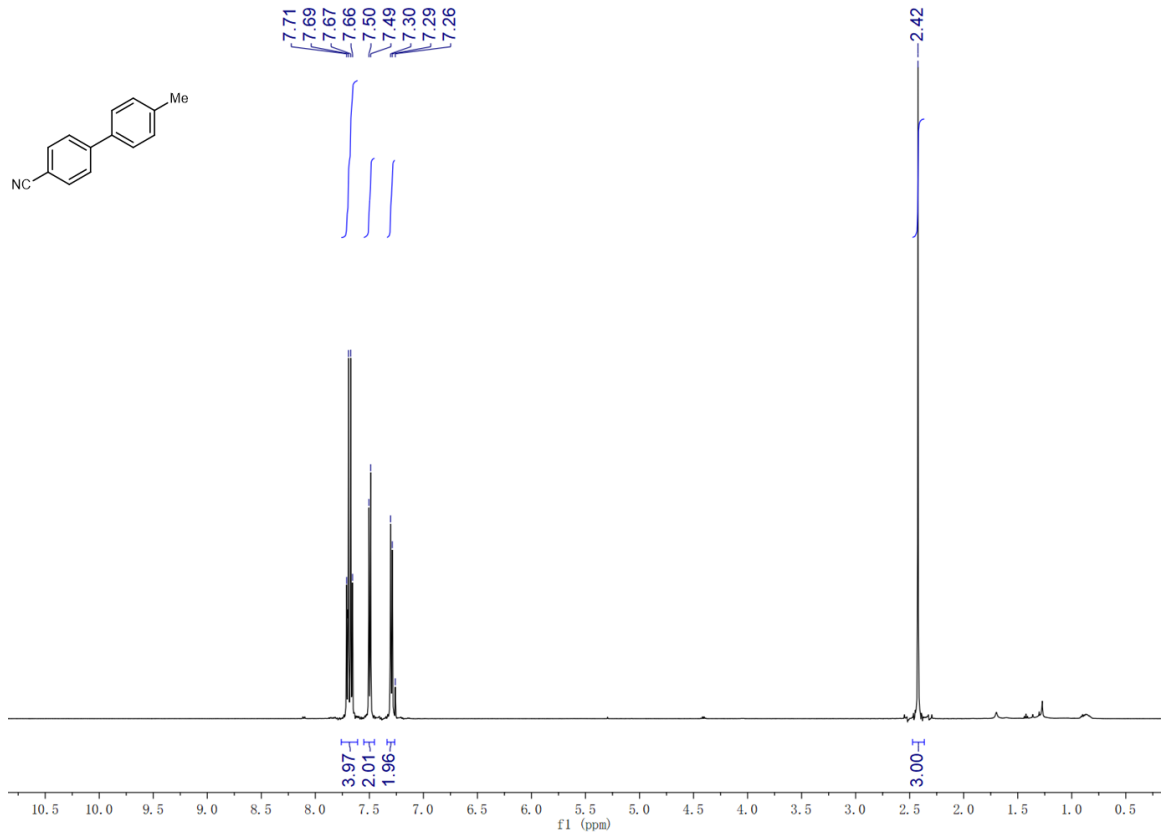

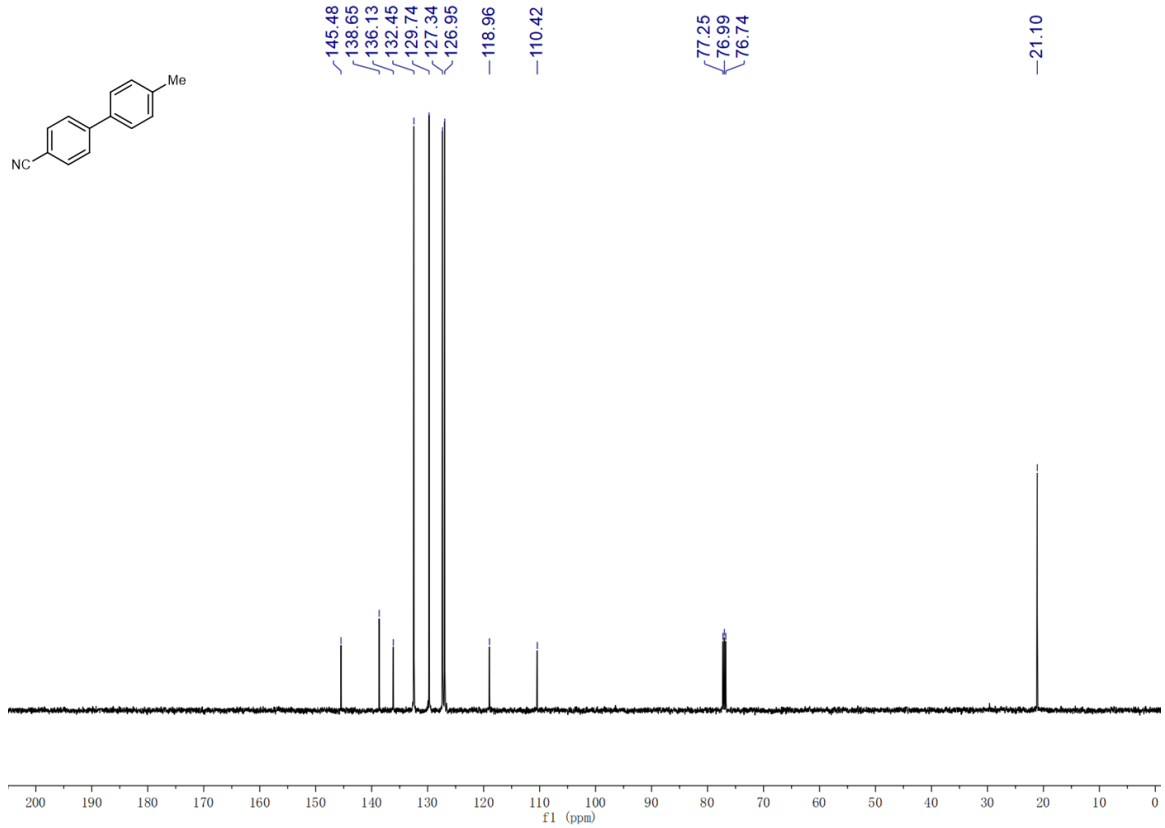

^{1}H and ^{13}C-NMR spectra of product 4x.

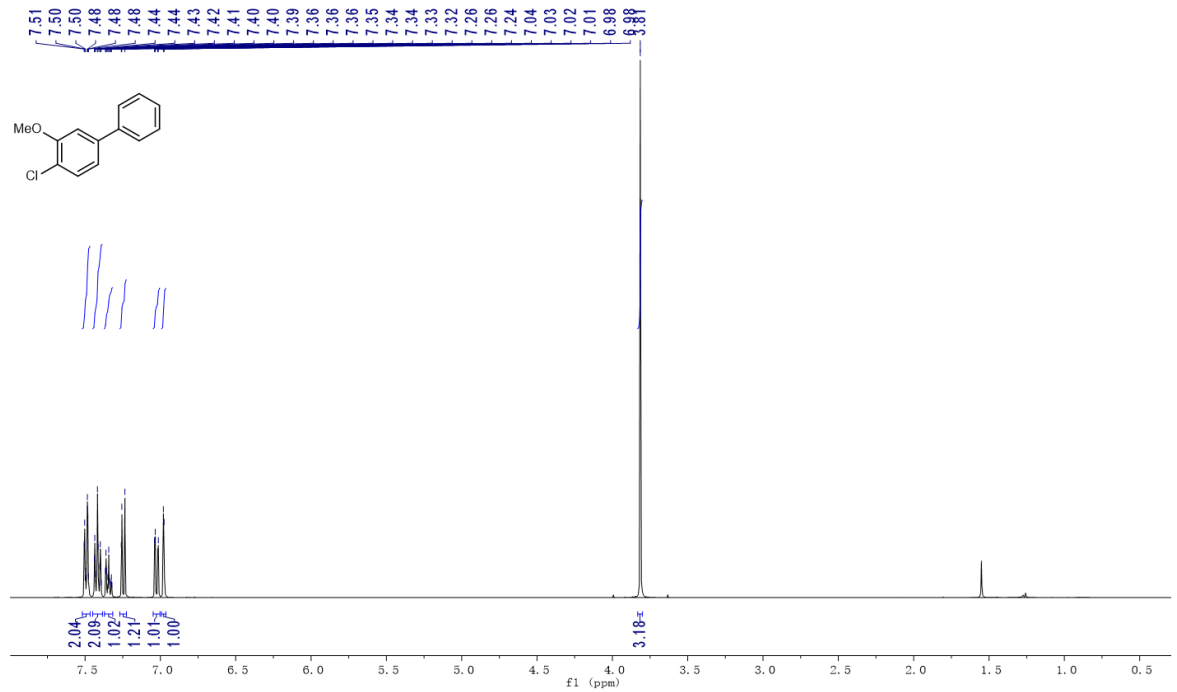

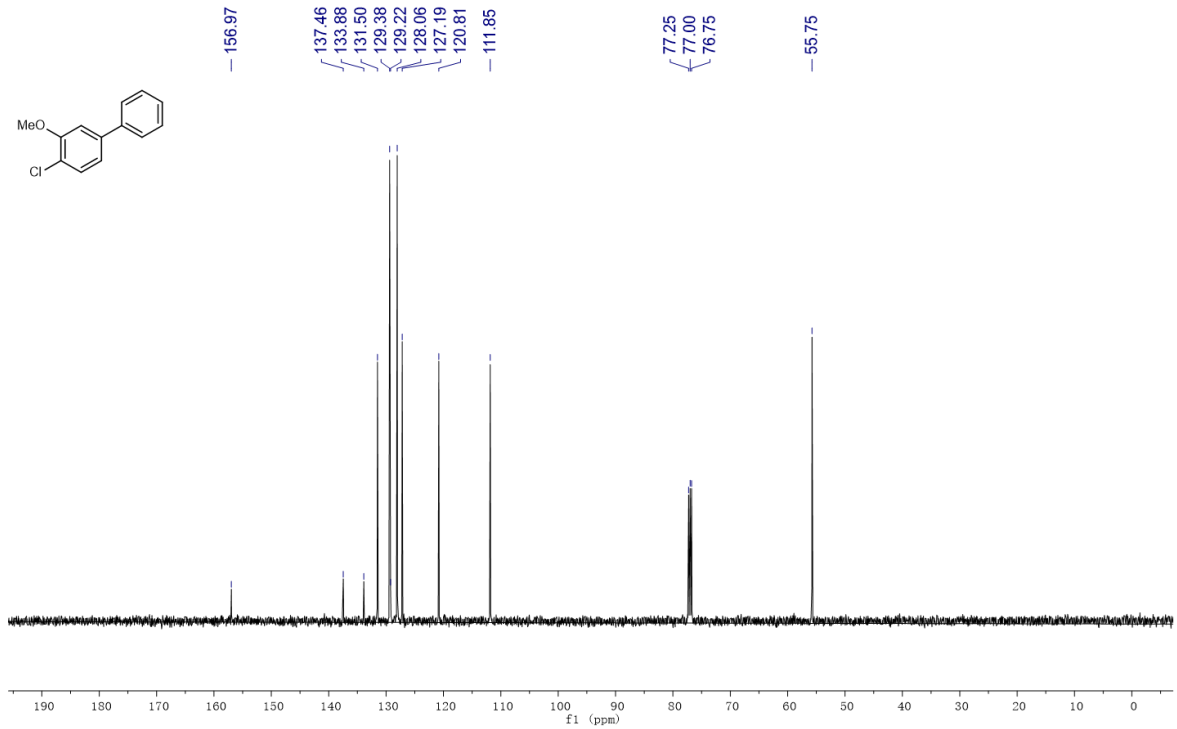

^{1}H and ^{13}C-NMR spectra of product 4y.

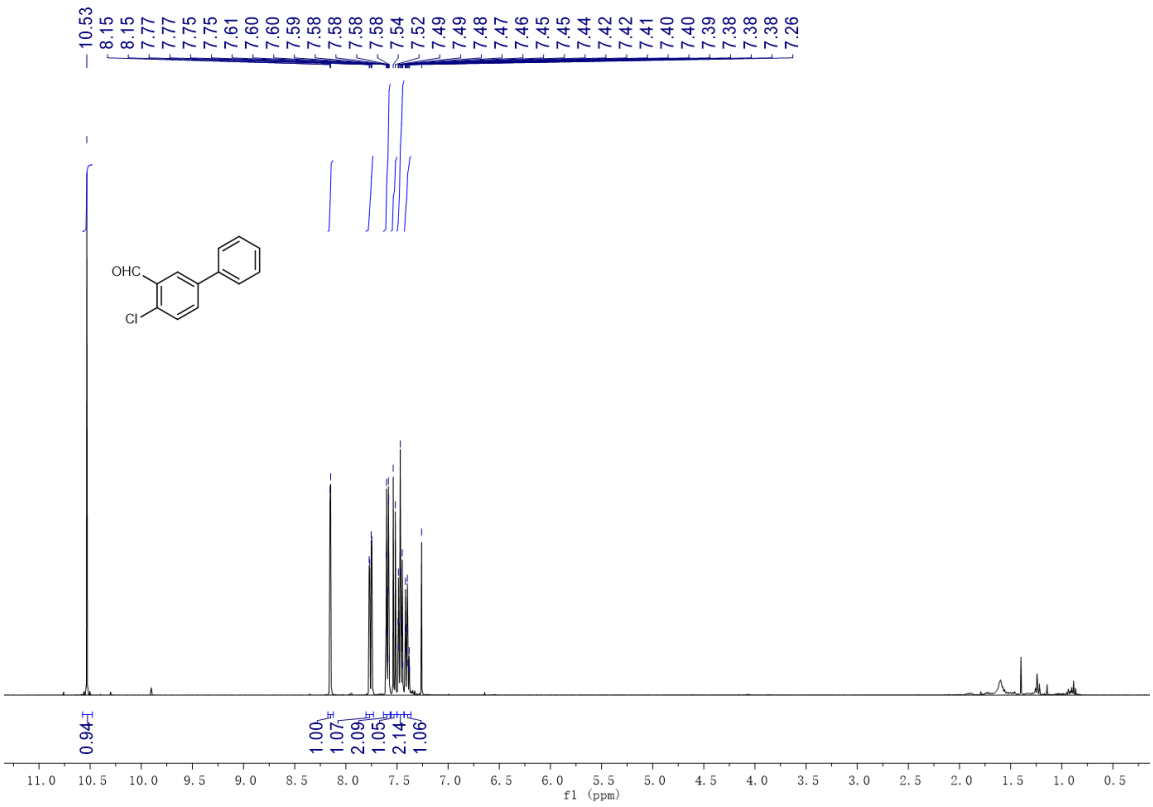

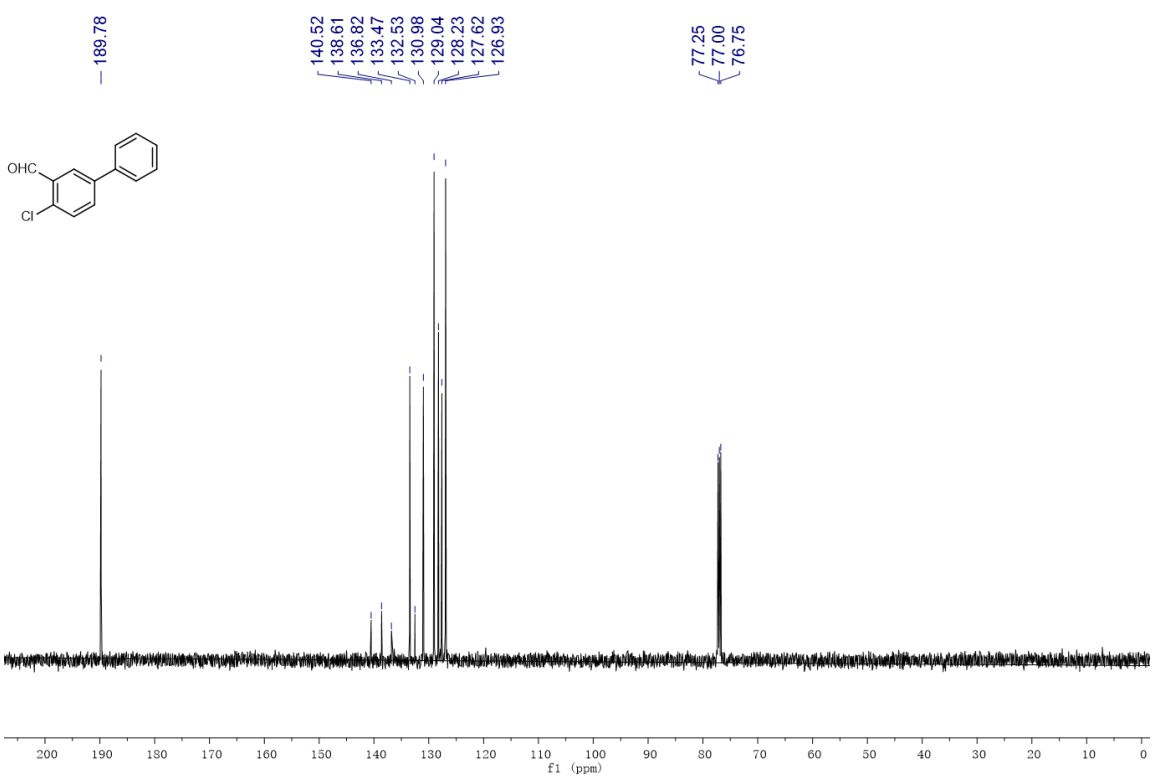

^{1}H and ^{13}C-NMR spectra of product 4z.

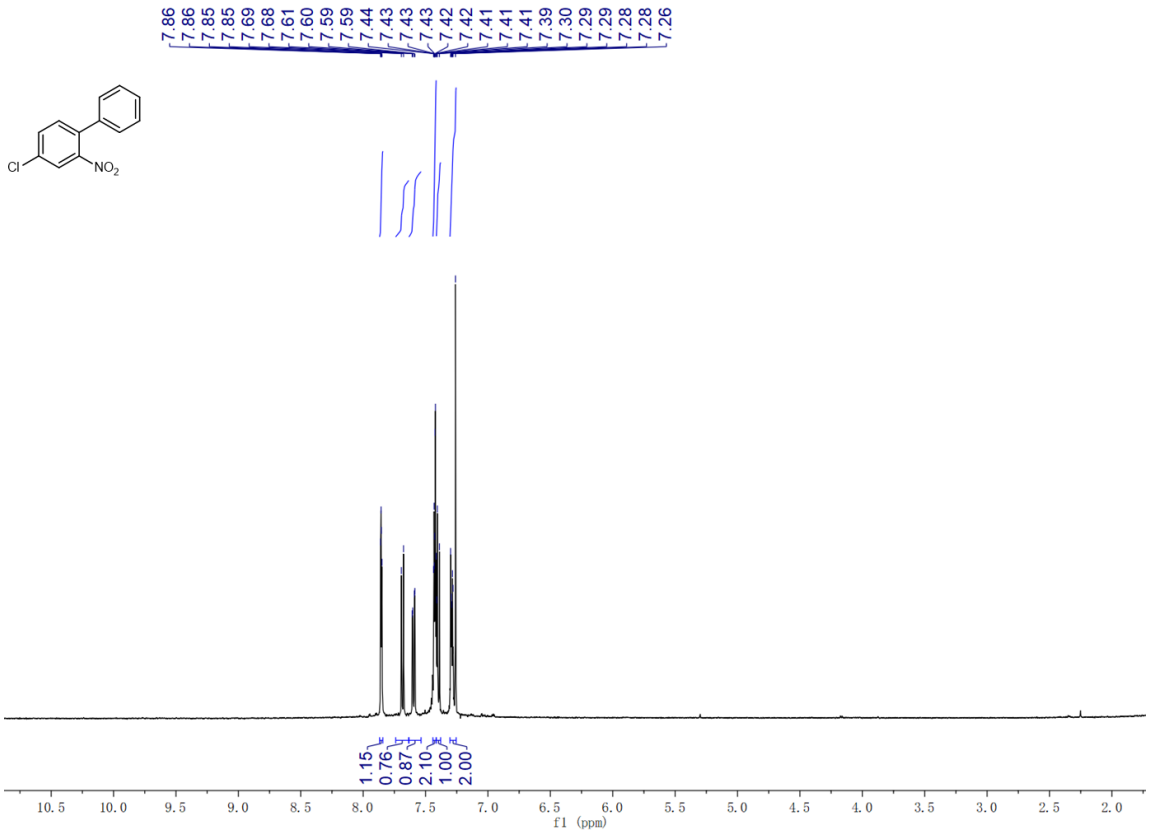

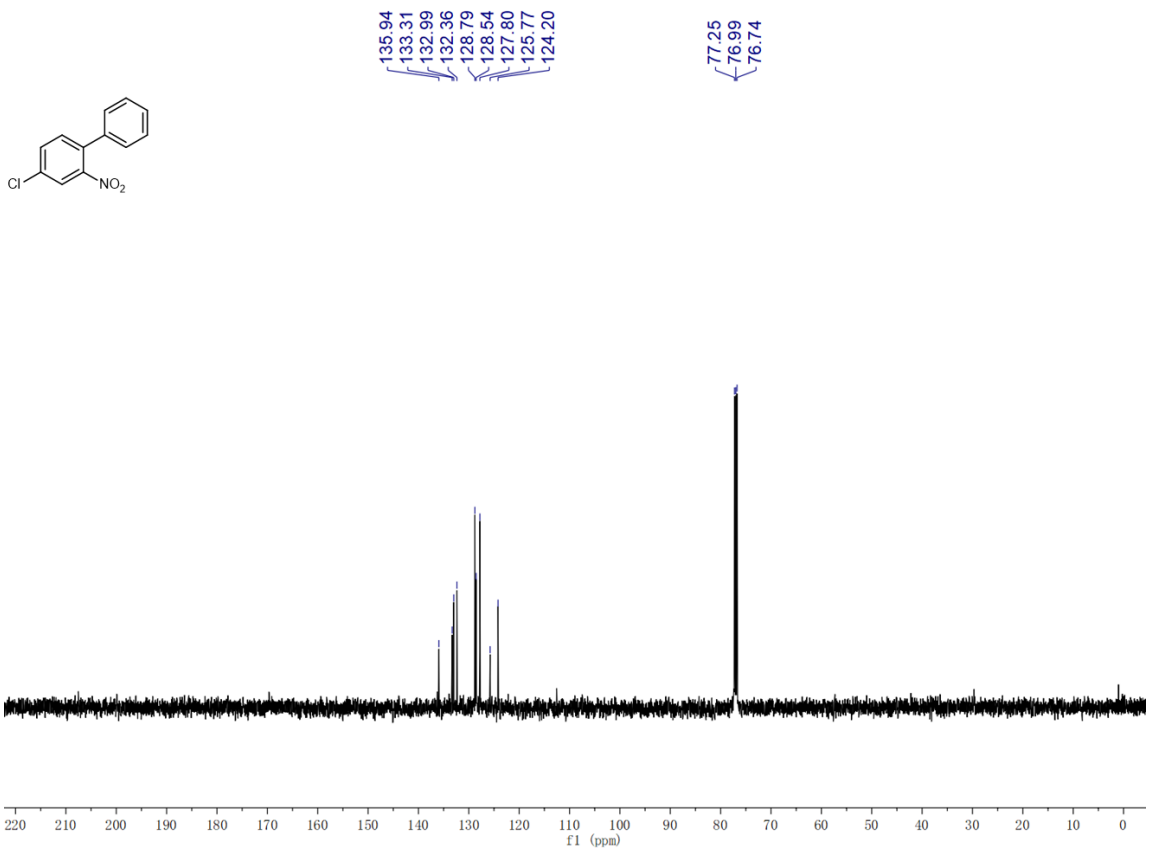

^{1}H and ^{13}C-NMR spectra of product 4aa.

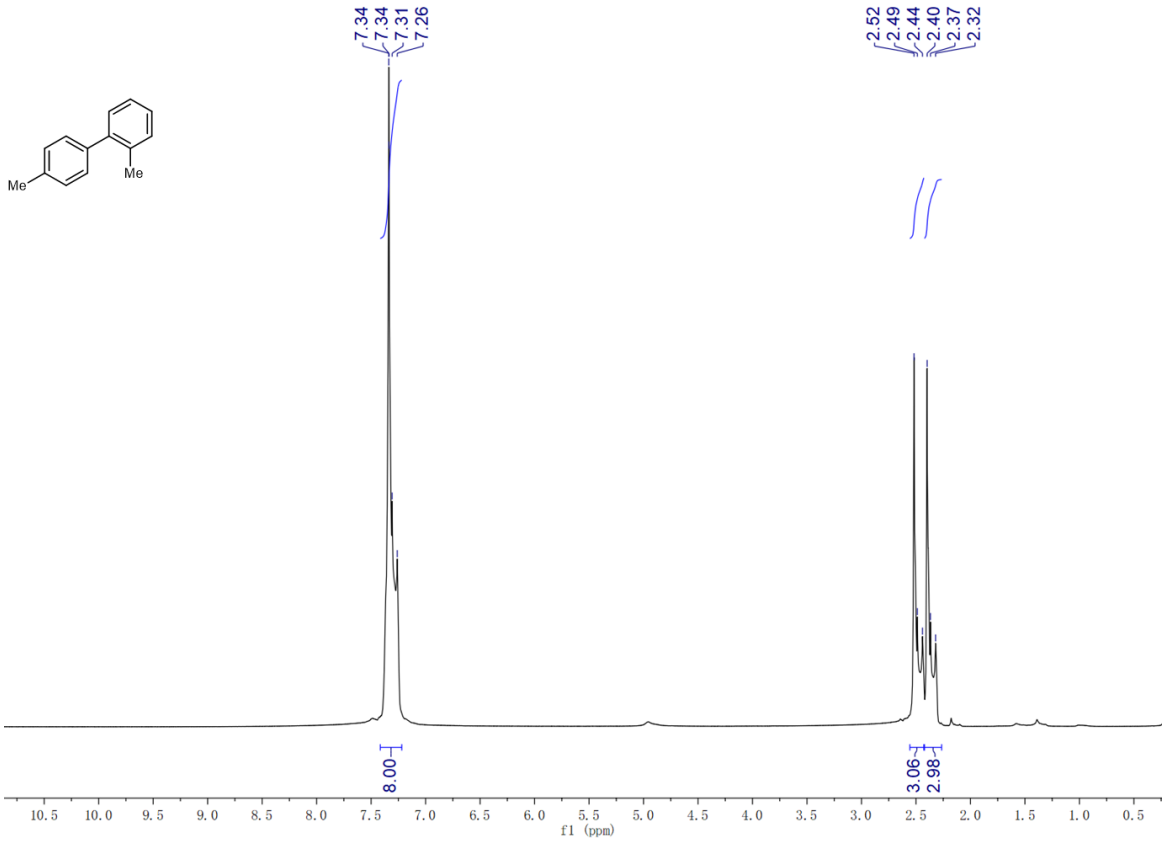

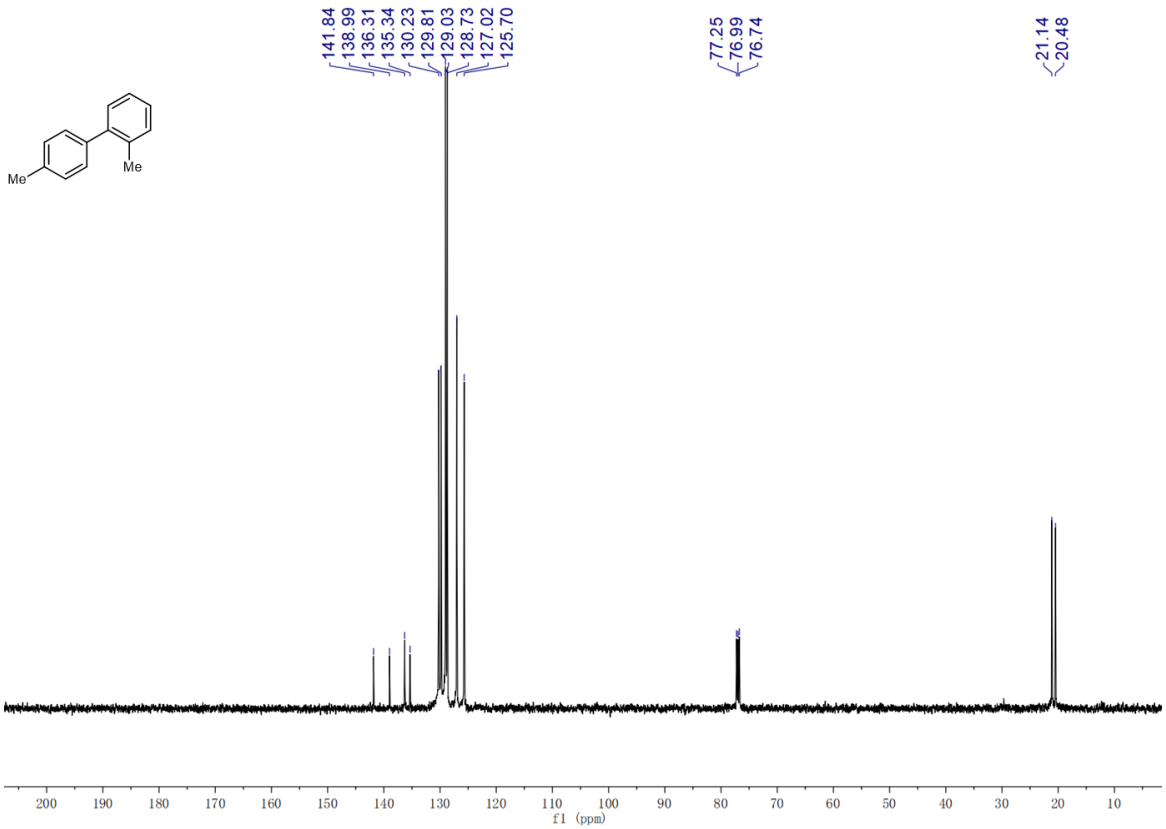

^{1}H and ^{13}C-NMR spectra of product 4ab.

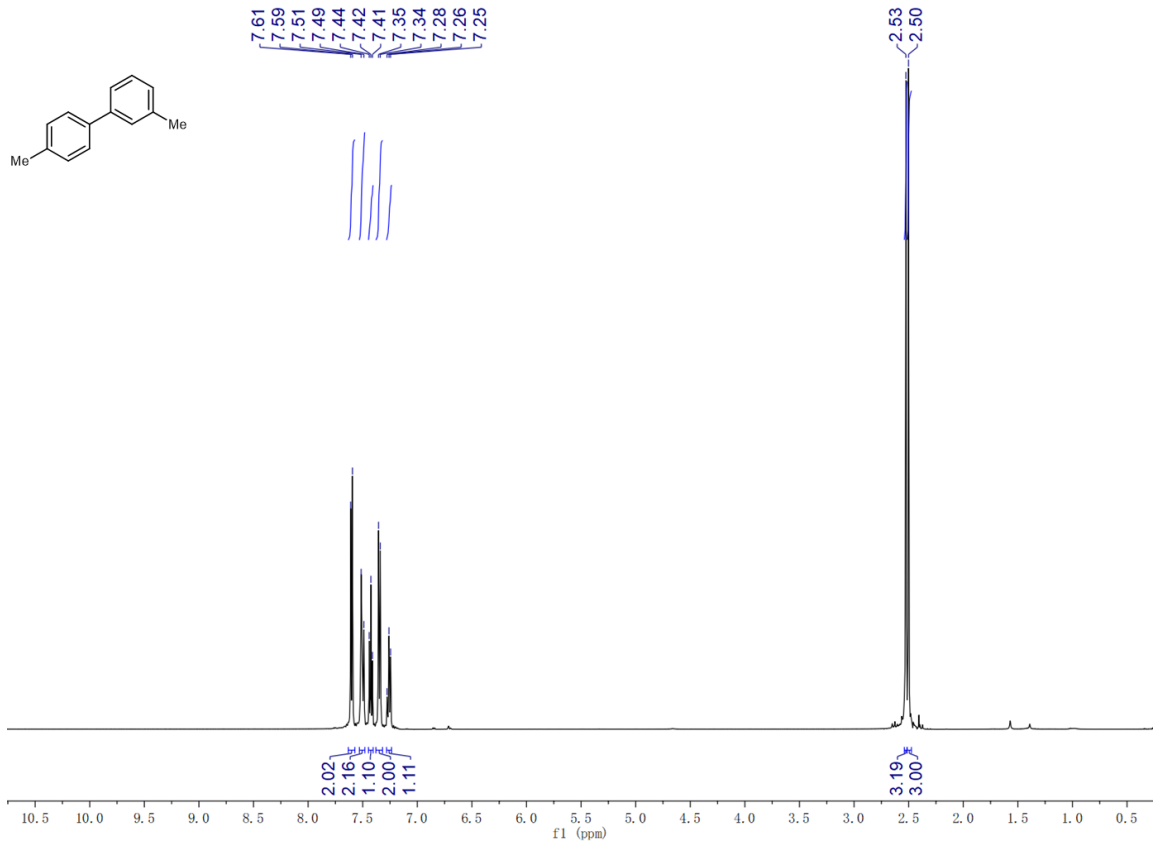

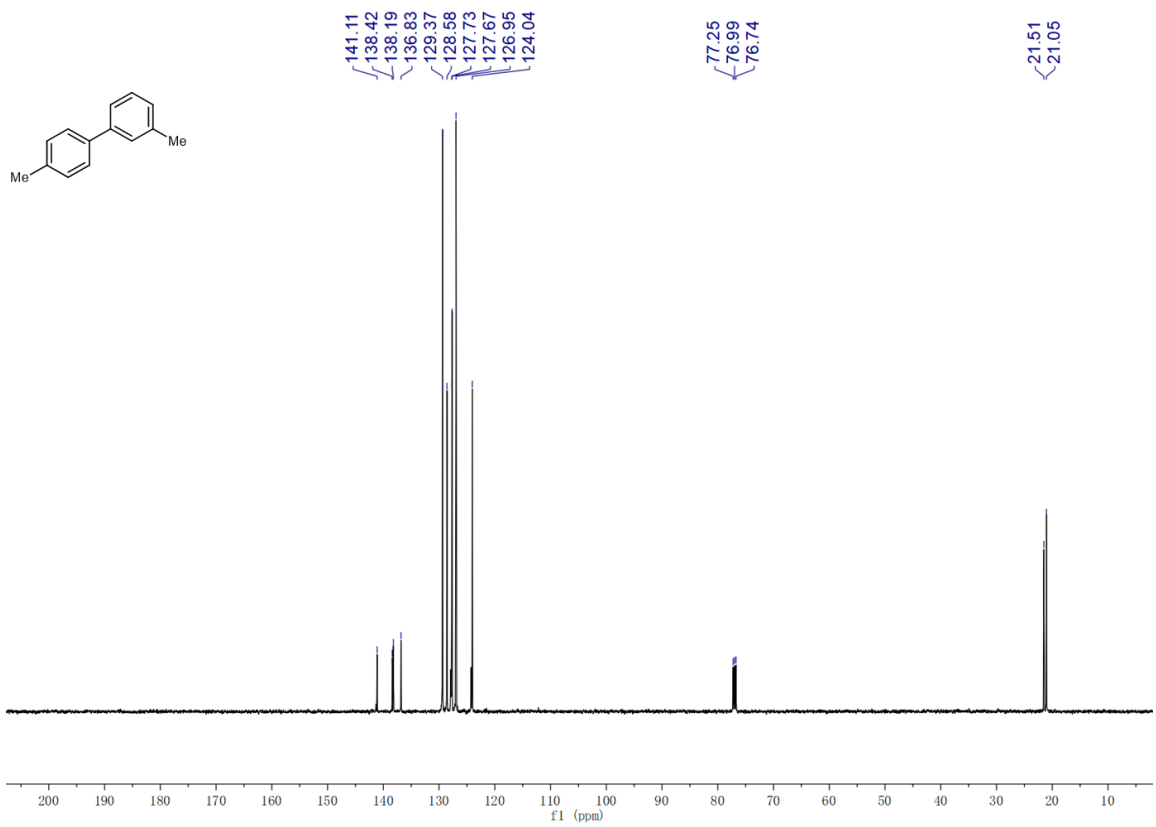

^{1}H and ^{13}C-NMR spectra of product 4ac.

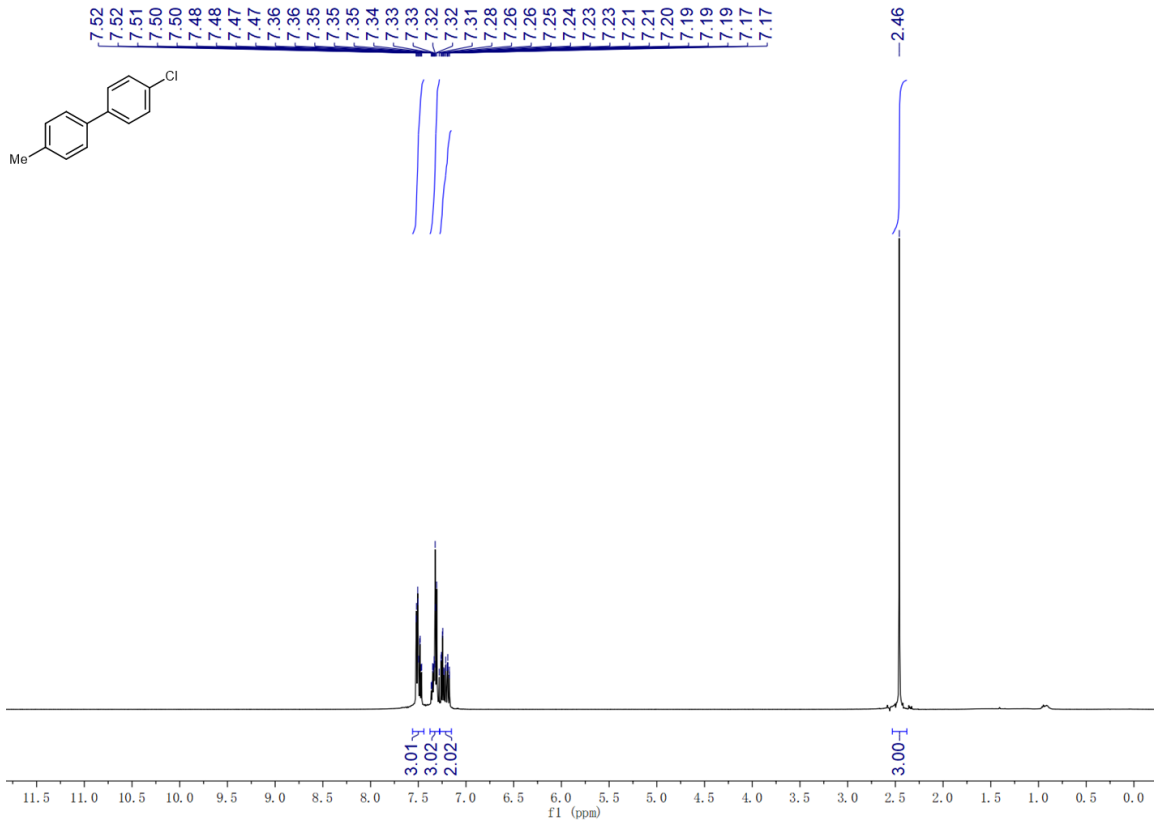

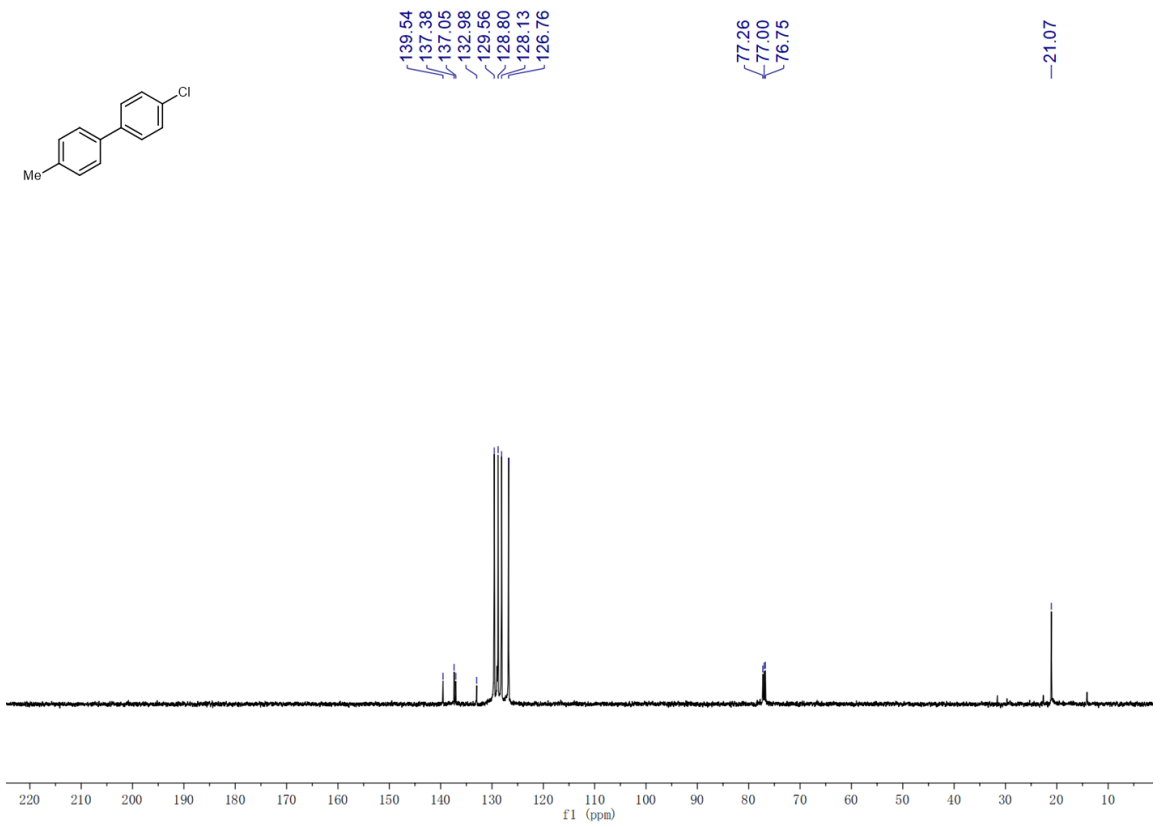

^{1}H and ^{13}C, ^{19}F-NMR spectra of product 4ad.

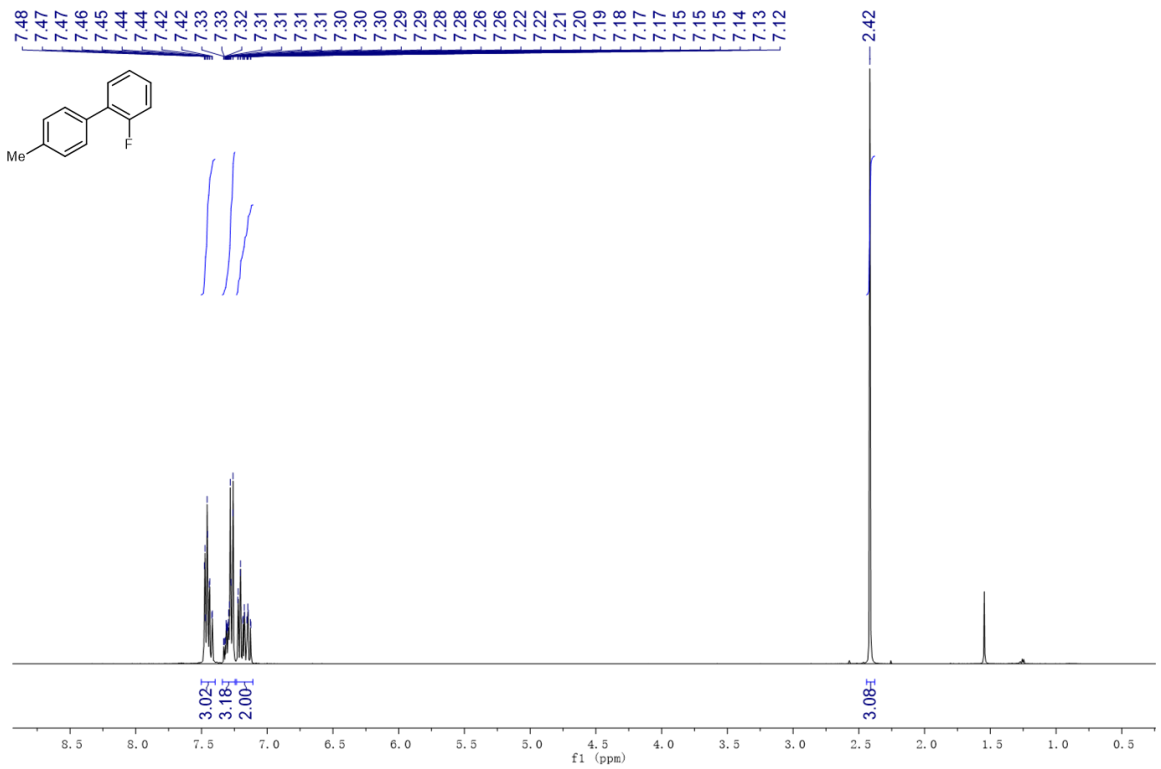

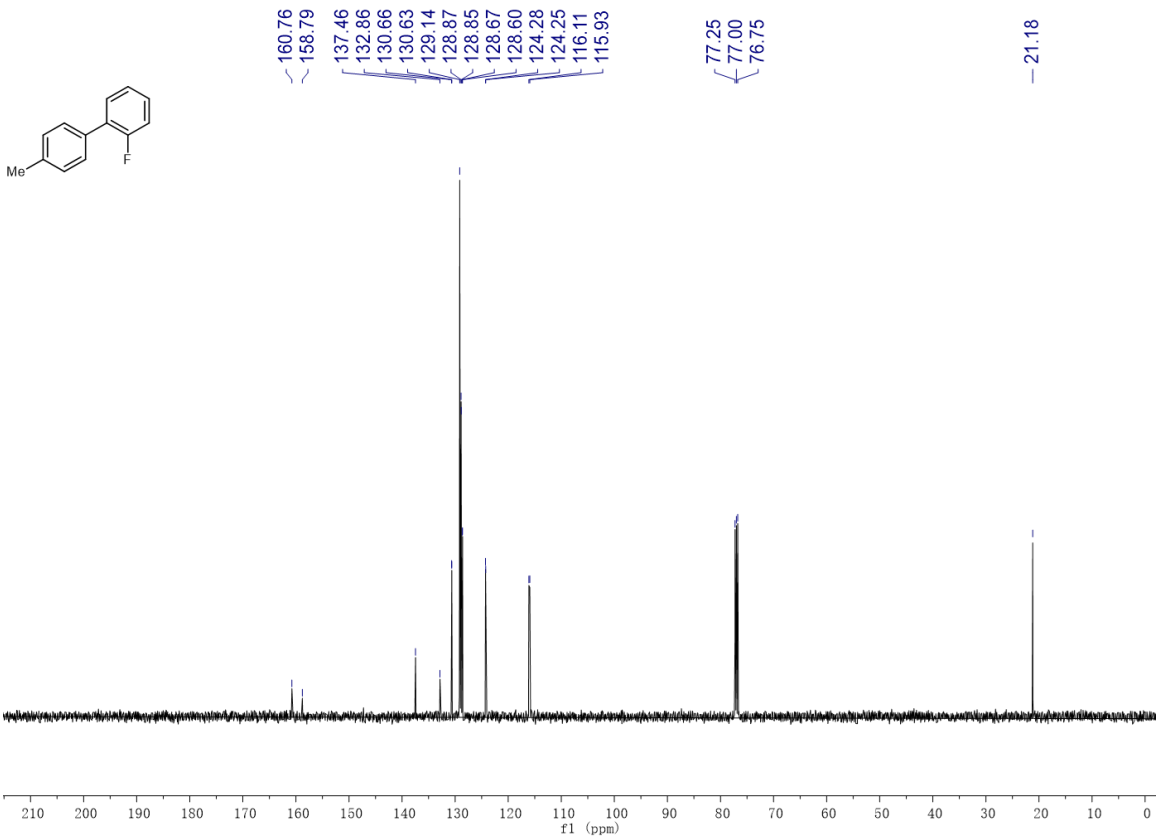

1195

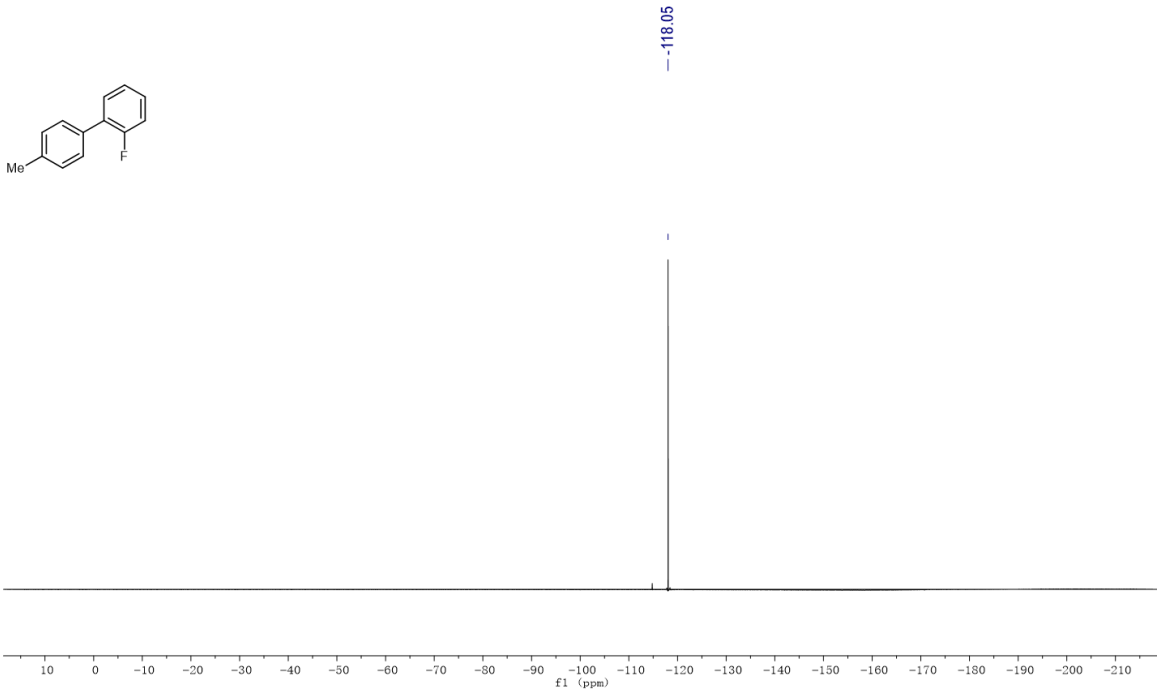

1196

1197

^{1}H and ^{13}C-NMR spectra of product 5a.

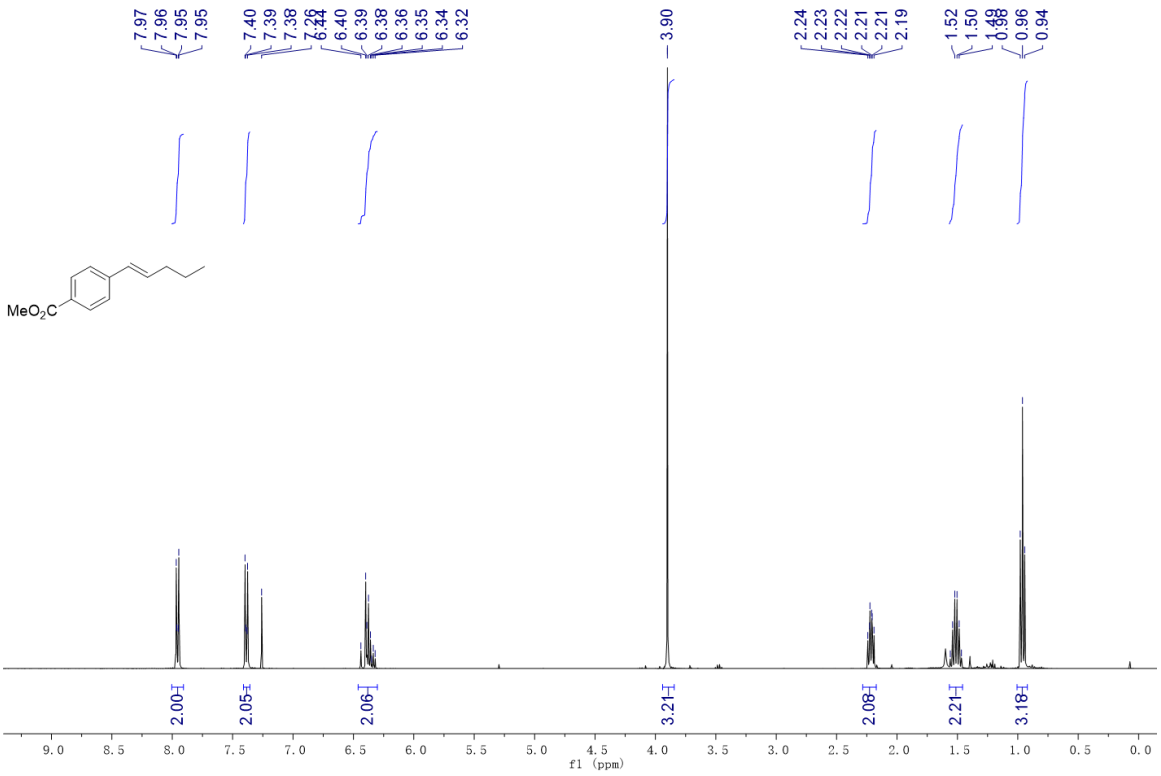

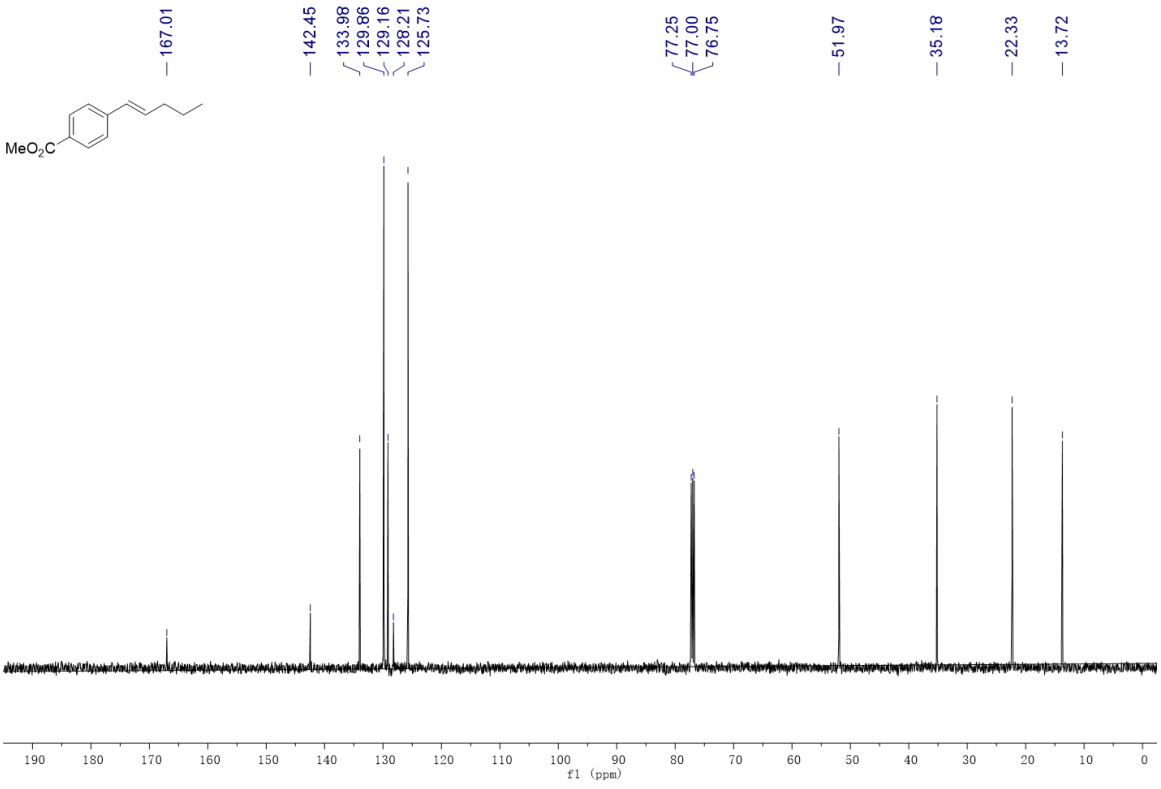

[1]Hand [13]C-NMR spectra of product 5b.

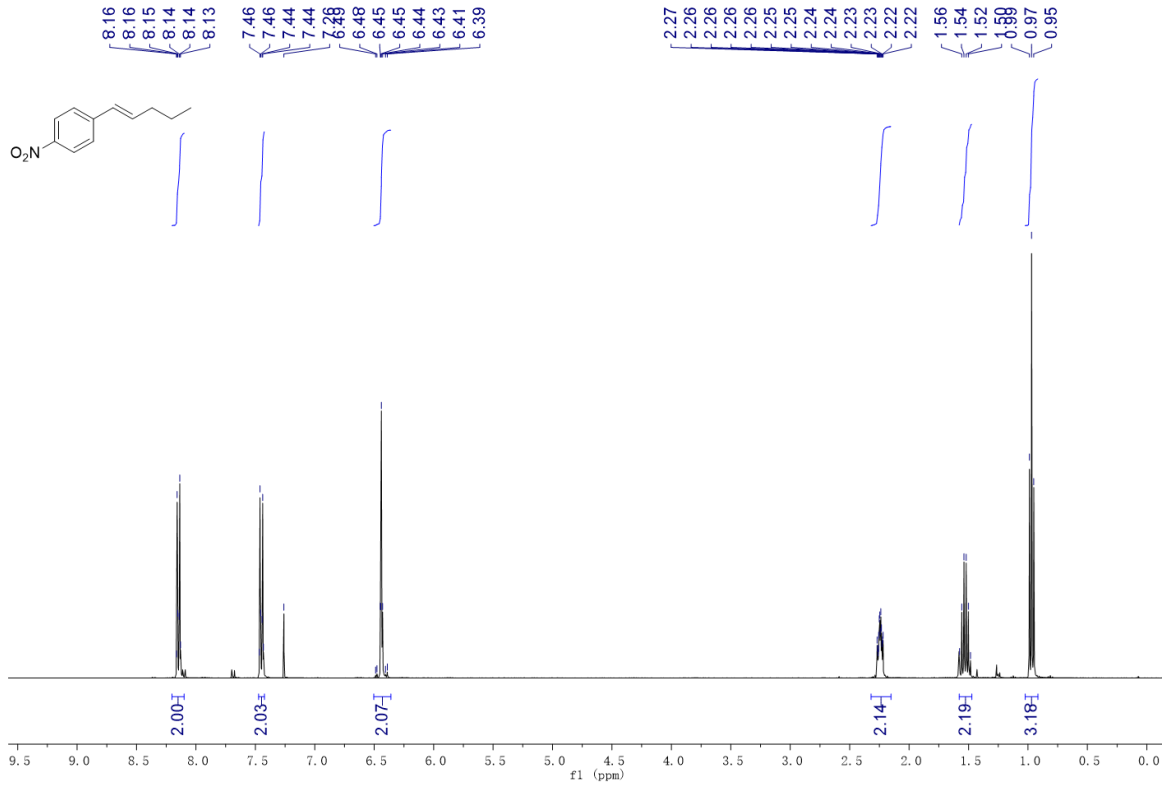

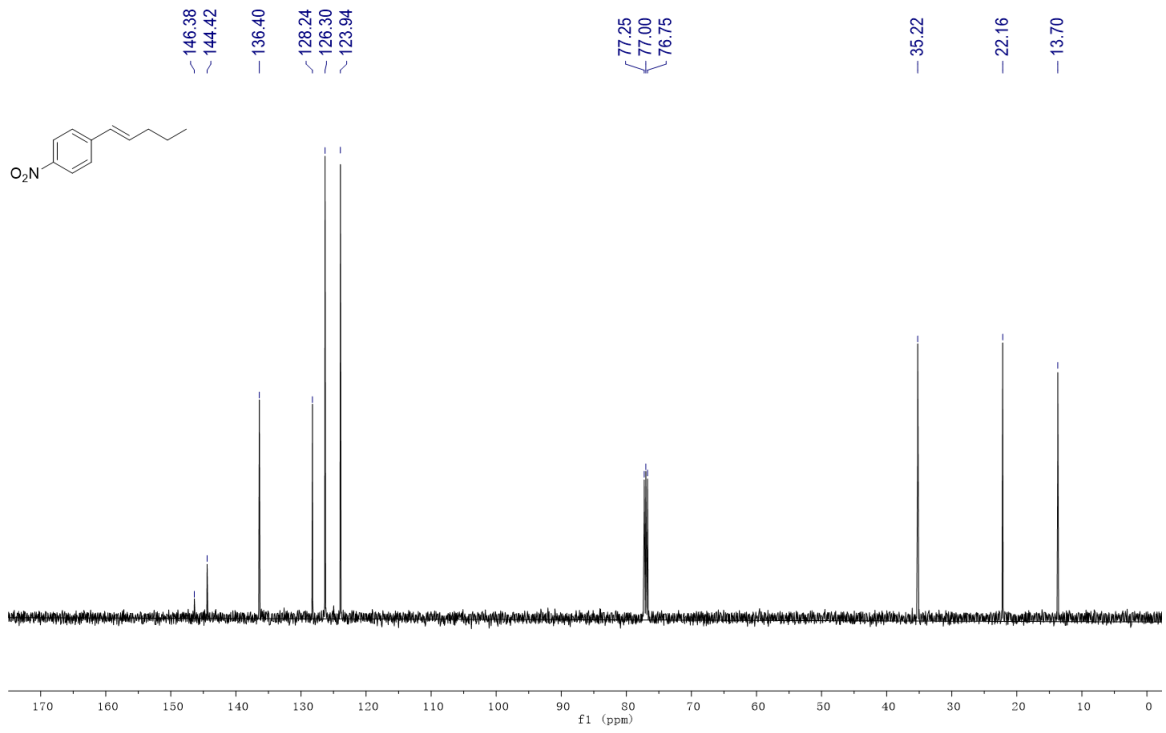

^{1}H and ^{13}C-NMR spectra of product 5c.

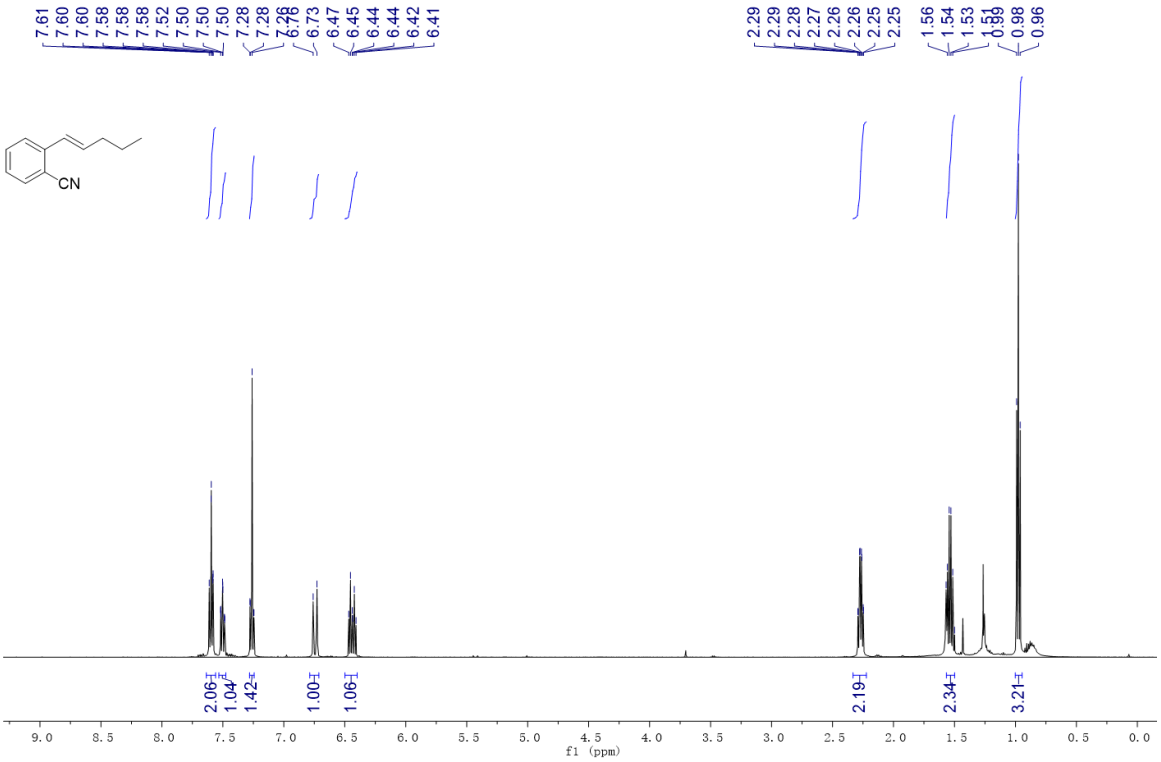

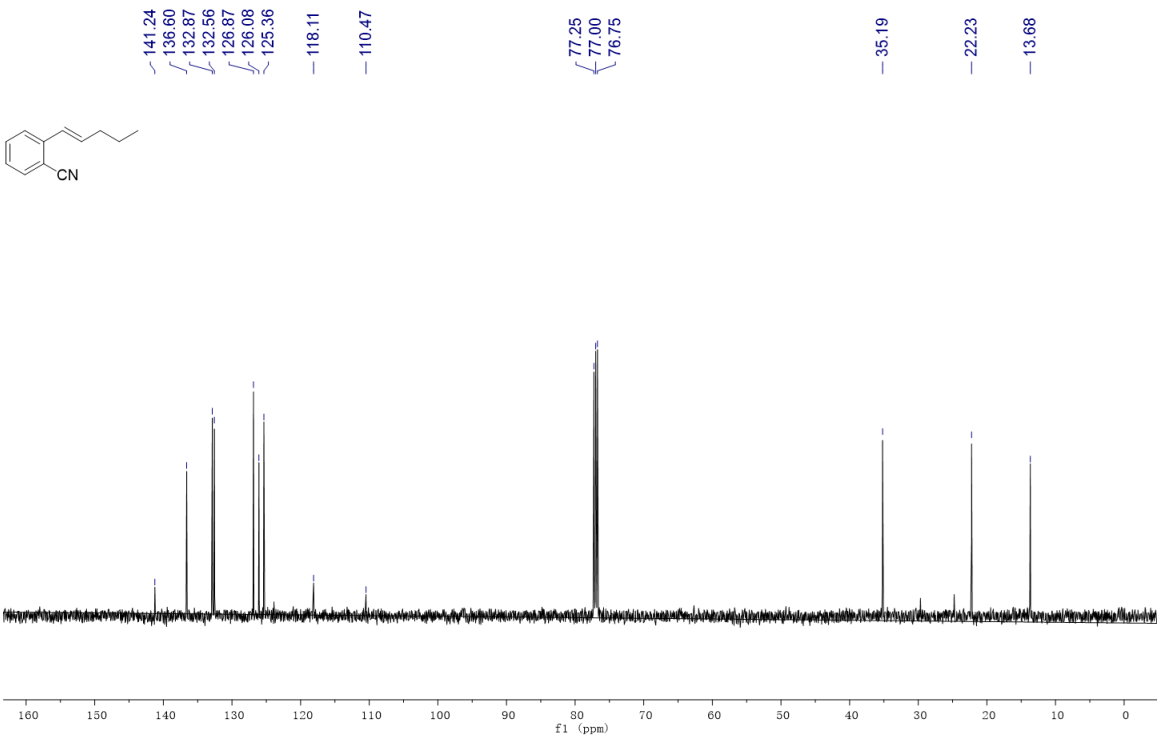

^{1}H and ^{13}C-NMR spectra of product 5d.

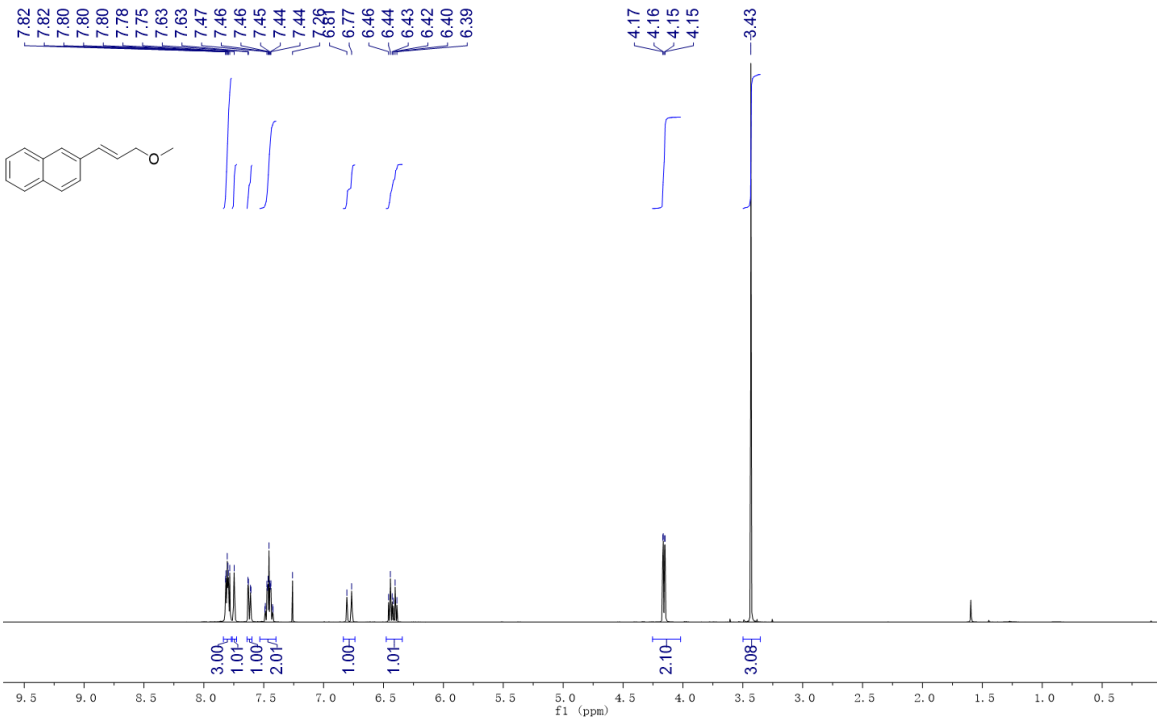

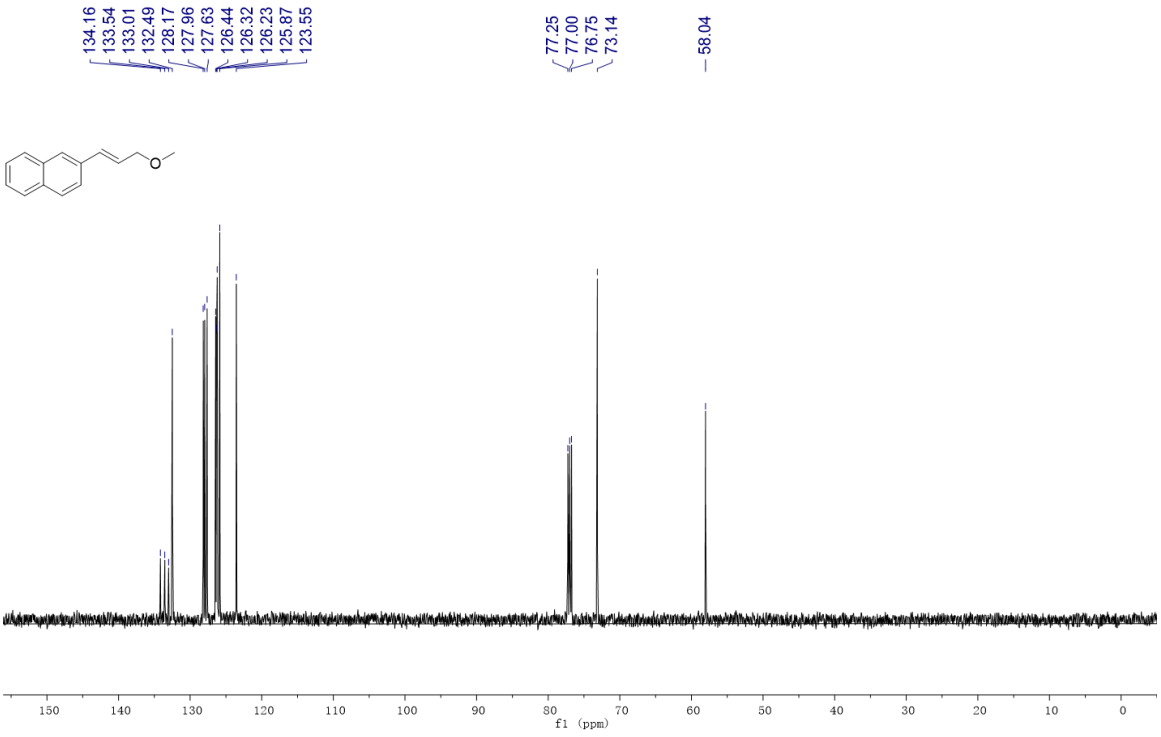

^{1}H and ^{13}C-NMR spectra of product 5e.

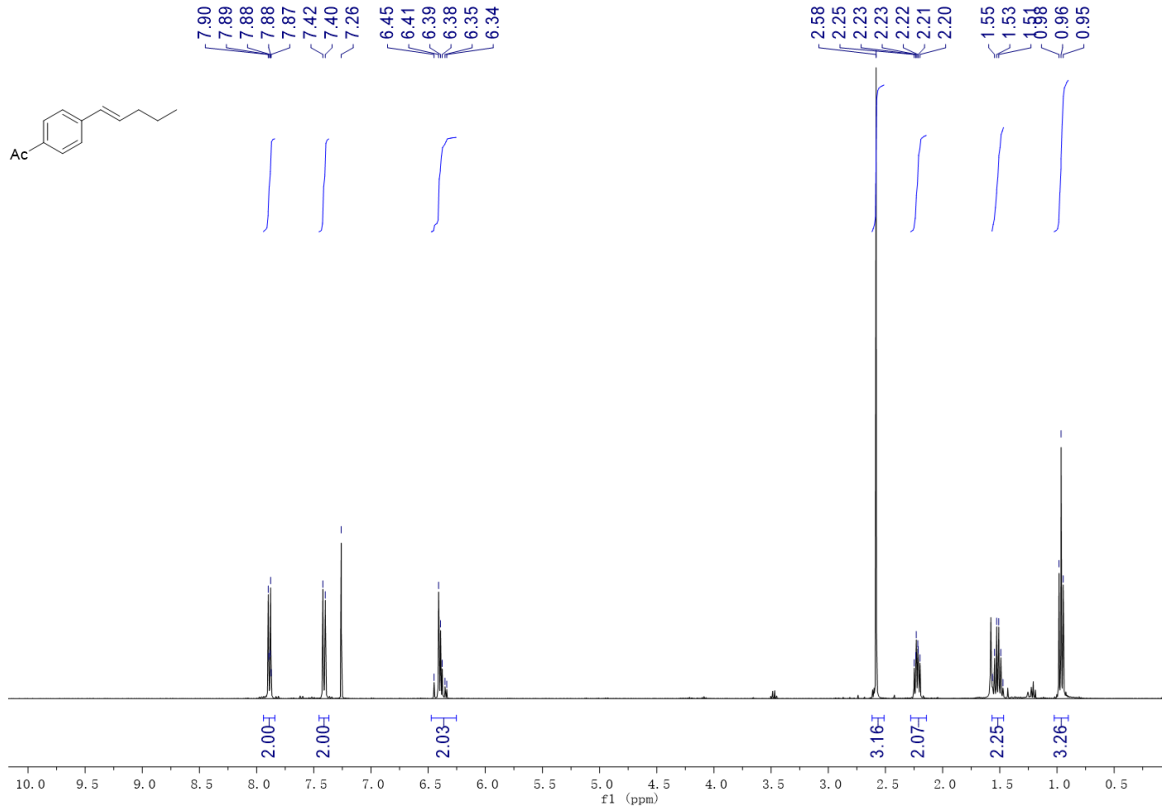

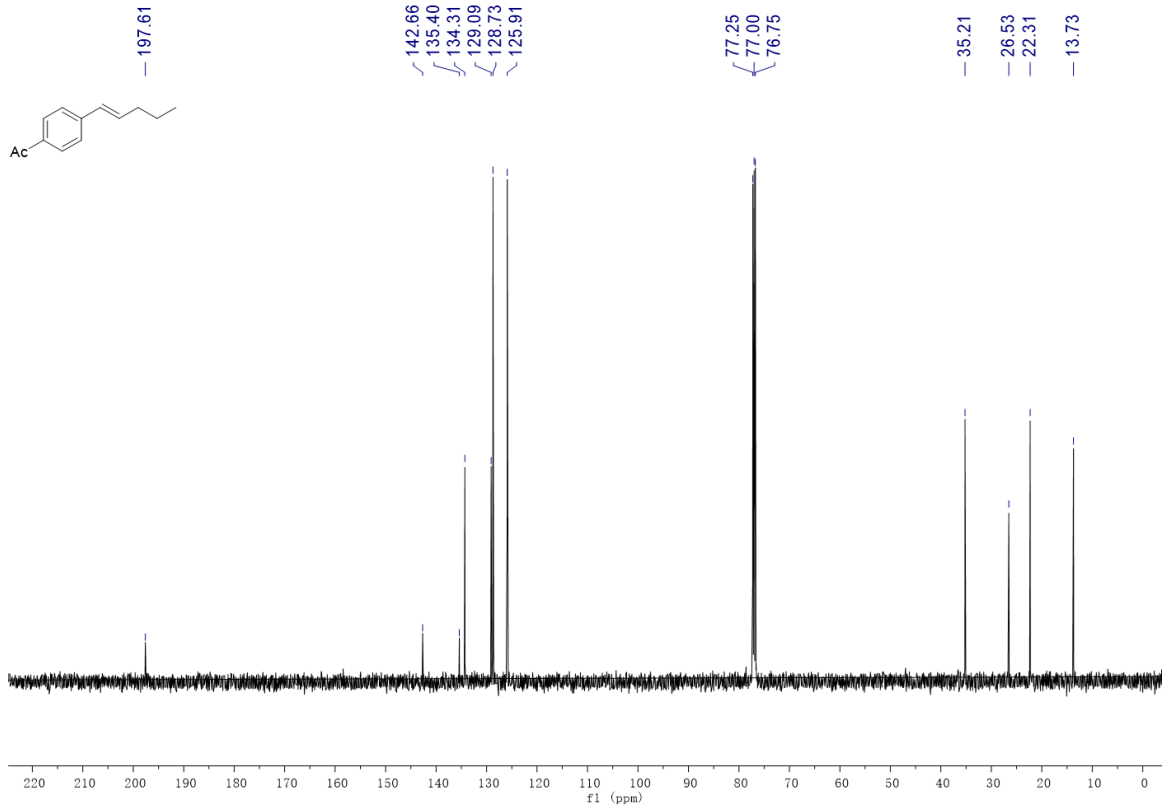

^{1}H and ^{13}C-NMR spectra of product 5f.

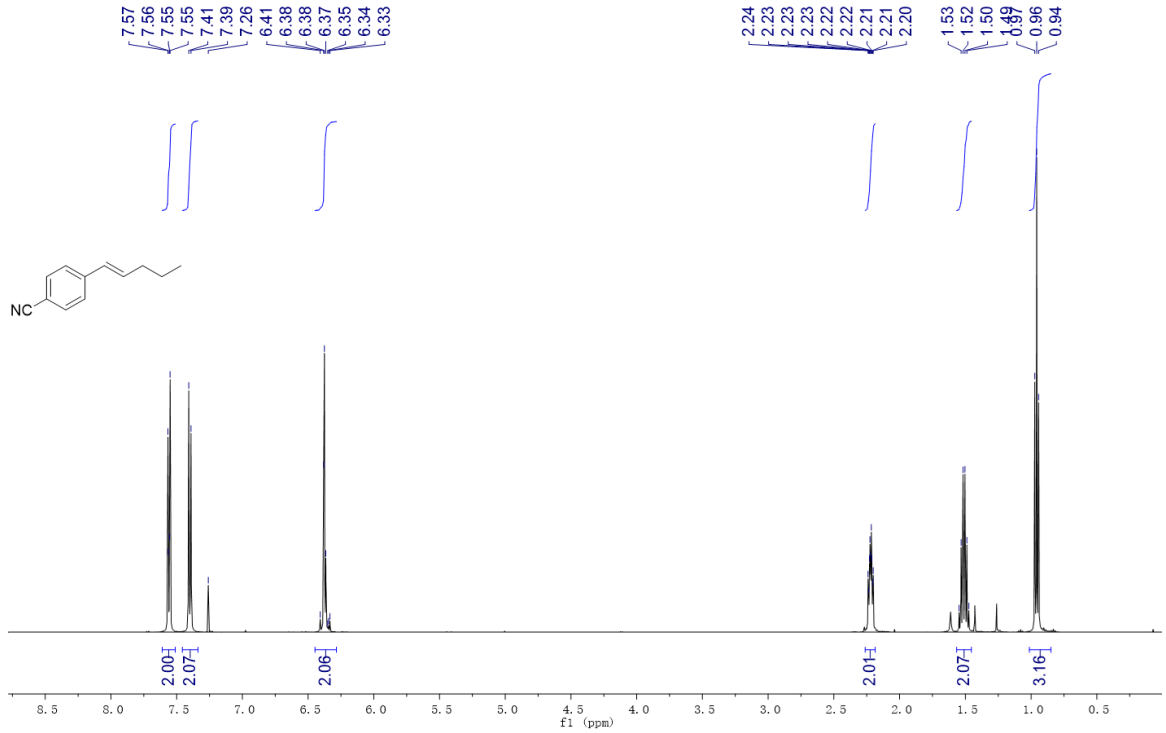

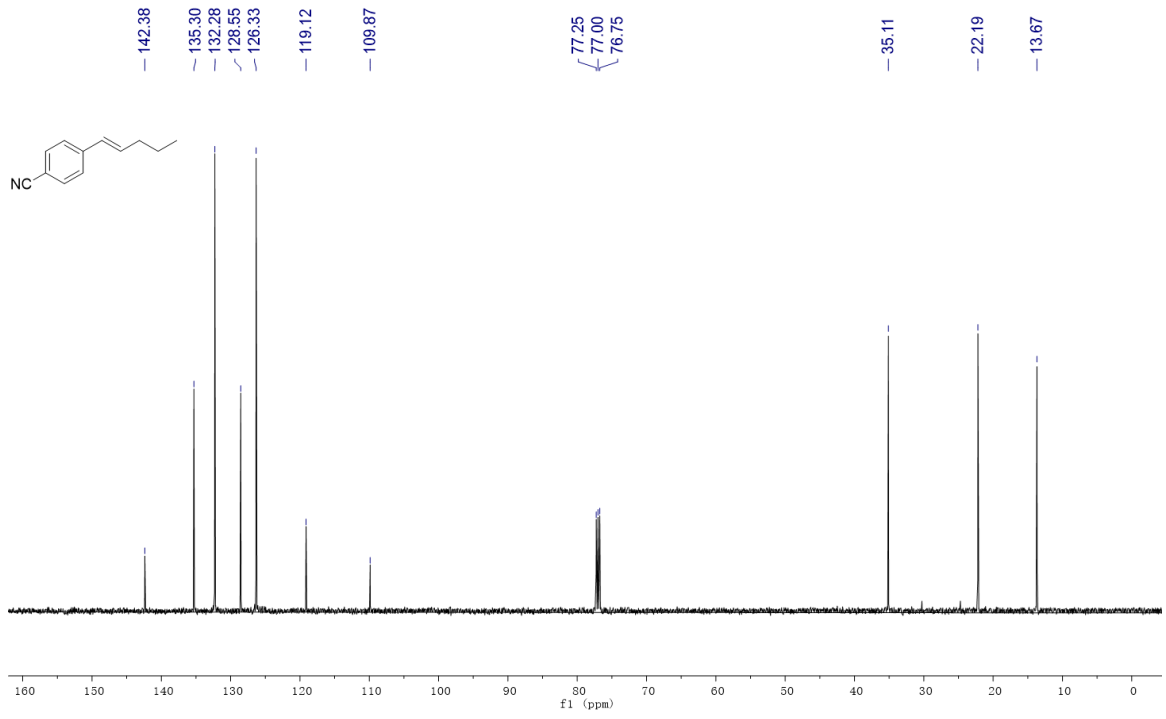

^{1}H and ^{13}C-NMR spectra of product 5g.

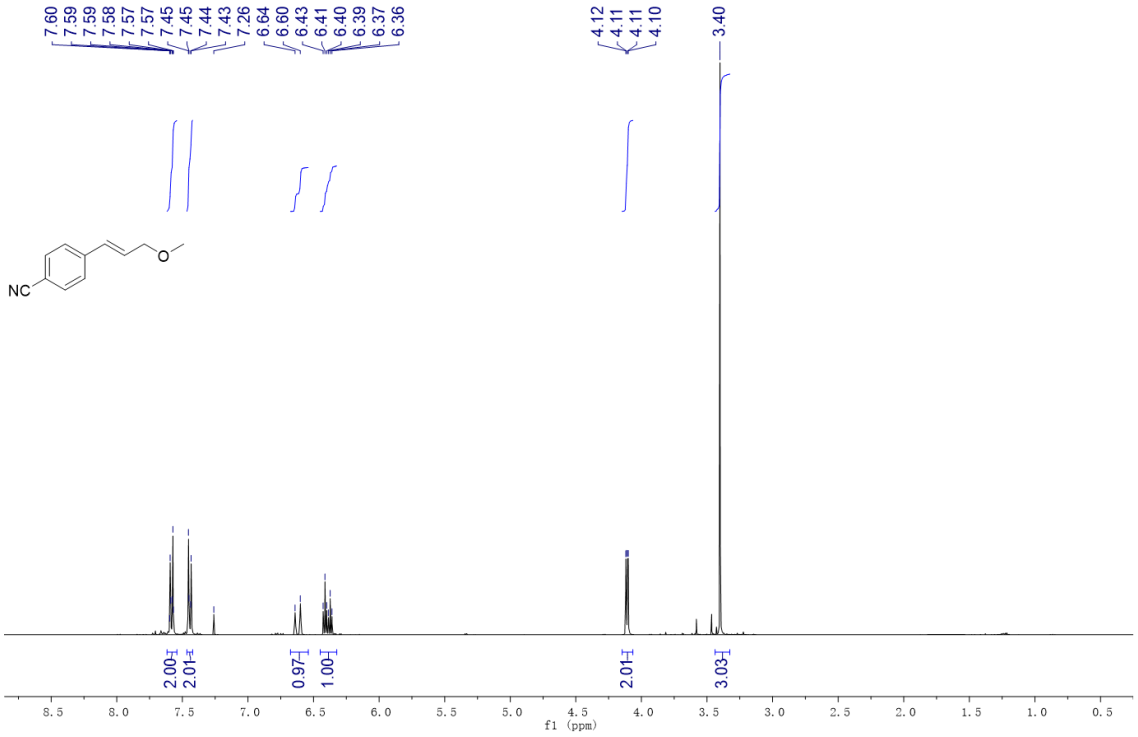

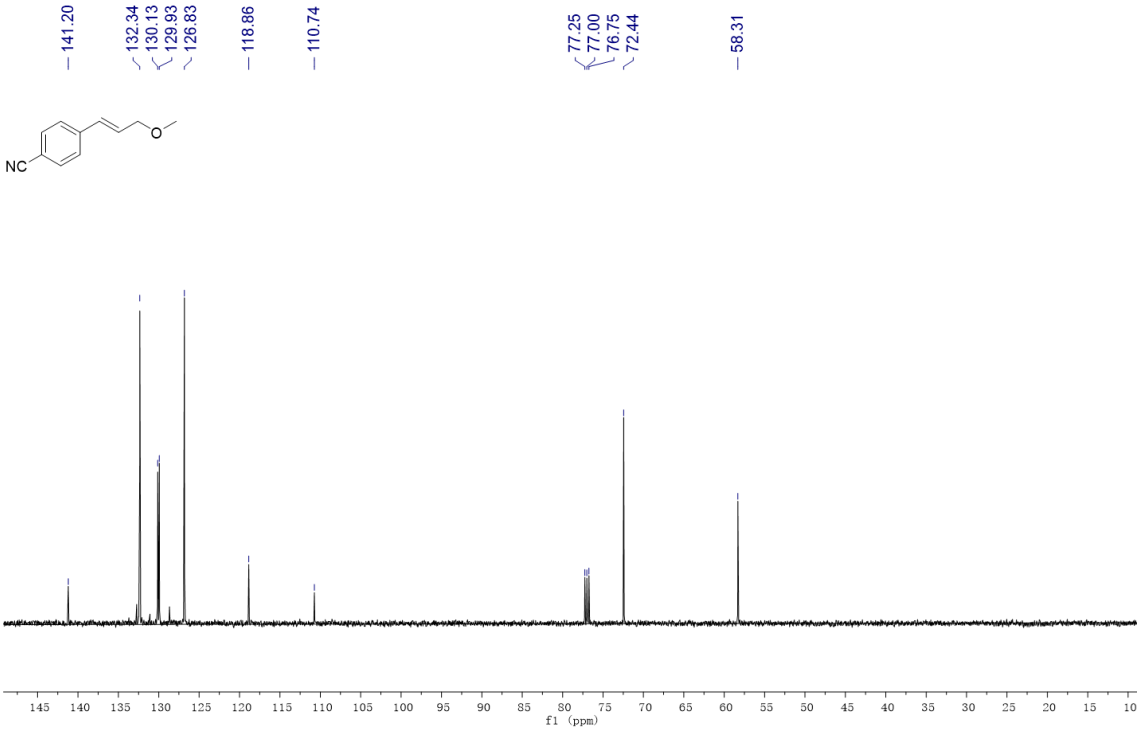

^{1}H and ^{13}C-NMR spectra of product 5h.

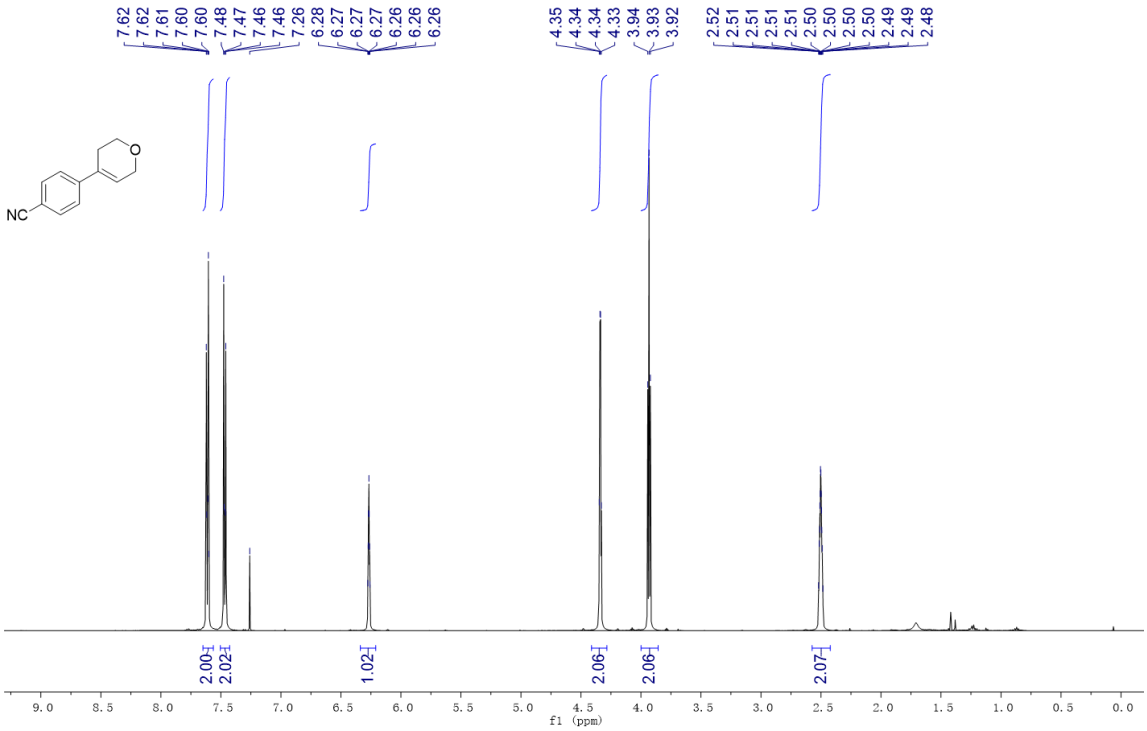

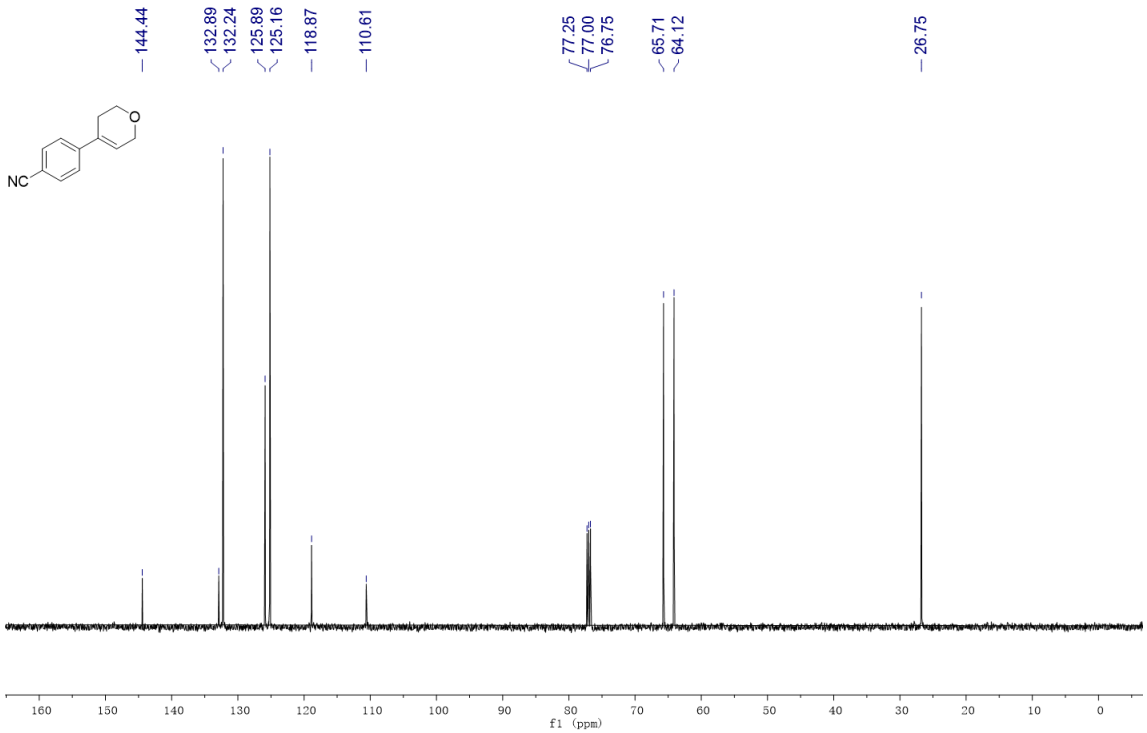

^{1}H and ^{13}C-NMR spectra of product 5i.

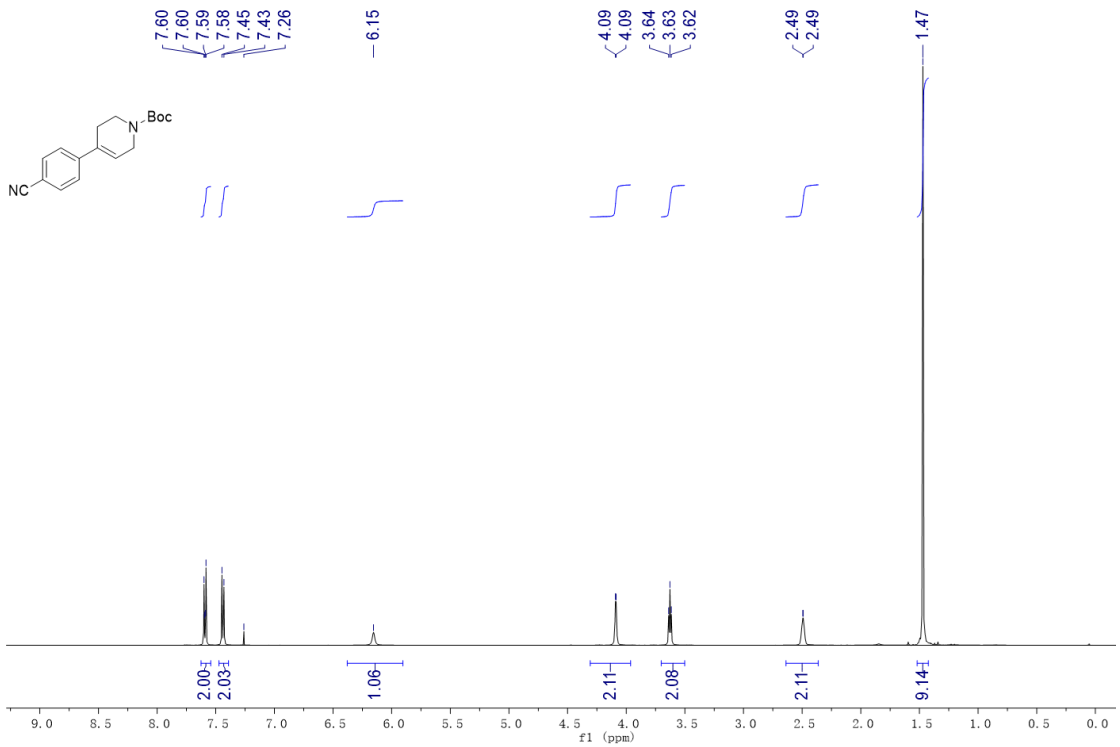

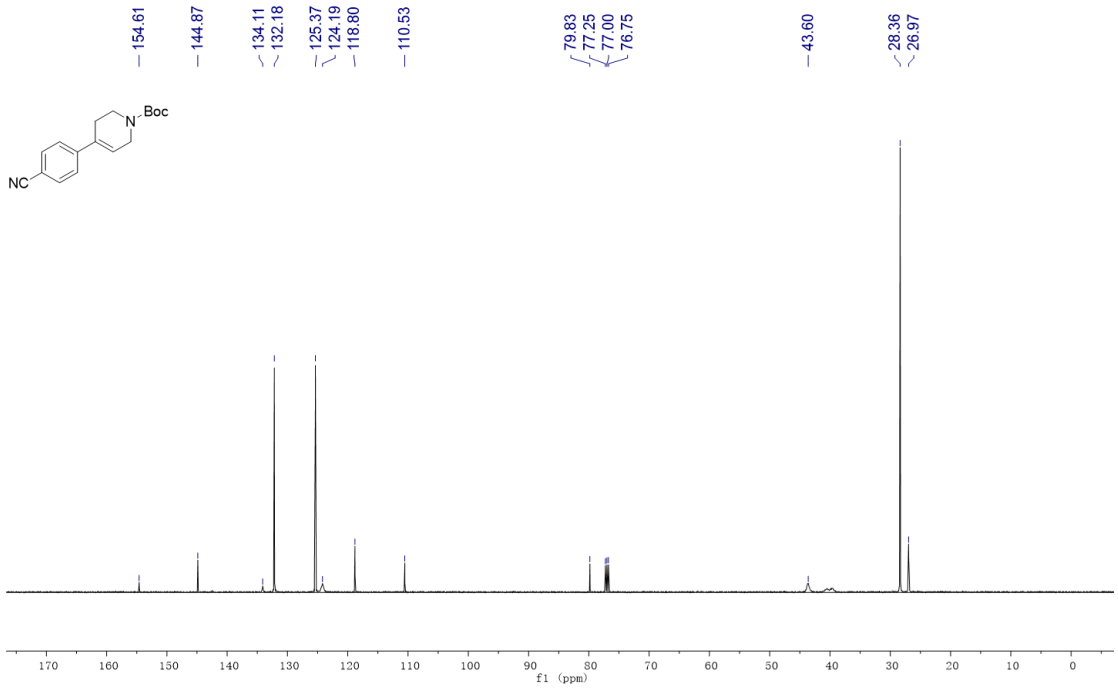

^{1}H and ^{13}C-NMR spectra of product 5j.

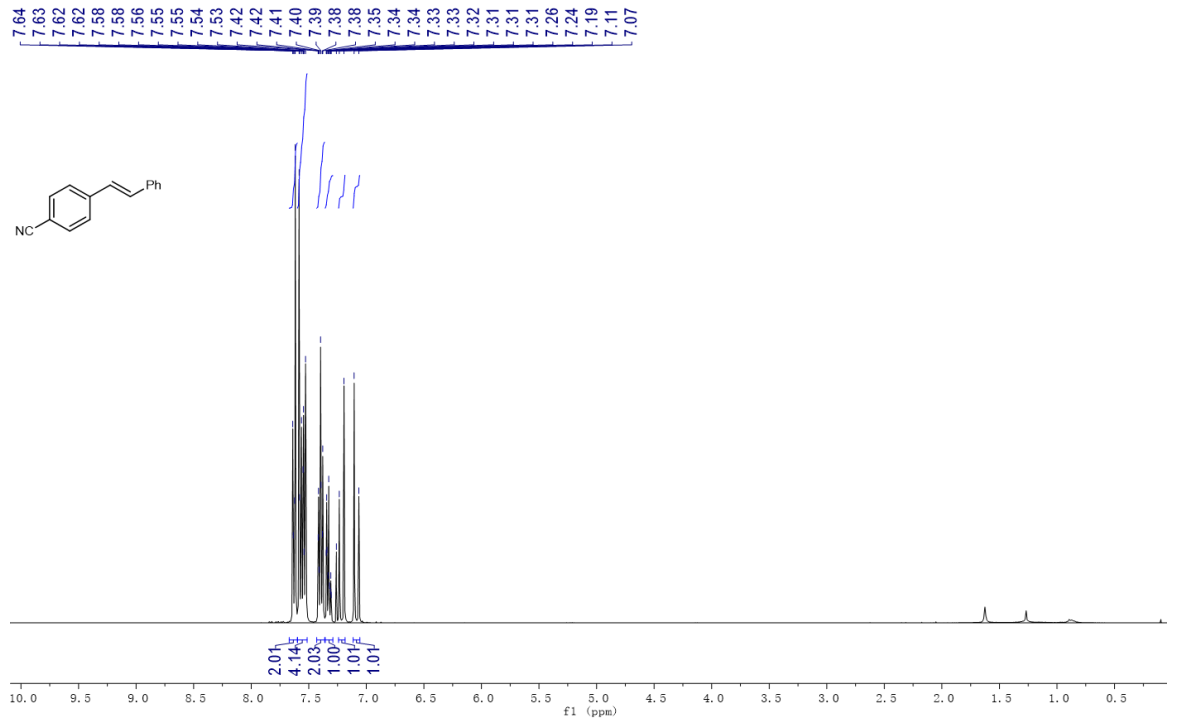

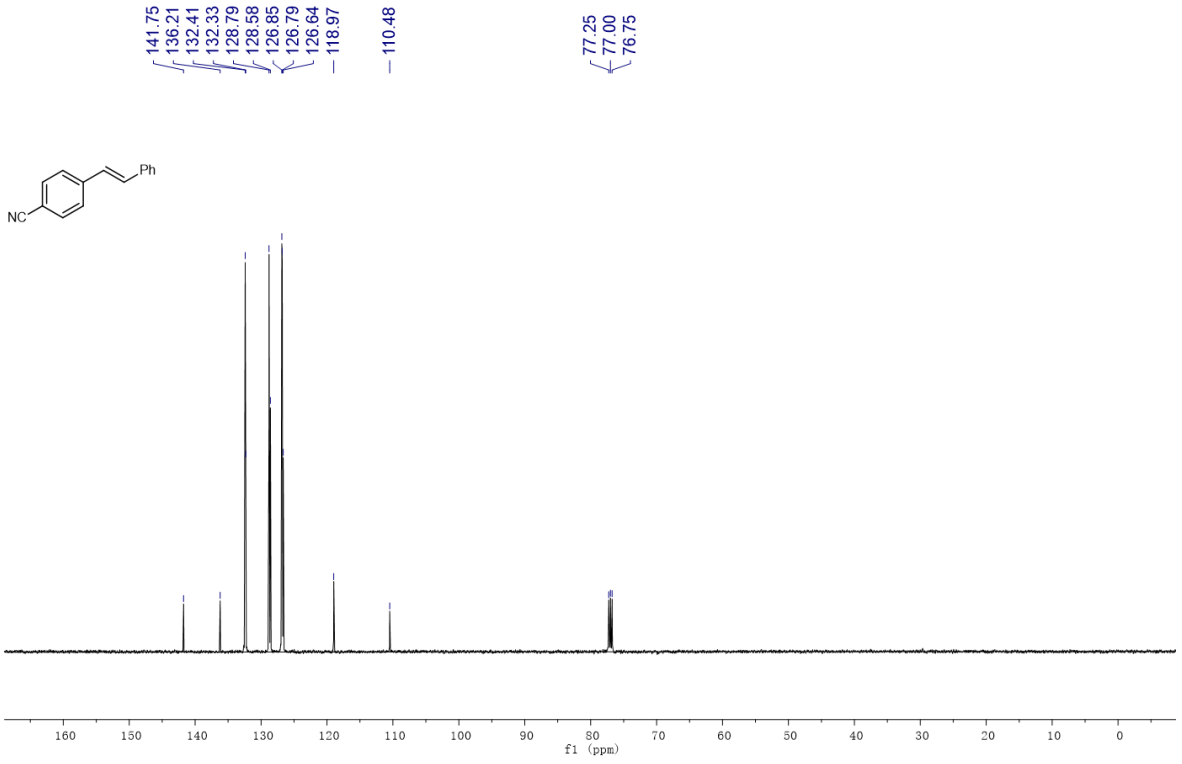

^{1}H and ^{13}C-NMR spectra of product 5k.

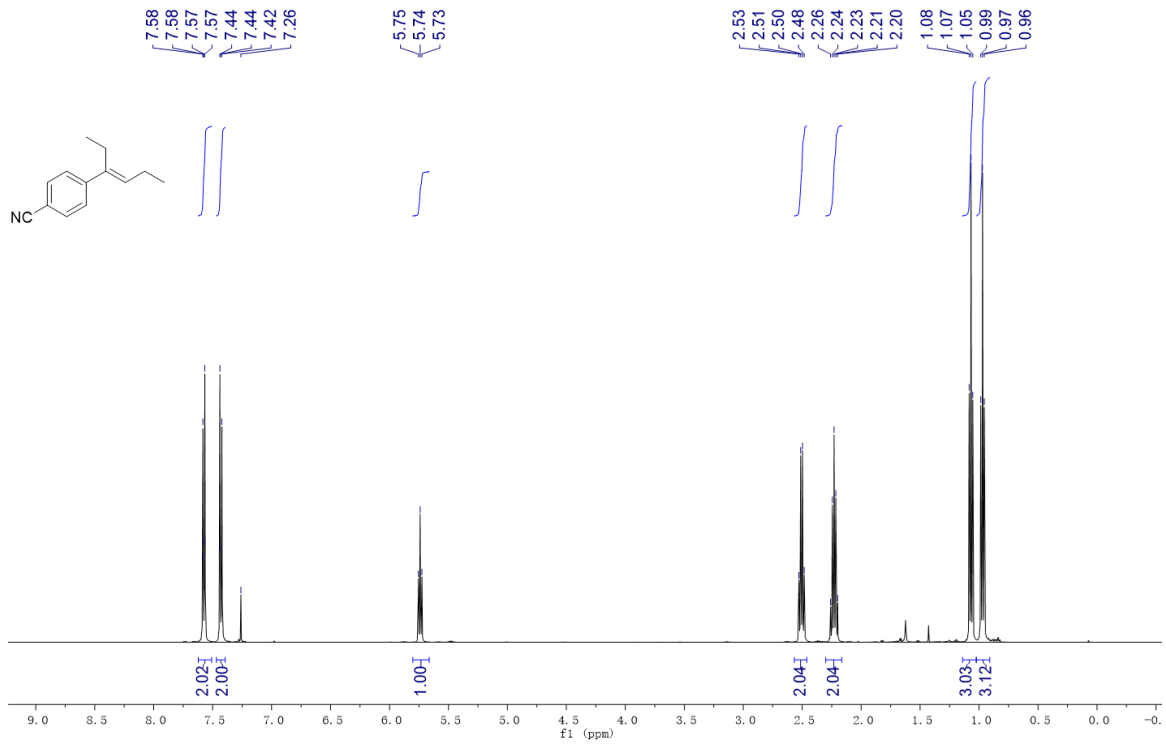

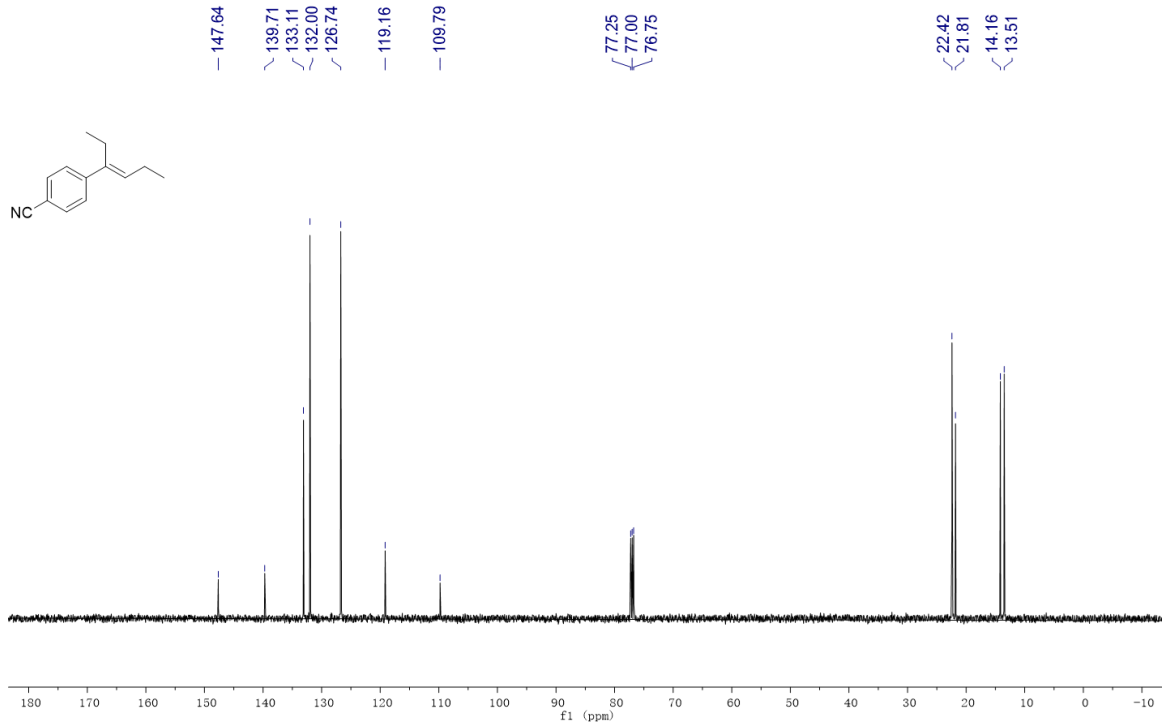

^{1}H and ^{13}C-NMR spectra of product 5l.

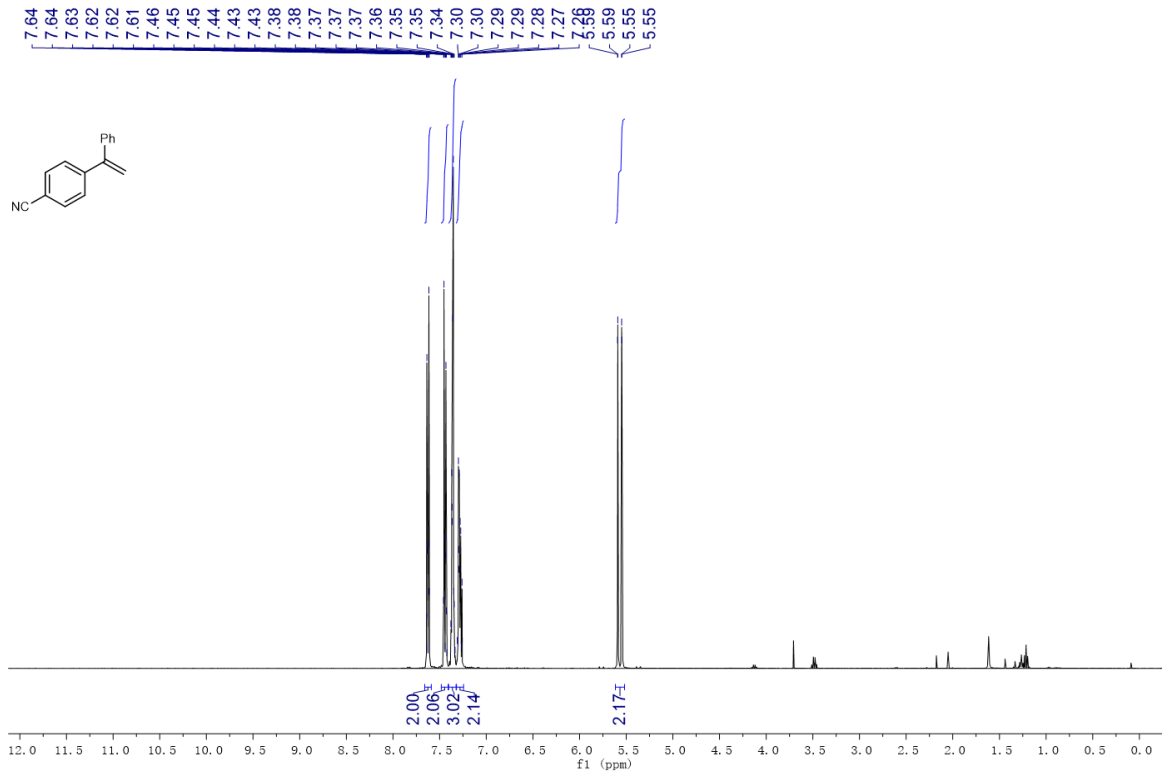

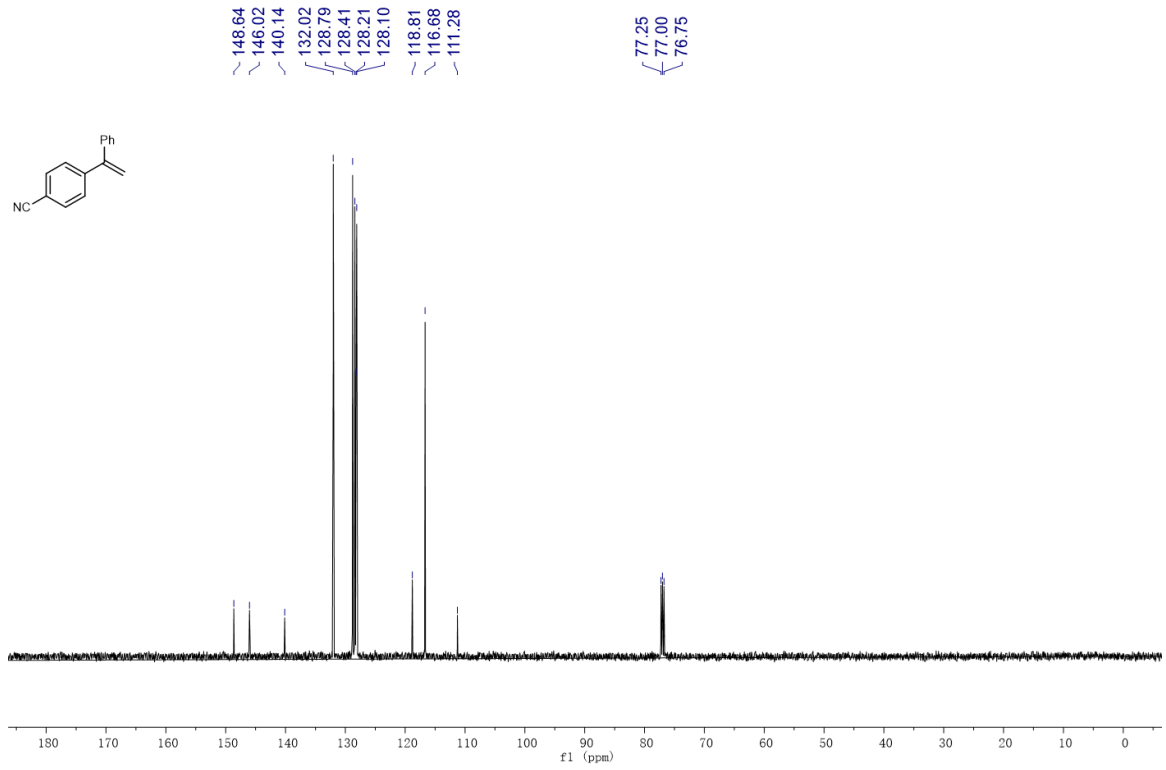

^{1}H, ^{13}C-NMR spectra of product 4ae.

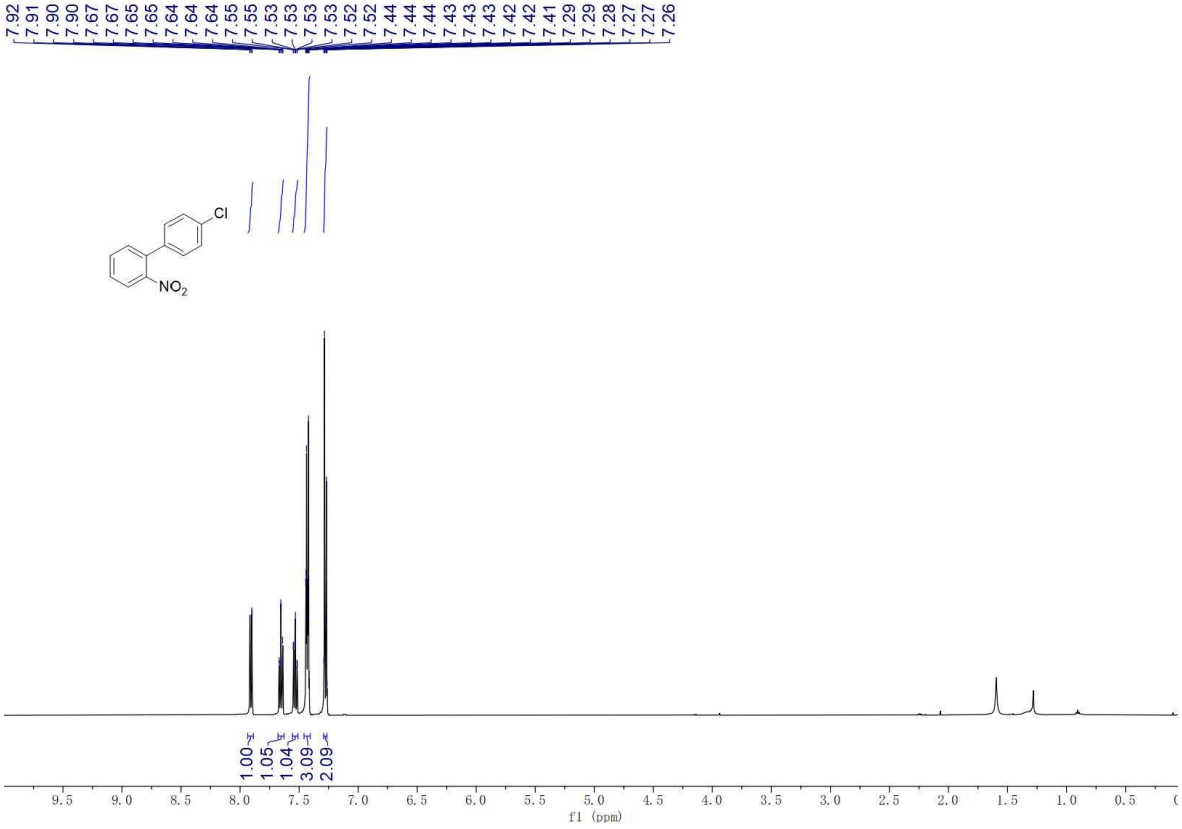

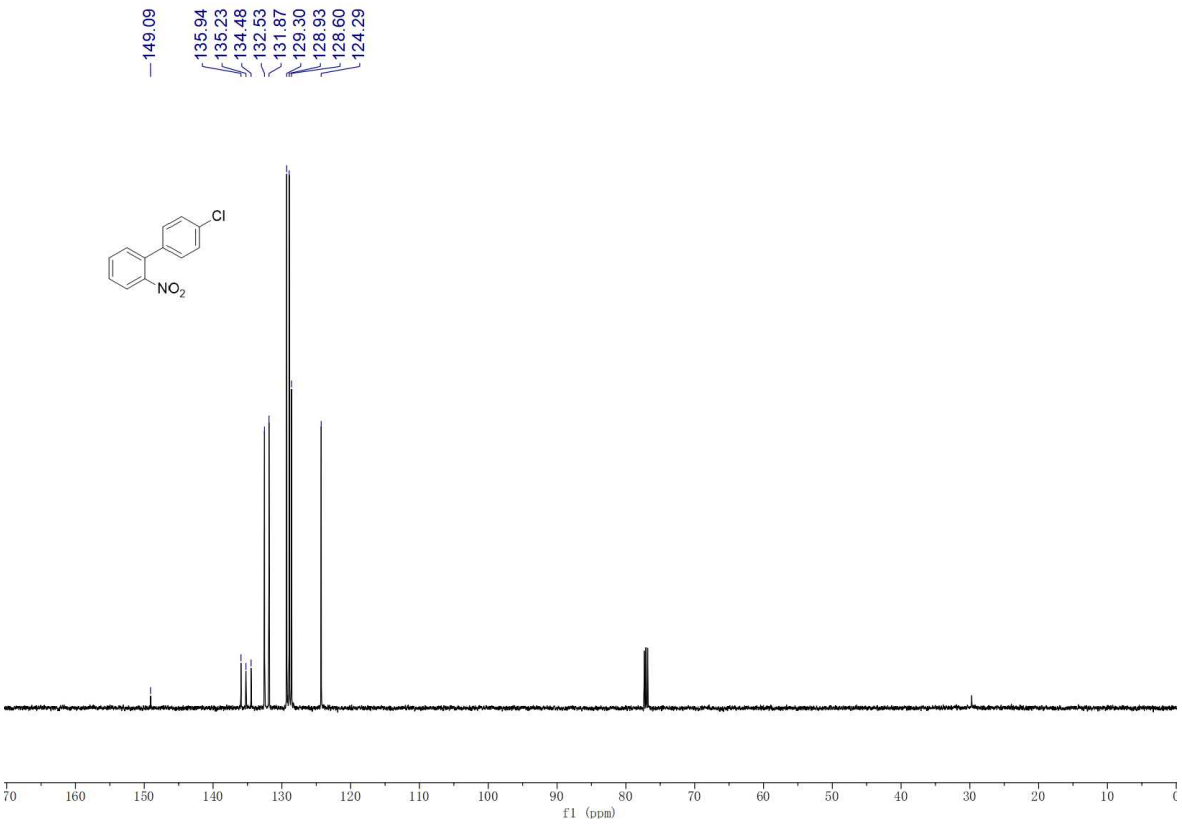

^{1}H,^{13}C and ^{19}F NMR of product 4af.

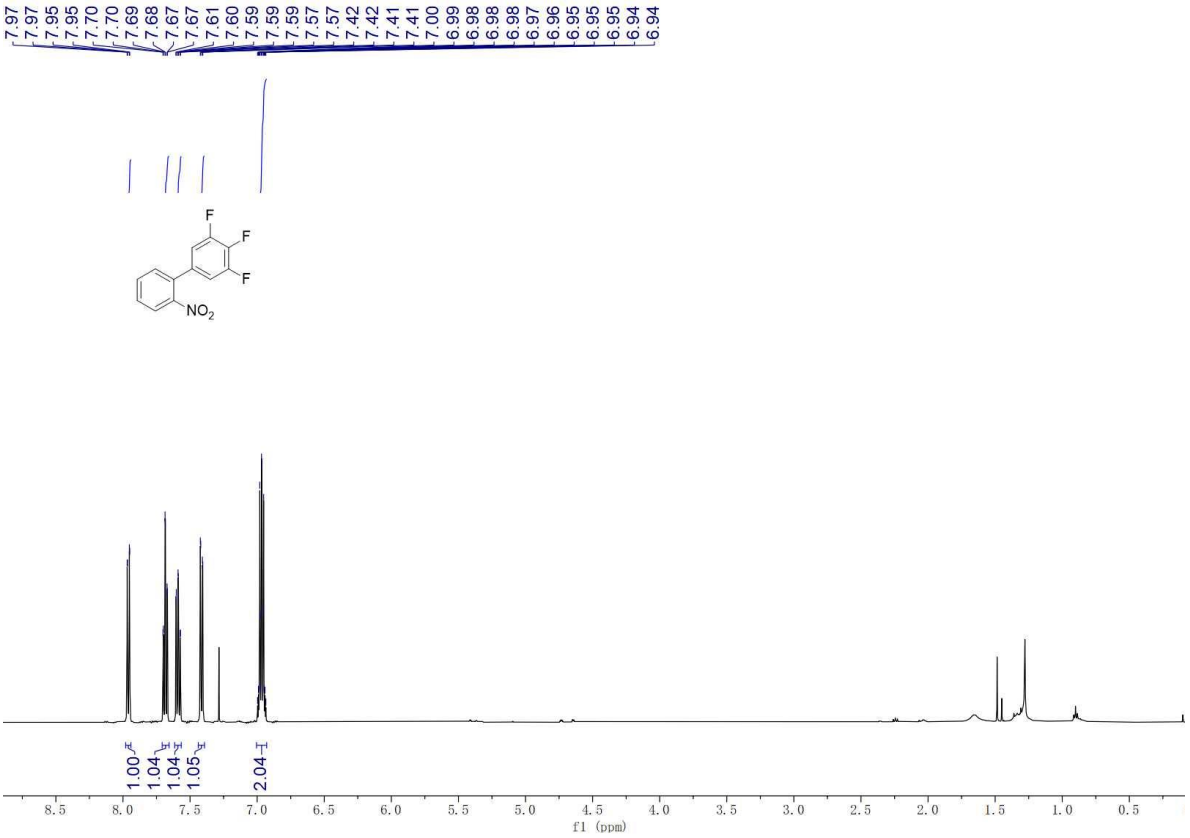

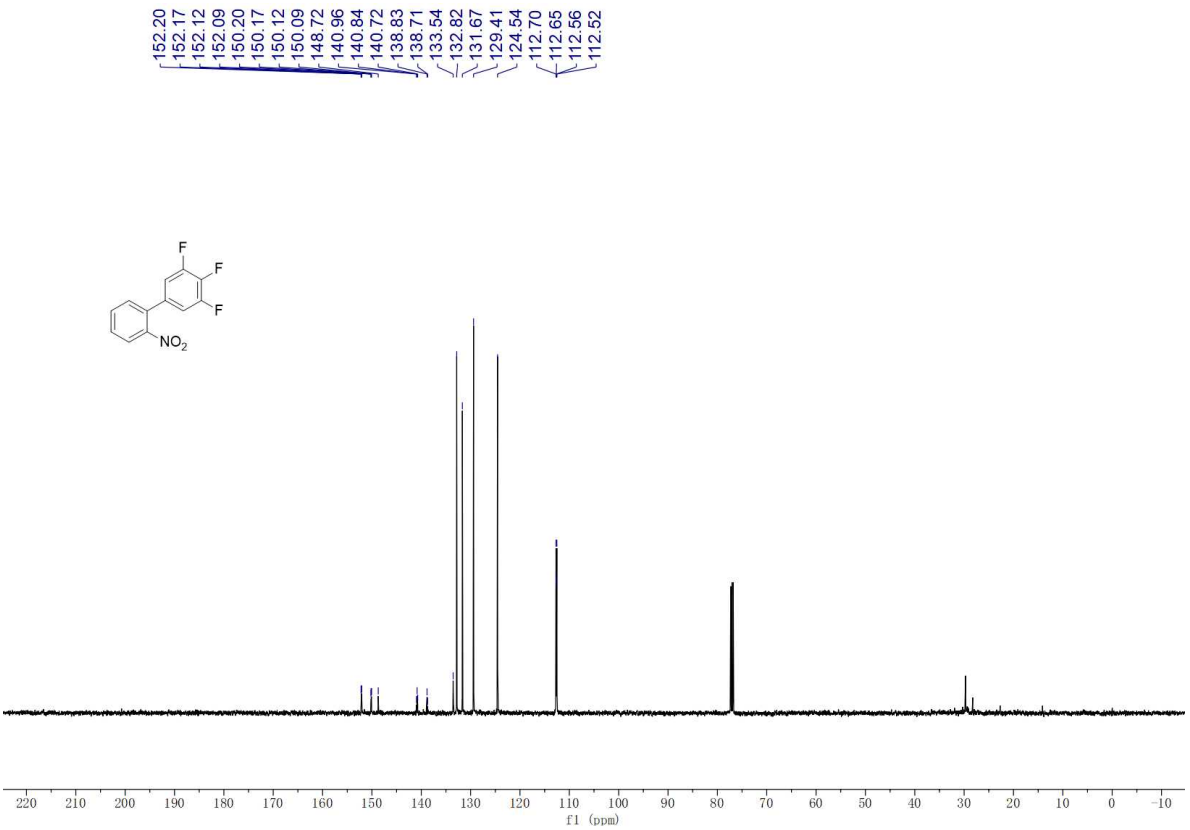

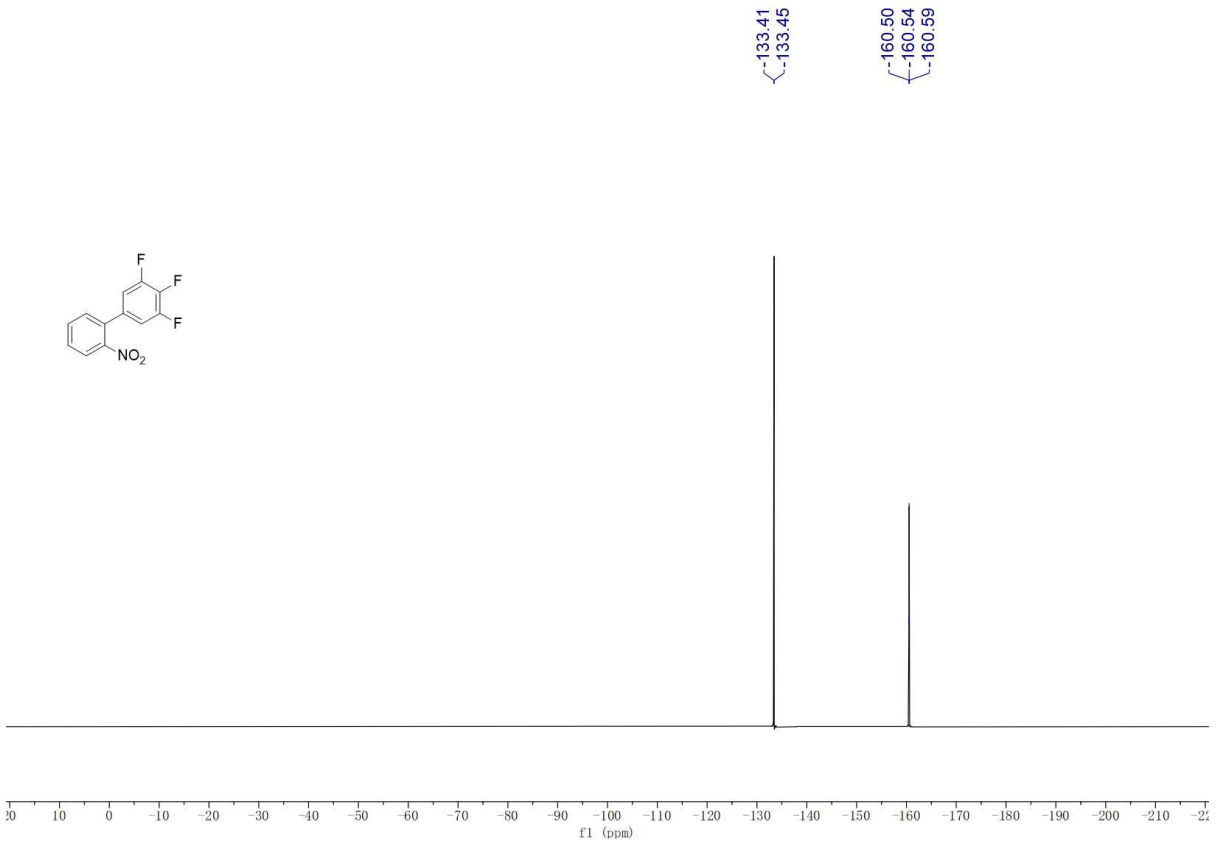
-133.41
-133.45
-160.50
-160.54
-160.59
F
F
F
NO2
10
0
−10
−20
−30
−40
−50
−60
−70
−80
−90
−100
−110
−120
−130
−140
−150
−160
−170
−180
−190
−200
−210
f1 (ppm)

1270

1271

^{1}H and ^{13}C spectra of product 4ag.

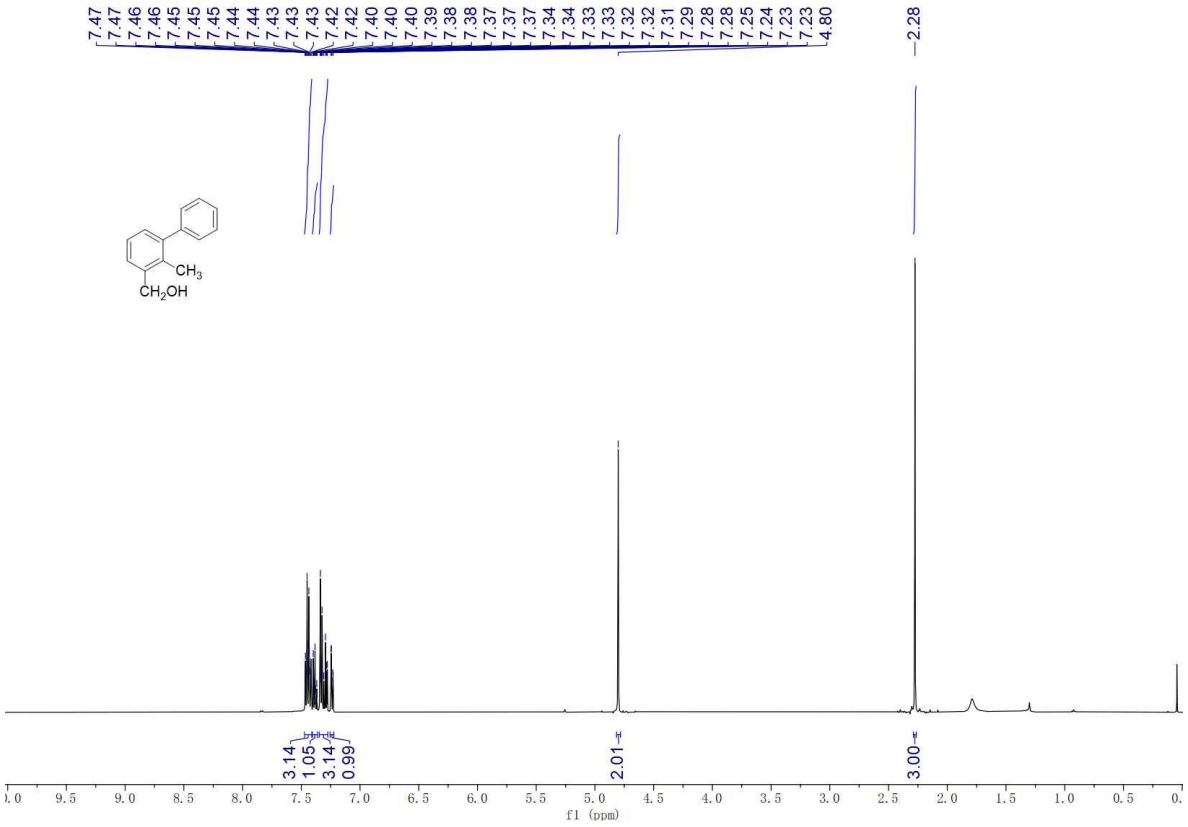

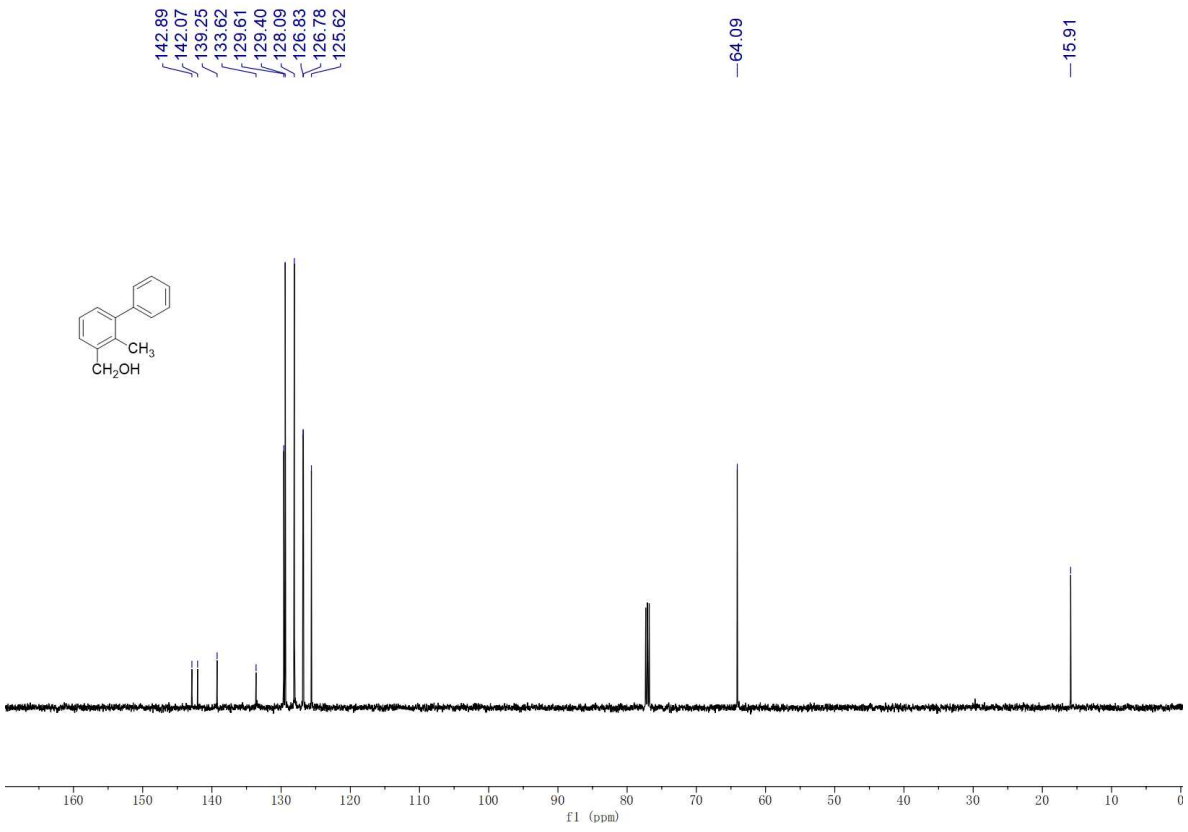

^{1}H,^{13}C and ^{19}F NMR spectra of product 4ah.

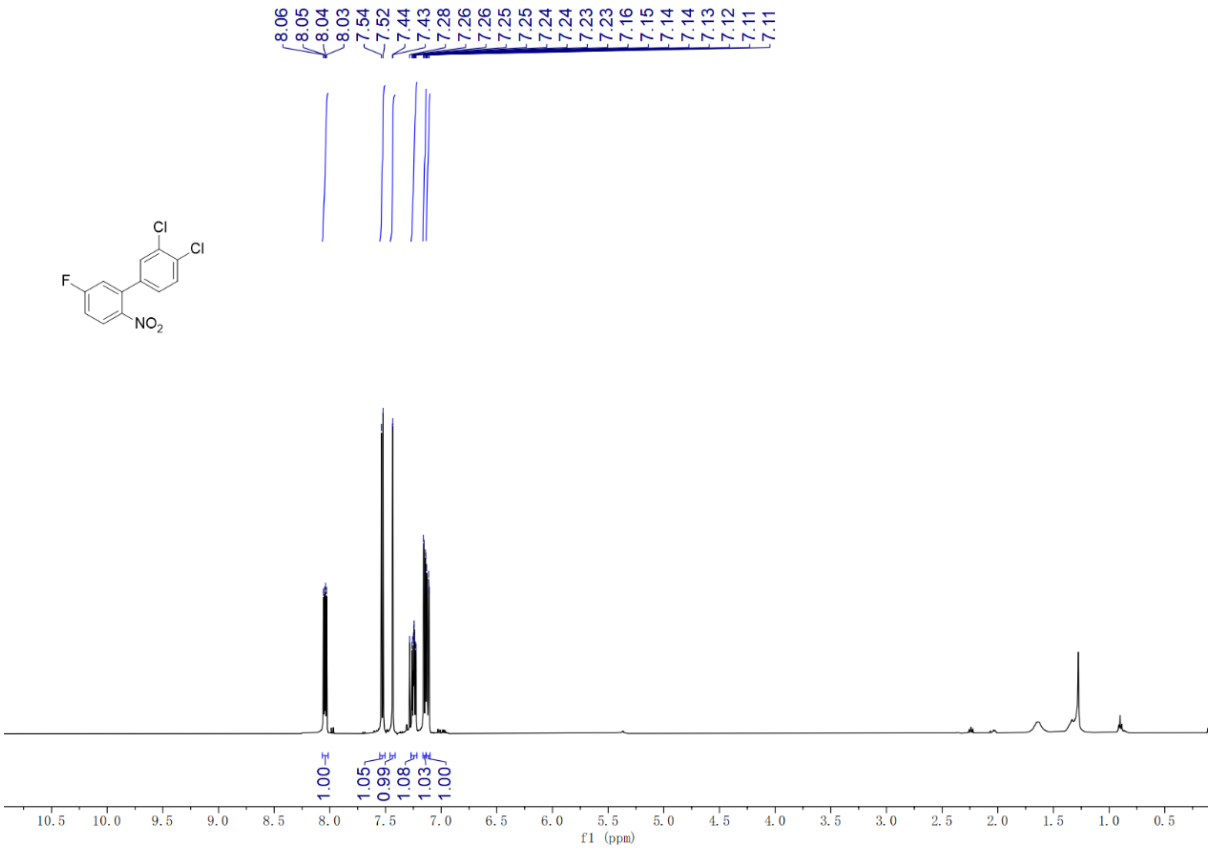

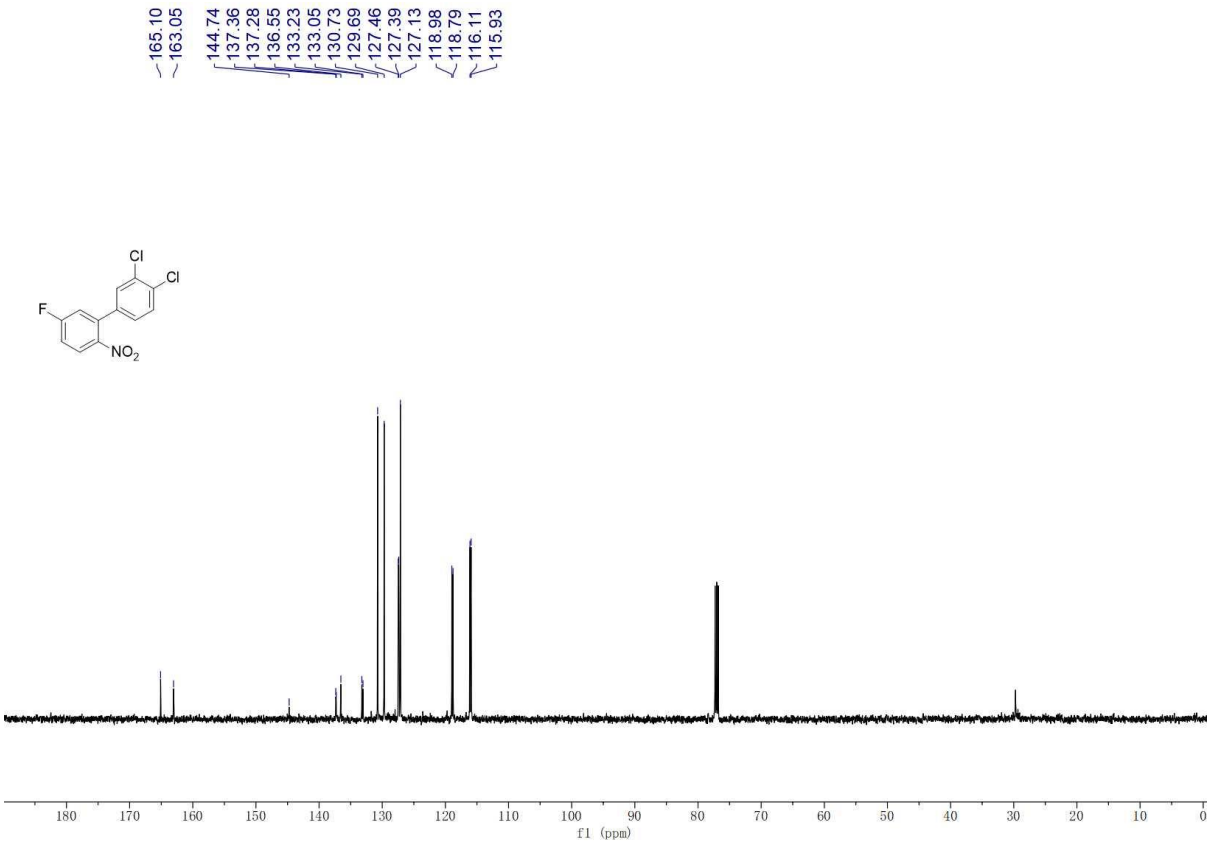

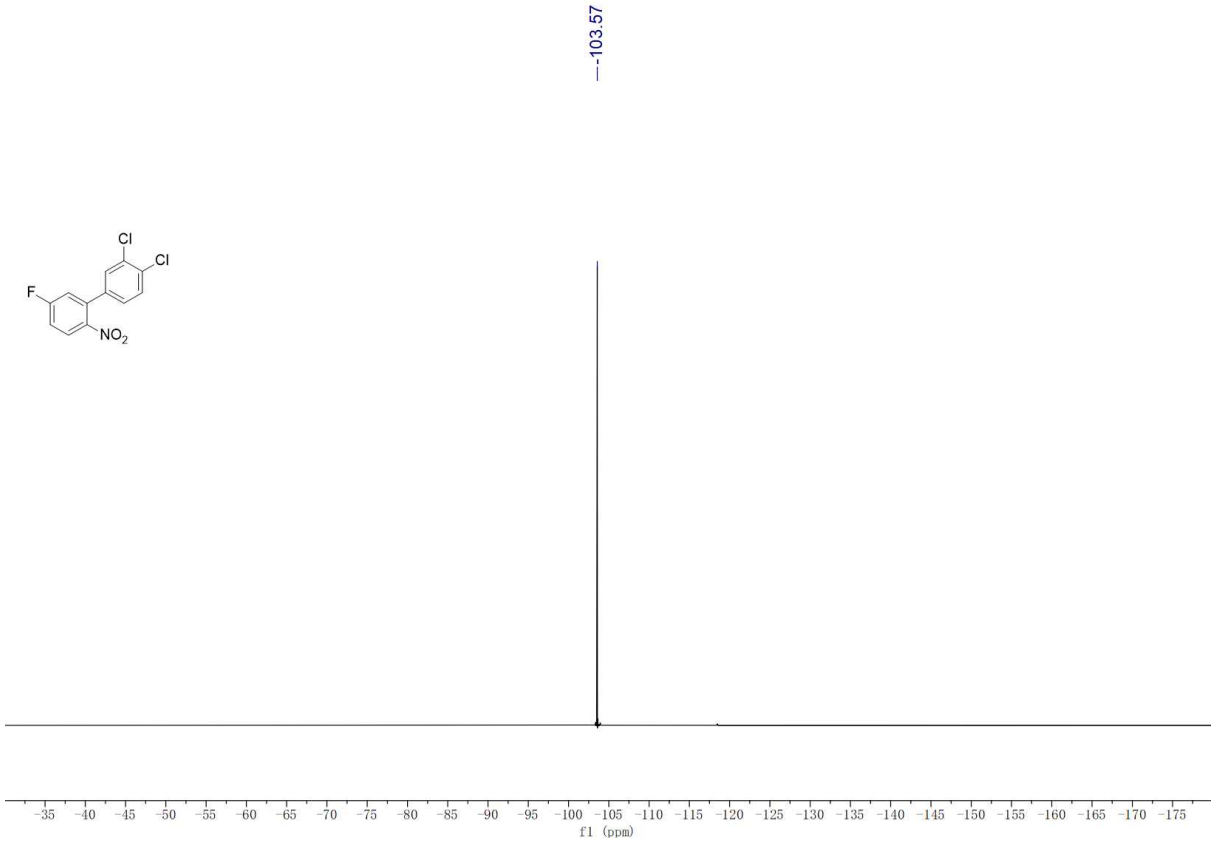
-103.57
Cl
Cl
F
NO2
-35 -40 -45 -50 -55 -60 -65 -70 -75 -80 -85 -90 -95 -100 -105 -110 -115 -120 -125 -130 -135 -140 -145 -150 -155 -160 -165 -170 -175
f1 (ppm)

1279

1280

^{1}H,^{13}C and ^{19}F NMR spectra of product 4ai.

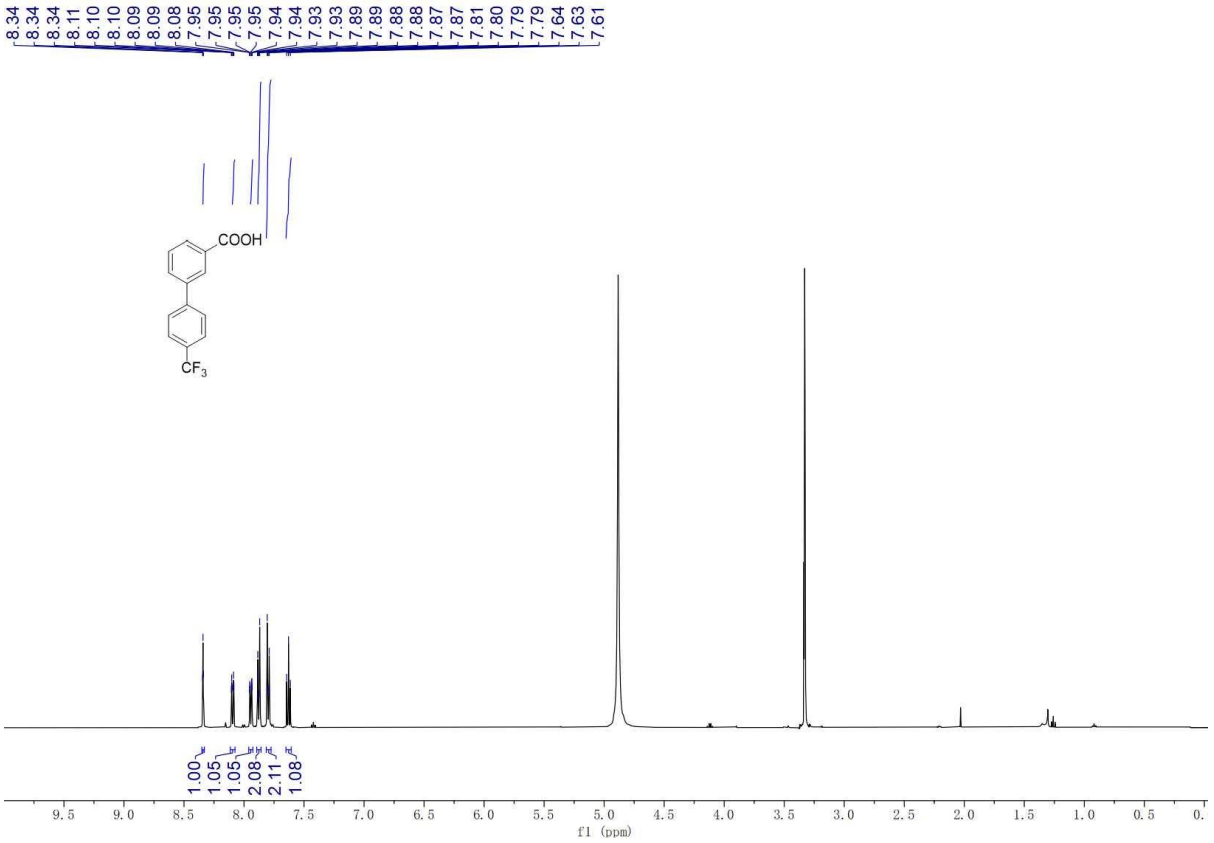

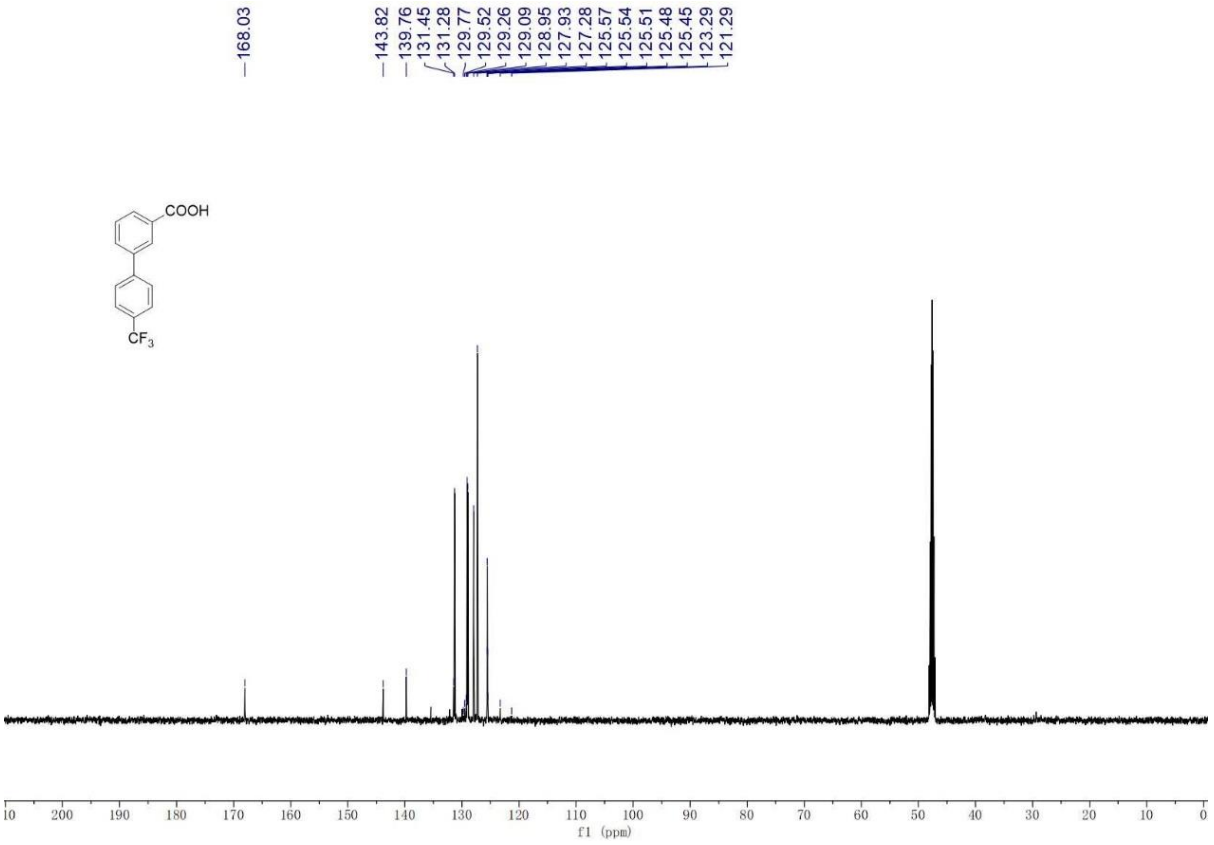

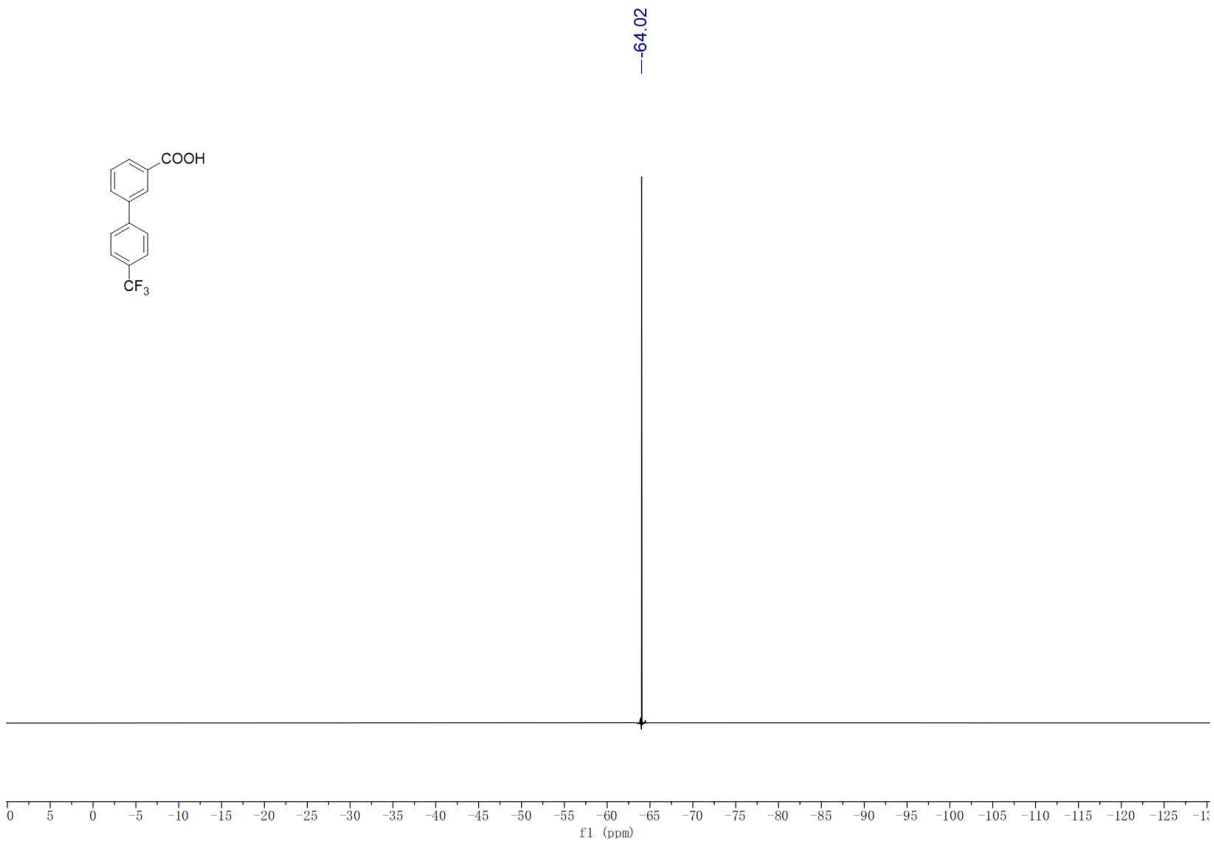
-64.02
COOH
CF3
0 5 0 -5 -10 -15 -20 -25 -30 -35 -40 -45 -50 -55 -60 -65 -70 -75 -80 -85 -90 -95 -100 -105 -110 -115 -120 -125
f1 (ppm)

1285

1286

^{1}H,^{13}C and ^{19}F NMR spectra of product 4aj.

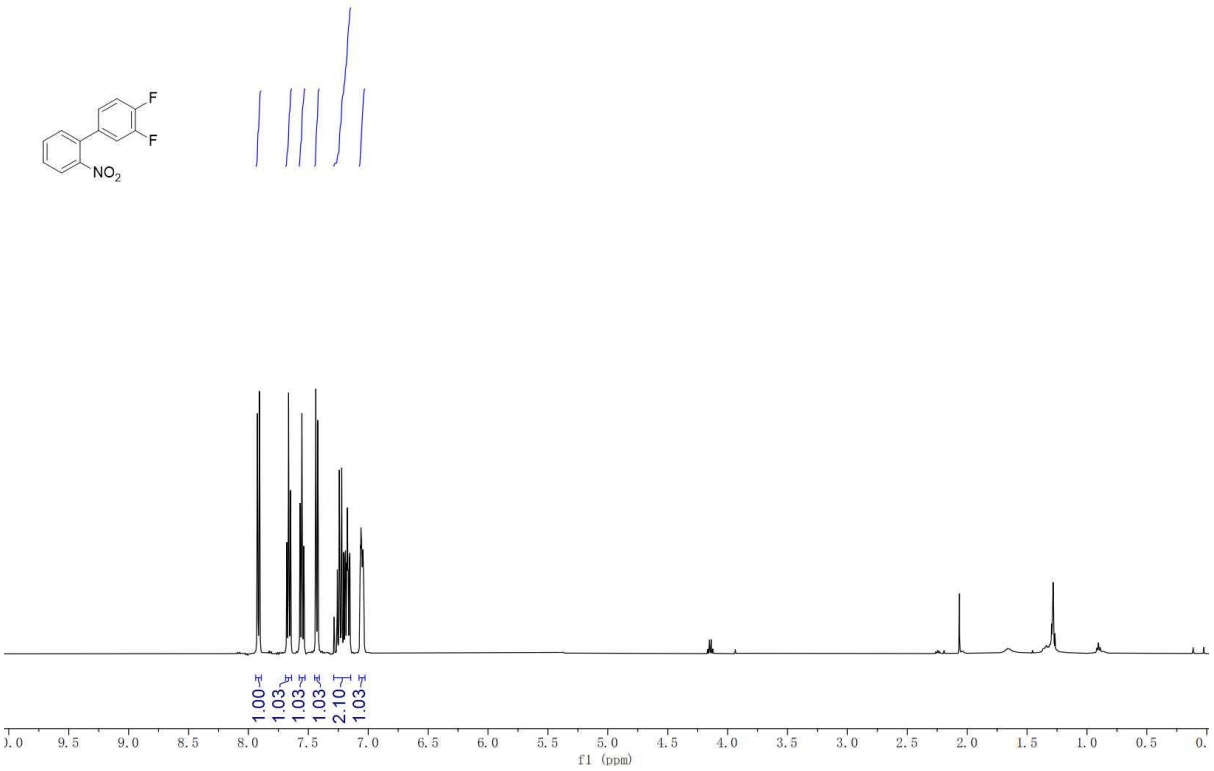

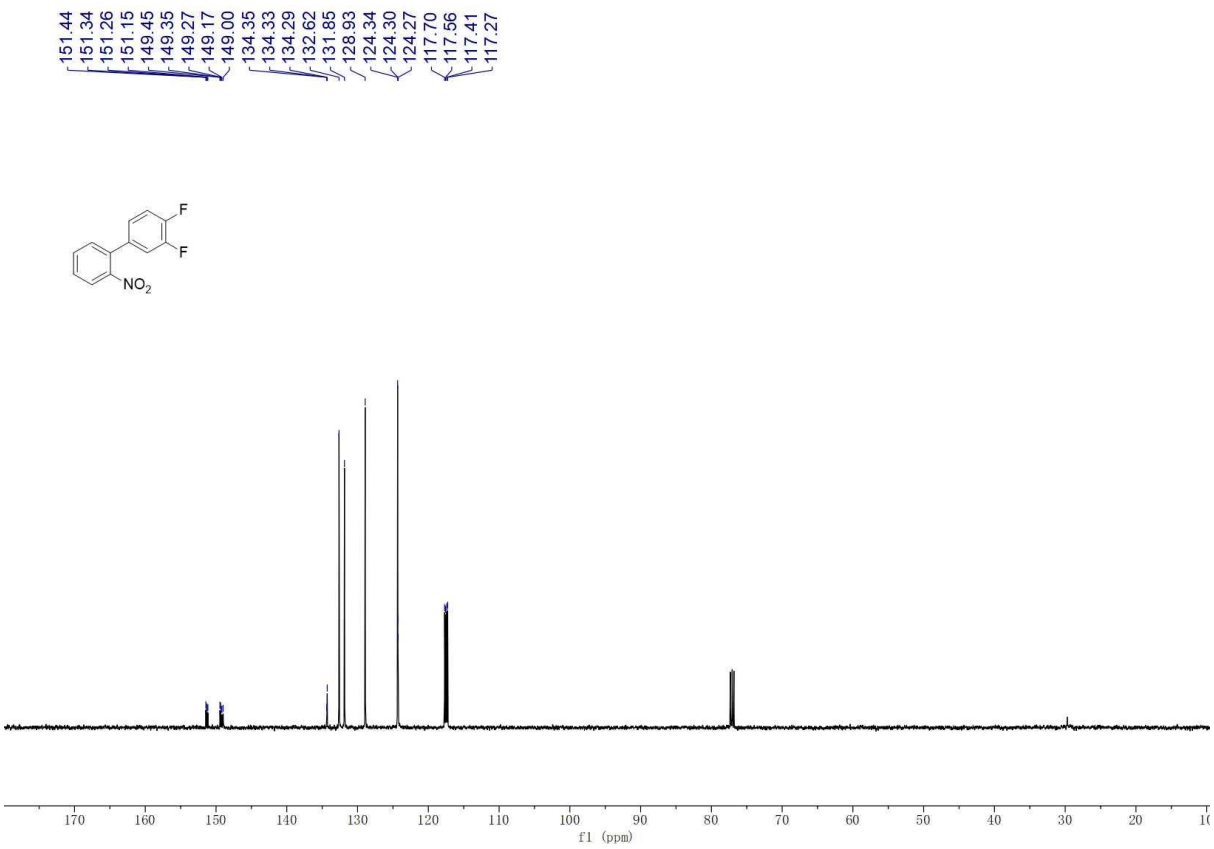

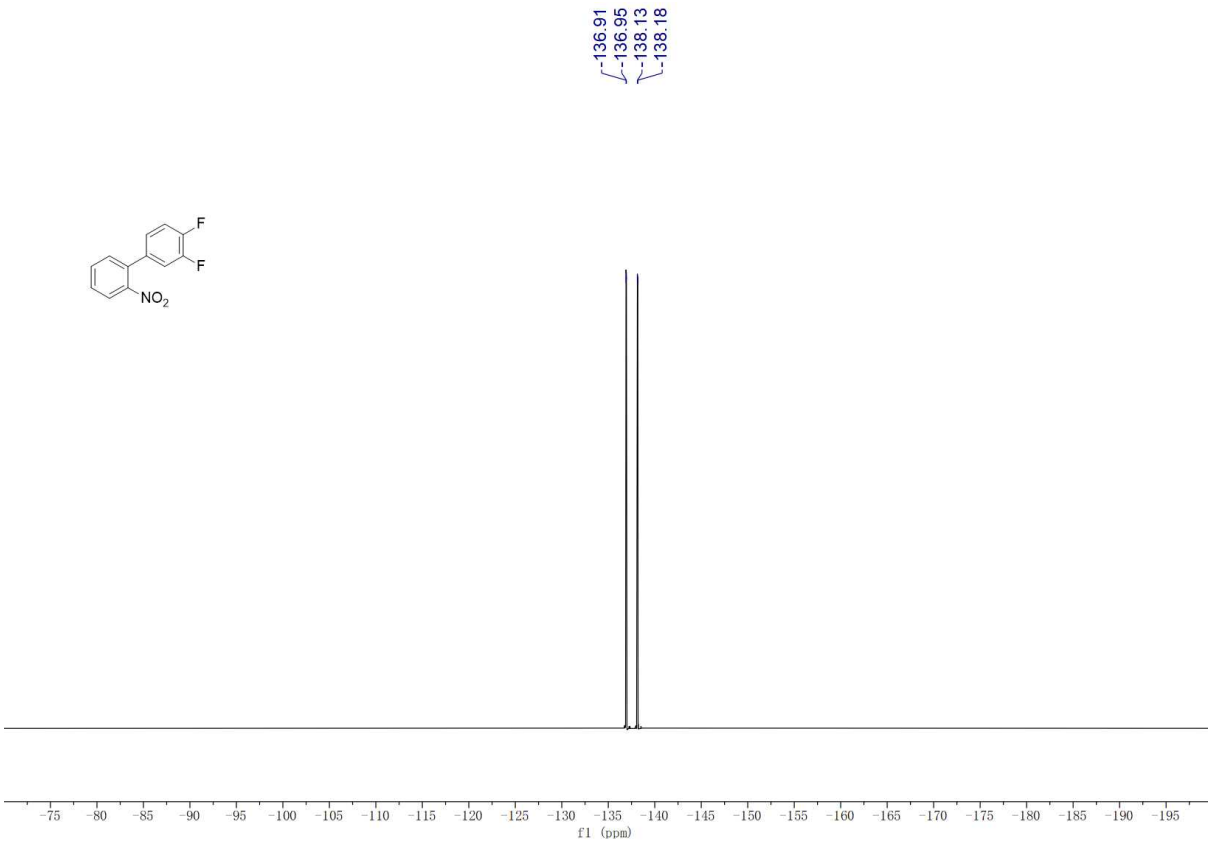
-136.91
-136.95
-138.13
-138.18
F
F
NO2
-75 -80 -85 -90 -95 -100 -105 -110 -115 -120 -125 -130 -135 -140 -145 -150 -155 -160 -165 -170 -175 -180 -185 -190 -195
f1 (ppm)

1291

1292

^{1}H and ^{13}C NMR spectra of product 4ak.

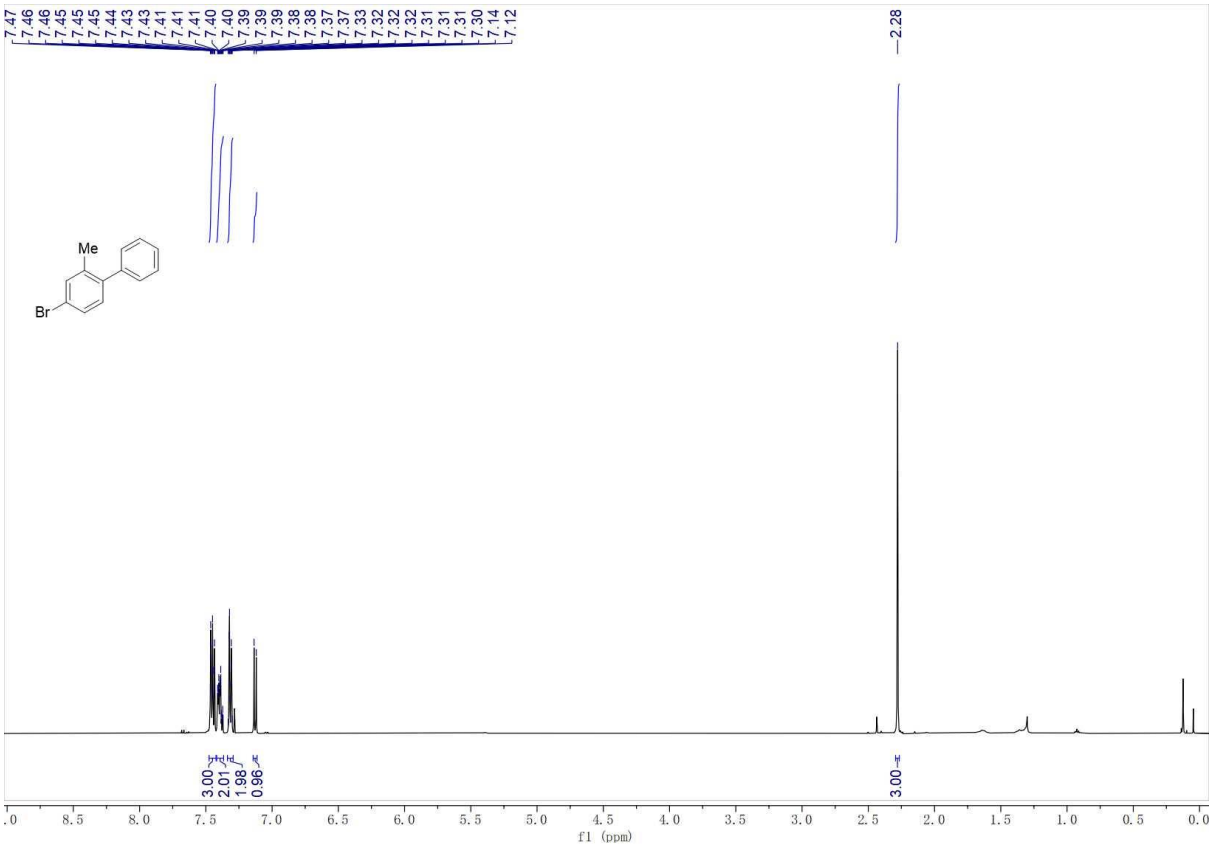

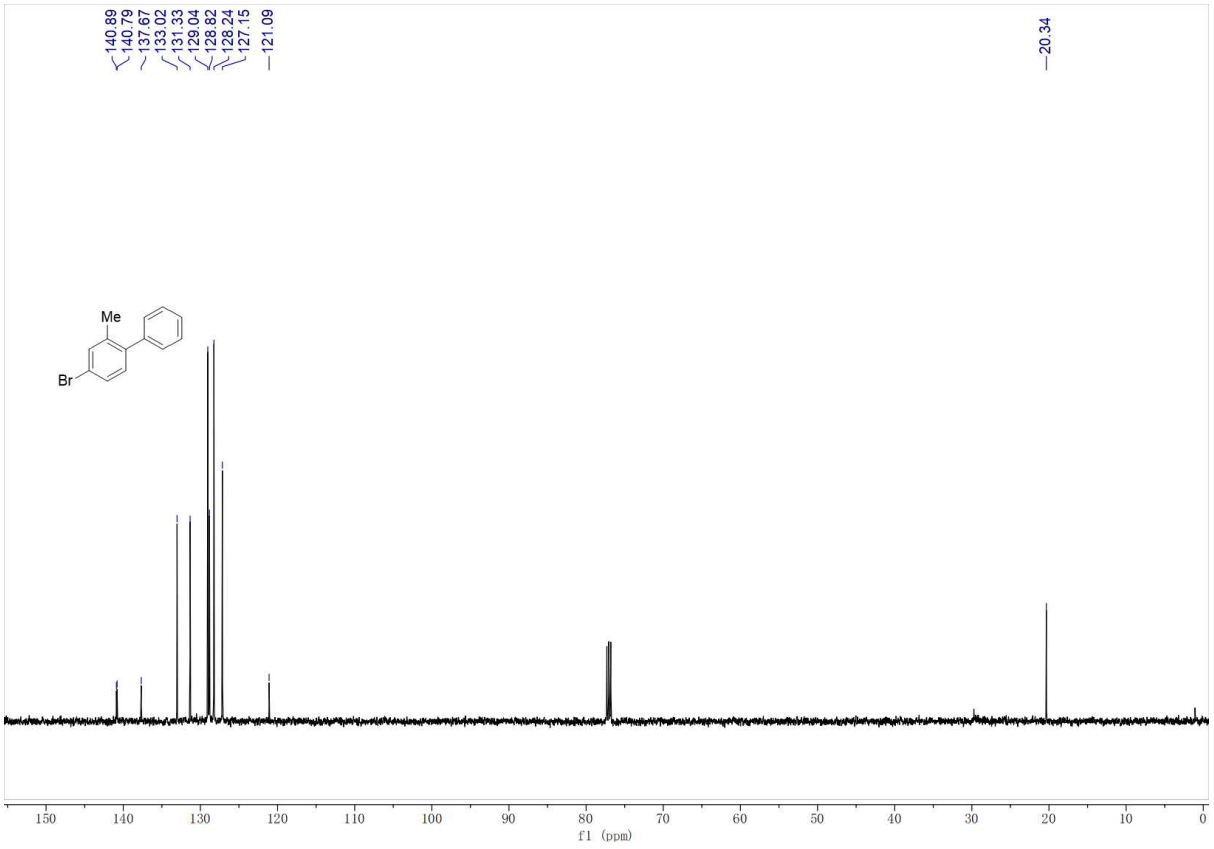

^{1}H and ^{13}C- NMR spectra of product 4al.

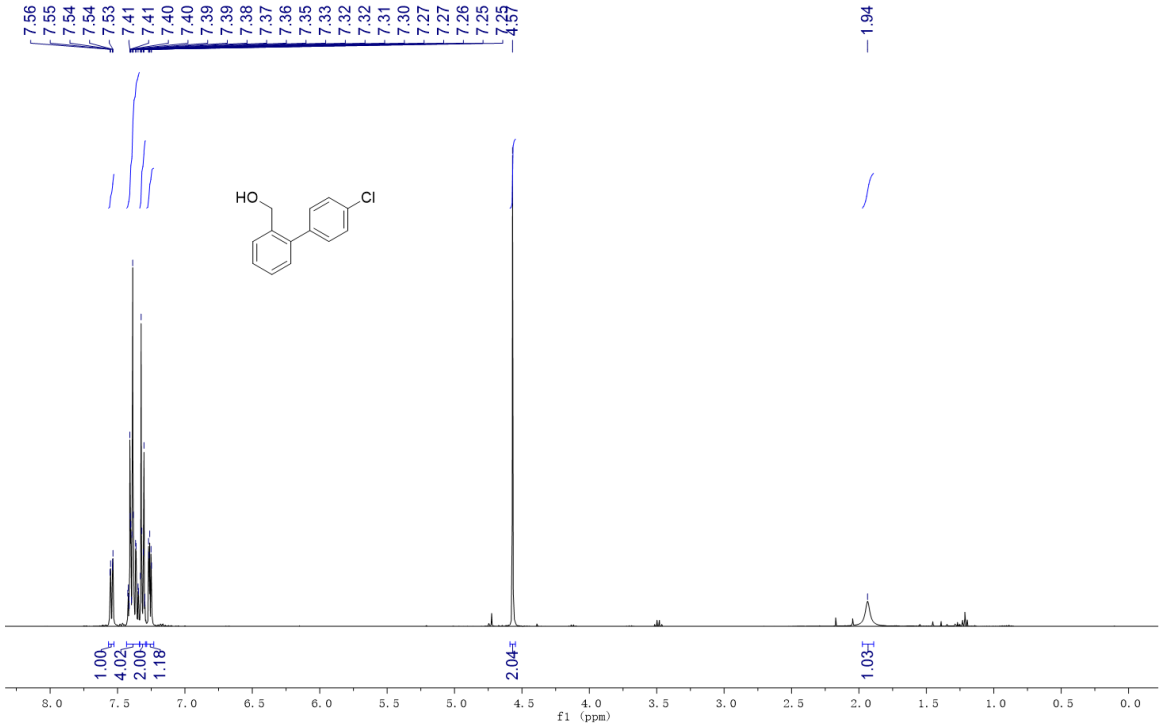

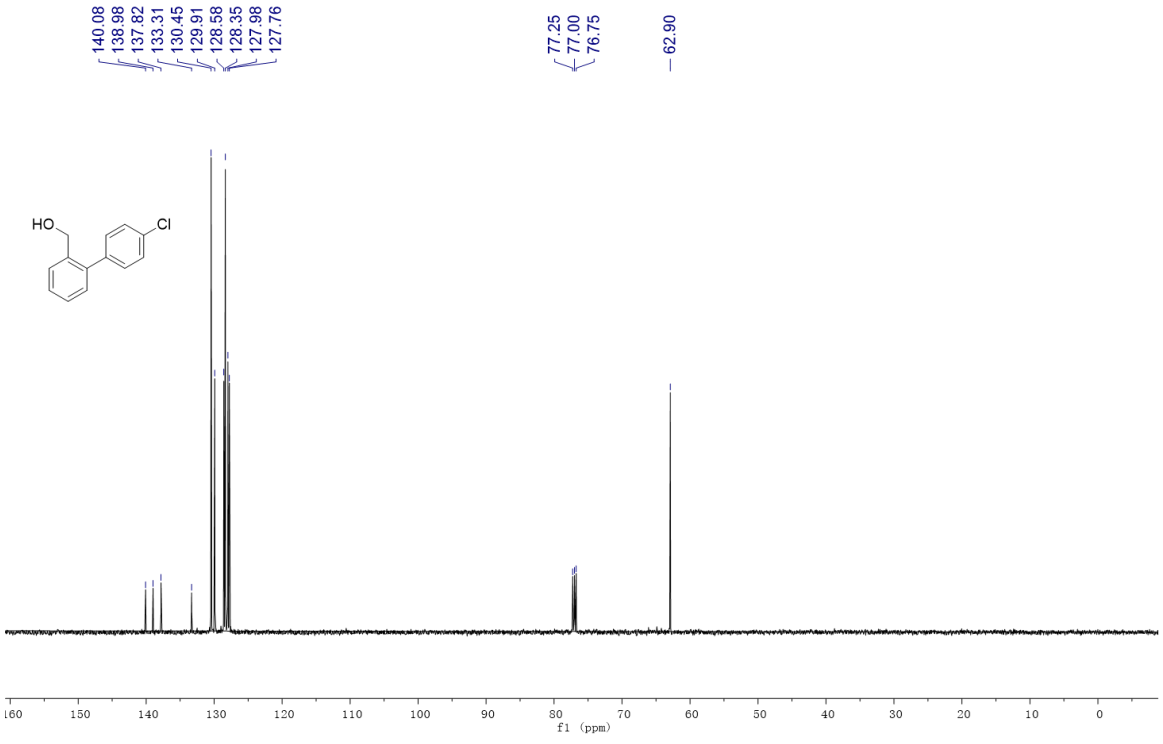

^{1}H and ^{13}C spectra of product 4am

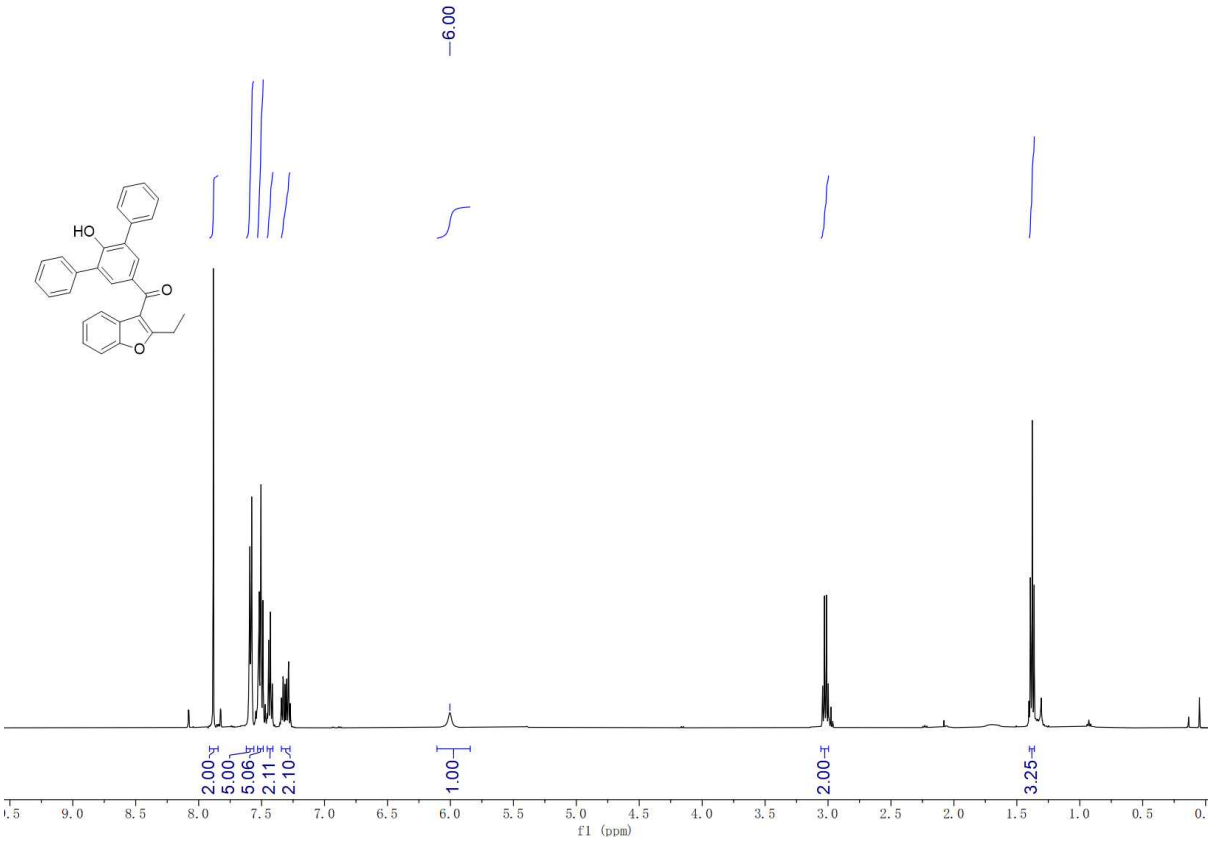

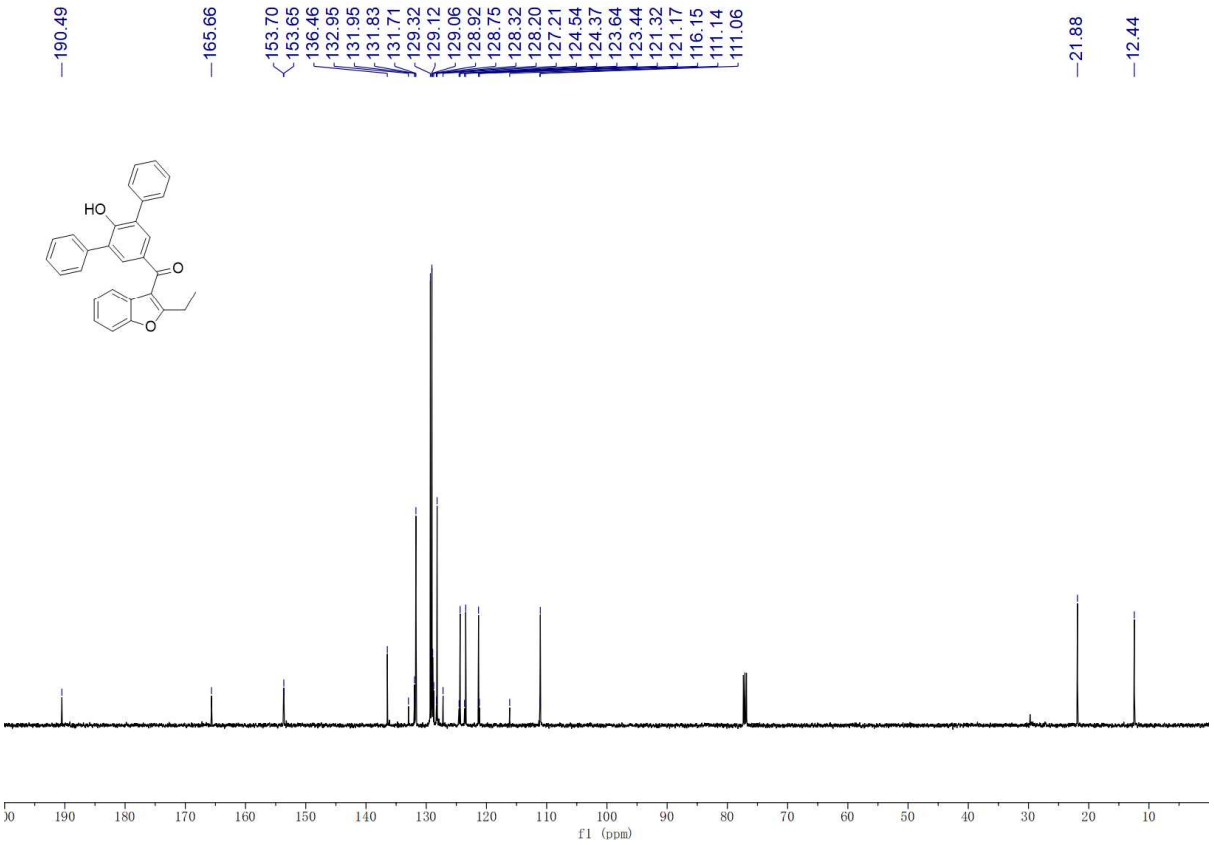

^{1}H and ^{13}C spectra of product 4an

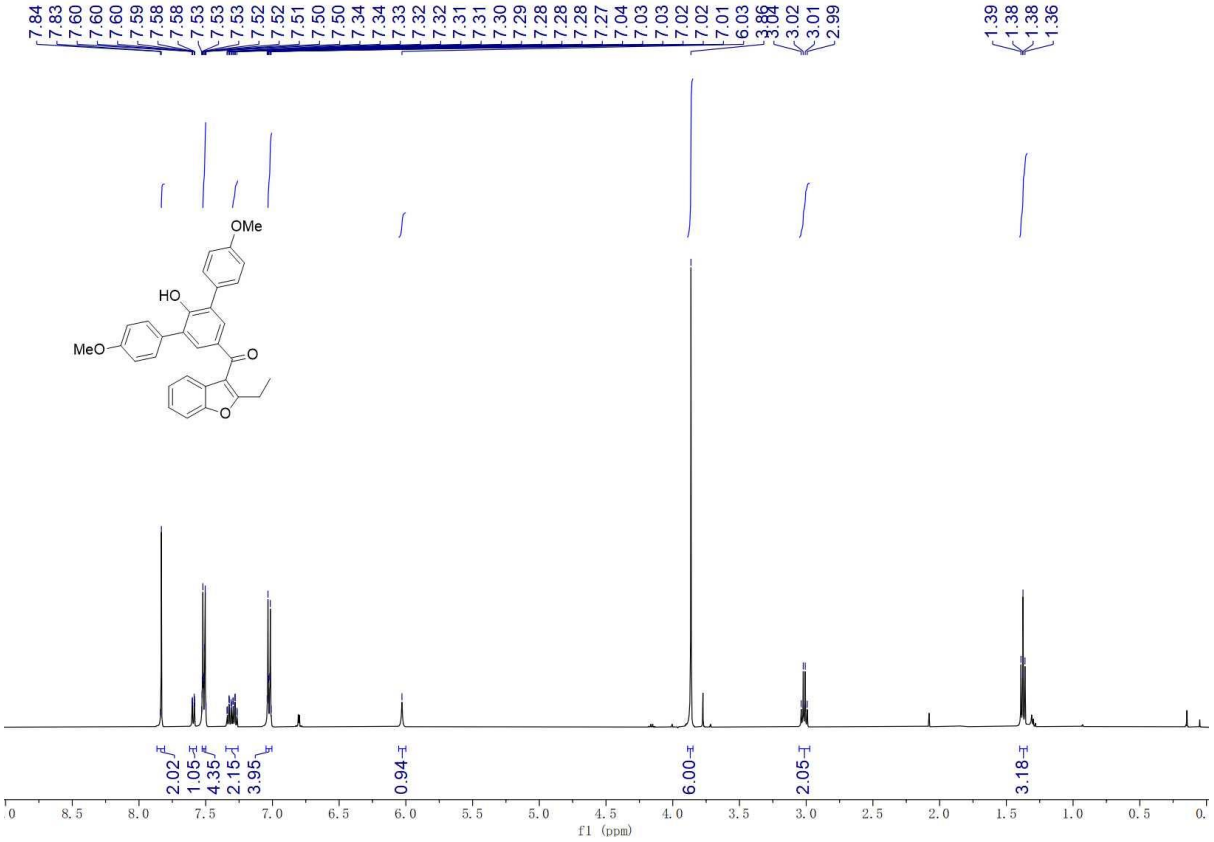

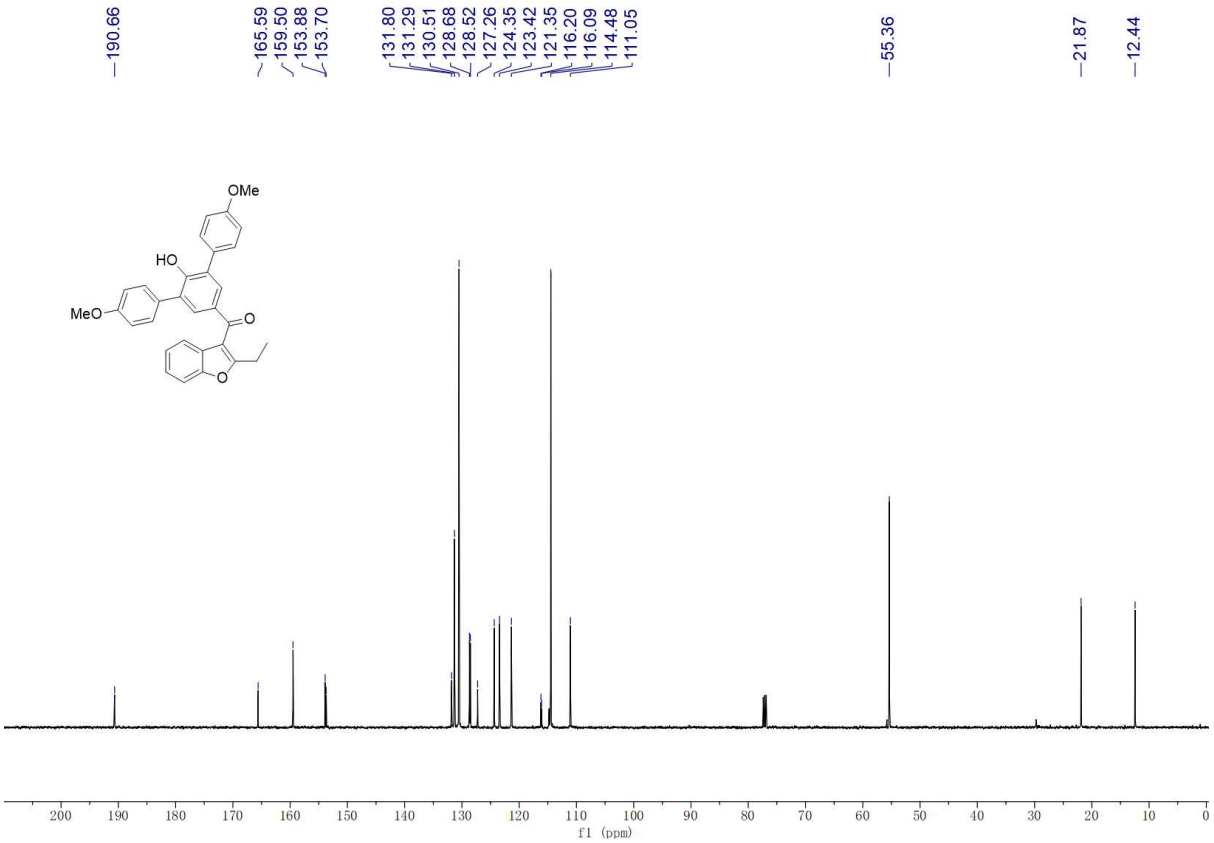

^{1}H and ^{13}C spectra of product 4ao

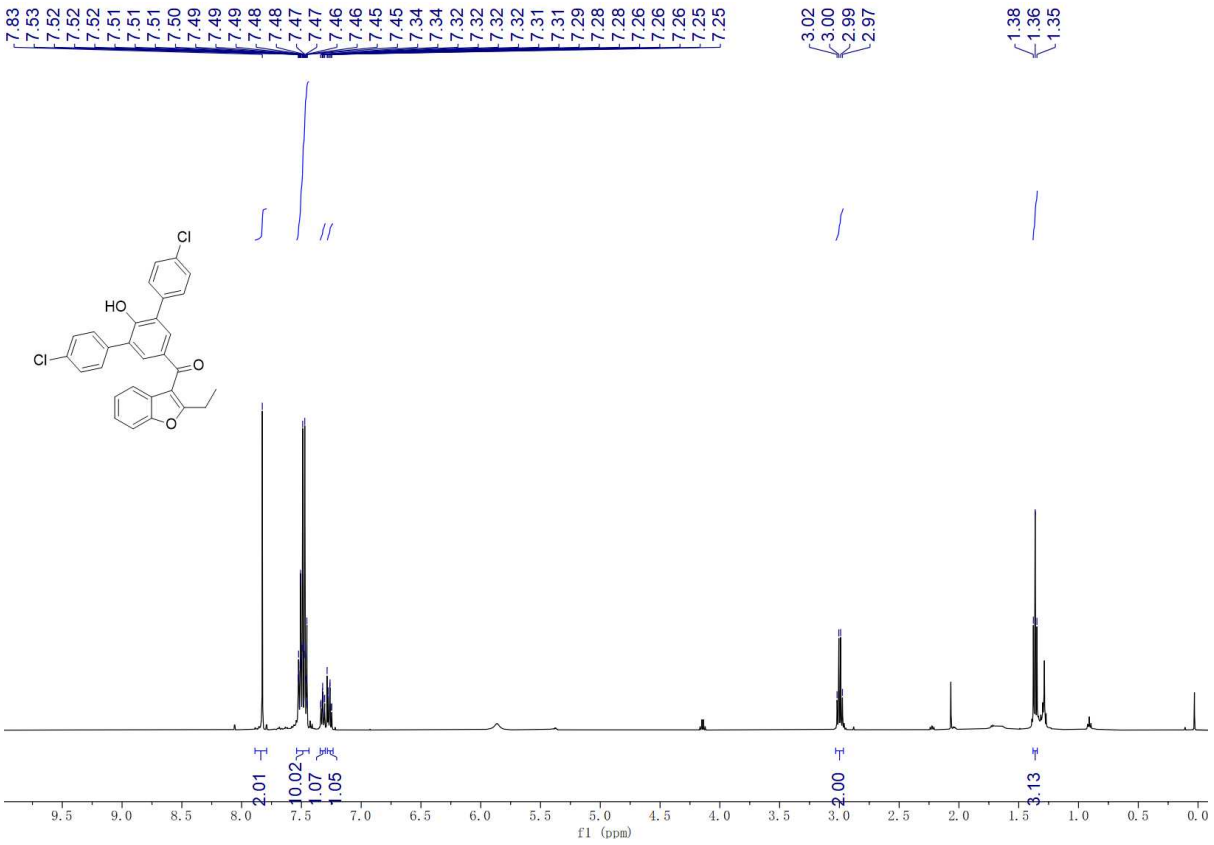

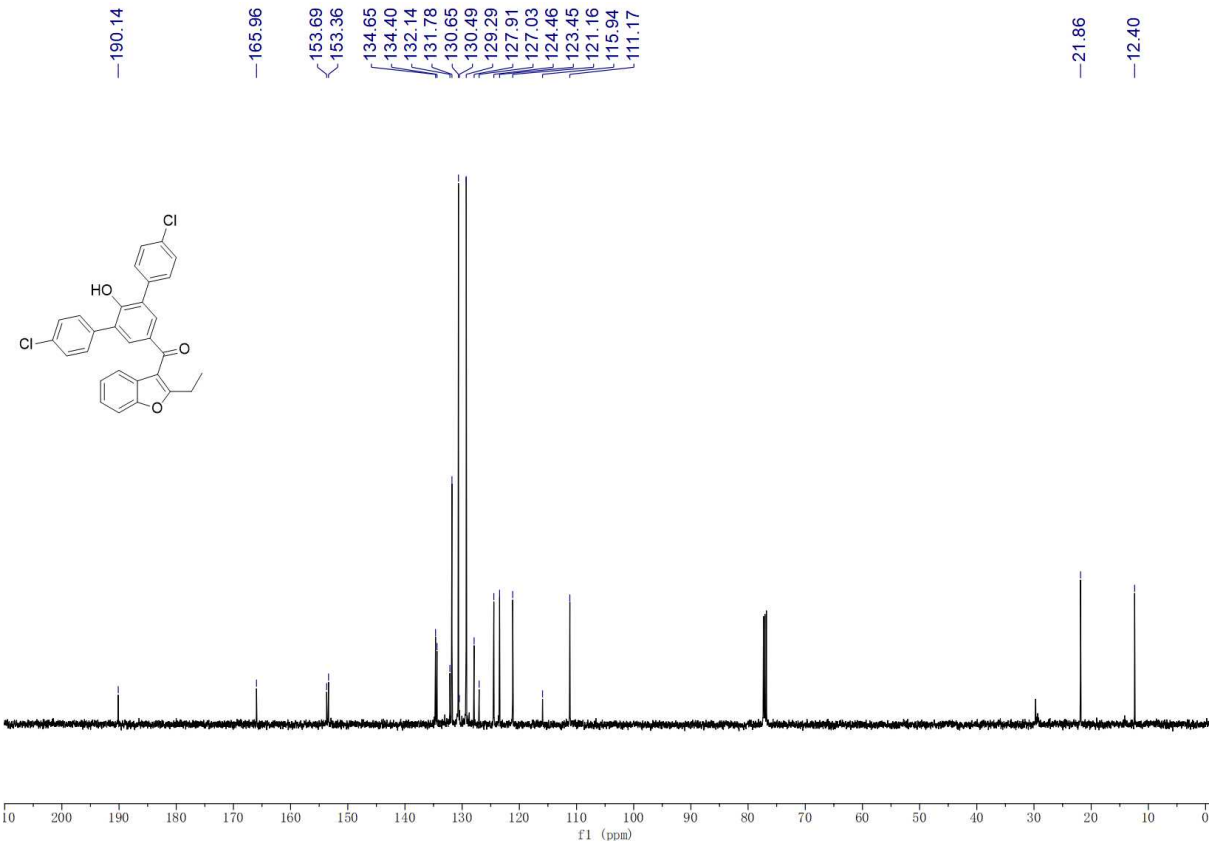

^{1}H and ^{13}C- NMR spectra of product.

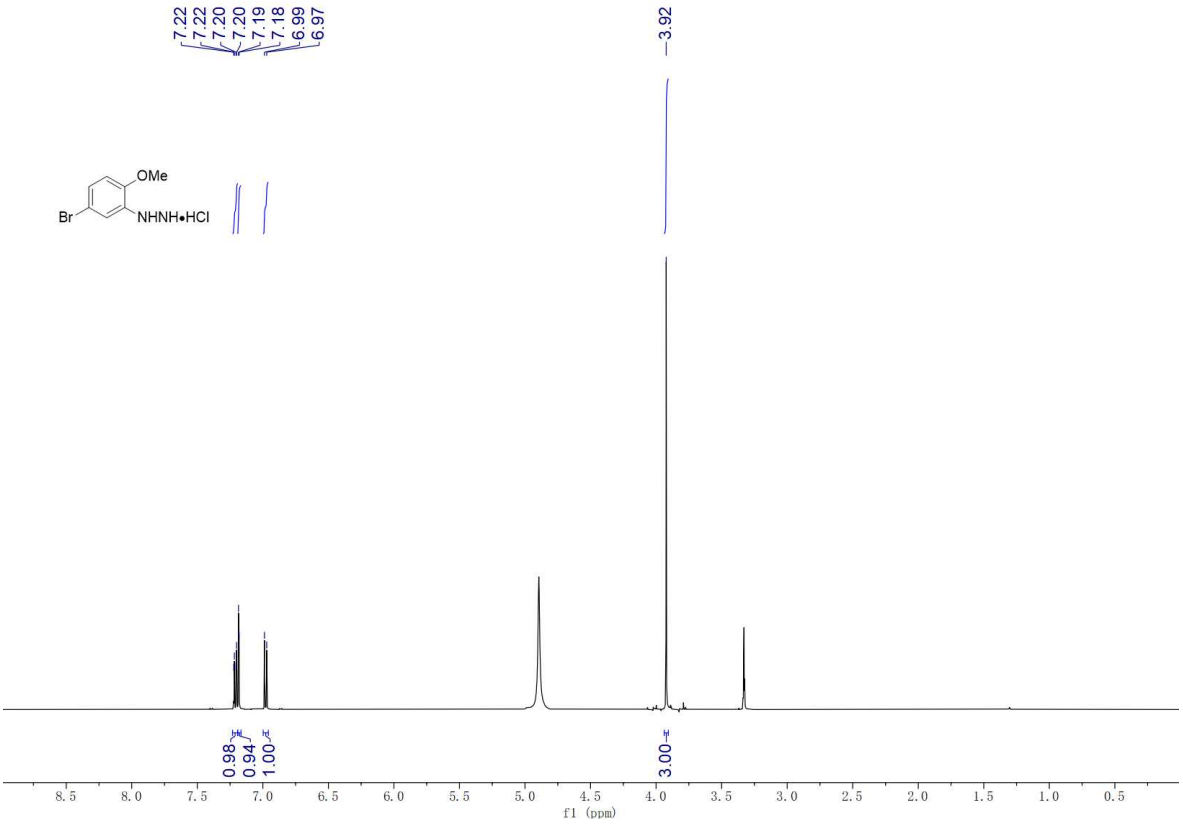

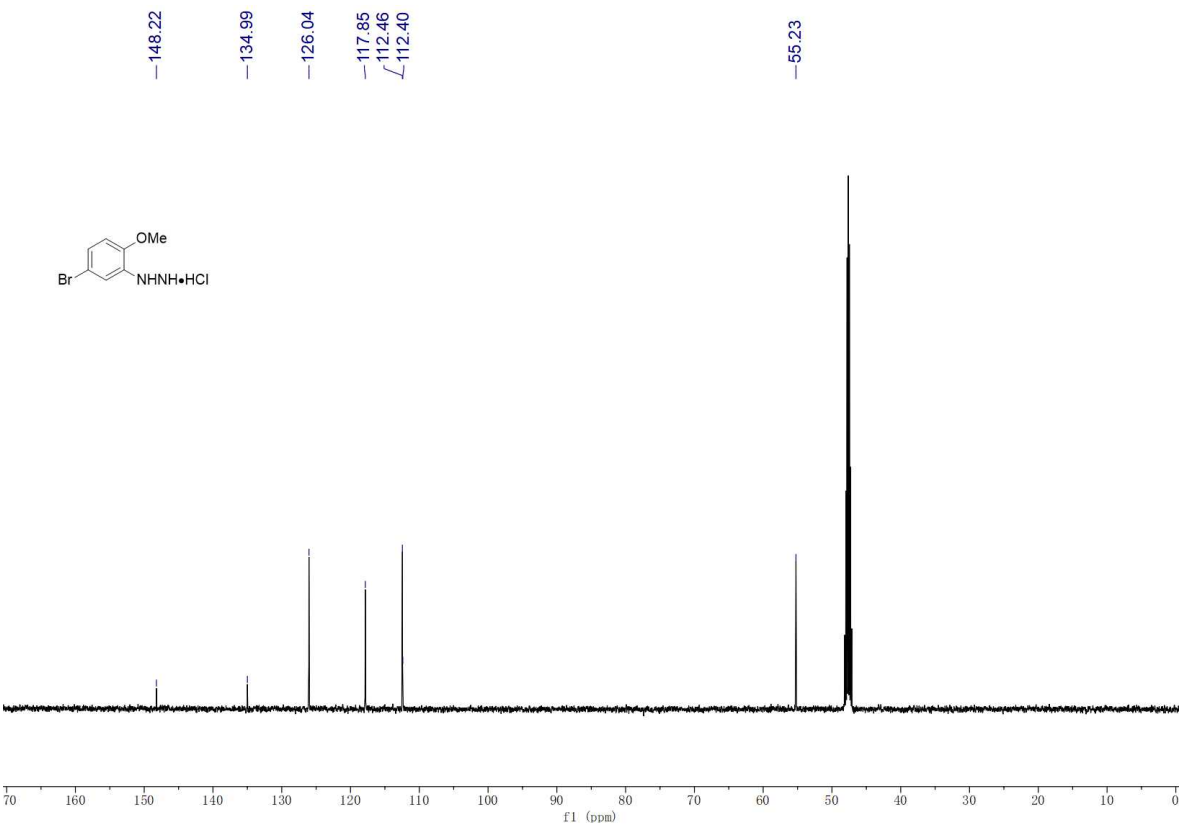

^{1}H and ^{13}C spectra of product 1aa

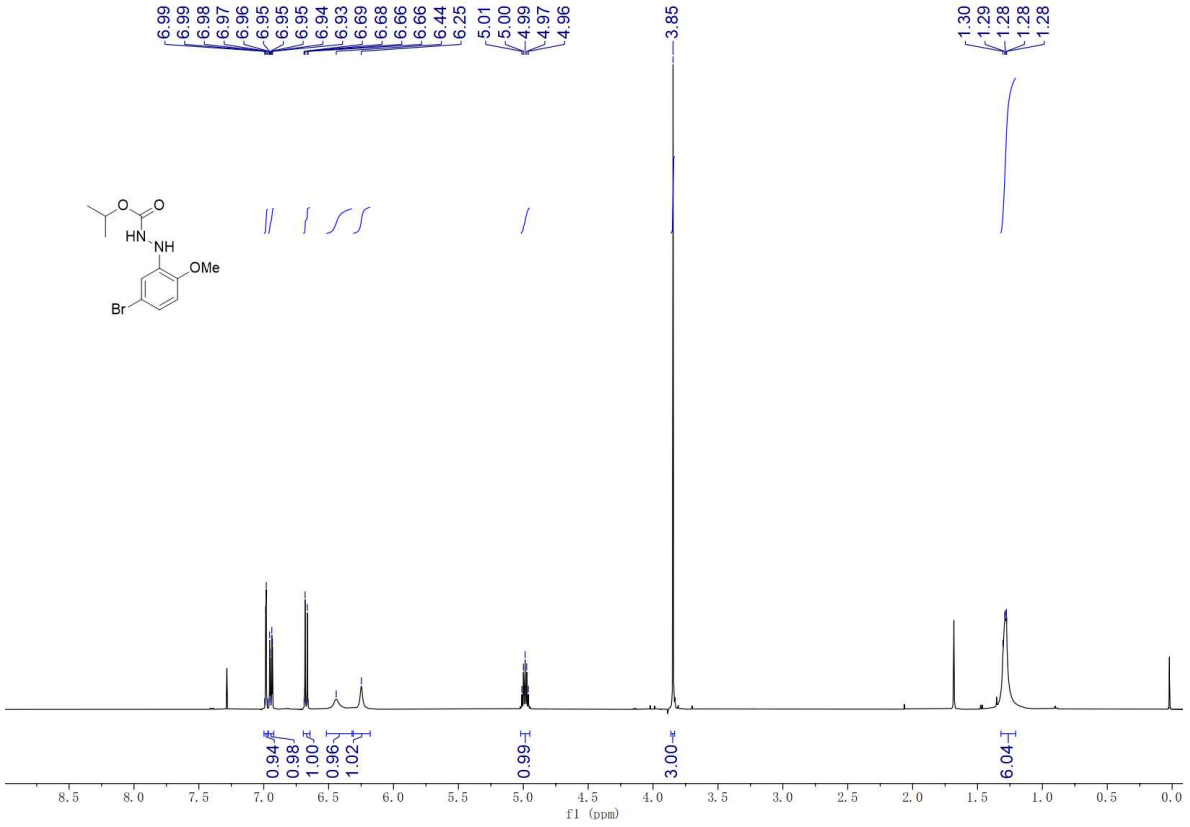

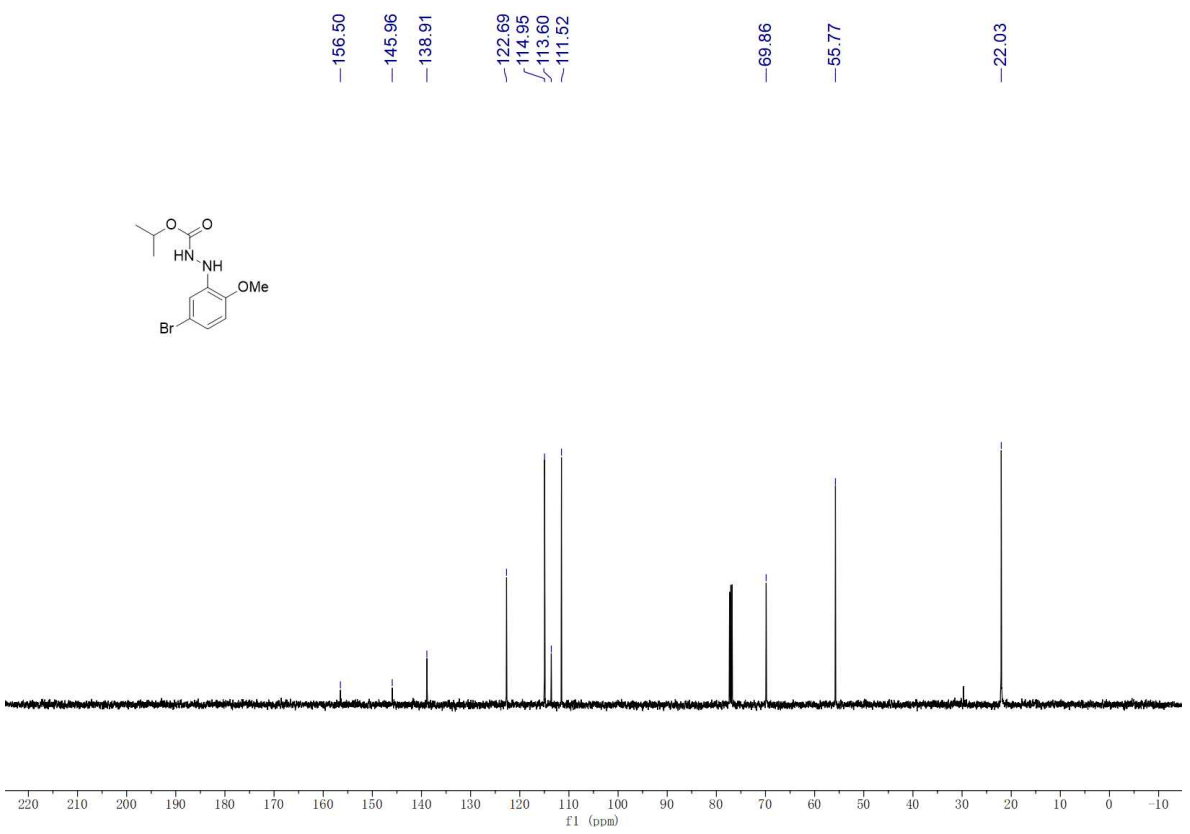

^{1}H and ^{13}C spectra of product bifenazate.

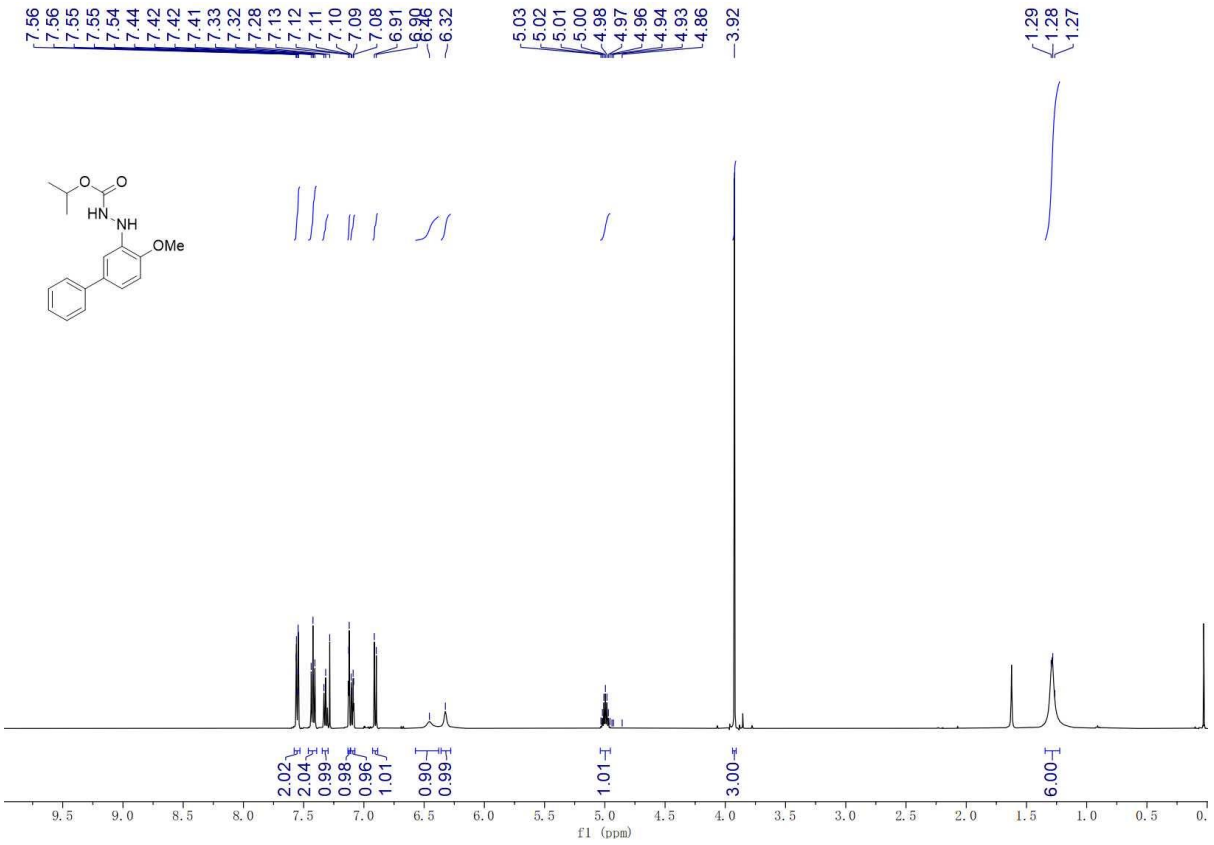

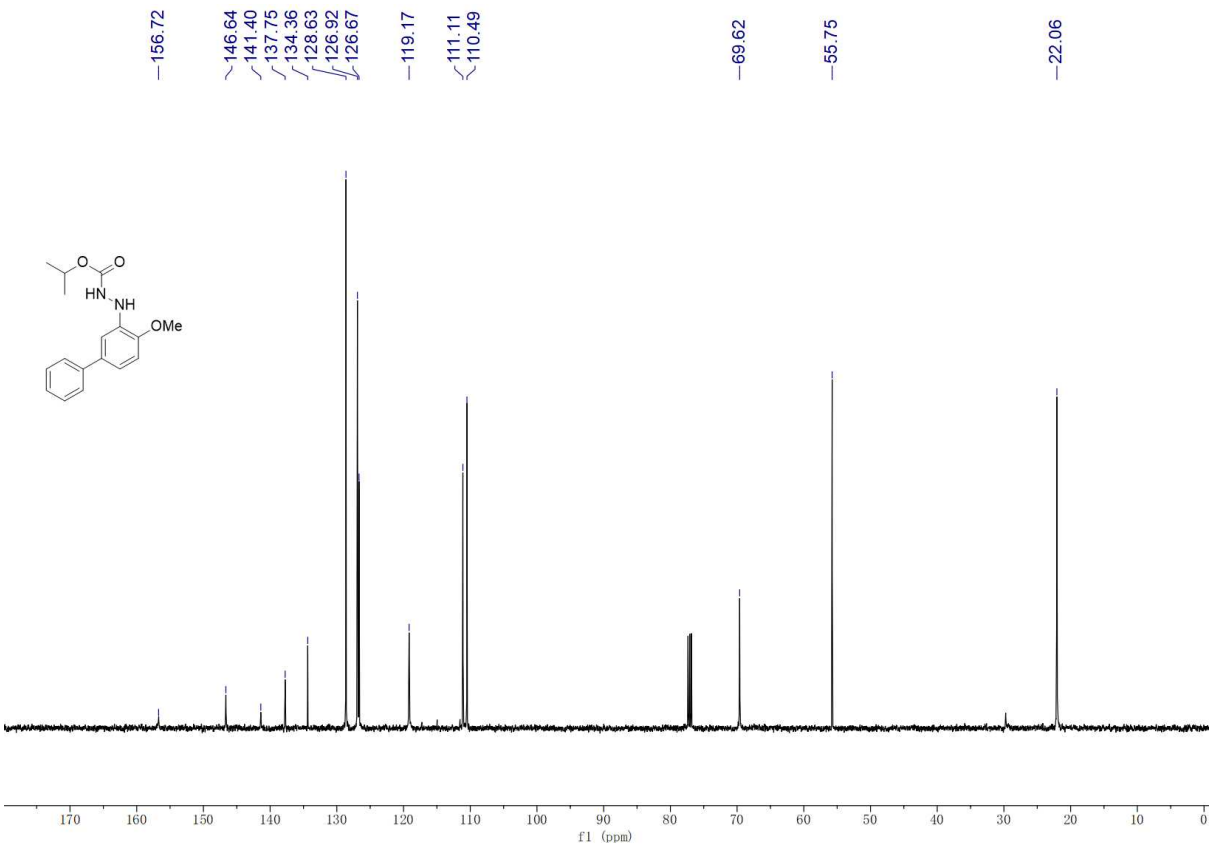

^{1}H and ^{13}C-NMR spectra of product 8a.

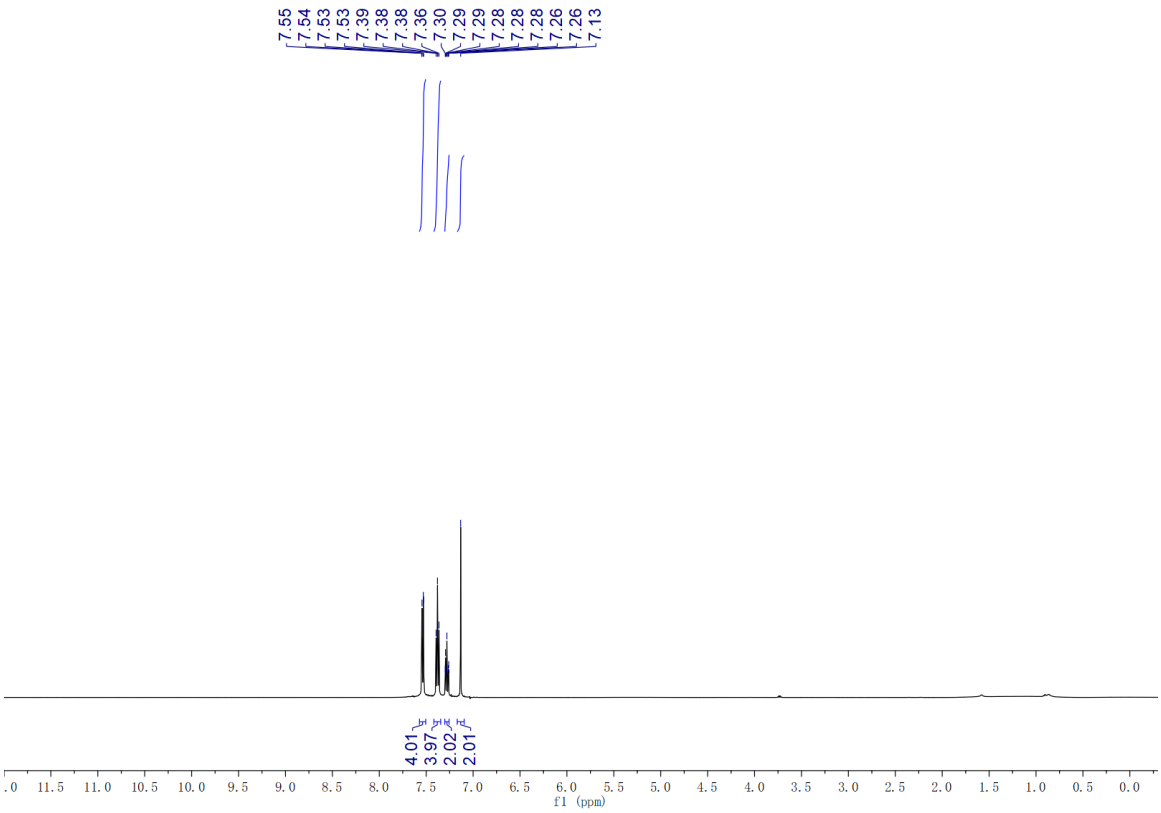

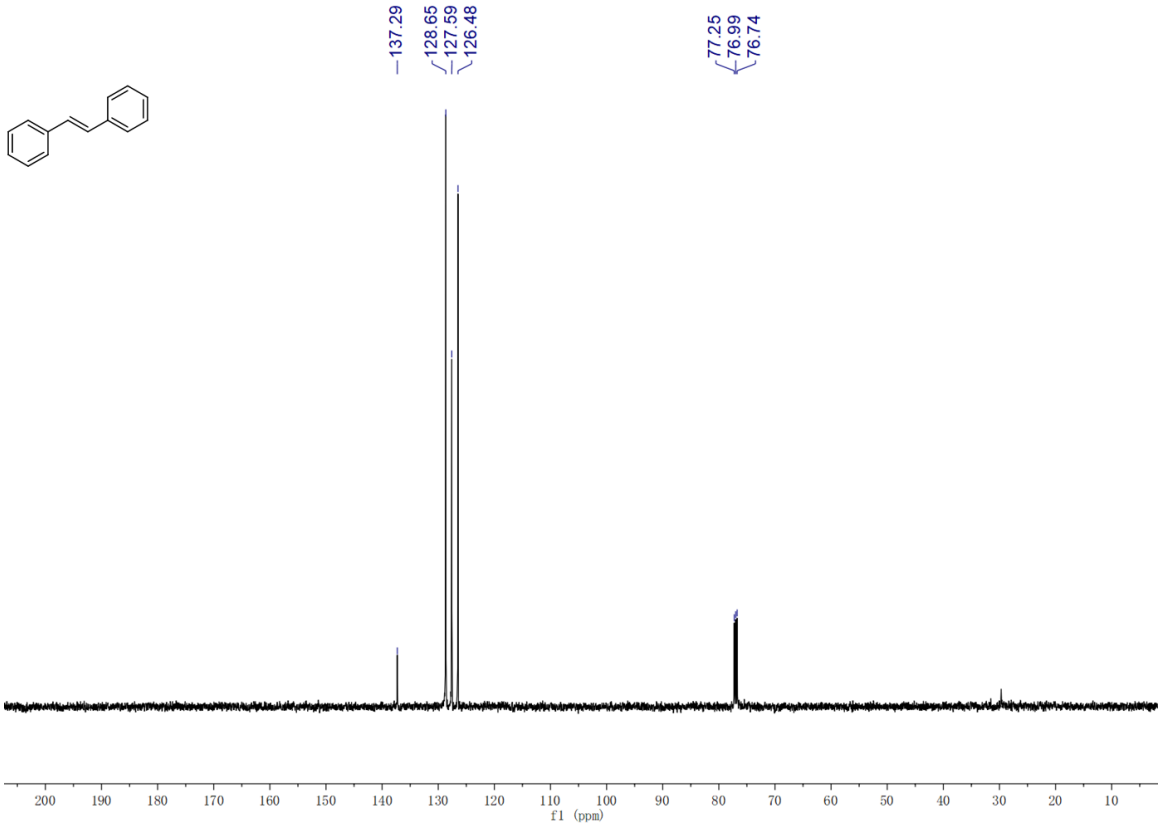

^{1}H and ^{13}C-NMR spectra of product 8b.

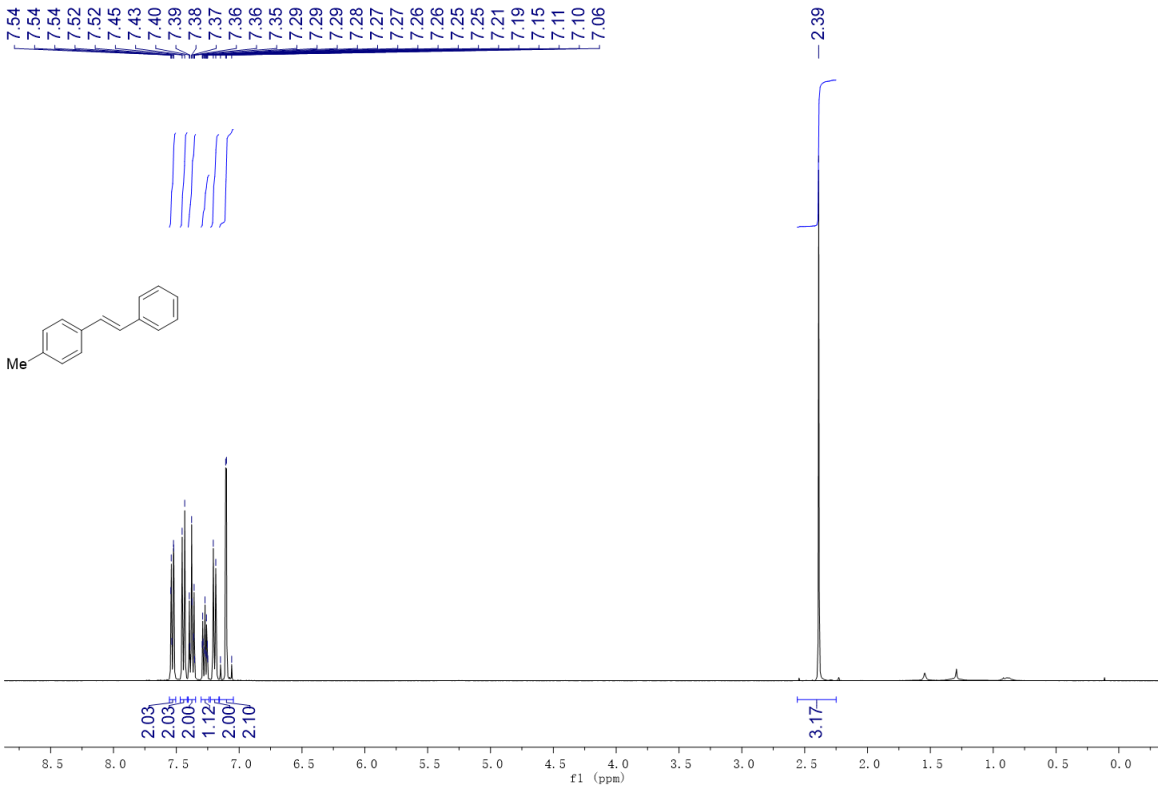

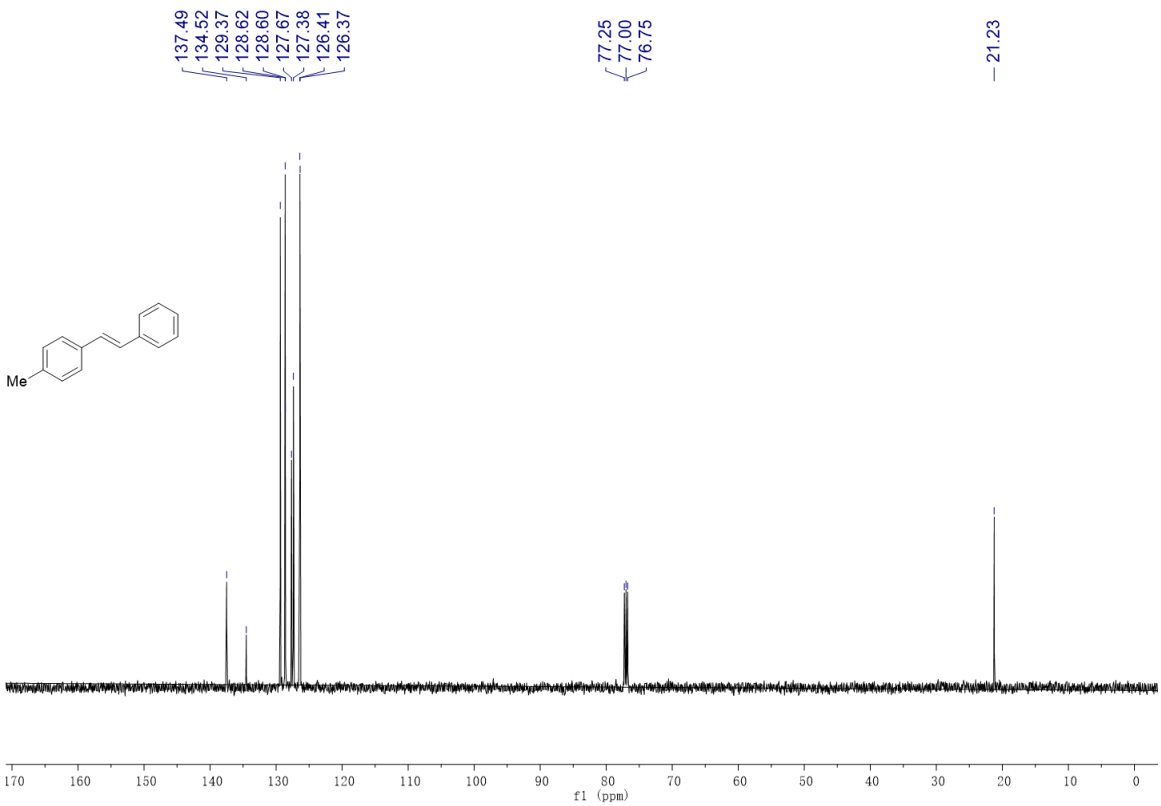

^{1}H and ^{13}C-NMR spectra of product 8c.

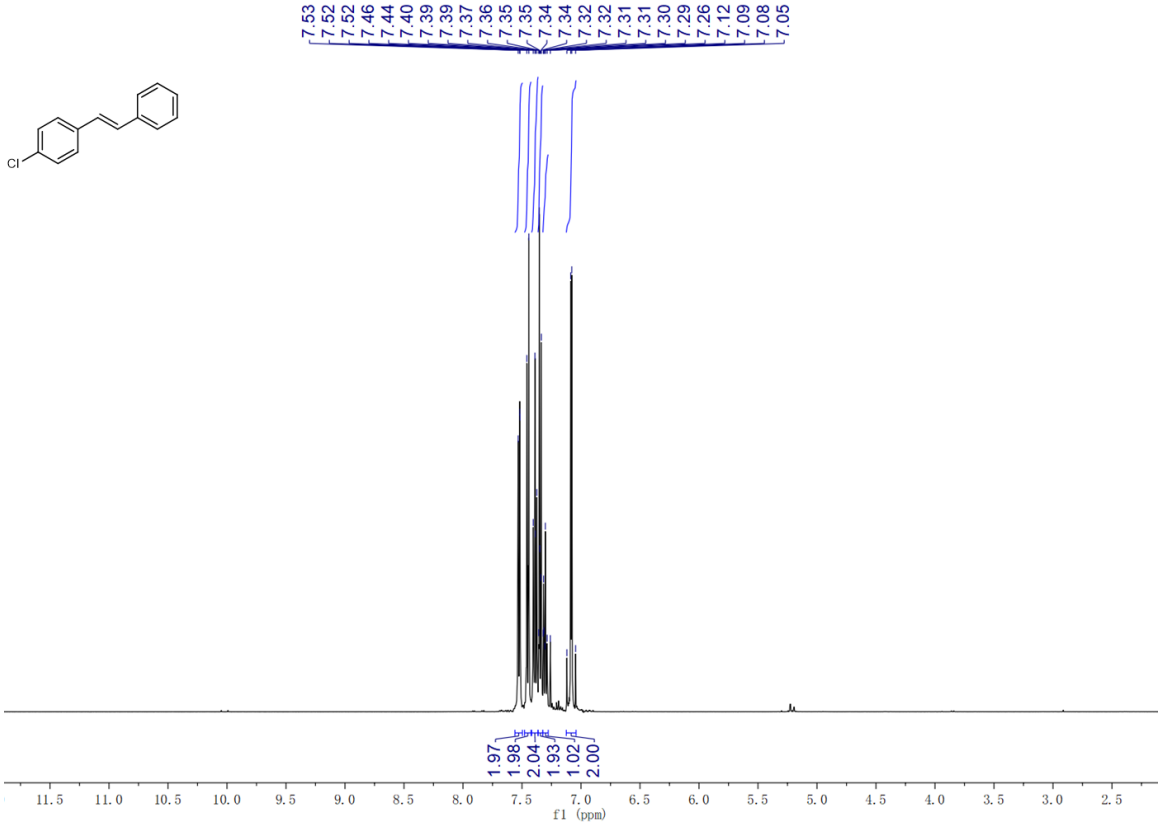

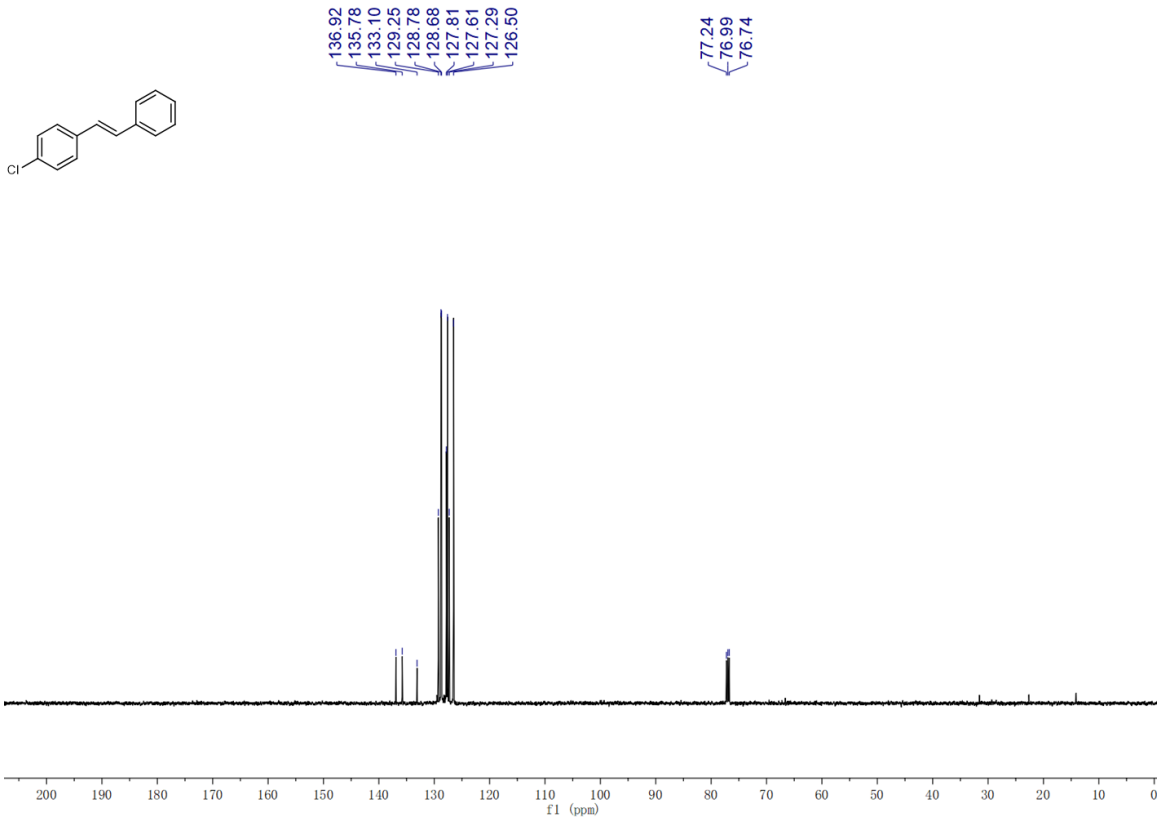

^{1}H and ^{13}C, ^{9}F-NMR spectra of product 8d.

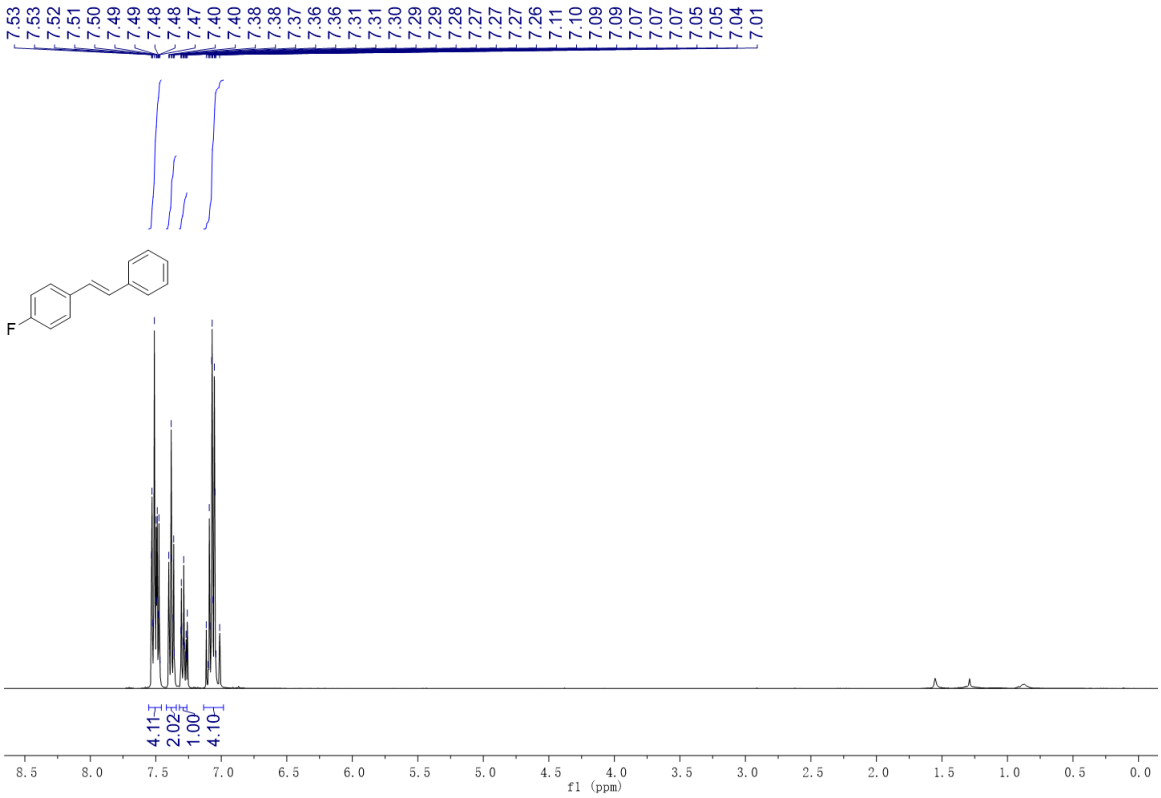

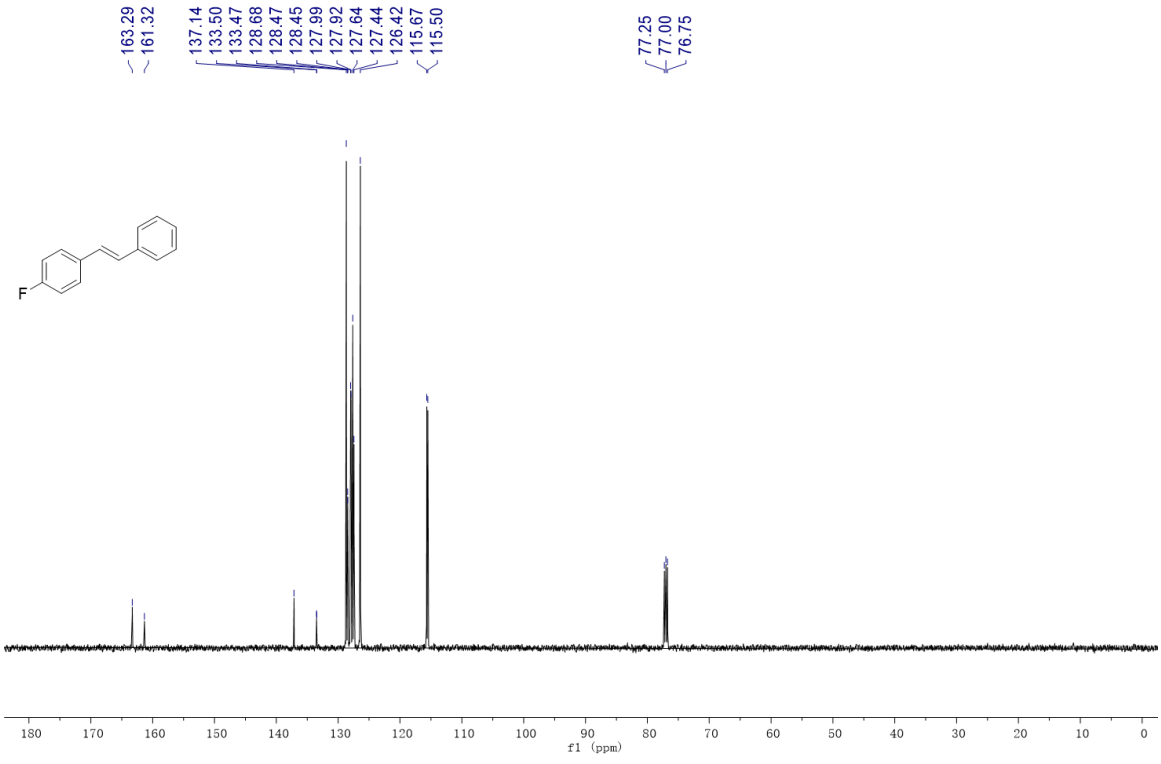

1346

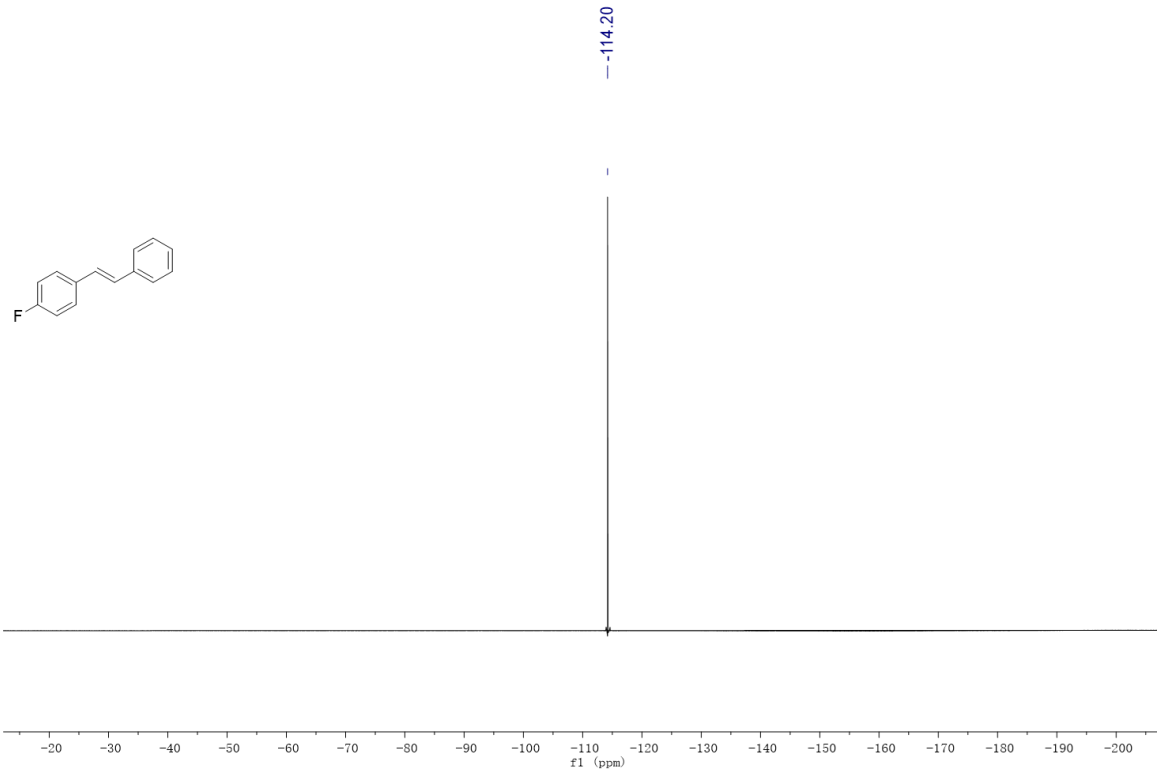

1347

1348

^{1}H, ^{13}C-NMR spectra of product 8e.

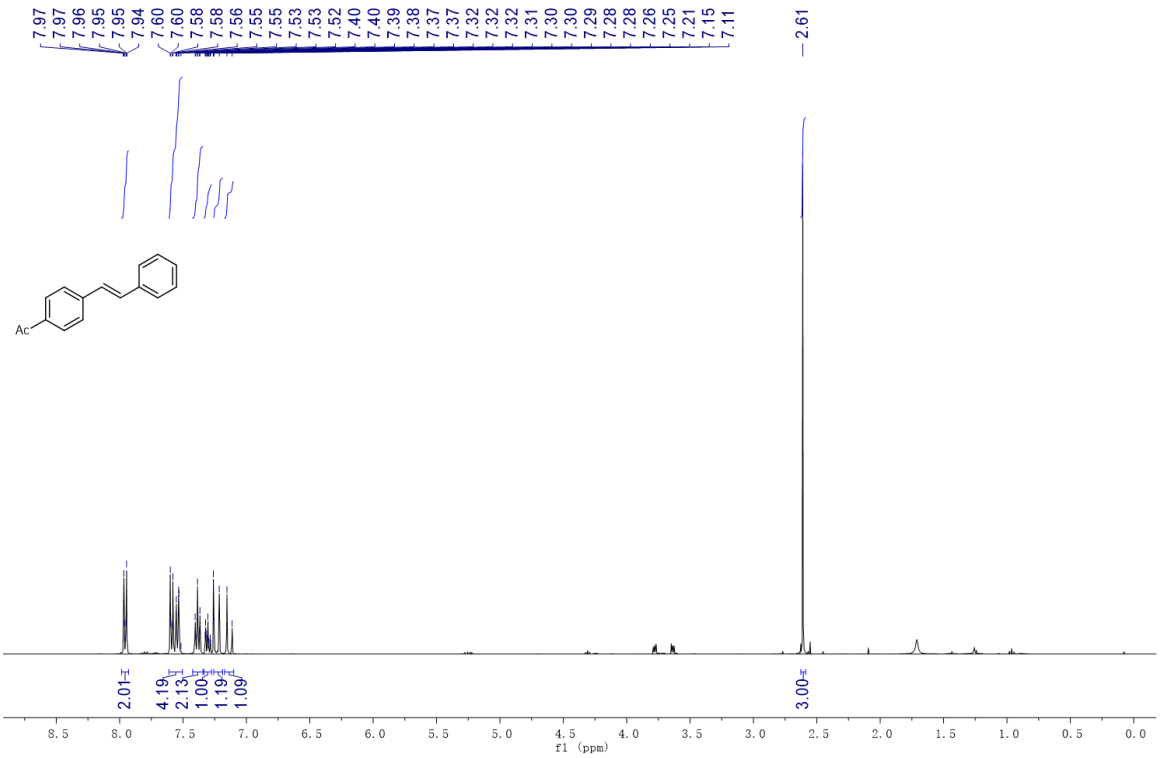

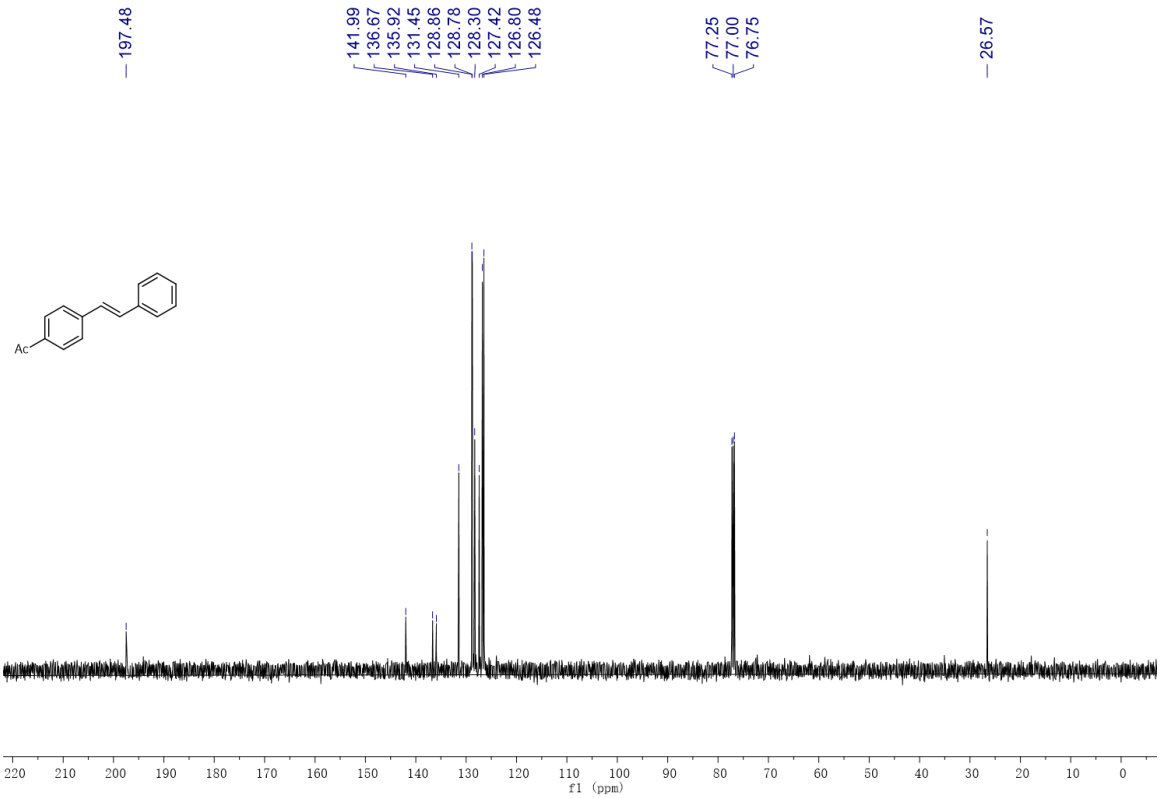

^{1}H, ^{13}C-NMR spectra of product 8f.

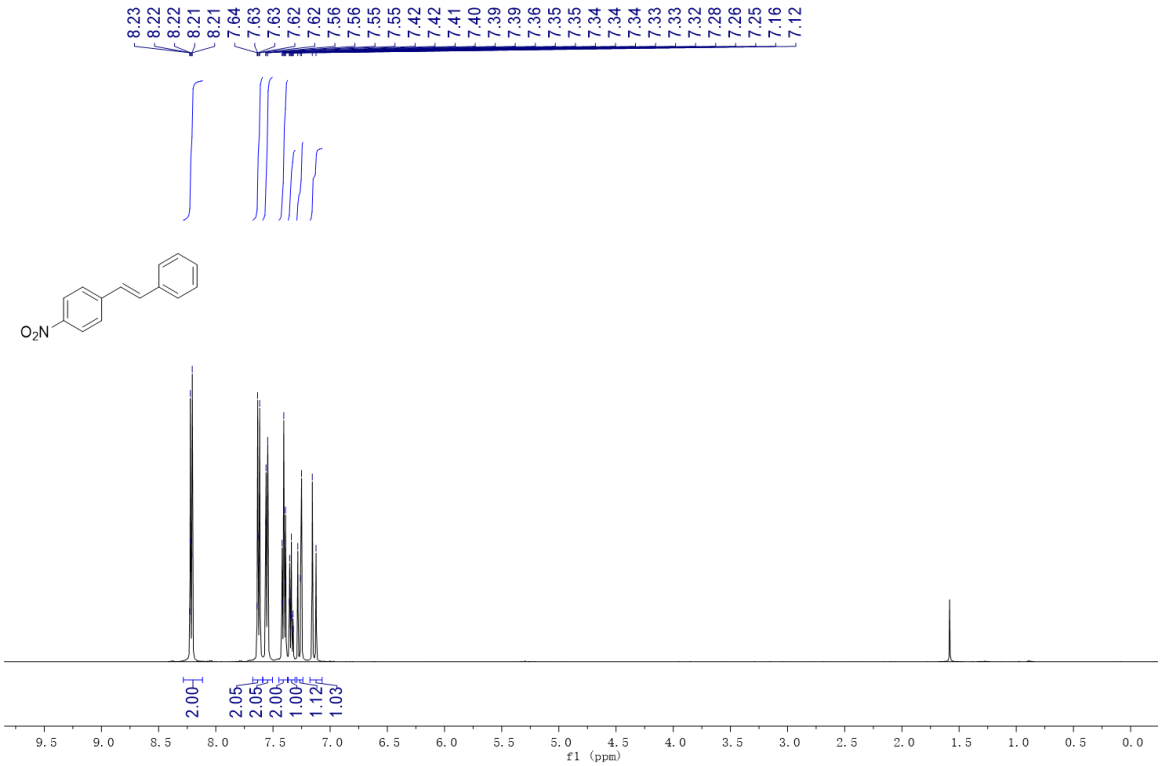

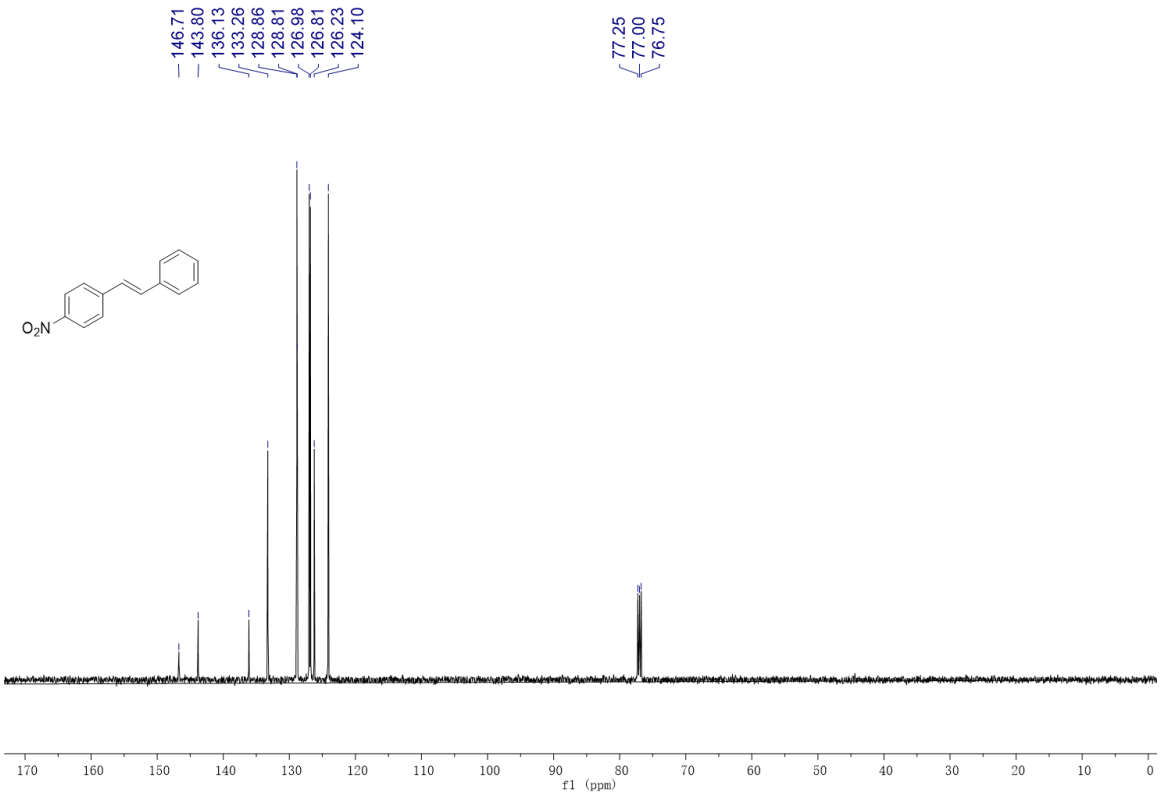

^{1}H, ^{13}C-NMR spectra of product 8g.

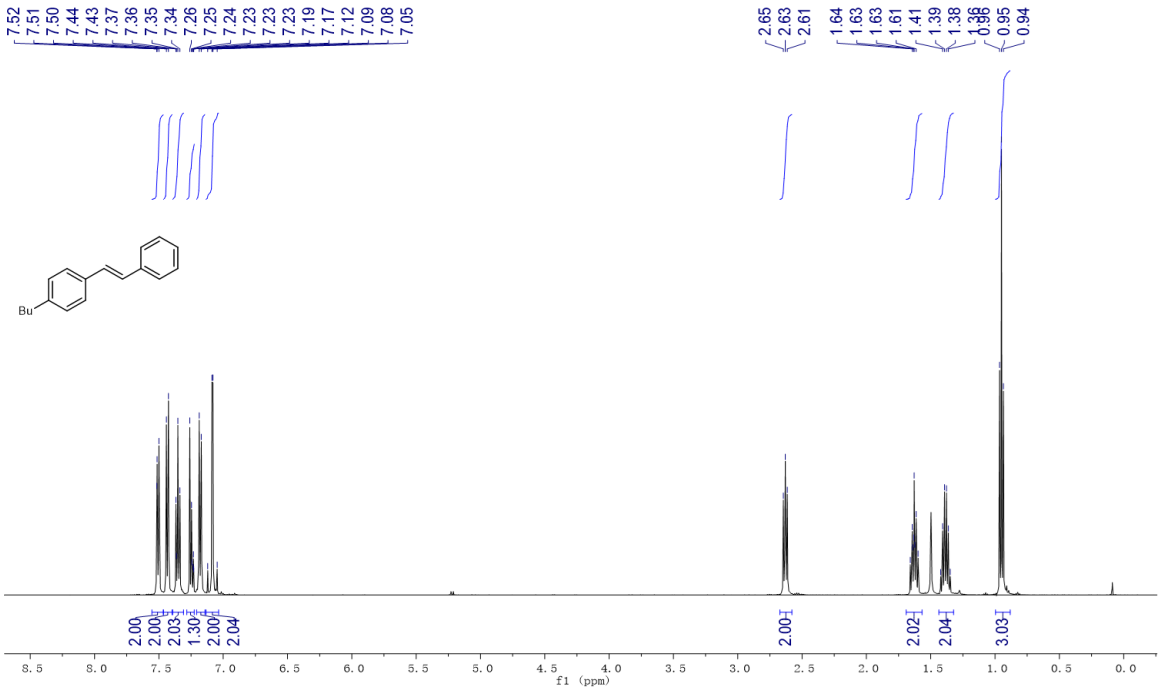

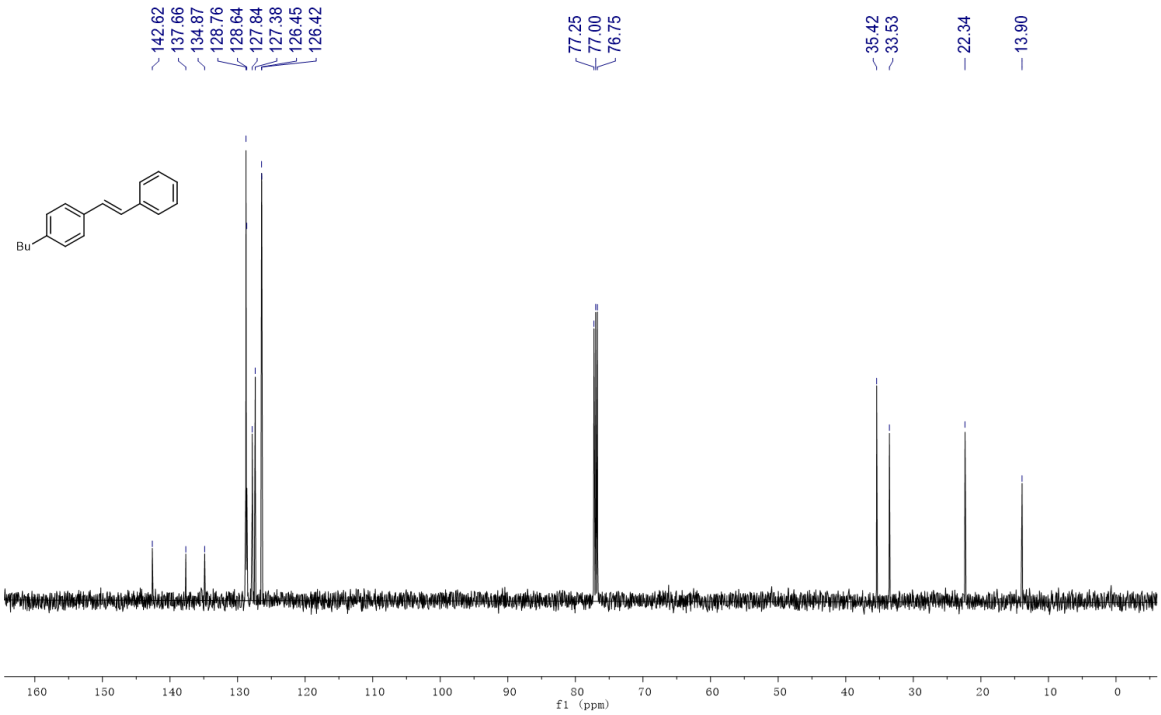

^{1}H and ^{13}C-NMR spectra of product 8h.

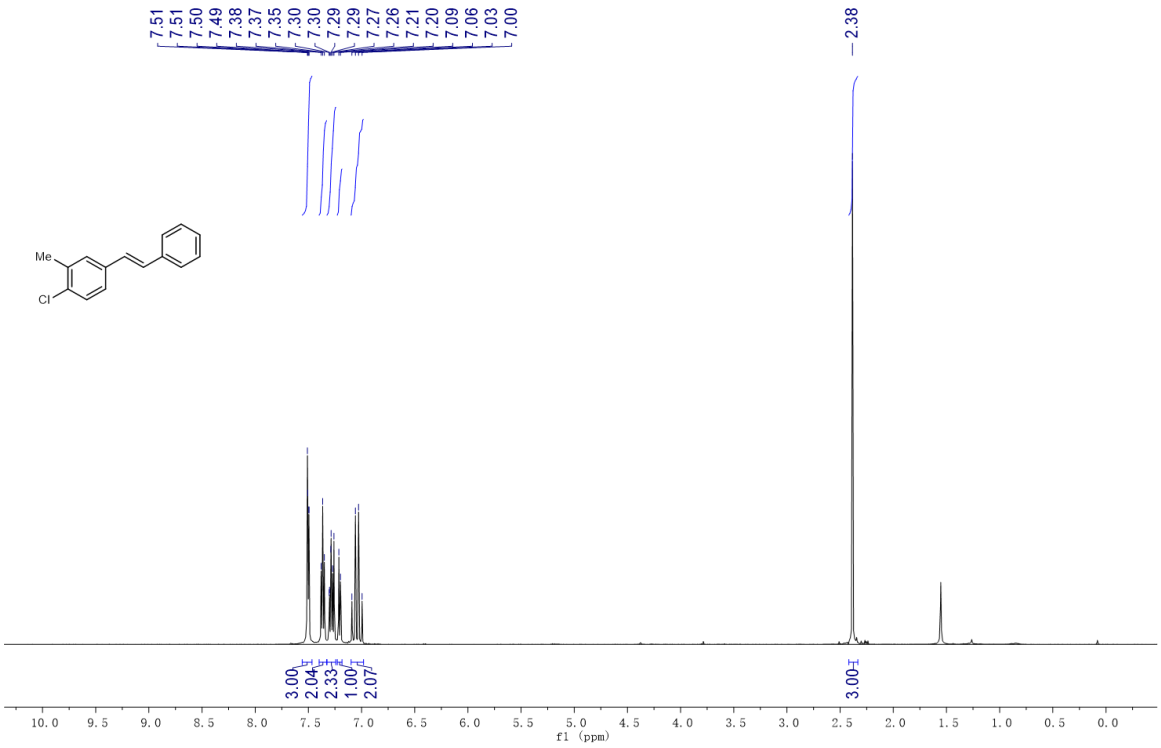

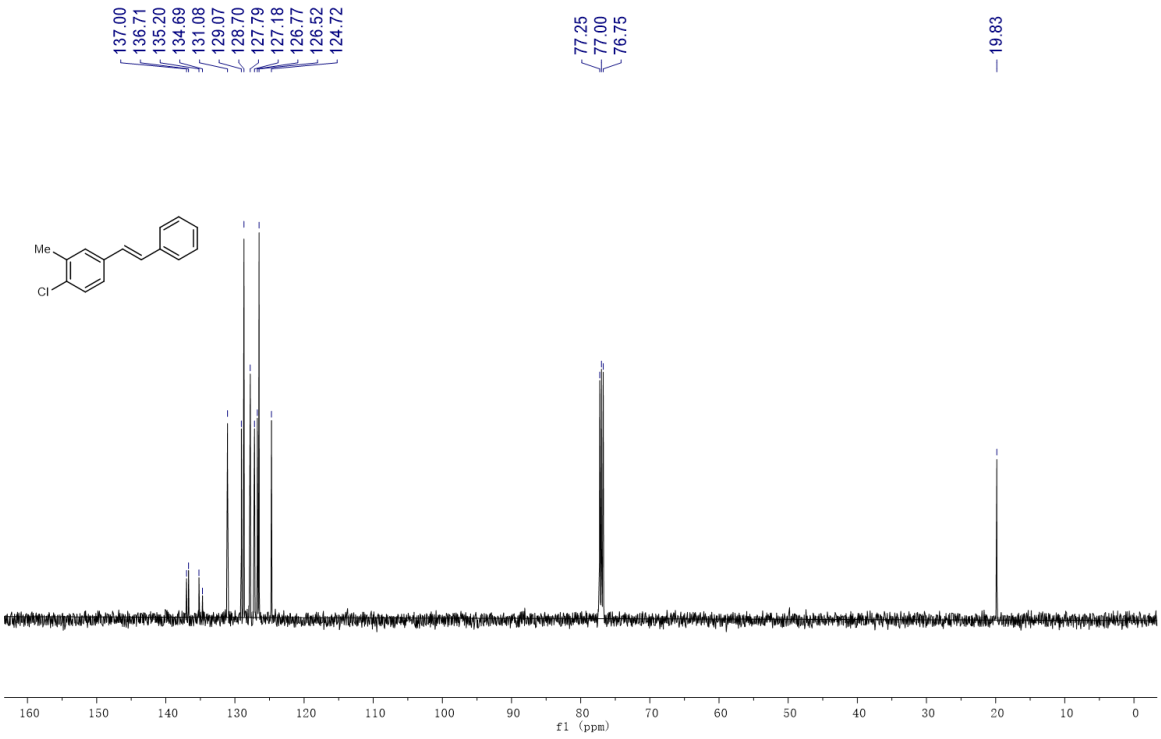

^{1}H and ^{13}C-NMR spectra of product 8i.

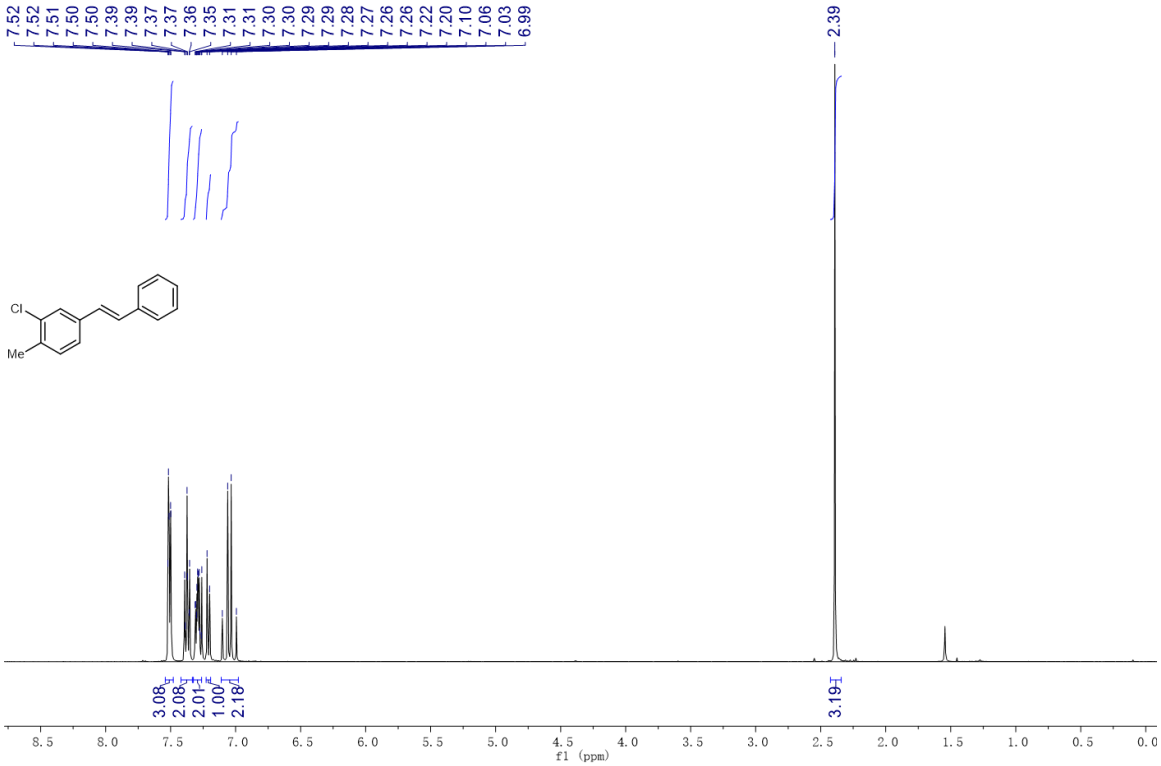

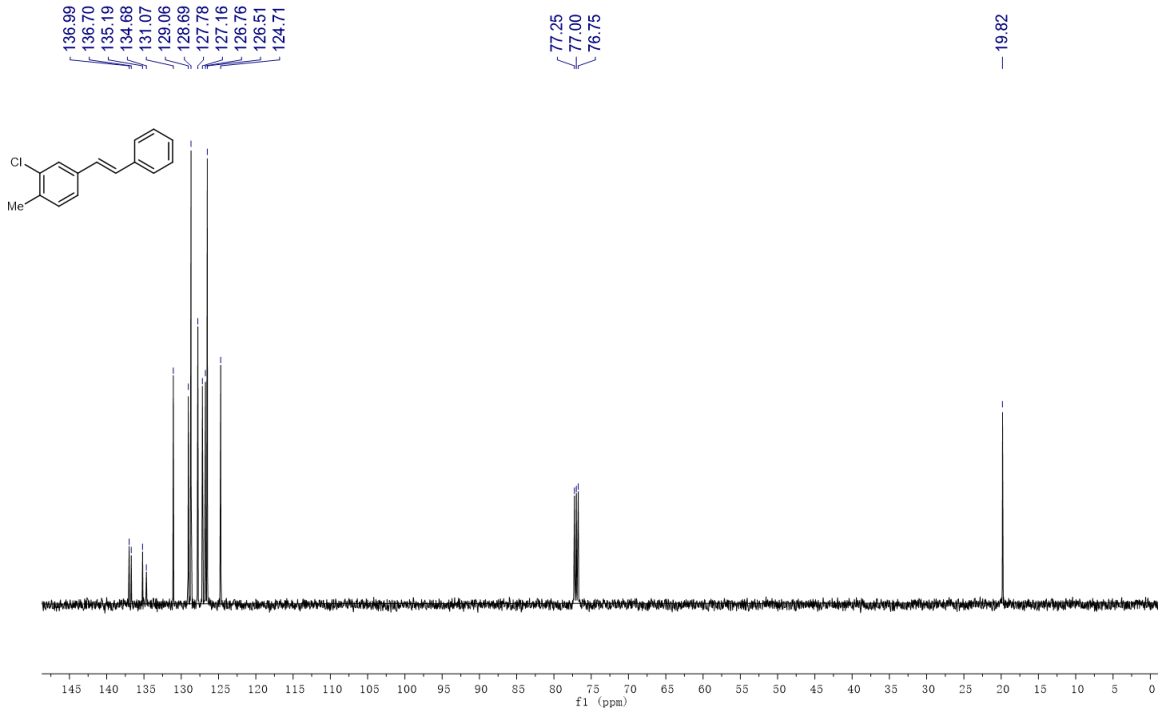

^{1}H and ^{13}C-NMR spectra of product 9a.

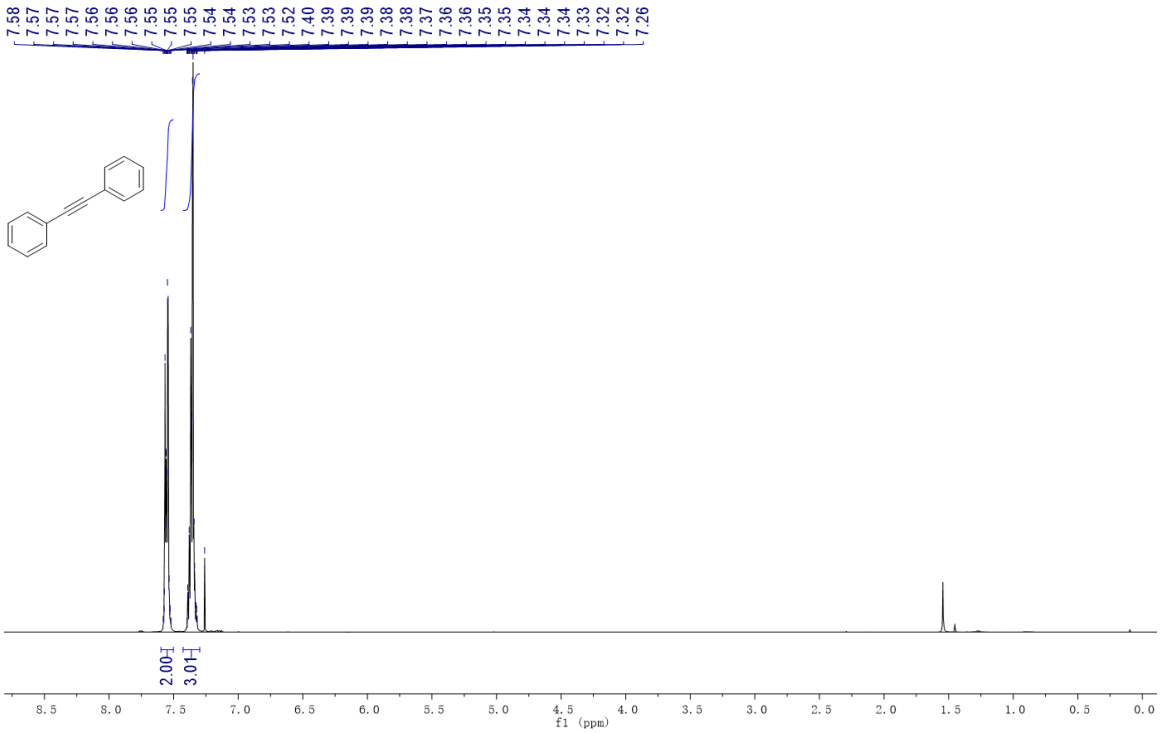

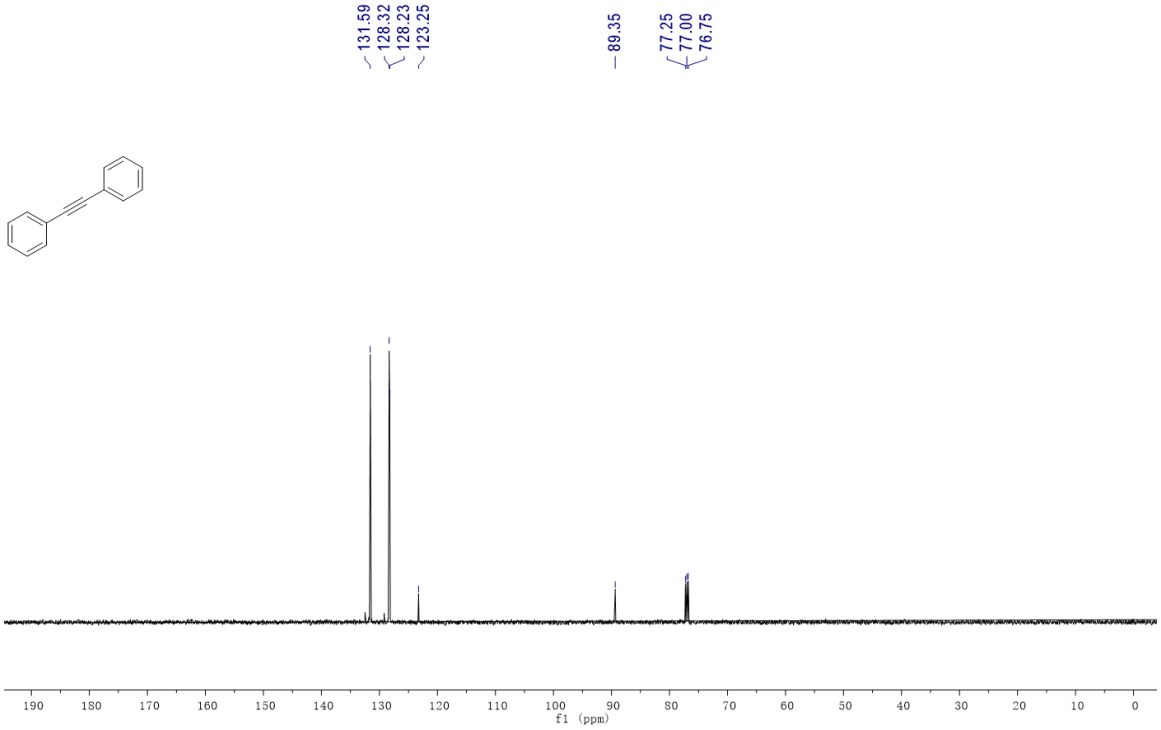

^{1}H and ^{13}C-NMR spectra of product 9b.

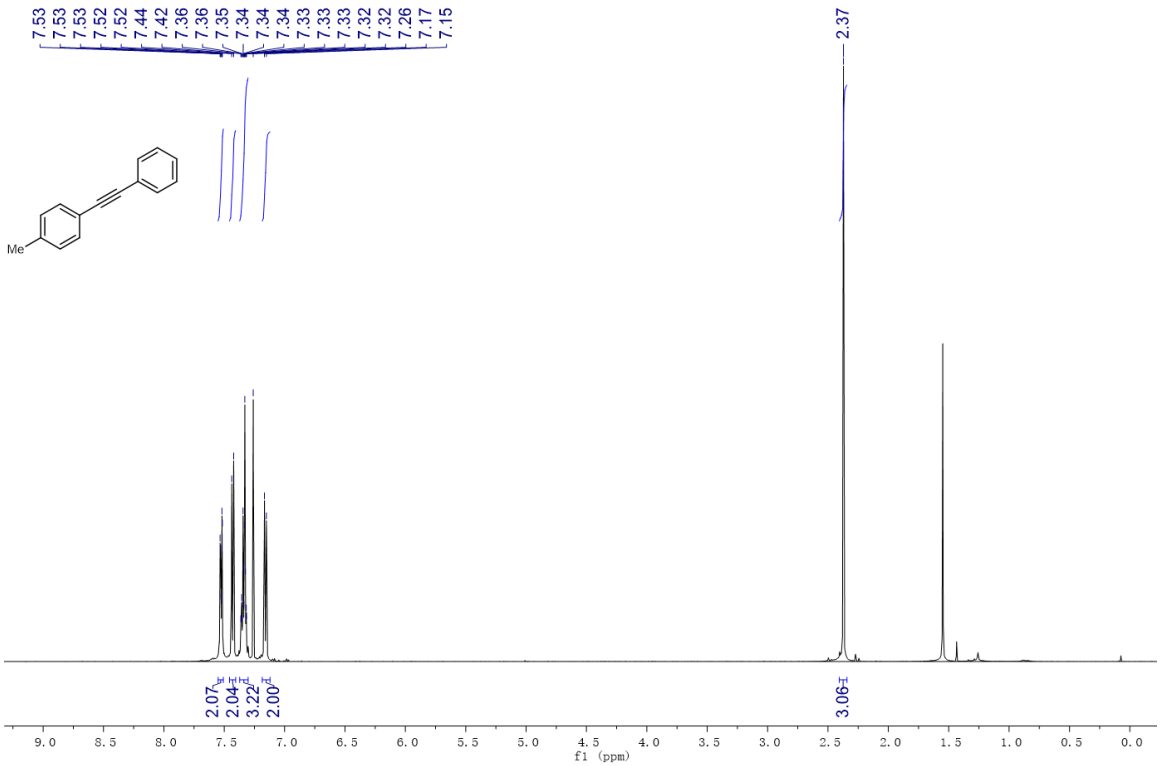

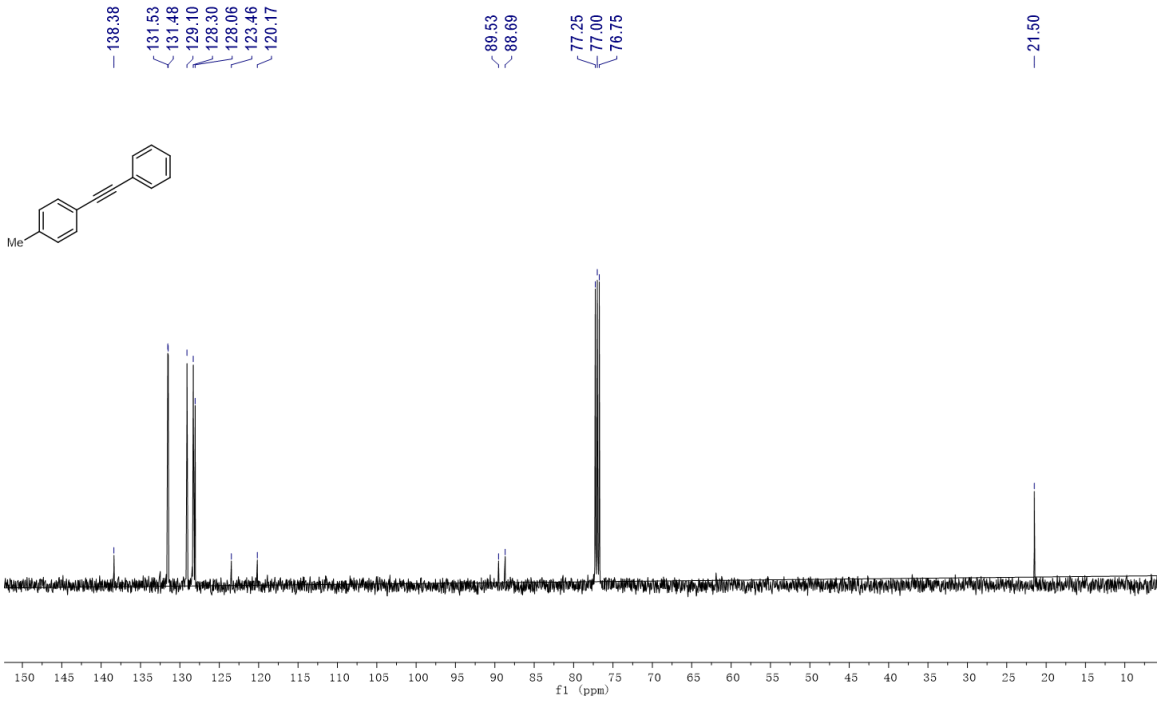

^{1}H and ^{13}C-NMR spectra of product 9c.

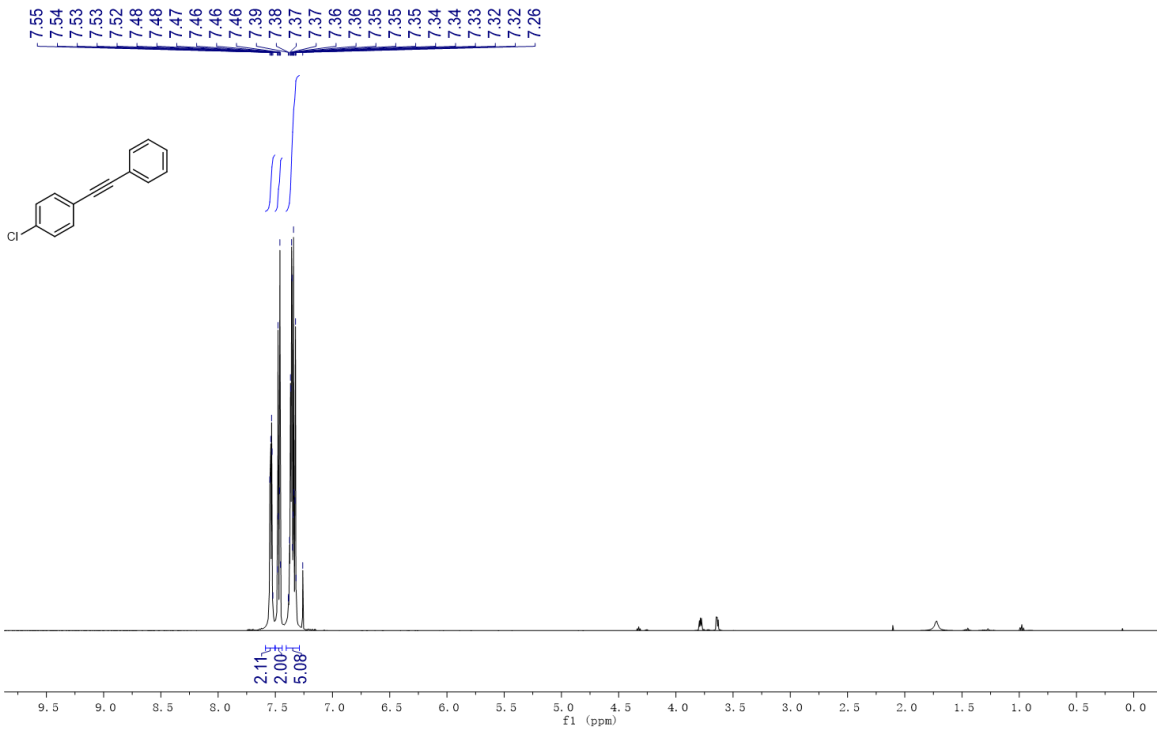

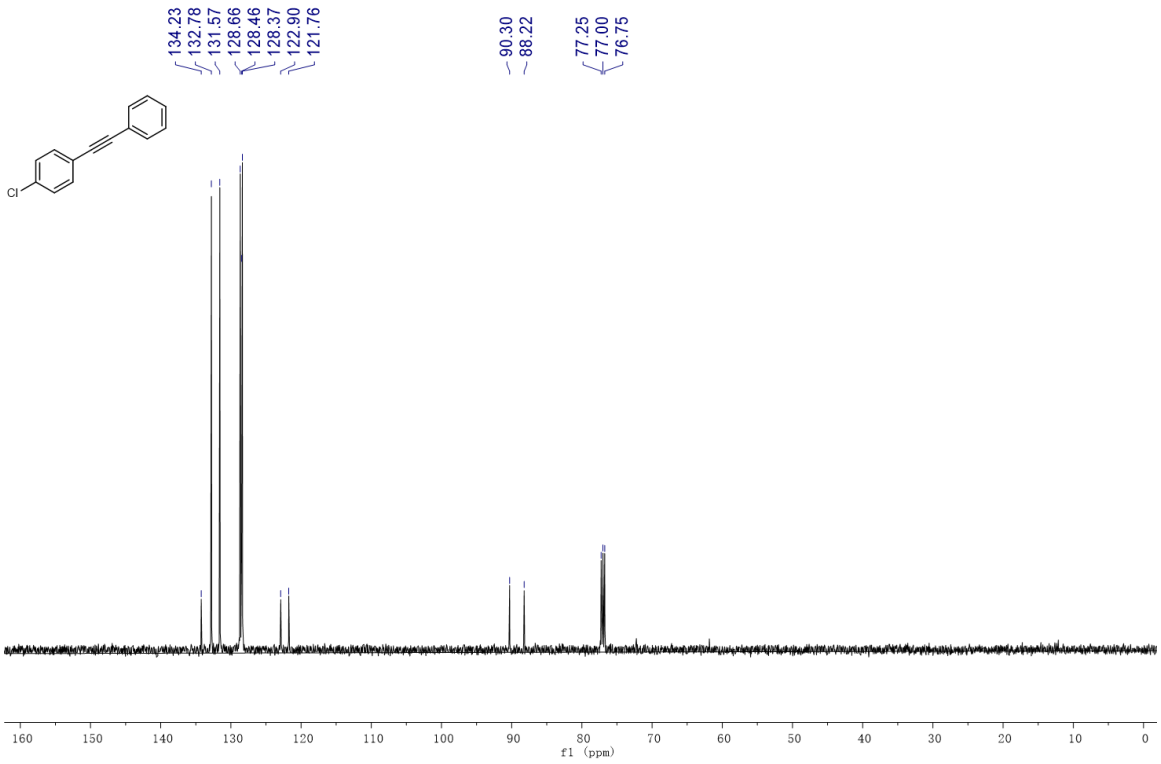

^{1}H and ^{13}C, ^{19}F-NMR spectra of product 9d.

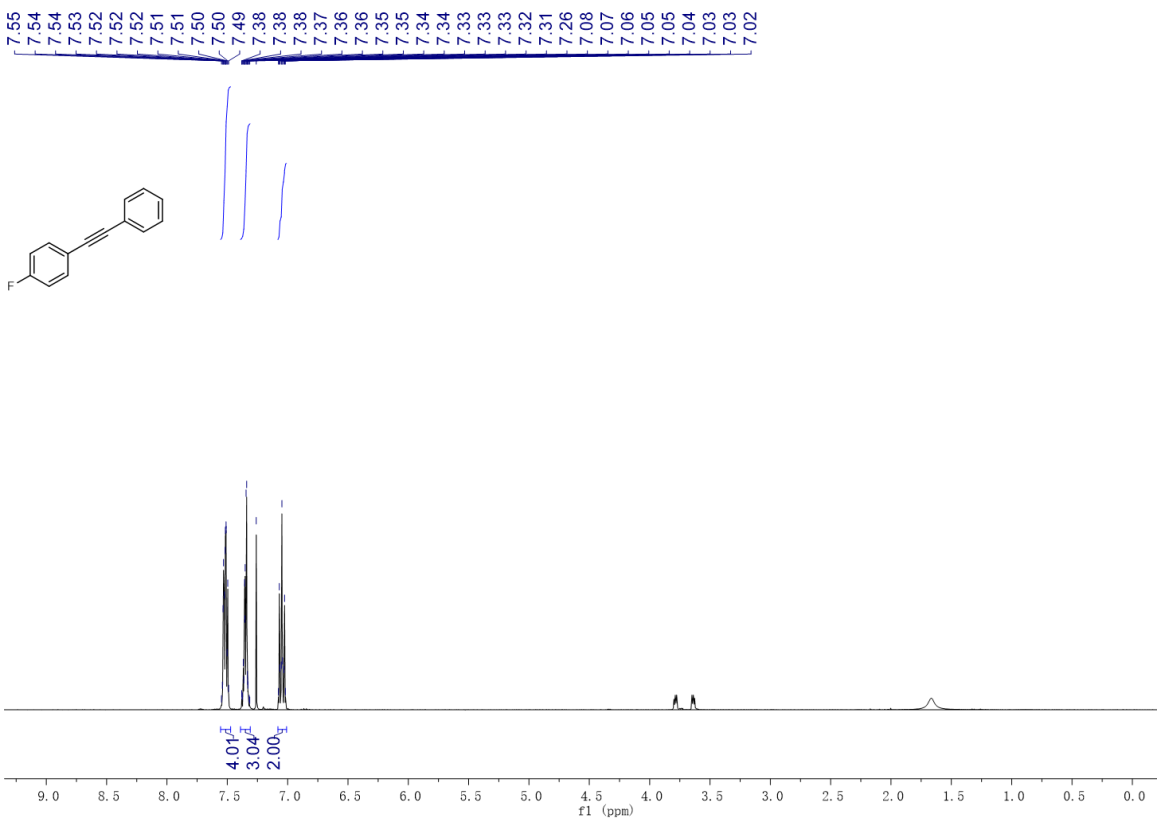

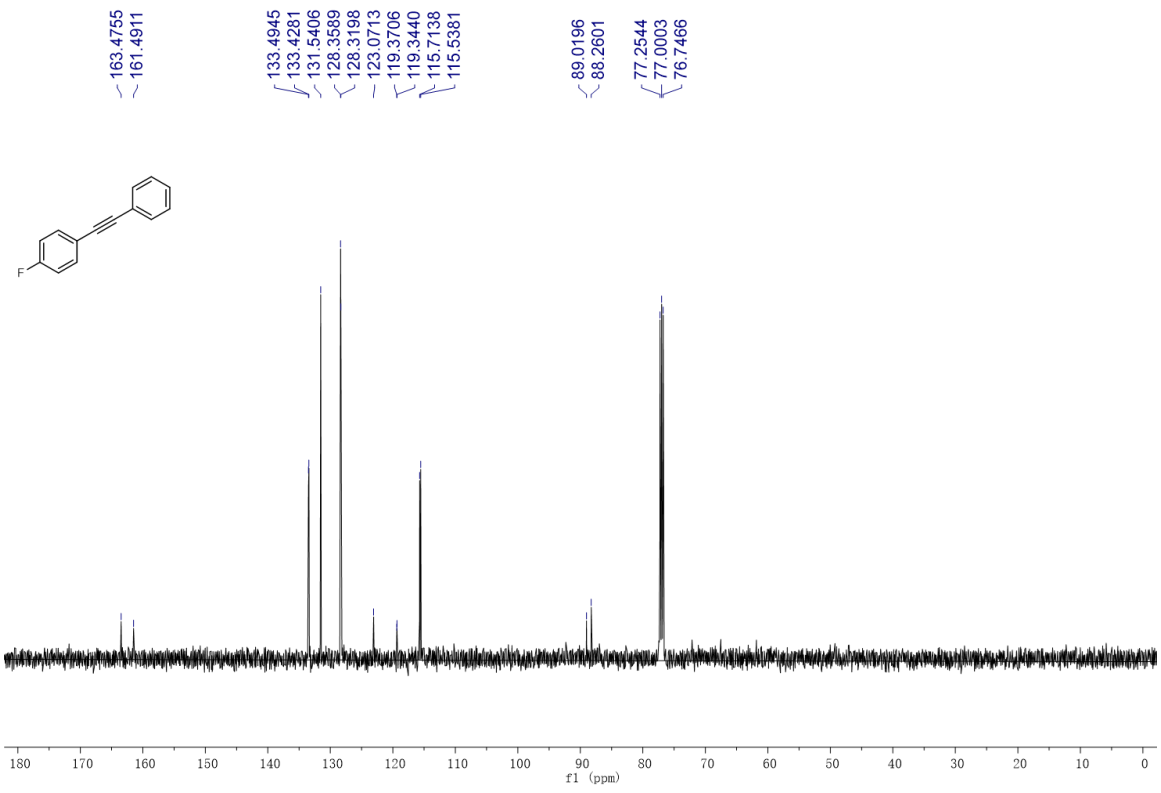

1402

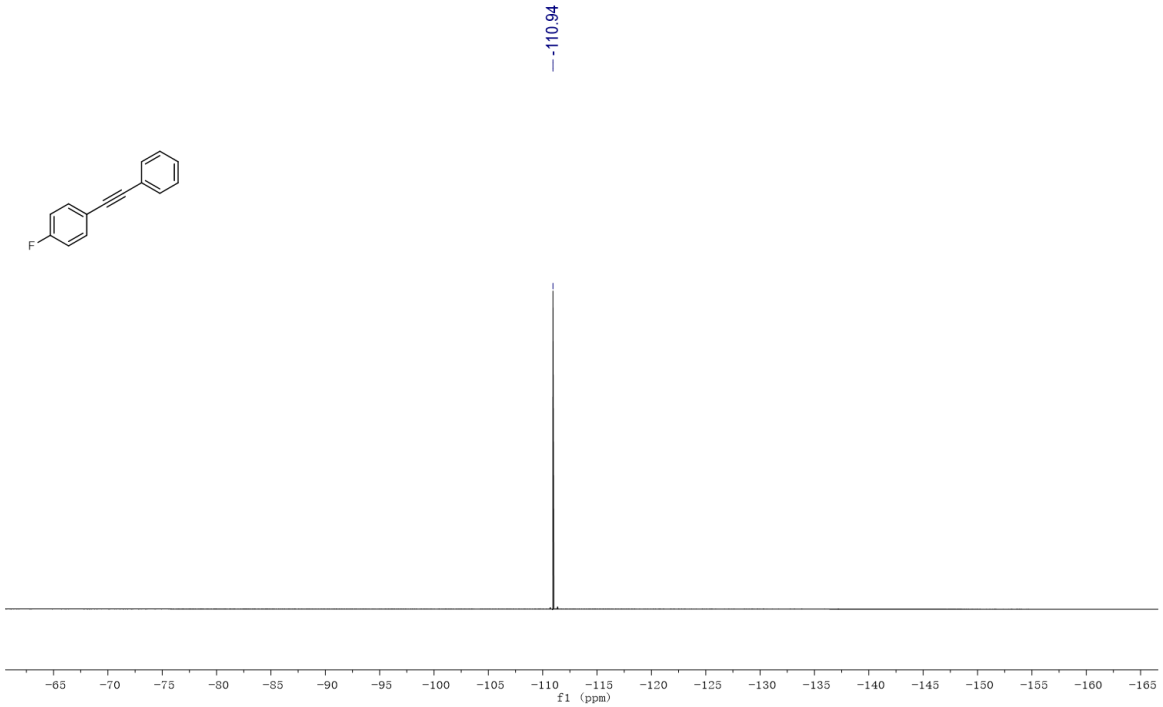
-110.94
F
-65
-70
-75
-80
-85
-90
-95
-100
-105
-110
-115
-120
-125
-130
-135
-140
-145
-150
-155
-160
-165
f1 (ppm)

1403

^{1}H and ^{13}C-NMR spectra of product 9e.

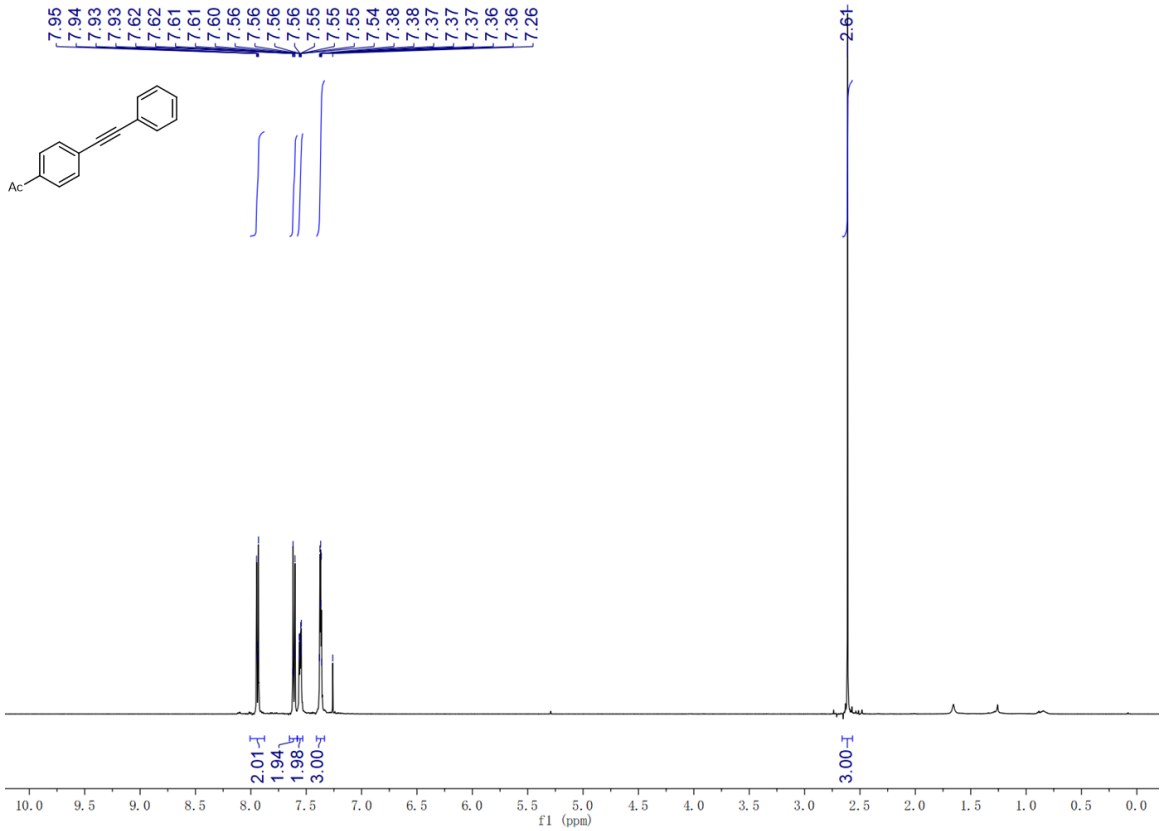

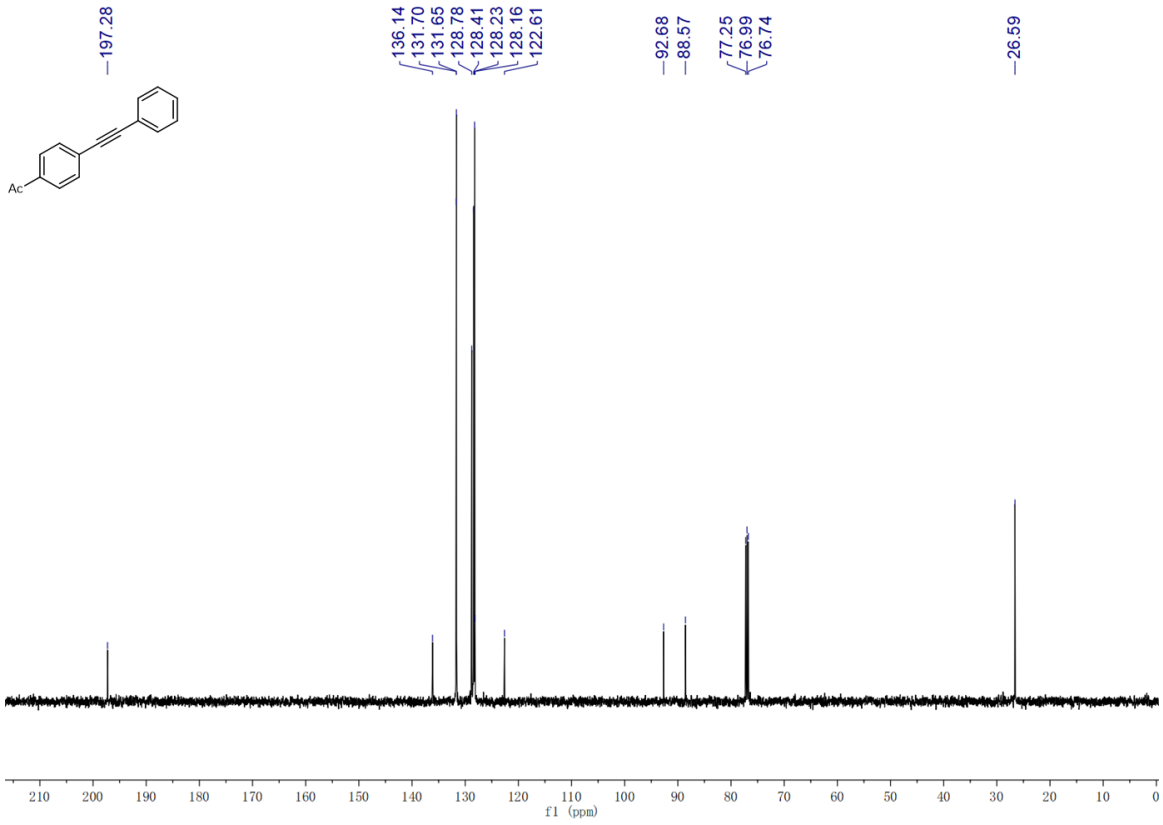

^{1}H and ^{13}C-NMR spectra of product 9f.

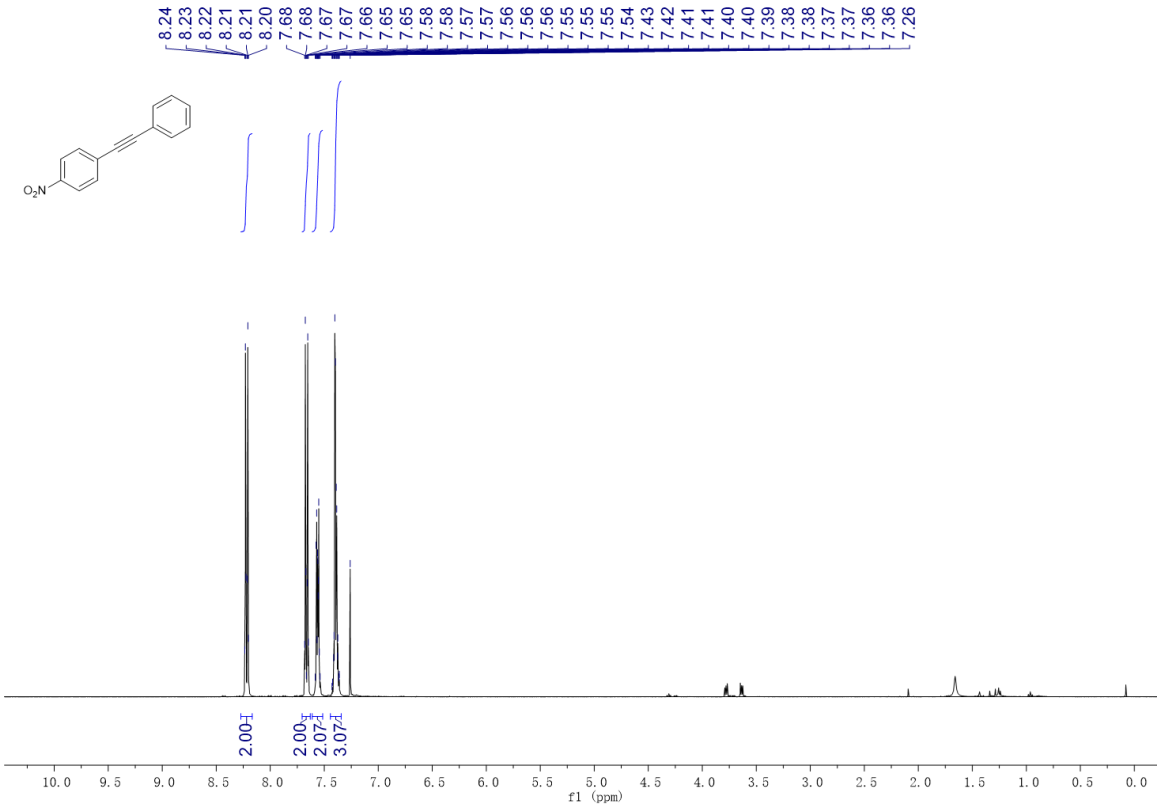

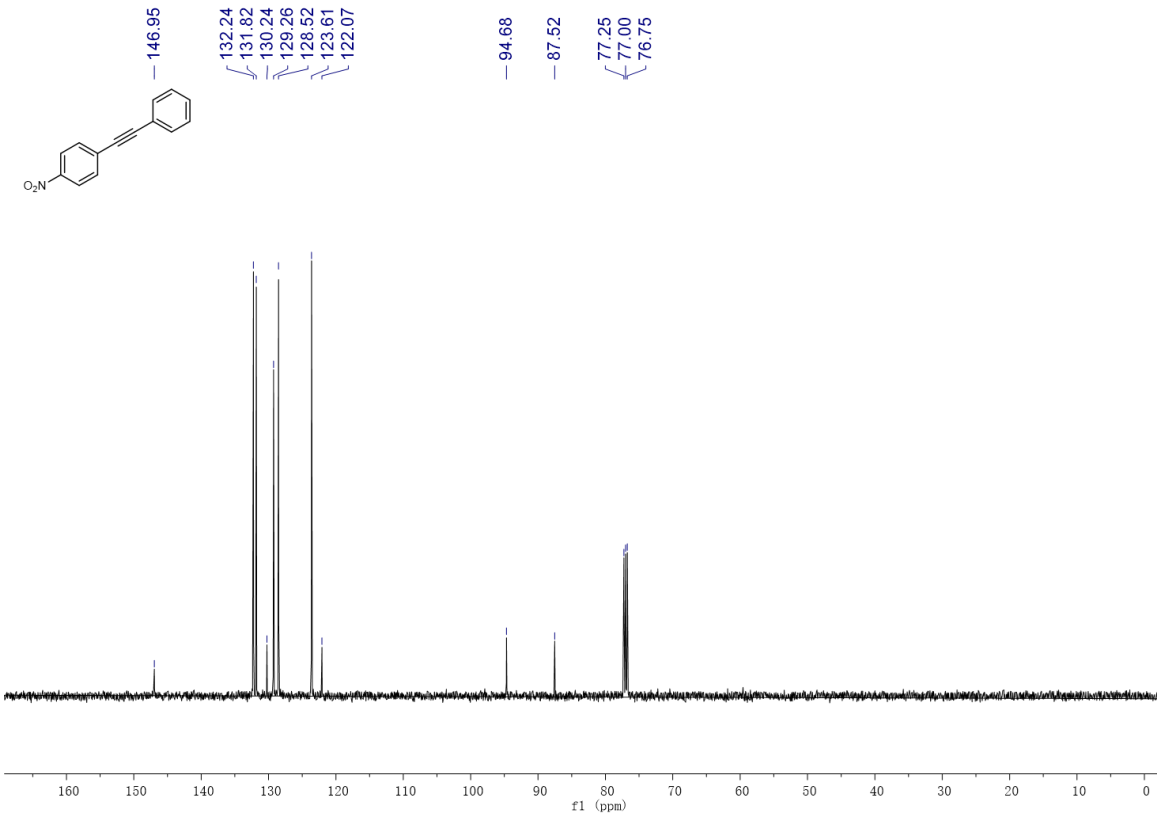

^{1}H and ^{13}C-NMR spectra of product 9g.

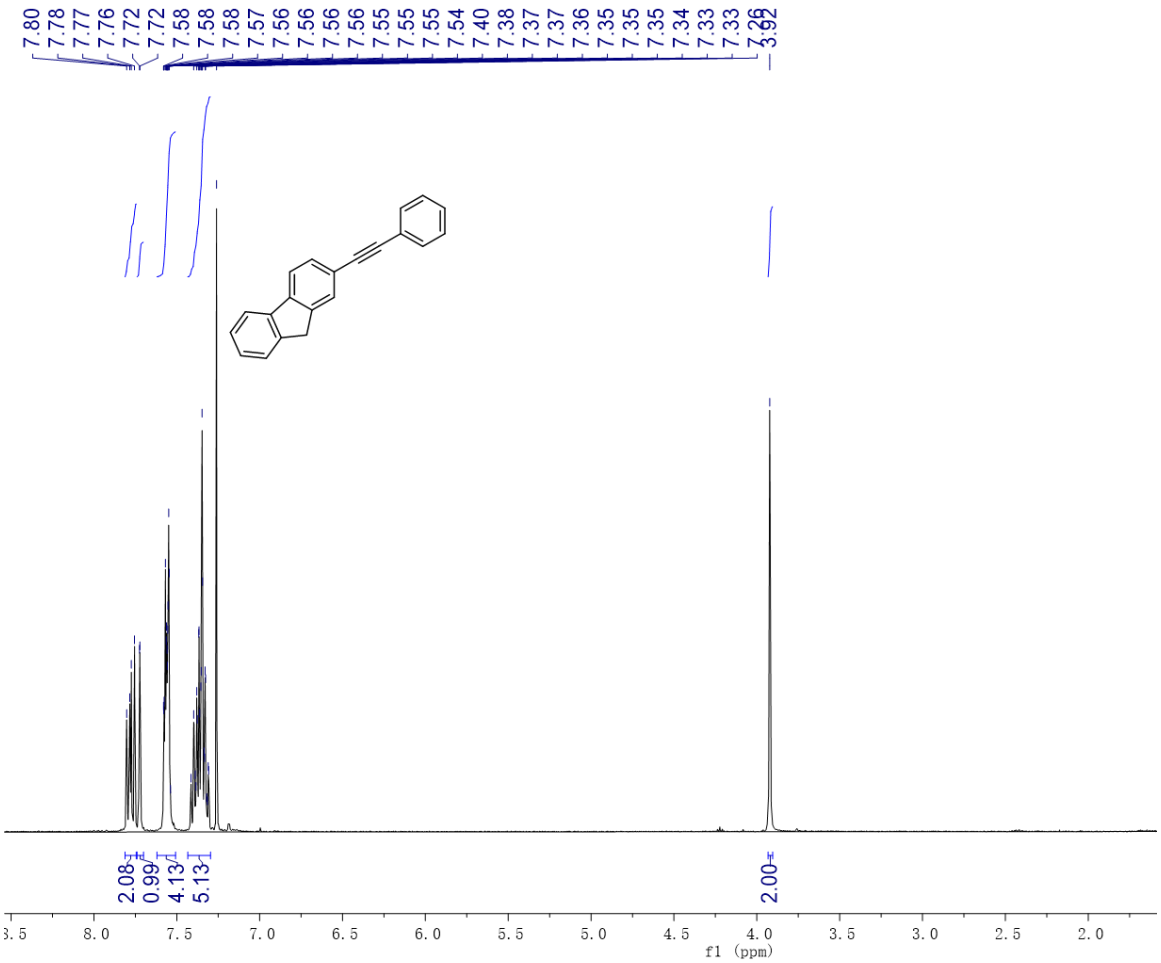

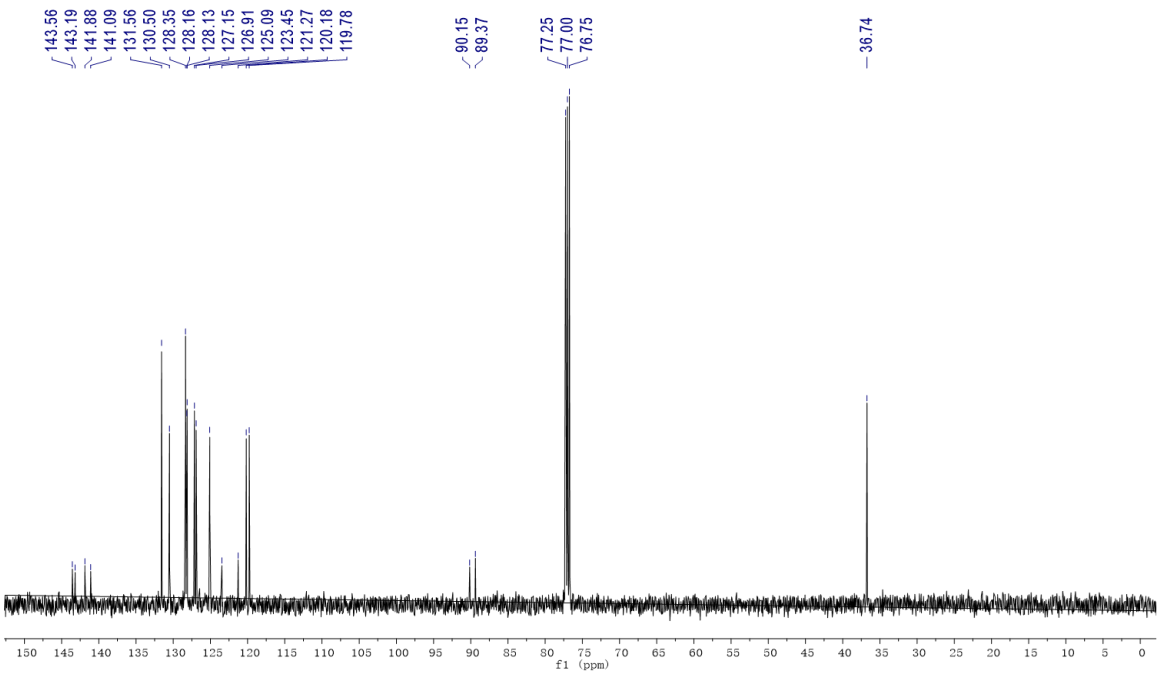

^{1}H and ^{13}C-NMR spectra of product 9h.

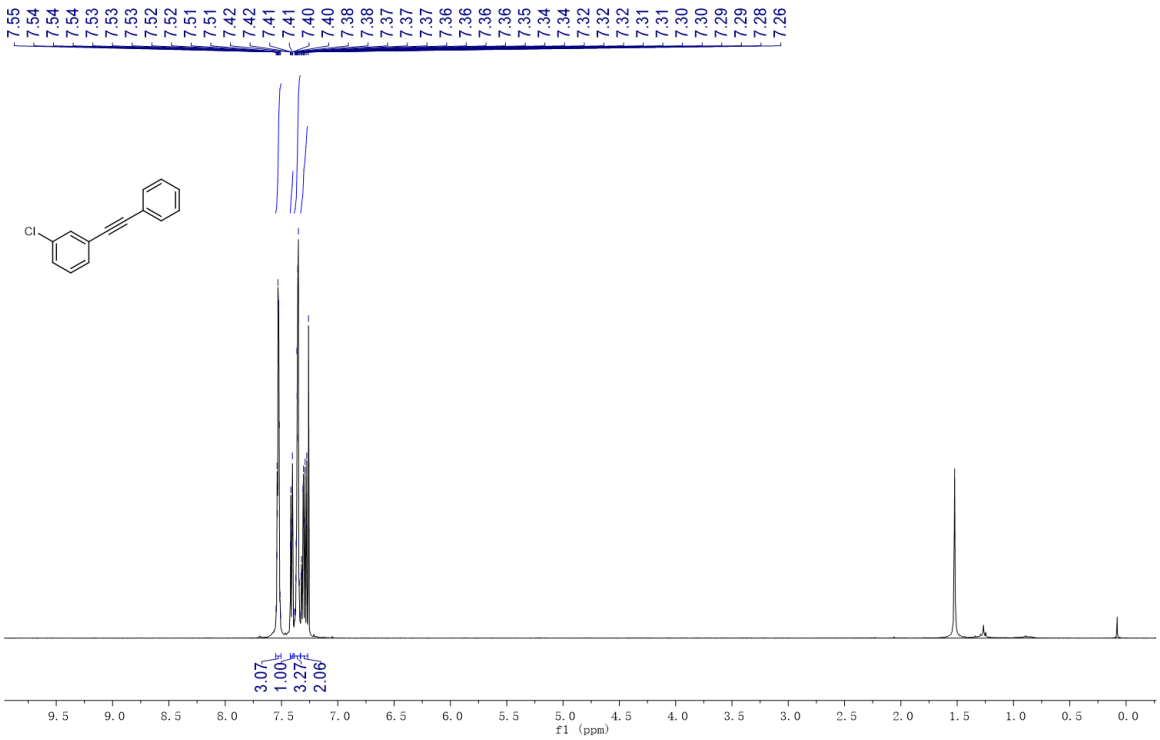

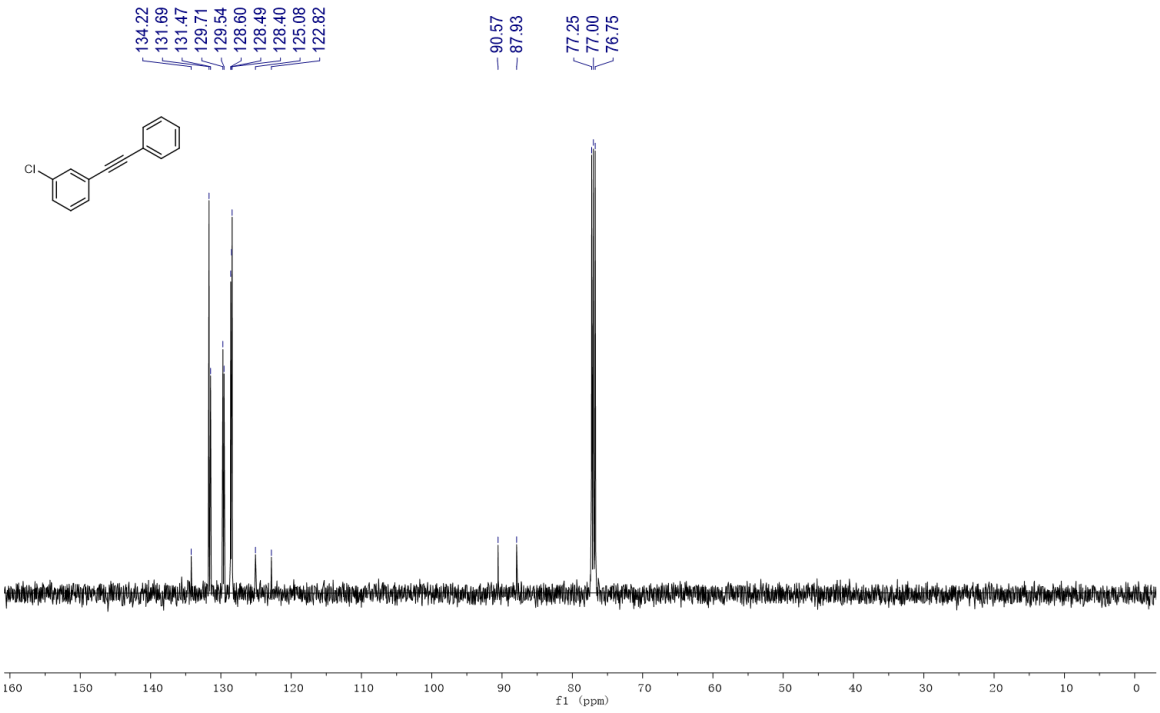

^{1}H, ^{13}C-NMR spectra of product 9i.